

https://dspace.org/

The relationship between material displacement and pressure reduction in a mass flow hopper during initiation of flow

Haupt, Colin

2021
https://hdl.handle.net/10539/31866

Downloaded from a DSpace repository. https://dspace.org/

The relationship between material displacement and pressure reduction in a mass flow hopper during initiation of flow

Colin Haupt

Faculty of Engineering and the Built Environment

University of the Witwatersrand

Johannesburg, South Africa.

Supervisor:

Mr. T Frangakis

A research report submitted to the Faculty of Engineering and the Built Environment, University of the Witwatersrand, Johannesburg, in partial fulfilment of the requirements for the degree of Master of Science in Engineering.

Johannesburg 2020

Declaration

I declare that this research report is my own unaided work, except where otherwise acknowledged. It is being submitted for the degree of Master of Science in Engineering in the University of the Witwatersrand, Johannesburg. It has not been submitted before for any degree or examination at any other university.

A conference paper was presented on the preliminary results at the Beltcon 20 conference held in Pretoria, South Africa, 31 July to 1 August 2019, see Haupt and Frangakis (2019) [17]



……

Signed on the …25th… day of …..December 2020…

Colin Haupt

Abstract

The methods for calculation of material pressures in a mass flow hopper are well researched and documented by multiple authors. The imposed material pressures directly relate to the pull-out tension of a belt feeder or apron feeder, or a shutoff gate.

It is well documented that the initial filling condition imposes a high ‘initial’ pressure on the feeder, and after commencement of a small amount of material withdrawal, the pressure state reduces to a ‘flow’ condition.

Very little research has been presented to demonstrate the amount of material displacement that is required to achieve this change in pressure state, although it is generally understood that the transition takes place rapidly, after only a small amount of material movement.

A laboratory scale test programme was performed to measure the initial and flow pressures and record the relationship between material displacement and actual pressure at the hopper bottom.

The tests were repeated with a variety of material types and hopper configurations, which assisted in understanding the observed effects in terms of a wider range of production scale applications. Parameters that were varied were hopper half-angle, outlet opening width, height of bin filling, differing bulk materials and wall materials. Additional tests were performed to demonstrate the effects of inertial compaction during filling, and a test was performed to gain insight into the time response during slow withdrawal of material

The required displacement for all cases was substantially lower than originally expected prior to performing the test programme.

The results give insight into the design of feeder and hopper interfaces and sizing of mechanical components of feeders. They also provide some guidelines to the requirements of possible load relieving mechanisms.

Dedication

This work is dedicated to my loving and patient wife Carey Haupt for holding everything together during the many hours I spent working on this, and to our two children, Martin and Helen, who always encouraged me to continue to the end without being stressed.

Acknowledgement

I would like to acknowledge and thank Mr Terrence Frangakis for his thorough support and commitment in guiding my efforts in this research, and doing so during some of the most inconvenient of times.

Also, I am grateful to the staff at North West Engineering laboratory for their efforts in construction of the test rig, as well as the Tunra Bulk Solids Africa team who provided support in performing the testing work.

Contents

Declaration ii

Abstract iii

Dedication iv

Acknowledgement v

Contents vi

List of Figures xi

List of Tables xiv

Nomenclature xvi

Chapter 1 Introduction and Background 1

1.1 Summary of Chapter 1 1

1.2 Research Background/Context 1

1.2.1 Initial and flow stress conditions 1

1.3 Industrial Application 3

1.4 Research Motivation 5

1.5 Problem Statement 5

1.6 Hypothesis 6

1.7 Research Questions 7

1.8 Objectives 7

Chapter 2 Literature Review 9

2.1 Introduction 9

2.2 Theoretical Analysis 9

2.3 Experimental and Theoretical Investigations 12

2.4 Industry Experience 13

2.5 Practical Design Recommendations 14

2.6 Numerical Analysis (by DEM simulation) and Comparison to Analytical Methods.. 14

2.7 Summary of literature review 16
Chapter 3 Experimentation 17
3.1 Introduction 17
3.2 Test Rig 17
3.2.1 Design Basis 17
3.2.2 Material pressures and strength design of the test rig 17
3.2.3 Variations in configuration 21
3.2.4 Load cell design and calibration 22
3.3 Material Properties 23
3.3.1 Selected materials and parameters to consider 23
3.3.2 Selection of moisture content for moist sand test cases 24
3.3.3 Bulk density measured vs. selected values 24
3.3.4 Wall friction inclined chute test 26
3.3.5 Selected wall friction and internal friction angles 26
3.4 Testing Procedures 27
3.5 Selection of tests to perform to isolate relevant tests 29
3.6 Data Processing 31
Chapter 4 Observations 38
4.1 Introduction 38
4.2 Range of pressures encountered during testing, compared to design 38
4.3 Behaviours noted during testing action 39
4.4 Initial observations in test result data 40
4.4.1 Comparisons between calculated and measured initial and flow pressures 40
4.4.2 Rate of pressure reduction 40
4.4.3 Effects of experimental events and anomalies. 41
4.5 Dimensional scaling of calculated loads and test rig dimensional constraints 42
Chapter 5 Results 44

5.1 Introduction 44
5.2 Test Set 2, 20-degree, 120 mm, dry sand, bin filled (levelled) 44
5.3 Test Set 3, 20-degree, 120 mm, dry sand, hopper filled 45
5.4 Test Set 4, 20-degree, 150 mm, dry sand, bin filled (levelled) 46
5.5 Test Set 5, 30-degree, 150 mm, dry sand, hopper filled 47
5.6 Test Set 6, 30-degree, 120 mm, dry sand, bin filled (levelled) 48
5.7 Test Set 7, 30-degree, 120 mm, dry sand, hopper filled 49
5.8 Test Set 8, 20-degree, 150 mm, dry sand, hopper filled 50
5.9 Test Set 9, 20-degree, 120 mm, dry aggregate, hopper filled 51
5.10 Test Set 10, 20-degree, 120 mm, moist sand, hopper filled 52
5.11 Test Set 11, 20-degree, 120 mm, moist sand, hopper filled – PVC lined 53
5.12 Test Set 12, Time response test 54
5.13 Summary of test data 55
5.14 Comparative presentation of test data 57
5.14.1 Variation of material types (fixed configuration) 57
5.14.2 Variation of wall angle (fixed materials, width and fill configuration) 58
5.14.3 Variation of opening width (fixed materials, angle and fill configuration) 60
5.14.4 Variation of fill configuration (fixed materials, angle, and opening width) 62
5.14.5 Variation of wall friction (fixed materials, angle, fill configuration and opening width) 64
5.14.6 Variation of rate of filling (fixed all other parameters) 64
5.15 Overall summary of pressure reduction rates, all cases 66
Chapter 6 Discussion 67
6.1 Introduction 67
6.2 Effects of material properties 67
6.3 Comparison to theoretical calculations 70
6.4 Hopper wall angle 70

6.5 Hopper opening width 72
6.6 Fill configuration (hopper only or filled bin) 74
6.7 Wall material 75
6.8 Rate of filling 75
6.9 Time effects 76
6.10 Increasing pressures on hopper 77
6.11 Review of experimentation methods 78
6.12 Summary and response to research questions. 79
6.13 Recommendations for operational sized installations 82
Chapter 7 Conclusion 83
7.1 Recommendations for future work 84
References 85
Appendix A Hopper and gate pressure calculation methodology 87
A.1 Initial Filling Case – Vertical bin Section 87
A.2 Flow Case – Vertical Bin Section 89
A.3 Mass-Flow Hopper Pressures 90
A.3.1 Hopper Initial pressures 91
A.3.2 Hopper Flow pressures 91
A.3.3 Surcharge pressure applied to the mass-flow hopper 92
A.4 Hopper loads on Feeder/Gate 92
A.4.1 Initial Filling Condition 94
Appendix B Calculation of withdrawn material mass 96
Appendix C Loadcell calibration and tare weight evaluation 99
Appendix D Test material properties 105
D.1 Bulk density 106
D.2 Moisture content 107
D.3 Particle size distribution 112

D.4 Poured angle of repose 114
D.5 Inclined chute test 115
Appendix E Friction Angle Sensitivity Analysis 116
Appendix F Sample Calculations 122
F.1 Calculation of hopper initial and flow pressures 122
F.2 Calculation of material withdrawal volume 125
Appendix G Test Results 126
G.1 Set 2, 20-degrees, 120 mm slot, dry sand, bin levelled full 127
G.2 Set 3, 20-degrees, 120 mm, dry sand, hopper only filled 129
G.3 Set 4, 20-degrees, 150 mm, dry sand, bin levelled full 131
G.4 Set 5, 30-degrees, 150 mm, dry sand, hopper filled 133
G.5 Set 6, 30-degrees, 120 mm, dry sand, bin levelled full 135
G.6 Set 7, 30-degrees, 120 mm, dry sand, hopper filled 137
G.7 Set 8, 20-degrees, 150 mm slot, dry sand, hopper filled 139
G.8 Set 9, 20-degrees, 120 mm, aggregate, hopper only 141
G.9 Set 10, 20-degrees, 120 mm slot, moist sand, hopper filled 143
G.10 Set 11, 20-degrees, 120 mm, moist sand, hopper filled, PVC lined 145
G.11 Set 12, Time response test 147
Appendix H Test Rig Design Drawings 152

List of Figures

Figure 1-1 Silo principal stress (σ1) fields and normal wall pressures (p_n) 2
Figure 3-1 Schematic of test rig with two hopper angle configurations and two opening widths 19
Figure 3-2 Test rig, (a) assembled, and (b) during a test (dry sand) 20
Figure 3-3 'High position' installation, indicating setup angle measurements 20
Figure 3-4 Inclined chute test of moist material on vinyl wall surface – slip at 38 degrees ... 26
Figure 3-5 Shape of material between hopper outlet and bottom plate 32
Figure 3-6 Set 9, Case 10 - Loadcell volt readings per nut rotation (raw data) 35
Figure 3-7 Set 9, Case 10, 20-degrees, 120 mm, 13 mm aggregate, hopper only - full range of test 35
Figure 3-8 Set 9, Case 10, 20-degrees, 120 mm, 13 mm aggregate, hopper only - range 1-5 mm 36
Figure 3-9 Set 9, Case 10, demonstration of uncertainty and weight corrections, range 40-50 mm 36
Figure 3-10 Result curves on Set 9 test repetitions 37
Figure 5-1 Set 2, 20-degree, 120 mm, dry sand, Levelled 44
Figure 5-2 Set 3, 20-degree, 120 mm, dry sand, Hopper filled 45
Figure 5-3 Set 4, 20-degree, 150 mm, dry sand, Levelled 46
Figure 5-4 Set 5, 30-degree, 150 mm, dry sand, Hopper filled 47
Figure 5-5 Set 6, 30-degree, 120 mm, dry sand, Levelled 48
Figure 5-6 Set 7, 30-degree, 120 mm, dry sand, Hopper filled 49
Figure 5-7 Set 8, 20-degree, 150 mm, dry sand, Hopper filled 50
Figure 5-8 Set 9, 20-degree, 120 mm, dry aggregate, Hopper filled 51
Figure 5-9 Set 10, 20-degree, 120 mm, moist sand, Hopper filled 52
Figure 5-10 Set 11, 20-degree, 120 mm, moist sand, Hopper filled – PVC Lined 53
Figure 5-11 Set 12, 20-degree, 120 mm, moist sand, hopper filled – PVC wall – time tesponse test 54
Figure 5-12 Set 12, plot of load to plate displacement – time response test 54
Figure 5-13 Load-displacement function of time response test – first 5 mm of deflection 55
Figure 5-14 Comparative behaviours of materials with varying properties 57

Figure 5-15 Comparative behaviours resulting from angle variation 20-degree to 30-degree - filled 120 mm 58
Figure 5-16 Comparative behaviours resulting from angle variation 20-degree to 30-degree – hopper, 120 mm 59
Figure 5-17 Comparison of behaviours from angle variation, 20-degree to 30-degree - Hopper 150 mm 59
Figure 5-18 Comparison of the effect of outlet opening width - dry sand, filled bin, 20-degree hopper 60
Figure 5-19 Comparison of the effect of outlet opening width - dry sand, hopper filled, 20-degree hopper 61
Figure 5-20 Comparison of the effect of outlet opening width - dry sand, hopper filled, 30-degree hopper 61
Figure 5-21 Effect of fill configuration, hopper only vs. filled bin, dry sand, 120 mm, 20-deg 62
Figure 5-22 Effect of fill configuration, hopper only vs. filled bin, dry sand, 120 mm, 20-deg 63
Figure 5-23 Effect of fill configuration, hopper only vs. filled bin, dry sand, 120 mm, 20-deg 63
Figure 5-24 Effect of wall friction at hopper surface 64
Figure 5-25 Fast-pour compaction effects - dry materials 65
Figure 5-26 Fast-pour compaction effects - moist (cohesive) materials 65
Figure 5-27 Rate of pressure reduction per test case, to 50% and 80% reduced 66
Figure 6-1 Stress field at hopper outlet, when presenting higher than expected loads 78

Figure A- 1 Silo principal stress ($\sigma 1$) fields and normal wall pressures (p_n) 87
Figure A- 2 Loads on feeder 93

Figure B- 1 Geometry of withdrawn material pile 96
Figure B- 2 Sloped (dry) and near-vertical (moist) repose angles from dry and moist sand .. 98

Figure C- 1 Loadcell and amplifier 100
Figure C- 2 Loadcell datasheet 104

Figure D- 1 Inclined chute test 115

Figure E- 1 Friction properties sensitivity – quartz aggregate 117
Figure E- 2 Friction properties sensitivity – dry sand..... 118
Figure E- 3 Friction properties sensitivity – moist sand 120

Figure G- 1 Test Set 2, 20-degrees, 120 mm, dry sand, bin filled to top level..... 128
Figure G- 2 Test Set 2, 20-degrees, 120 mm, dry sand, bin filled to top level – 1-5 mm range 128
Figure G- 3 Test Set 3, 20-deg, 120 mm, dry sand, hopper filled 130
Figure G- 4 Test Set 3, 20-deg, 120 mm, dry sand, hopper filled 130
Figure G- 5 Test Set 4, 20deg, 150 mm, dry sand levelled full..... 132
Figure G- 6 Test Set 4, 20-deg, 150 mm, dry sand, levelled full 132
Figure G- 7 Test Set 5, 30-degrees, 150 mm, dry sand, hopper filled 134
Figure G- 8 Test Set 5, 30-degrees, 150 mm, dry sand, hopper filled, 1-5 mm range..... 134
Figure G- 9 Test Set 6, 30-degrees, 120 mm, dry sand, bin levelled full 136
Figure G- 10 Test Set 6, 30-degrees, 120 mm, dry sand, bin levelled full, 1-5 mm range .. 136
Figure G- 11 Test Set 7, 30-degrees, 120 mm, dry sand, hopper filled 138
Figure G- 12 Test Set 7, 30-degrees, 120 mm, dry sand, hopper filled, 1-5 mm range..... 138
Figure G- 13 Test Set 8, 20-degrees, 150 mm, dry sand, hopper filled 140
Figure G- 14 Test Set 8, 20-degrees, 150 mm, dry sand, hopper filled, 1-5 mm range..... 140
Figure G- 15 Test Set 9, 20-degrees, 10 mm, Aggregate, hopper filled 142
Figure G- 16 Test Set 9, 20-degrees, 10 mm, Aggregate, hopper filled, 1-5 mm range..... 142
Figure G- 17 Test Set 10, 20-degrees, 120 mm, moist sand, hopper filled..... 144
Figure G- 18 Test Set 10, 20-degrees, 120 mm, moist sand, hopper filled, 1-5 mm range .. 144
Figure G- 19 Test Set 11, 20-degrees, 120 mm, moist sand, hopper filled..... 146
Figure G- 20 Test Set 11, 20-degrees, 120 mm, moist sand, hopper filled, 1-5 mm range .. 146
Figure G- 21 Results from Case 12, time response test 151
Figure G- 22 Case 12, time response test, load-displacement plot..... 151
Figure G- 23 Case 12, time response test, load-displacement plot: 1-5 mm..... 151

List of Tables

Table 2-1 Parameters affecting friction properties 12
Table 3-1 - Nominal vs. Actual hopper dimensions 22
Table 3-2 - Measured and selected bulk density parameters..... 26
Table 3-3 - List of test result cases and test sets 31
Table 3-4, Example test record sheet (Set no. 9, Case no. 10) – Aggregate, 20-deg, 120 mm, Hopper only 34
Table 4-1 Error correction on nut turn direction..... 41
Table 4-2 Error recording - rig bumped during time consolidation test 42
Table 4-3 Step change in pressure due to Delayed reading..... 42
Table 5-1 - Summary of material drawdown per test set 56
Table 6-1 – Expected behaviours of the selected materials 68
Table 6-2 - Effects of variation to, hopper wall angle 72
Table 6-3 Effects of variation to hopper opening width 73
Table 6-4 Effects of variation to fill configuration 74
Table 6-5 Effects of variation to wall friction 75
Table 6-6 Effects of variation to filling rate (cohesive materials) 76
Table 6-7 Required deflection to achieve 80% load reduction, per material type..... 81

Table C- 1 Loadcell 1 calibration worksheet..... 101
Table C- 2 Loadcell 2 calibration worksheet..... 102
Table C- 3 Calculation of tare weight 103

Table D- 1 Bulk density, sand (dry and moist)..... 106
Table D- 2 Bulk density, 13 mm quartz aggregate 106
Table D- 3 Sand – initial moisture content test record..... 107
Table D- 4 Sand – saturation moisture content test record 108
Table D- 5 Summary of water addition to give selected moisture content (50% saturation) 109
Table D- 6 Quartz aggregate – initial moisture content test record 110
Table D- 7 Quartz aggregate saturation moisture test record 111
Table D- 8 Particle size distribution of sand 112

Table D- 9 Quartz aggregate particle size distribution 113
Table D-10 Poured angle of repose - photographic record 114

Table E- 1 Quartz aggregate, internal friction sensitivity (ϕ_w = 28°) 116
Table E- 2 Quartz aggregate, wall friction sensitivity (δ= 47°) 116
Table E- 3 Dry sand, internal friction sensitivity..... 118
Table E- 4 Dry sand, wall friction sensitivity..... 118
Table E- 5 Moist sand, internal friction sensitivity..... 119
Table E- 6 Moist sand, wall friction sensitivity..... 119

Table G- 1 Test Set 2, 20-degrees, 120 mm, dry sand, bin filled..... 127
Table G- 2 Test Set 3, 20-degrees, 120 mm, dry sand, hopper filled 129
Table G- 3 Test Set 4, 20-degrees, 150 mm, dry sand, bin levelled full..... 131
Table G- 4 Set 5, 30-degrees, 150 mm, dry sand, hopper filled..... 133
Table G- 5 Test Set 6, 30-degrees, 120 mm, dry sand, bin levelled full..... 135
Table G- 6 Test Set 7, 30-degrees, 120 mm, dry sand, hopper filled 137
Table G- 7 Test Set 8, 20-degrees, 150 mm, dry sand, hopper filled 139
Table G- 8 Test Set 9, 20-degrees, 10 mm, Aggregate, hopper filled 141
Table G- 9 Test Set 10, 20-degrees, 120 mm, moist sand, hopper filled..... 144
Table G- 10 Test Set 11, 20-degrees, 120 mm, moist sand, hopper filled, PVC lined..... 145
Table G- 11 Set 12, Time response test. 20-degrees, 120 mm, moist sand, hopper filled, PVC lined..... 148

Nomenclature

Symbol	Description	Units
A_o	Area of hopper outlet	m^2
B	Hopper outlet width or diameter	m
c_c	Parameter for plane flow or axi-symmetric flow	-
c_{nf}	Jansen pressure reduction factor	-
d_c	Diameter of the circular bin section	m
D	Width of rectangular bin upper section	m
g	Acceleration due to gravity	m/s^2
h_b	Total effective head of stored solid	m
h_c	Height of material contacting bin vertical walls	m
h_h	Dimension from top of hopper to intersection of projections of sloped side walls	m
h_s	Effective surcharge head	m
H_s	Actual surcharge head	m
j	Hopper exponent	-
k	Lateral pressure ratio	-
k_h	Hopper parameter	-
k_{hi}	Hopper parameter – initial condition	-
k_{hf}	Hopper parameter – flow condition	-
L	Hopper outlet length	m
m	Symmetry parameter for plane flow hoppers	-
m_s	Surcharge parameter	-
M_{90}	Mass of withdrawn material with 90-degree repose angle	kg
M_{wd}	Mass of withdrawn material	kg
n	Vertical bin formula constant = 0.06	-
p_s	Surcharge pressure at transition from vertical bin to sloped hopper	kPa
p_n	Normal wall pressure at vertical bin section	kPa
p_{nh}	Normal wall pressure at sloped hopper wall section	kPa
p_{no}	Normal wall pressure at highest contact of material onto vertical wall	kPa
p_{ni}	Normal wall pressure on bin vertical walls in initial state	kPa
p_{nhi}	Normal wall pressure at sloped hopper wall section in initial state	kPa
p_{nhf}	Normal wall pressure at sloped hopper wall section in flow state	kPa

p_v	Vertical pressure in the vertical-wall section of the bin	kPa
p_{vh}	Vertical pressure in the hopper section	kPa
p_{vhf}	Vertical pressure in the hopper section in flow state	kPa
p_{vhi}	Vertical pressure in the hopper section in initial state	kPa
p_{vf}	Vertical pressure in the vertical bin section in flow state	kPa
p_{vi}	Vertical pressure in the vertical bin section in initial state	kPa
p_{vo}	Average vertical surcharge pressure at top position of material contact onto vertical wall	kPa
q	Non-dimensional surcharge factor	-
r	Radius of cone developed by material at repose angle	m
r_c	Hydraulic radius	m
V	Load onto feeder	kN
V	Measured voltage	V
V_{90}	Volume of withdrawn material with 90-degree repose angle	m^3
V_c	Volume of corner cones composite	m^3
V_r	Volume of rectangular prism	m^3
V_t	Volume of triangular prism composite	m^3
V_w	Volume of all withdrawn material	m^3
y	Height of material contact on the vertical bin side wall, measured from the top position of contact	m
z_g	Hopper height from top to outlet	m
z_h	Distance from top of hopper to position of interest	m
α	Hopper half-angle	degrees
α	Compressibility coefficient	-
γ	Bulk specific weight (the product of ρ and g)	N/m^3
δ	Effective angle of internal friction	radians
η	Angle between major consolidation stress vector and normal of the wall	degrees
μ	Coefficient of wall friction	-
ρ	Bulk density	kg/m^3
ρ_{loose}	Loose poured bulk density	kg/m^3
$\rho_{compact}$	Tapped bulk density	kg/m^3
σ_1	Major principal stress	kPa
σ_2	Minor principal stress	kPa
ϕ_w	Wall friction angle	degrees
ϕ_r	Repose angle	degrees

Chapter 1 Introduction and Background

1.1 Summary of Chapter 1

Chapter 1 consists of the background, problem statement, research question.

1.2 Research Background/Context

In the field of Bulk Materials Handling, the structural design of bulk storage bins, hoppers, silos, or stockpiles requires accurate analysis of the pressures induced by the stored material. This analysis is also significant for the design and sizing of the feeder equipment that controls the discharge of material from these facilities.

The calculation of material-induced pressures is fairly complex, resulting from the nature of bulk solids which, unlike fluids, can maintain a certain amount of internal shear force without any shear motion. Variables that directly affect the flow of materials include bulk density, bulk compressibility, wall friction, internal friction, consolidation pressure and cohesive effects. These variables are affected by a number of material parameters including the material type, particle shape, surface roughness, size distribution, moisture content, etc. Additionally, the bulk material flow properties do not remain as constants in a particular application because they are affected by applied consolidation pressure and also other parameters such as dwell time.

Many analytical methods are available for predicting pressures within storage equipment such as silos, bins, or stockpiles, and have been developed from empirical methods. Accurate prediction of flow properties requires the bulk material to be comprehensively tested under a range of consolidation pressures and differing moisture levels in order to arrive at a set of data that are appropriate for design calculations.

1.2.1 Initial and flow stress conditions

When a bulk solid storage system, for example a silo, is loaded with material from an empty condition, the material is gradually loaded on top of the material already in place. As a result, the weight of each particle resolves directly downwards. Lateral forces on silo walls also develop as far as is required to restrain the material from lateral movement, but the direction of the major principal stress field is essentially, vertically downwards. This results in a high

pressure on the bottom surfaces of the silo (including any feeders which are used to control the flow of material from the silo). This stress condition is typically referred to as a 'peaked' or 'active' stress field because the major principal stress is vertical over the full height of the silo and reaches its maximum at the bottom of the hopper section as shown in Figure 1-1(a).

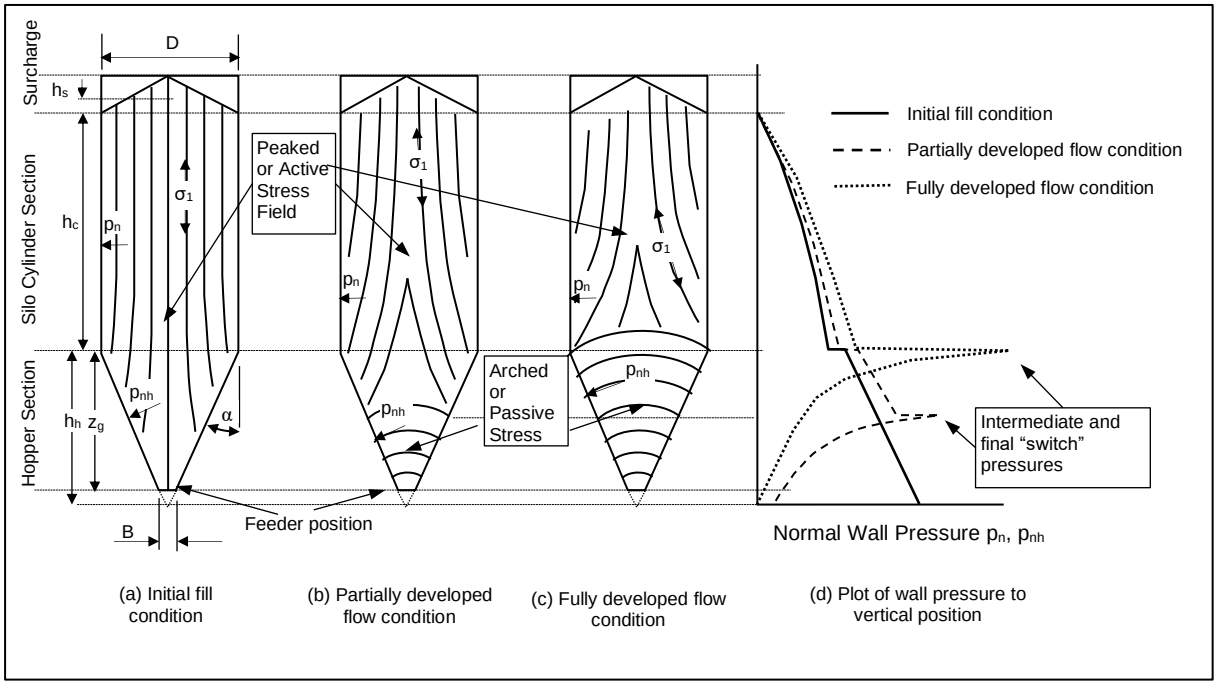


Figure 1-1 Silo principal stress (σ1) fields and normal wall pressures (p_n) based on Roberts [4]

When the bottom opening in the silo is opened (i.e. the feeder is operational) and a small amount of material is allowed to flow out, the flow of material downwards in the bottom zone begins to re-orient the particles such that the loads can resolve laterally to a greater degree and the new direction of the stress field becomes close to normal against the hopper walls. This induces an altered stress field shaped like an arch above the hopper's bottom opening, which is, therefore, known as an 'arched' or 'passive' stress field. This arched stress field directs the vertical component of the weight onto the hopper walls instead of these being resolved vertically onto the bottom of the hopper. As a result, the vertical pressure on the hopper's bottom section is reduced from a high, almost hydrostatic pressure to a substantially lower pressure. Initially, the arched stress field develops close to the bottom of the hopper, and as additional material is withdrawn, the arch expands upwards until it reaches the junction between the hopper and the silo's vertical wall by which time the flow pattern is fully developed (see Figure 1-1(b) and Figure 1-1 (c)). An arched stress field may also be partially developed if, instead of drawing material out of the hopper, the feeder located at the bottom of the hopper is lowered. This requires that some flexibility is built into the system

where the feeder is located, or a mechanism is included to allow the feeder to be manually lowered.

In the arched stress condition, a high magnitude normal pressure is present at the junction between the silo's vertical section and hopper. This pressure, termed the 'Switch Pressure' is the result of the arch over the hopper directing the weight of the material above the arch against the sloped walls of the hopper with a large horizontal force component. At positions below the junction the hopper wall pressure reduces, initially rapidly and then at a more gradual rate. In this manner the arch partially supports the weight of the material above it. If the arch has sufficient strength to carry the full weight of material above, further material cannot be withdrawn, and the hopper becomes blocked. If the arch has less than this required strength, it reduces the pressure applied to the feeder but not all the way to zero. Within the arch portion, the pressure applied onto the hopper wall continues to tend lower towards the intersection of the hopper planes and, at this position the calculated theoretical pressure on the hopper walls tends toward zero. The pressure curves of the switch pressure can be seen in Figure 1-1 (d), as well as the reduction in pressure in the hopper section as material flows towards the outlet.

After this re-orientation of the stress field, the original vertical stress field cannot be re-established unless the silo is emptied and then refilled from empty and the new stress field remains in place regardless of whether the material is in motion or stationary. The result of this is that when pressures on a feeder underneath the silo are reduced due to the initial flow, they do not rise again provided sufficient material remains in place to maintain an arch over the bottom opening. In this instance, the pressure configuration remains as shown in the hopper portion of Figure 1-1 (c).

1.3 Industrial Application

In a typical industrial application, a gravity reclaim system will make use of a feeder located underneath the bin, hopper, silo, or stockpile. Feeders may take several forms including belt feeders, apron feeders or vibrating pan feeders. In all cases, the feeder is intended to maintain a controlled reclaim rate of the material through an opening at the bottom end of the storage facility.

With material flow properties determined from laboratory testing, the hopper opening should be a minimum width as calculated to avoid material bridging over the opening (thereby preventing discharge), and also to ensure a sufficient 'live' volume percentage (this being the percentage of the stockpile that successfully flows down into the hopper opening) as opposed to the portion remaining on the sides of the stockpile, silo of bin as 'dead' volume (the volume of material that cannot be reclaimed by gravity means alone).

It is also possible to calculate the geometry required for reliable flow over the desired flow regime, for example 'mass-flow' (in which all material is in continuous motion during flow) or 'funnel flow' (in which a central column flows downwards after which adjacent static material slides diagonally down into the central column). These calculations will also determine the wall pressures and pressures on mechanical feeders.

The feeder mechanical components firstly, are selected so as to have sufficient strength for the maximum possible loads experienced by the feeder under all possible loading conditions. Secondly, the feeder must deliver the required volumetric flow rate out of the silo. During normal operation, the feeder operates in the flow condition, but that condition is only present after the feeder has started and has withdrawn sufficient material out of the hopper to transition the stress fields. The flow condition persists provided the bin does not empty to below the transition from the cylindrical section to the hopper section of the silo. In the initial condition (when the peaked stress field is present), after the bin has been loaded but no material has yet been drawn out of the silo, the maximum pressure is present at the feeder location. This can be a very significant load, in the order of 2 to 10 times the load in the flow condition (when the arched stress field is established). The ruling theory of the above is summarised by Roberts [4]. Sizing the feeder motor and mechanical components for this initial case leads to the feeder being significantly over-designed compared to the normal operational condition.

The loads on the feeder systems are normally relieved somewhat due to some flexibility of the feeder mechanical components, or from some particle re-orientation occurring during compression of the bulk material that occurs during initial loading, but the degree to which this will occur is typically unknown. Therefore, various empirical 'rules-of thumb' have been developed in order to present a reasonable basis for selecting a lower starting pressure condition than that indicated in the bin wall load calculations. However, there is not a clear methodology for designers to apply and, therefore, the industry tends to default up to a load

estimation significantly higher than actually required because of concern of under-specifying the system. Typically, in industry, feeders are selected at a factor of two to three times stronger than are required on the basis of the actual loads that would occur. These over-estimations are often made for very large feeder systems, and the outcome is the very large costs associated with the feeder. Furthermore, project owners typically do not record the actual loads or motor start-up currents after systems have been commissioned. Therefore, the industry often does not receive valuable feedback relating to the actual loads on these components. This lack of information tends to perpetuate the cycle of over-design in bulk solids feeders.

Designers tend to design some mechanical flexibility into the feeder arrangement, such that the pressures applied cause the feeder to deflect downwards and relieve the pressure somewhat by starting the transition to the arched state. These measures improve the probability of a lower initial start-up load, but as there is no clear method to relate displacement of the feeder to reduced initial loads, feeders are often designed to the maximum theoretical load in any case, and the flexibility is used as an 'extra design margin' rather than a main input into the design.

1.4 Research Motivation

There is a need to better understand the reduction in pressure on a feeder resulting from the initial withdrawal of material, and the factors that affect this process so that the industry-wide problem of over-design of bulk material feeders can be addressed. If it is possible to more accurately predict the reduced pressure on the feeder as a function of the volume of material withdrawn during the first small displacement of material (due to designed flexibility, for example), a significant reduction in feeder costs may be achieved.

1.5 Problem Statement

It is well known in the materials handling industry that when the first flow starts to occur from a silo, the pressures in the region of the exit decrease rapidly, from the initial condition to the flow condition. Also it is accepted that it only requires a relatively small amount of material withdrawal to observe a major reduction in pressure, as can be seen in Figure 1-1 (d).

Despite this, there is a shortage of reference information available to be used as a design guideline for the design of large feeders. As a result, large expensive feeders are often substantially over-designed in order to eliminate the risk of the feeder failing to initiate flow of material in the initial load condition (if a feeder fails to start, the overall operation can be subjected to costly delays and production losses). Therefore, the opportunity to reduce the sizing of a feeder system by taking advantage of the system's flexibility, is often not realised.. Also, the opportunity of designing in additional flexibility (for example by the use of mounting springs, hydraulics, or screw assemblies for the feeder) is often not taken advantage of, even though these may reduce initial feeder loads by a significant factor.

Whether the first portion of material is withdrawn from the hopper by action of starting the feeder, by lowering the feeder by deliberate effort, or by mechanical flexibility, the effect on the hopper stress condition is the same. In all instances the initial downward flow of material in the hopper re-orients the particles, thereby forming the arch which relieves the vertical pressure on the feeder at the bottom of the hopper.

It is not documented what form of mathematical function would relate the displacement of material to the force reduction. It is expected not to be linear, but rather to show rapid reduction with the first onset of flow, tending towards a more gradual rate of reduction as the remainder of the required volume is withdrawn until the arched stress field is fully established.

1.6 Hypothesis

It is well established that a significant pressure reduction will occur on a feeder located below a mass flow hopper when the feeder is lowered appropriately, so as to result in a re-orientation of material in the hopper and a change in stress state from active (peaked) to passive (arched).

The hypothesis is that significant reductions in pressure may be achieved by lowering the feeder by a small dimension compared to the system dimensions (millimetres, but certainly less than 5% of hopper opening width)

This research aims to gain insight into the relationship between the vertical pressure on a flat base at the bottom of a mass flow hopper and the vertical displacement of the material at that

position. The vertical displacement of the flat baseplate simulates the withdrawal of material from the hopper by a mass flow feeder.

Because several variables are known to affect the initial and final load states, it is inferred that these variables will also affect the pressure transition behaviour from active to passive conditions. In order to evaluate the effects of these variables, several of the parameters will be adjusted independently so as to isolate the effect of each one. The variables that are considered as likely to influence the change in stress pattern are the following:

- Hopper / bin geometry, including,
    - Ratio of hopper width to bottom opening width
    - Hopper half-angle
    - Loading configuration (only hopper loaded, or bin above also loaded, potentially also with a surcharge pile on top)
- Friction angle between bulk solid and hopper wall material or liner
- Internal friction angle of the bulk solid sliding on additional bulk solid material
- Particle size
- Particle shape
- The degree of cohesiveness of material (free flowing or presenting internal cohesive strength after application of a consolidating pressure).

1.7 Research Questions

1. Is it possible to achieve a significant pressure reduction on the feeder in a mass flow hopper (at least 80% of the difference between initial and flow pressures) by drawing down material or manually lowering the feeder by 5% of opening width or less?
2. Which variables among particle size, hopper half-angle, opening width, internal friction and wall friction play a dominant role in how rapidly the pressure is reduced?

1.8 Objectives

1. Develop a scale model plane flow storage bin with parameters adjustable including bin wall angle, and outlet opening width. The model design requirements include a flat plate underneath the outlet with the functionality for lowering in a controlled way and measuring the vertical load using loadcells.

2. Assess the relationship between feeder pressure and plate deflection using building sand (dry and wet state) and 13 mm aggregate (dry state) with the following variables:

    - Hopper half-angle 20-degrees and 30-degrees
    - Hopper outlet width 120 mm and 150 mm
    - Bin filled to top level of vertical portion of bin
    - Bin filled to top of sloped hopper portion only
    - Hopper lined with PVC sheeting for comparison of wall friction angle.

Chapter 2 Literature Review

2.1 Introduction

This section will review some of the theoretical basis for understanding the manner in which loads and stress fields develop in bins and hoppers for the initial filling and the flow conditions. It also considers how these relate to the loads onto the gate or feeder at the bin outlet.

Thereafter, a review of previous research is presented in relation to methodologies available to calculate the loads quantitatively, and to provide understanding of the qualitative behaviours inside a bin and hopper. A summary is then provided of published reports and guidelines developed from industrial experience covering aspects of feeder start-up load management methods.

Finally, a discussion is presented on previous investigation performed using numerical analysis (discrete element method, referred to as DEM). This provides some insight into the topic of the current research in that the method uses direct simulation of movement of particles in a bed. The scope of application was seen to be limited due to aspects relating to material characterising for DEM and validation against operational cases. It is however, of interest for comparative purposes.

2.2 Theoretical Analysis

A large portion of the body of knowledge used to perform material properties evaluation and analysis of pressures and flow of bulk solids in containers is based on the works of Janssen [1] and Jenike [2].

Developing largely from the theoretical basis of [1] and [2], and supplemented by various other pieces of subsequent research, the Australian Standard AS3774-1996 [12] was developed, which defines the required methodology to calculate the loads on bulk solids containers such as bins and silos, and also includes loads on gates and feeders. It is a statutory code in Australia and it also provides methodologies for consideration of the effects of material momentum induced compaction inside a container. The method presented by Roberts [5] and [6] uses a similar theoretical calculation but with different nomenclature and calculation forms to those used in [12].

The methods developed by Roberts and [6] for calculation of bin wall pressures and feeder loads together with that of Arnold et al [7] which expands on the feeder loads calculation methodologies, have been widely used and are considered reliable for the analysis of feeder loads. These methods provide an estimate of loads for the initial and flow conditions but do not provide guidance with regard to the material displacement required in order to effect the transition from the one load case to the other.

Roberts [6] does, however, provide a method by which to consider the flexibility of the feeder, by using the hopper exponent, 'j'. This is a dimensionless parameter which can have values of between 0.0 and 1.0, where 0.0 is for an infinitely rigid feeder operating underneath a bed of totally incompressible bulk material, and 1.0 is for a highly compressible material, and a feeder with significant flexibility. Practical values of between 0.1 and 0.9 are suggested, but no meaningful method is presented by which to quantitatively select this value. Industry typically defaults to a value of between 0.25 and 0.4. The same variable j may have higher values than 1.0 when the system is in the passive state after the onset of flow, and the methodologies to calculate the flow condition determine j based on the material properties and the system geometry.

Within the analysis of [6], the graphical presentations of the stress fields in the bottom bin areas, slightly above the feeder, show a zone that does not reach the theoretically calculated maximum initial pressures. This is supported by equations for calculating feeder start-up load, which include consideration of limitations to pressures at the outlet. A discussion is presented that notes various unavoidable features present at the outlet including inherent flexibilities in the feeder, clearances at the outlet, as well as the effects of compressibility. These load-reducing edge effects are also expected to present in the current research, in terms of some loads not matching with calculated initial and flow loads.

Because this method was the basis of comparative calculations in the present research, a summary of the ruling equations from Roberts [5], [6], and portions of the derivation thereof, are presented in Appendix A.

Jenike and Johanson [3] presented a summary of methodologies to calculate bin wall loads and included a presentation of how the switch pressures develop and propagate upward in the hopper and bin, while increasing in magnitude up to the cylinder-hopper transition for mass flow bins, and also above the transition for funnel flow bins which experience a switch

pressure at an effective transition location. Also included in [3], is an assessment of how material compressibility has the effect of reducing the initial pressure at the bottom of a hopper. This was done by defining a coefficient of compressibility 'α'. This coefficient is useful in determining the position and magnitude of the switch pressure in a mass flow hopper. The analysis does not, however, include an assessment of the load onto the feeder as a function of the coefficient of compressibility. It also does not estimate the volume of material to withdraw in order to complete the transition of the pressure state. The current research has not attempted to develop or define these relationships, but does consider that the effects of compressibility are expected to significantly affect both the initial pressure (reducing it) and the load behaviour during withdrawal (results to be observed from results in the current research).

Roberts [4] presents the methodologies used for characterisation of bulk solids. This includes compressibility, internal friction angles, wall friction angles, and cohesive material behaviours. Also included is a basis for evaluating the minimum requirements to ensure reliable mass flow as:

- Avoidance of mechanical arching, which requires a minimum opening width of four times maximum lump size.
- Avoidance of cohesive arching, which is a function of bin geometry as well as material properties of friction, density, and cohesive properties.
- Ensuring mass flow in the hopper, as opposed to funnel flow (a function of geometry and flow properties).

Internal flow angle and wall friction angles of bulk materials are a result of the combined effect of several parameters noted by Roberts [4] and listed in

Table 2-1.

Table 2-1 Parameters affecting friction properties

Bulk Solid Characteristics	Wall Surface Characteristics	Loading and Environmental Characteristics
Particle size and distribution	Surface Roughness	Normal pressure of bulk material onto wall surface
Particle shape	Hardness	Relative sliding velocity
Particle hardness	Chemical Composition	Temperature and humidity conditions
Particle density		Vibrations on the container
Moisture content		
Chemistry characteristics on surface		
Temperature		
Time in storage, undisturbed		

Jenike [2] noted that effective internal friction of solids have been measured in the range of 30° to 70° for various materials, and that in general fine and dry materials display low angles of effective internal friction, whereas coarse and wet materials display higher angles. In this context the moisture effects are largely related to cohesion of small size fractions (below 4 mm and dominated by portions smaller than 250 μm), whereas for coarse materials it relates to friction between lumps where there is not a significant effect of fines residing in-between lumps, which typically represent the failure planes for materials sets containing mixed lumps and fines content.

2.3 Experimental and Theoretical Investigations

Holmes [8] performed a laboratory-scale experimental programme to compare start-up and running loads on conveyor belt feeders as calculated by several analytical and empirical methods. The test apparatus was designed as a scale model of an existing belt feeder installation but the dimensions of the test apparatus (hopper bottom opening of 600 mm long by 200 mm wide) were sufficiently large that boundary effects at the hopper outlet did not substantially affect the measured values. This was seen from the relatively close correlation between the loads as calculated by some theoretical methods, with the method of Arnold [7] giving the closest predictions.

Although the data and analysis presented in Holmes' study are relevant in terms of the cases before and after commencement of flow, no data was collected relating to the displacement of material required to re-orient the stress fields.

Roberts et al [9] performed an experimental investigation into the loads onto a laboratory-scale rail load-out bin model as typically used for iron ore or coal products. This investigation suggested that initial loads are likely to correlate with values calculated for highly compressible materials and that the loads are likely to be significantly lower than the values typically selected as per the method following the Australian code. The results suggested that a value of j=1.8 was appropriate, whereas Roberts, [4] and Standards Australia [12] suggest a maximum value of j=0.9, even for flexibly supported feeders and highly compressible materials.

This is significant because the test rig used by Roberts et al [9] intended to mimic a rigidly supported gate with low compressibility material which would traditionally be expected to match a value of j that was within the range of 0.1-0.45, whereas the behaviour of the system demonstrated a significantly higher value for j.

Guo [10] performed an experimental study relating to the pull-out tensions of belt feeders, also considering the pattern of pressures on the outlet. This study gave insight into the behaviour of the hopper-feeder interface, considering the effects of the material arching above the feeder interface. It presented a phenomenon whereby material at the outlet of the hopper located underneath the passive stress field arch, and which is not supported by cohesive forces, continues to apply a load onto the feeder underneath even when a stable arch is present inside the material bed. The application to the current research is that a partially supportive (but not cohesively stable) arched stress field at the outlet of a hopper may be unable to provide support to material at the lower extents of the hopper, and loads at the outlet may be higher than expected in the flow condition. This assisted understanding of an increasing load at the outlet after full development of the flow condition

2.4 Industry Experience

The presentation by Leech [13] described initial and flow loads as measured from a large coal storage bin belt feeder, and demonstrated how these were significantly lower than the loads used in the calculation. This provided an example of how large belt feeders are frequently over-sized for loads, because of a lack of accuracy in theoretical models. The two feeders considered were over-sized by a factor of between 2.4 and 2.7 for the flow condition, and between 3.3 and 4.4 for the initial fill condition. This over-estimation in especially the initial case and which was used for equipment mechanical design, is an example of the failure to

consider the partial transition between the initial and flow case that tends to take place as a result of flexibility of the feeder and compressibility of the bulk solid. The loads used for design in the cases presented by Leech [13] and Roberts [11] were all based on initial conditions, with no account taken of the possibility to reduce loads based on the principle of feeder flexibility.

It is worth noting that the calculations used by Leech [13] used a value of 0.25 for j as described by Roberts [6]. From the comparison to the actual initial loads encountered by Leech [13] it is apparent that the calculation should have been made with a value for j greater than 0.25 and which coincides with lower design loads.

2.5 Practical Design Recommendations

McGee and Bates [14] made reference to design considerations for feeder loads and included in the recommendations that several options were available to designers, including mounting the feeder on a flexible arrangement or allowing the feeder to be manually lowered before starting. No method was presented to quantify the recommended flexibility or displacement, and no method was suggested to estimate the reduced force. Therefore, although these were useful recommendations, they could not be practically incorporated into a design guideline because the required deflection, as well as the degree of force reduction, was not defined. Therefore, designing to a lower force would present a significant risk in terms of possibly under-sizing equipment or structures. This was because the consequence of under-specifying the load would carry the risk of structural failure or failure to perform the feeding duty. For this reason, large size mineral feeders have frequently been overdesigned by a substantial margin, which remains a common practice.

2.6 Numerical Analysis (by DEM simulation) and Comparison to Analytical Methods

Hose [15] presented an analysis of an industry-scale feeder hopper at Richards Bay Coal Terminal, which was added as a portion of the Phase V Expansion Project. The material pressures and loads were calculated analytically for the initial and running cases of the belt feeder operation. These calculated loads compared very well to the actual loads measured during the belt feeder commissioning. However, a relationship between displacement and load during the *transition* from initial to flow condition was not calculated analytically

(especially in the absence of a method to calculate this). Also, this data was not recorded during the field commissioning. However, a Discrete Element Modelling (DEM) exercise presented some information relating to the initiation of flow. The intention of the DEM analysis was to compare the feeder loads before and after initiation of flow. Some reasonable agreement was found to exist between the loads calculated through the DEM method and the loads identified analytically and experimentally. This would possibly suggest a reasonable match between the displacement of material required, as calculated by DEM, against the loads actually encountered in a real-world application.

The time response of loads as a function of flow on the belt feeder, and therefore as a function of displacement through the hopper, was presented by Hose in [16] as a set of further data following on from [15].

Using the data presented by the DEM analysis, it was apparent that the calculated maximum belt pull-out tension occurred after a material displacement of approximately 1.8% of the hopper opening width. A notable reduction in load to approximately 80% of the initial load condition took place after a displacement of approximately 10% of opening width. A steady state load condition, which would correlate approximately with the flow condition in mass flow hoppers, was seen to have been established after a displacement of approximately 35% of opening width.

Relevant parameters of this system described by Hose in [15][16] were an opening width of 1000 mm, clean export coal with size of 95 percent passing a 50 mm mesh, moisture content of up to 20% and bulk density from 700 to 800 kg/m^3. These properties correlate with typical expectation of a material with moderately high properties of cohesiveness and compressibility.

It is noted specifically that these simulated data were not validated against practice in any way and, therefore, are only of general comparative interest. An additional consideration is that the DEM analysis uses significantly larger particle size than any practical fines-containing material and therefore the effects of contained fines cannot be incorporated into a DEM model. It has been noted by numerous DEM-focused design presentations and also in work by software developers that it is feasible to determine loads from bulk solids in packed beds. This is, however, not a fully refined process yet and there are multiple DEM software suppliers who have each developed their models based on different mathematical and

solution methods. Evaluation of the development of the switch pressure in a bin or hopper can likely be performed successfully with appropriately set up DEM models. This may be a field for subsequent research. However, the current study was focused on the traditionally used analytical methods as well as measured data.

2.7 Summary of literature review

Although there is significant research available to described the load states prior to the onset of flow, and after fully establishing flow, there is relatively limited research available to indicate how much material removal is required to establish this shift, either in whole or in part. On occasions where completed research included some limited information about the volumes of material that were withdrawn, this was not the primary research focus of the research and was not reported thoroughly in the resulting literature

Industry experience generally aligns with the expectation that the transition is rapid, requiring only a small amount of material to be withdrawn, in comparison to the overall capacity of the bin system.

The literature that is available to describe the process of *transition* from the initial fill (peaked stress field) to the flow condition (arched stress field) describes the progression of the loads and how the stress fields re-orient. They do not however present any quantitative analysis into how much movement of material is required to achieve this, or the shape of the deflection-force curve that results, or what parameters of the system have which effects.

Chapter 3 Experimentation

3.1 Introduction

To provide insight into the behaviour of the pressures at the bottom of a mass flow hopper, and to demonstrate the effects of different materials and geometric configurations, a laboratory-scale test rig was constructed and used to perform appropriate measurements.

This chapter describes the design and calibration of the test rig, the properties of the materials tested and the testing procedures.

The methods of processing the data are also described.

3.2 Test Rig

3.2.1 Design Basis

A laboratory-scale test rig was manufactured which mimics typical industry installations of mass flow hoppers using the 'plane flow' type of arrangement. Plane flow was selected in this case because most large feeders use this arrangement. Additionally, measured data from a test rig using this arrangement was likely to be more precise and repeatable than would be expected for an axi-symmetrical type hopper due to the two-dimensional material flow.

The plane flow hopper also allowed practical utilisation of hopper walls with less-steep angles than would be the case for an axi-symmetrical hopper.

The test rig included a flat plate underneath the hopper opening supported by two loadcells which allowed measurement of the vertical force of the material in the hopper opening. The loadcells were loaded in tension and fitted with a threaded rod underneath each loadcell which were used for lowering the flat plate when the hopper was full. The width of the flat plate was such that it could hold a sufficient volume of material drawn out of the hopper to ensure complete transition from initial to flow loading state. One end plate of the rig was made from Perspex allowing insight into movements of materials inside the hopper.

3.2.2 Material pressures and strength design of the test rig

Due to the small dimensions compared to typical industry-sized installations, there was an expectation of some precision loss due to edge-effects (clearances, and material effects with

corners and valleys) and low-pressure conditions (which have the potential to not suitably capture effects of cohesive properties). Although many of the phenomena present in large-scale installations do display their effects in low pressure conditions, it was preferable for initial pressures to be in the range of several kPa, which is typically where most materials begin to show the effects of cohesive properties[1].

The design intended that test pressures be as high as practicable for the small scale of the test rig. As an example, high density bulk materials such as iron ore or chrome ore (with densities in the range of 2700 to 3000 k/m^3) are preferable to low density bulk materials such as potash or coal (which have densities in the range of 900-1200 kg/m^3), because they are more likely to achieve sufficient pressures to demonstrate the effects of cohesion.

The test rig design was of sufficient strength to handle test samples with bulk densities in the range of 3000 kg/m^3 to allow for future testing of mineral ores (this equates to a maximum working load rating of 800 N per loadcell). In terms of load sensitivity, the loadcells were selected so as to allow an accurate load reading in a working range of 20 N to 1000 N. This selection allows for both low- and high-density ores also to be tested in future.

Although the strength design is appropriate, and the loadcell instrumentation is selected to be accurate in the associated load range, it is possible that the experimental accuracy when testing light ores may be lower than for denser ores. Potential future tests with light ores and loads should include an assessment of the experimental measurement uncertainties related to such testing. In general principle, however, the equipment including the loadcells was designed with an accuracy suitable for such experimentation.

The above relates only to the design of the experimental equipment whereas the current research was limited to sand and stone materials with testing densities in the range of 1200-1600 kg/m^3.

The design of plates and stiffeners was performed to provide sufficient strength to maintain deflection of less than 1/500th of the span, measured in the direction of the angles used for

[1] The author's preference to encounter several kPa of pressure in the test rig in order to demonstrate cohesive behaviours is based on the author's personal experience of analysing bulk ore flow properties reports and handling system designs. No published design guideline is available which requires such pressures.

stiffening, and calculated on the basis of maximum expected test material density. This resulted in a bin that may be considered a high rigidity bin, thereby minimising possible deflection of the structure which could affect load measurements.

A schematic of the test rig is shown in Figure 3-1 and the manufacturing drawings are included in Appendix H

The design of the rig was such that geometries of the bin could be adjusted in terms of the bottom opening width and the slope angle of the side plates. This was achieved by means of two sets of mounting bolt holes on the front and back plates to facilitate installation of the front and back plates in the ‘high position’ or in the ‘low position’.

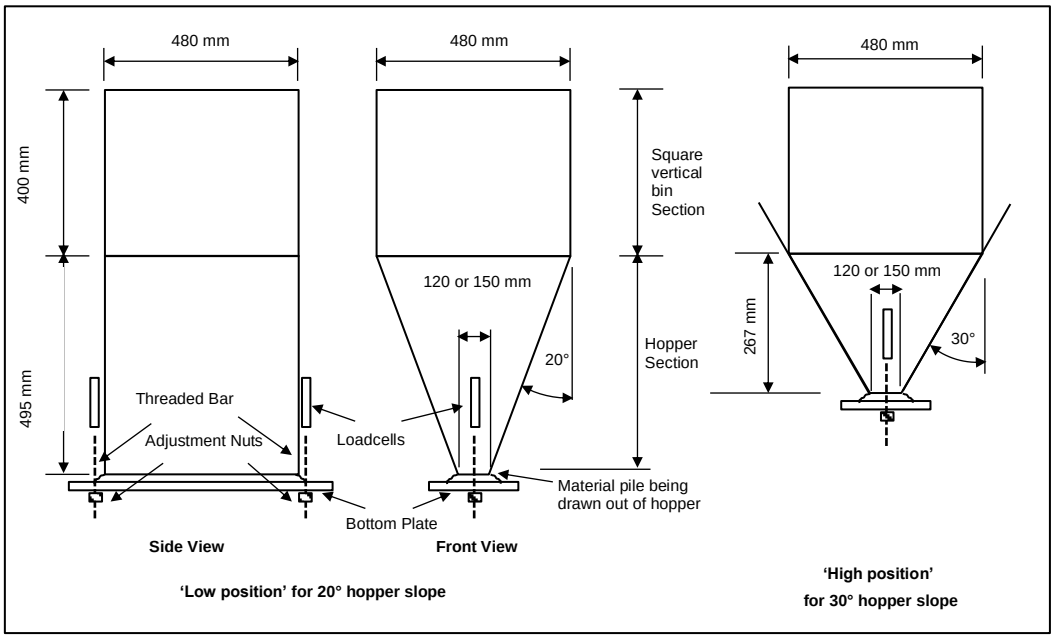


Figure 3-1 Schematic of test rig with two hopper angle configurations and two opening widths

Photographs of the test rig assembled in ‘low position’ (20° hopper), and during a test, are shown in Figure 3-2



(a) **(b)**

Figure 3-2 Test rig, (a) assembled, and (b) during a test (dry sand)

The assembly installed in 'high position' is shown in Figure 3-3.



Figure 3-3 'High position' installation, indicating setup angle measurements

The test rig included a flat plate underneath the hopper opening supported by two loadcells which allowed measurement of the vertical force of the material in the hopper opening. The loadcells were loaded in tension and fitted with a screwed rod underneath each loadcell. As the plate was lowered by turning the screws with the hopper full, the pressure on the plate was measured incrementally.

The width of the flat plate was such that it could hold material withdrawn from the hopper while the plate was lowered a sufficient distance to demonstrate stabilised hopper pressures, which coincided with a completed transition between initial and flow pressure regimes. The width of the plate was sufficient to accommodate usage varied hopper opening widths. The plate is used to mimic a discharge feeder and is termed a ‘feeder plate’.

3.2.3 Variations in configuration

The test rig allowed for variations in the configuration as follows:

- Opening width – nominally 120 mm to 150 mm, adjustable by using slotted holes at the bottom connection of the side walls to end walls.
- Wall slope angle – nominally 30-degrees from vertical and 20-degrees from vertical, adjustable by unbolting the front and back plates and installing them either in a ‘high position’ corresponding to 30-degrees, or a ‘low position’ corresponding to 20-degrees.
- Material surface of hopper – either mill scale mild steel or lined with PVC sheeting (to give higher wall friction coefficient)
- Material fill height could be varied as desired and can be either of:
    - Filled to hopper level (at the position where the sloped walls meet the vertical walls)
    - Filled to top of vertical bin level (taken as 50 mm below top, to allow freeboard and avoid spillage). ‘Freeboard’ here refers to an empty, unused portion of the available height of a container, to provide for practical usage and avoidance of spillage.
    - Filled to top of vertical bin level with added surcharge pile on top of vertical bin level.

The practicality of the system design and construction was such that test dimensions were not exactly on 150 mm /120 mm opening and 30°/20° slope. The configurations are as listed in Table 3-1.

Table 3-1 - Nominal vs. Actual hopper dimensions

Nominal dimensions		**Measured dimensions**		**Actual dimensions (average)**	
Opening (mm)	Angle (°)	Opening (mm) North / Mid / South	Angle (°) West / East	Opening (mm)	Angle (°)
150	20	145 / 145 / 148	17.6 / 19.0	146	18.3
150	30	140 / 140 / 140	27.4 / 28.5	140	28.0
120	20	120 / 121 / 120	18.7 / 20.2	120.3	19.4
120	30	120 / 120 / 119	28.7 / 29.8	119.7	29.2

In all analyses and calculations, the average measured dimensions listed in the right two columns were used. In discussion and graphing and for ease of discussion, these configurations are named according to the nominal dimensions.

3.2.4 Load cell design and calibration

The loadcell used was an S-type loadcell with load rating 100 kg. The calibration records, calculations, and datasheet are presented in Appendix C

The calibration formula for Loadcell 1 and Loadcell 2, along with R-squared value are:

Loadcell 1: Mass=24.739 x (Voltage) + 0.0532 (1)

R2 = 0.999 999 3

Loadcell 2: Mass=25.116 x (Voltage) - 0.323 (2)

R2 = 0.999 988

From observing the calibration curves of the two loadcells together, it was apparent that the errors of the two loadcells offset each other resulting in the overall system being more accurate than either individual loadcell in terms of conversion from recorded volts to measured load.

Uncertainty of load readings for the overall system, in the load range of interest to the present research is 0.2%. This uncertainty was considered sufficiently to not carry through to data

processing and analysis. The loads calculated from recorded volts were used as measured loads.

3.3 Material Properties

3.3.1 Selected materials and parameters to consider

Three material sets were identified and characterised for the purposes of the testing. The intention in using the different materials was to gain some insight into the effects of the varying material properties. The following three material sets were chosen:

- 13 mm quartz aggregate – dry
- 8 mm river sand (as used for fine concrete aggregate) – dry
- 8 mm river sand (as used for fine concrete aggregate) – moist

A set of tests was performed on each material set to appropriately select and define the material sets. The following tests were performed, and the results are listed Appendix D:

- **Bulk density, loose poured**
  Placed carefully in the test bucket to measure minimum uncompacted density.
- **Bulk density, tapped**
  Compacted in the test bucket by tapping to achieve consolidation, this denotes the maximum density.
- **Particle size distribution**
  By screening with square aperture wire sieves, agitated mechanically, the mass fraction of the portion passing each sieve size is defined.
- **As received moisture percentage**
  By weighing the received sample and thermally drying and then weighing the dried sample, the as-received moisture is defined.
- **Saturation moisture percentage**
  By submerging the thermally dried sample into water using a porous drainable cone container, then removing the sample and allowing it to drain to a stable moisture content, the remaining moisture content is defined as saturation moisture on a wet mass basis.
- **Poured angle of repose**
  The angle that a heap of carefully poured material makes relative to the horizontal, when

poured with a constant velocity from a low height. The angle is measured from a photograph taken on with a horizontal camera angle.

- **Inclined chute friction angle test**

  This method includes placing a retaining ring onto a sample of the selected wall material. The ring is filled with the bulk material sample and then consolidated with a defined load. Removing the test weight and observing the angle at which first movement commences, this provides insight into the relative angle of friction of the bulk material against the selected wall material sample. (This test does not directly measure wall friction angle)

3.3.2 Selection of moisture content for moist sand test cases

From the author's experience of various bulk solid handling testing projects, Maximum cohesive properties typically occur at moisture levels in the range of 50-60% relative to saturation moisture. From inspection of the moistened material, it was apparent that from 60% and higher relative moisture, the material could be difficult to work with due to adhesion to test equipment. It was apparent then that 60% was possibly more wet than would be ideal for practical experimental purposes. For this reason, the test moisture was selected as 50% which equates to 8.2% absolute moisture content, on a wet mass basis. The moist sand test sample was made up by adding the appropriate mass of water to a defined mass of dry material (containing only as-received moisture). The moist sand sample was thoroughly mixed in enclosed buckets to give the intended moisture.

3.3.3 Bulk density measured vs. selected values

To perform load calculations, it was necessary to determine an appropriate basis for bulk density in the test environment. This bulk density is by necessity greater than the loose poured bulk density, which is a lower limit that can't be practically encountered when applying larger loads in a test bin. The test bulk density also is by necessity lower than the tapped density which is an upper limit to density, already including significant mechanically induced compaction not present in a static (un-agitated) test environment in the test rig. The selection of the test bulk density requires a degree of assumption because it is not practical to directly measure actual bulk densities within the test rig.

The moist sand had a significantly lower loose poured bulk density than other materials tested in the study, owing to the friction and cohesion between particles which limits consolidation

under low pressures. The dry materials by contrast had higher loose poured bulk density but a lower percentage of compaction from loose poured to tapped.

The densities for the reference calculations were chosen based on 25% consolidation for the dry materials, and 50% consolidation for the moist product, on the basis that higher pressures would occur in the test bin than in the 5 litre bucket that was used for the density tests. Therefore by self-weight, the moist sand was assumed to compact to 50% of the difference between loose and tapped, whereas the dry materials were assumed to only compact to 25% of the difference, on the basis that minimal agitation was present to assist such compaction.

Bulk densities for use in calculation were therefore chosen as follows:
For dry material:

$$\rho = \rho_{loose} + 0.25 \cdot (\rho_{compact} - \rho_{loose}) \quad (3)$$

which can be rewritten as,

$$\rho = 0.75 \cdot \rho_{loose} + 0.5 \cdot (\rho_{compact}) \quad (4)$$

Similarly for moist material,

$$\rho = 0.5 \cdot \rho_{loose} + 0.5 \cdot (\rho_{compact}) \quad (5)$$

These densities correspond to bulk density consolidated 25%, and 50% respectively where ρ_{loose} is the loosely poured bulk density and $\rho_{compact}$ is the bulk density compacted by tapping.

The bulk density parameter calculated in this way was used for the analytical calculation of the initial and flow pressures (for comparison to measured loads), and for conversion of the measured load on loadcells (including material already drawn out from the bin) into a pressure parameter at the position of the hopper outlet.

The measured values and the selected values, as calculated using the methodology above are shown in Table 3-2**.**

Because of the assumptions made with respect to the degree of consolidation, a basis of uncertainty was developed with regards to the calculated mass of withdrawn material. This was evaluated together with approximate uncertainty on the actual angles of repose encountered during the testing activities. The related uncertainty was calculated on the basis possible densities ranging from loosely poured to tapped.

Table 3-2 - Measured and selected bulk density parameters

Material Properties	Units	Dry Sand	Moist Sand	Aggregate
Bulk Density (loose)	kg/m^3	1458	1171	1459
Bulk Density (tapped)	kg/m^3	1643	1593	1536
Bulk Density (25% consolidated)	kg/m^3	1504	-	1478
Bulk Density (50% consolidated)	kg/m^3	-	1382	-

3.3.4 Wall friction inclined chute test

Inclined chute tests were performed for moist sand on two surfaces - Steel and PVC sheet. This was to provide a basis of assumption for variation in friction properties between the two surfaces, and it demonstrated the relative higher wall friction of the PVC sheet lined wall material.

The inclined chute tests, although informative as a qualitative basis, are of limited use in determining the wall friction angle ϕ_w for a packed bed bin application because the physics of the test does not replicate the configuration of a packed bin. The test does, however, give a basis for the selection of one material having a higher or lower friction angle than others. As an example of the inclined chute test, see Table 3-4 below. Slope angles were noted as 38° for the PVC lined wall and 35° for the moist material on steel.



Figure 3-4 Inclined chute test of moist material on vinyl wall surface – slip at 38 degrees

3.3.5 Selected wall friction and internal friction angles

Shear cell testing of friction flow angles and wall friction angles was not performed due to the high cost of comprehensive testing and also limitations in laboratory resource availability at the time of the testing programme. Instead, historical properties of similar sand products

from various mine sites, including quartz and limestone sand were considered to select appropriate values to use in the calculation[2]. The following friction properties were selected:

δ = Effective Internal Friction Angle,
= 47 degrees for dry materials and
= 55 degrees for wet materials
ϕ_w = Wall friction angle,
= 28 degrees for dry sand and for dry aggregate on mill-scale mild steel
= 30-degrees for moist sand on mill-scale mild steel
= 32 degrees for moist sand on walls with PVC applied to the sloped walls

It was considered acceptable to select these typical comparative values for δ and ϕ_w instead of definitely measuring them, because the focus of the present research was not on the theoretical calculation but rather on how the measured initial and flow properties relate to each other as a function of feeder plate displacement.

3.4 Testing Procedures

In order to ensure repeatability and accuracy of the tests, the testing sequence for each test was as follows:

- Select a testing configuration (wall slope, opening width, loading configuration as hopper fill or entire bin full, and any desired hopper liming material) and test material set based on planned comparisons between chosen parameters of interest. Also, record other test variances for example whether the bin should be filled slowly/loosely or if it should be filled fast to cause momentum induced compressive effects)
- Ensure dimensional set-up is appropriate and recorded, including measurements of opening width (at each end and in the midpoint of the slot) and slope angle of each side hopper. The dimensions are set up as close as practical to 120 mm, 150 mm, 20-degrees, and 30-degrees hopper wall slope.
- Check the position of each loadcell to ensure consistent volt to mass recording.
- Clean the hopper outlet and feeder plate of dust and debris using a hand brush.

[2] The reference information used to select flow properties were based on test results obtained from the author's employer which the author considered similar to the material test samples used in the current research.

- Lift the gate plate up to the hopper and lightly tighten the adjustment nut on each loadcell threaded rod to give minimum clearance but no contact between the hopper and the feeder plate. Minimum clearance is required to ensure accurate initial pressures, but direct mechanical contact can tensions into the loadcell which leads to incorrect evaluation of tension from the material bed.
- Record the tare voltage on the loadcells and compare with the typical tare voltage to confirm that there is no mechanical induced tension on loadcells or remaining material on the plate. This tare value is used as the zero point for applied load from material.
- Fill the bin to the desired height, taking care to place material carefully into the bin by hand with a small trowel without allowing momentum transfer or compaction. Only after a bed depth of at least two hopper opening widths is in place over the opening may the rate of loading increase, after which time it must continue to be gently loaded until filled to the desired level.
    - When intending to investigate the momentum effects to the compaction and relieving effects, a large bucket of material (approximately 12 kg) is poured rapidly into the bin, within a duration of approximately one second, one bucket at a time, in order to achieve the desired momentum effects. No levelling of material is performed between buckets of material).
    - Any such action should also evaluate whether the impact load of a single lump falling onto the plate may create transient loads of 100 N or more per loadcell, which may overload the loadcell and potentially lead to damage/loss of calibration.
- With the bin filled to the desired level, record the volt readings on each loadcell.
- Initially, turn the adjustment nuts one eighth of a turn and record the new voltage.
- Record the reduced voltage immediately, as soon as is practical do so, preferably within approximately 20 seconds. It is apparent that after the initial reduction in voltage after the lowering, the voltage does not remain static but increases gradually as the particles settle into new orientation. It is not practical to wait several minutes for the pressures to stabilise fully prior to continuing the test procedure. The time between turning of the adjustment nut and the measurement of the voltage should be as short as is practical to do consistently so as to avoid differing periods of time which can result in significant changes or steps in the pressure trend.
- Repeat with a series of one eighth turns, recording after each turn until a full rotation of the nut is complete.

- If the rate of reduction in voltage per one eighth rotation is low after the completion of the first full rotation (approximately less than10% reduction in load from the seventh to the eighth), then the rate of rotation between load recordings can increase from one-eighth to quarter turns. If the rate of reduction is still more than approximately 10% per rotation, continue recording rotations on one eighth increments for another full rotation.
    - To allow ease of usage of the data, only perform the change to one quarter turns after a completion of a full rotation of one-eighth turns. If collecting with differing increments of nut rotation per test it becomes complicated to process the data for comparative purposes. It is practical to use a full rotation of eight $1/8^{th}$ turns, followed by at least eight quarter turns.
- Continue with quarter turns until the voltages stabilise again to less than 10% reduction per quarter-turn, then change to half turns, full turns, double turns, etc. until the pressure changes are not significant or when there is no sufficient height available due to material starting to spill off the feeder plate. At the first sign of material spilling off the feeder plate, end the data collection. The first voltage reading after material has spilled off is not valid and the prior reading is the last valid measurement.
- Ideally, all comparative test sets should use the same increments of rotation.
- When the data collection is complete, lower the plate to the point where the material can be emptied out into the buckets and then repeat the test.

Besides the standard test described above, an additional test is performed to observe the time effects of lowering the plate. During this test, the voltage is measured immediately after turning the nuts, and then recorded once per minute until the voltage stabilises noticeably to a variation of less than approximately 2 mV per minute. After the voltage has stabilised appropriately the nut is turned again to the next position. Besides the action of collecting the time response data after each turn, the remainder of this test procedure is the same as the standard test procedure listed above.

3.5 Selection of tests to perform to isolate relevant tests

Due to the large number of variables considered, it was not feasible to test all combinations of variables as listed below:

- Bin wall angle – 2 parameters (20-degrees / 30-degrees)
- Bin opening width – 2 parameters (120 mm / 150 mm)
- Material sets – 3 parameters (aggregate / dry sand / moist sand)
- Wall friction parameter – 2 parameters (steel / PVC)
- Fill configuration – 2 parameters (hopper only / vertical section also)

If all the combinations of parameters were tested, this would have required 48 test sets requiring at least one test each, and a selection of test sets would be repeated sufficient times to demonstrate repeatability and accuracy of results. It was rather decided to conduct a sub-set of these in order to establish the main relationships and demonstrate the effects of the most significant parameters without testing all parameter combinations.

Each configuration (combination of set-up parameters, and test material) was denoted, and recorded as a test 'Set'.

Additional tests were performed including consideration of the effects of fast vs. slow filling, these were performed as variations to the main tests performed and only a small number of variation tests were performed, however these did provide sufficient insight into the effects of fast vs. slow filling.

In most test sets more than one test was performed to demonstrate the repeatability or reliability of results. Some test repeats included a fast fill as an additional test case. The test sets that were performed are as listed in Table 3-3, with noted case parameters and actual dimensions of the rig as configured

Where it is possible to separate out a test case from within a set of tests, this is listed sequentially as its own results case. This was done in order to separate out the results of the fast fill cases compared with the standard loose fill cases

The term 'levelled' is a reference to the filling configuration, which is the vertical bin section filled to 50 mm below the top of the vertical bin wall. Cases 1 to 9 represent dry sand, case 10 represents dry aggregate, and cases 11 to 15 represent moist sand.

Table 3-3 - List of test result cases and test sets

Case No.	Set No.	Description	Test angle (°)	Test width (mm)
1	2	20-degrees, 120 mm slot, dry sand, levelled	19.4°	120.3
2	3	20-degrees, 120 mm slot, dry sand, hopper only	19.4°	120.3
3	4	20-degrees, 150 mm slot, dry sand, levelled	18.3°	146
4	5	30-degrees, 150 mm slot, dry sand, hopper	28°	140
5	5 – fast fill	30-degrees, 150 mm slot, dry sand, hopper	28°	140
6	6	30-degrees, 120 mm slot, dry sand, levelled	29.2	119.7
7	7	30-degrees, 120 mm slot, dry sand, hopper only	29.2	119.7
8	7 - fast fill	30-degrees, 120 mm slot, dry sand, hopper only	29.2	119.7
9	8	20-degrees, 150 mm slot, dry sand, hopper	18.3°	146
10	9	20-degrees, 120 mm slot, 13mm aggregate, hopper only	19.4°	120.3
11	10	20-degrees, 120 mm slot, moist sand, hopper only	19.4°	120.3
12	10 - fast fill	20-degrees, 120 mm slot, moist sand, hopper only	19.4°	120.3
13	11	20-degrees, 120 mm slot, moist sand, hopper only-PVC Lined	19.4°	120.3
14	11- fast fill	20-degrees, 120 mm slot, moist sand, hopper only-PVC Lined	19.4°	120.3
15	12	20-degrees, 120 mm slot, moist sand, hopper only, time consolidation investigation	19.4°	120.3

3.6 Data Processing

The raw data collected was tabulated as voltage for each load cell as a function of the number of rotations of the adjustment nut to lower the feeder plate.

The number of rotations was converted to mm of displacement (based on 1.75 mm pitch for an M12 bolt), and the voltage was converted to Newtons based on the loadcell calibration and gravitational acceleration.

Prior to the first lowering of the plate, the measured load onto the plate was a valid measure of the pressure at the bottom opening of the hopper. After lowering by several turns of the nut however, a significant amount of material would have moved out from the bin and its weight was added to the plate. It was necessary subtract this from the measured load to give a correct measure of the load at the hopper outlet. The mass of the material between the hopper outlet and the plate was calculated as a function of the volume of the rectangular prism made by the hopper outlet projected to the bottom plate, with additional consideration of the material rolling down the slope according to the material repose angle.

The approximate shape of the material withdrawn is as shown in Figure 3-5

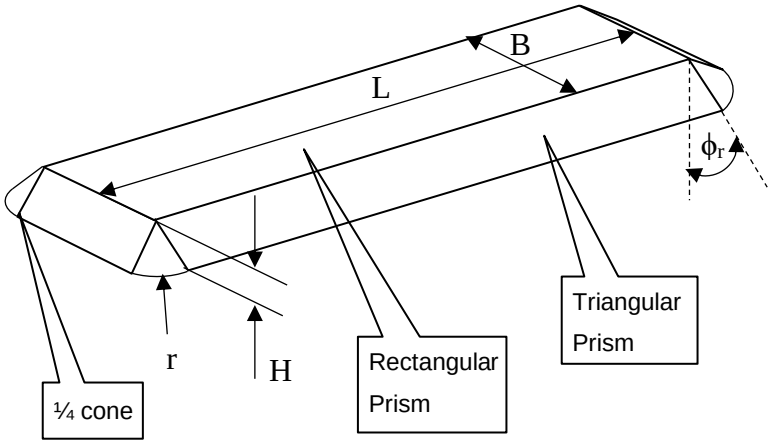


Figure 3-5 Shape of material between hopper outlet and bottom plate

The method of calculation of this material is presented in Appendix B, and equation (B.1) is repeated as equation (6).

$$= L \cdot B \cdot H + (L+B) \cdot H^2 / \tan \phi_r + \pi \cdot H^3 / (3 \cdot \tan^2 \phi_r) \qquad (6)$$

During testing, moist sand did not necessarily the same repose angle as tested from pouring tests because the consolidation from pressures at the bottom of the hopper caused the material to hold together and extrude out of the hopper outlet. For this reason, a near vertical angle was observed. As a result, it was decided to calculate the weight of moist sand withdrawn on the basis of a vertical (90 degrees) repose angle at the outlet.

An example of the measured data is shown in Table 3-4. The raw data for a sample test iteration (voltage as a function of number of turns for the two loadcells) is shown graphically on Figure 3-6, indicating each individual voltage reading. The full range of converted data for a single test iteration is shown on Figure 3-7.

The result sheet includes calculations to process these voltage readings into loads (using calibration functions), and then using the measured loads to back-calculate the load at the hopper outlet. This is achieved by subtracting the self-weight of the testing equipment supported from the loadcells, and also subtracting the calculated mass of the withdrawn

material as a function of the distance of plate lowering and the assumed material properties. This load was in all cases treated as a measured load.

A plot is then prepared for the curve of the converted pressure against the lowering distance of the feeder plate, with lowering distance as the product of the rotation of the adjustment nut with the pitch of the threaded bar.

Due to the uncertainty of the material properties at the outlet, which are based on assumption, there is some uncertainty to the conversion of measured voltage to pressure at the outlet. A curve of upper bound and of lower bound withdrawn mass has been tabulated in Table 3-4 and graphed in Figure 3-7. For the lower bound value, a minimum density and maximum repose angle have been used and the converse used for the upper bound value. Based on this, upper and lower bound values (denoted as Test 2 (H) and Test 1 (L) respectively) are plotted for the hopper pressure are calculated by subtraction and included in the results graph.

Figure 3-8 and Figure 3-9 are expanded views of Figure 3-7 showing the first 5 mm and last 10 mm of displacement respectively, allowing clearer view of the specific details in those zones.

The lower bound value relates to a calculation case with high density and low repose angle, which implies a greater mass of material withdrawn as a function of plate displacement.

This implies that if density was maximum (tapped bulk density) and repose angle was minimum (resulting in a wider pile), the mass of the pile would be higher. When subtracting this from the measured load, it defines the lower bound value, and the converse applies for low density with high repose angle which defines the upper bound value.

It is apparent that the uncertainty (the deviation between the upper and lower bound load lines) increases with increasing displacement. After plate displacement of 5.25 mm (3 rotations) the uncertainty range is -0.18% and +0.64%. After 49 mm displacement, the uncertainty increases to -4.3% and +19.7%. On the graphical presentation of each test set, the uncertainties are listed at feeder plate displacements of 5.25 mm and at 35 mm only, or where no available data is available at that point, the nearest available data point is used for comparison. The upper and lower result curves are not graphed for each set for reasons of results readability.

All further usage of results was based on the single calculated value based on assumed material properties for each test set. The 'Initial' and 'flow' lines are representations of the analytically calculated loads that compare to the measured loads.

Table 3-4, Example test record sheet (Set no. 9, Case no. 10) – Aggregate, 20-deg, 120 mm, Hopper only

Test Record Sheet		Hopper base plate lowering force curve							
Set Number	9								
Test Name	20 degrees, 120 mm slot, 13mm aggregate, hopper only								
Case Number	10								
Moisture	0.20%		(air dry)						
Max Lump	13	mm							
P80 Lump	11.2	mm							
Angle	19.4	degrees							
Width	120.3	mm							
Length	480	mm							
Spec. wt	14502	N/m3	(loose density +25% of difference to tapped density)			15068.2			
repose	43	degrees				35			
Initial:	414.6	N	Calculated			430.82			
Flow:	59.9	N	Calculated			62.23			
Tare	7.09	kg					0.182%		
Screw Pitch M12	1.75	mm				Low Repose			
						High Density			
		Test 2		Test 2 Loads		Test 2 (L)	Initial (calc.)	Flow (calc)	Average
Load record (screw turns)	Disp. (mm)	Volt 1-1	Volt 1-2	Draw Load (N)	Load-Test 1	draw	(calc)	(calc)	
Empty Load		128	157		0.0				
max (N)	379.7				379.7				
min (N)	33.5				34.1				
50% reduction (N)	206.6				206.9				
80% reduction (N)	102.8				103.3				
displacement to min (mm)	21.0				21.0				
displacement - 50% red. (mm)	0.274				0.274				
50% red displ as % of gap	0.23%				0.23%				
displacement - 80% red. (mm)	0.550				0.541				
80% red displ as % of gap	0.46%				0.45%				
0	0	913	925	0.00	379.7	0.00			380
0.125	0.219	566	661	0.18	230.3	0.19	415	60	230
0.25	0.438	377	470	0.37	137.2	0.38	415	60	137
0.375	0.656	310	375	0.55	97.3	0.58	415	60	97
0.5	0.875	300	340	0.74	86.1	0.77	415	60	86
0.625	1.094	280	317	0.93	75.4	0.97	415	60	75
0.75	1.313	261	292	1.12	64.4	1.16	415	60	64
0.875	1.531	261	301	1.30	66.5	1.36	415	60	66
1	1.750	246	281	1.49	57.7	1.56	415	60	58
1.25	2.188	247	281	1.88	57.6	1.97	415	60	58
1.5	2.625	231	270	2.26	50.6	2.37	415	60	51
1.75	3.063	231	265	2.65	49.0	2.79	415	60	49
2	3.500	231	266	3.05	48.8	3.21	415	60	49
2.25	3.938	239	263	3.44	49.6	3.63	415	60	50
2.5	4.375	223	261	3.84	44.8	4.06	415	60	45
2.75	4.813	231	273	4.25	49.3	4.49	415	60	49
3	5.250	223	256	4.66	42.8	4.93	415	60	43
3.5	6.125	226	252	5.48	41.7	5.82	415	60	42
4	7.000	228	253	6.33	41.6	6.74	415	60	42
4.5	7.875	223	260	7.18	41.2	7.67	415	60	41
5	8.750	221	251	8.06	37.7	8.63	415	60	38
5.5	9.625	230	257	8.94	40.5	9.60	415	60	40
6	10.500	221	249	9.84	35.4	10.60	415	60	35
7	12.250	227	255	11.69	36.5	12.66	415	60	36
8	14.000	237	263	13.60	39.0	14.81	415	60	39
9	15.750	242	270	15.58	39.9	17.04	415	60	40
10	17.500	245	278	17.61	40.6	19.36	415	60	41
12	21.000	238	276	21.87	34.1	24.27	415	60	34

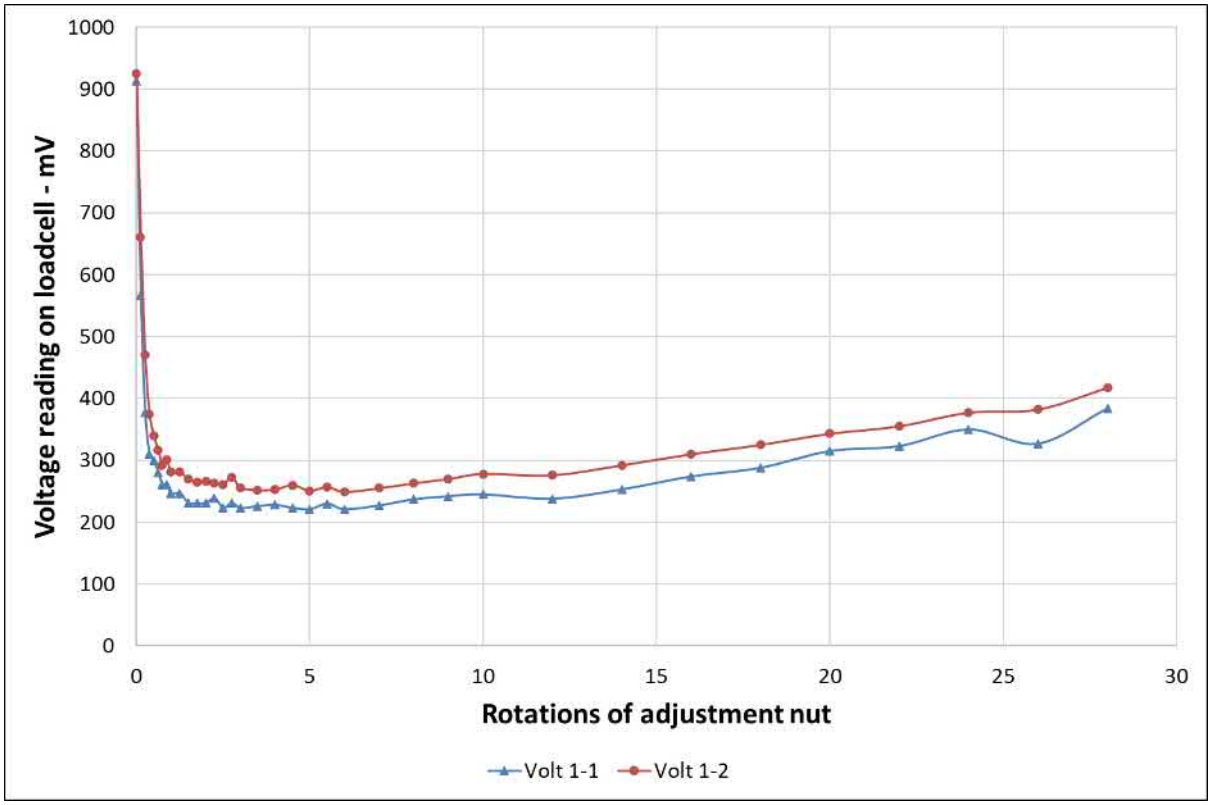


Figure 3-6 Set 9, Case 10 - Loadcell volt readings per nut rotation (raw data)

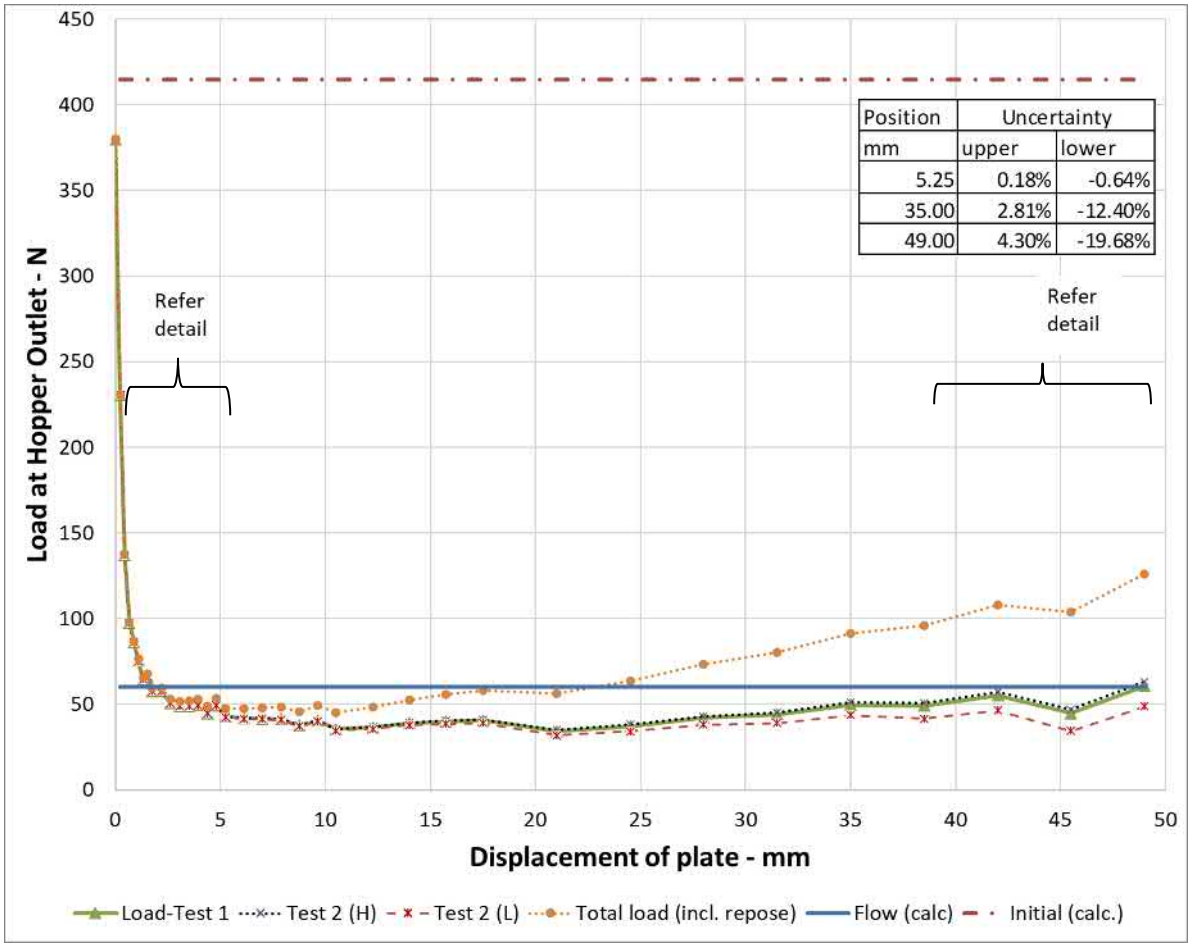


Figure 3-7 Set 9, Case 10, 20-degrees, 120 mm, 13 mm aggregate, hopper only - full range of test

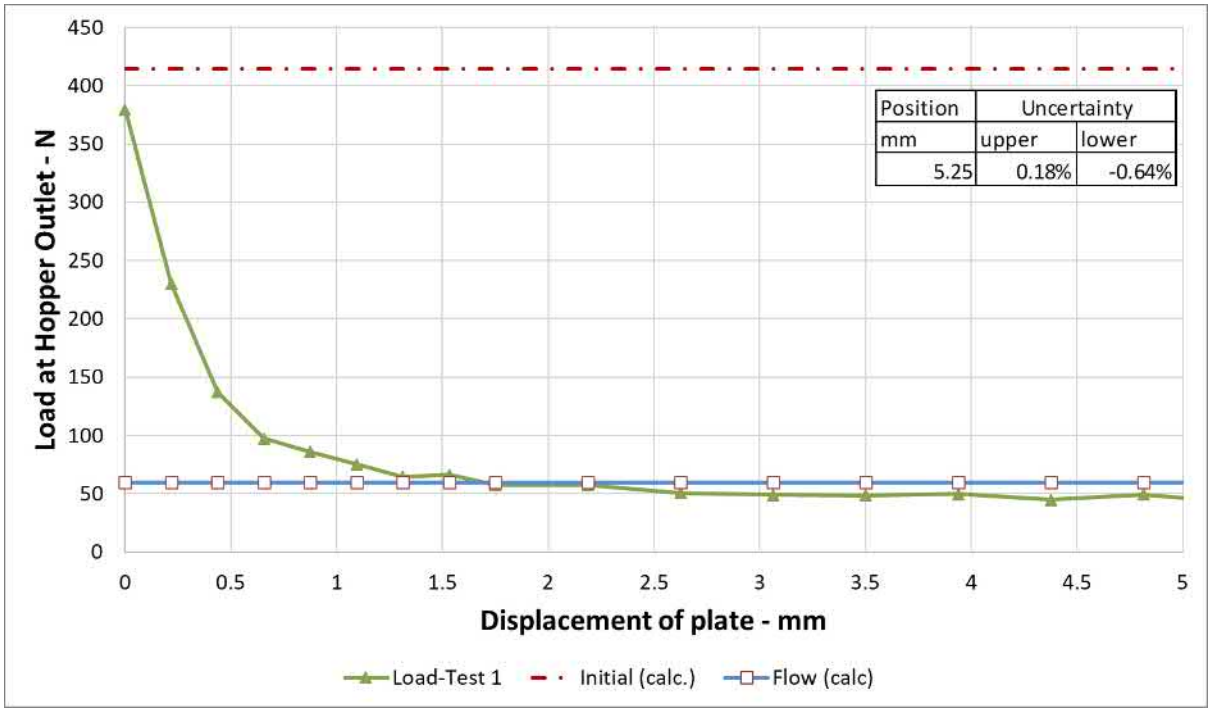


Figure 3-8 Set 9, Case 10, 20-degrees, 120 mm, 13 mm aggregate, hopper only - range 1-5 mm

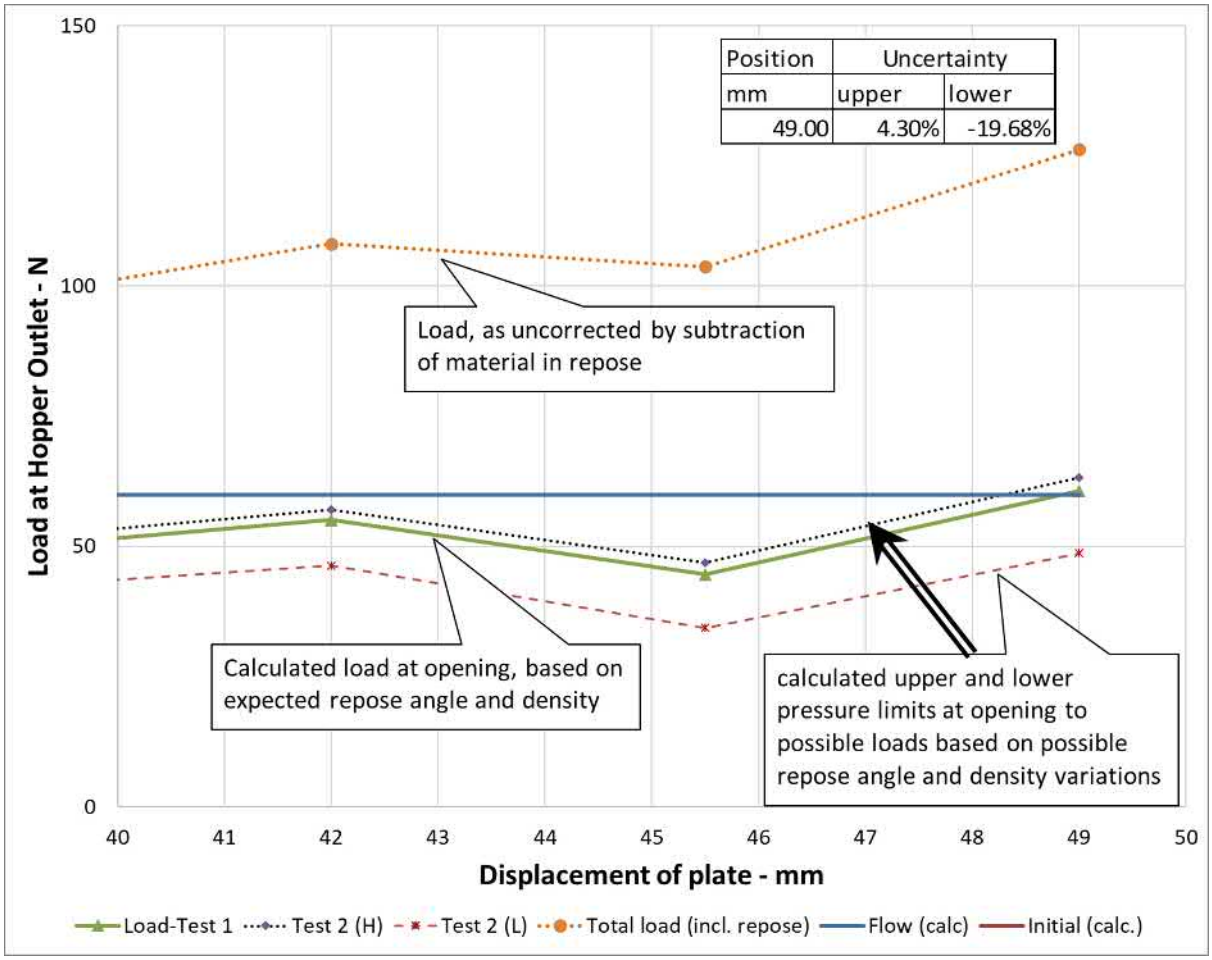


Figure 3-9 Set 9, Case 10, demonstration of uncertainty and weight corrections, range 40-50 mm

In most test cases, including the test case above (case 9), the test was repeated several times in order to demonstrate the repeatability of results. An example of the combination of test repetitions for Set 9 is shown in Figure 3-10.

Comparative data processing between the test cases were based on selection of the test result that most suitably demonstrated a correctly executed test.

In all cases, only the test case that presented the most reliable test result was used for comparisons and further analysis. In the example of Set 9, only Test 2 was selected for use in comparative analysis.

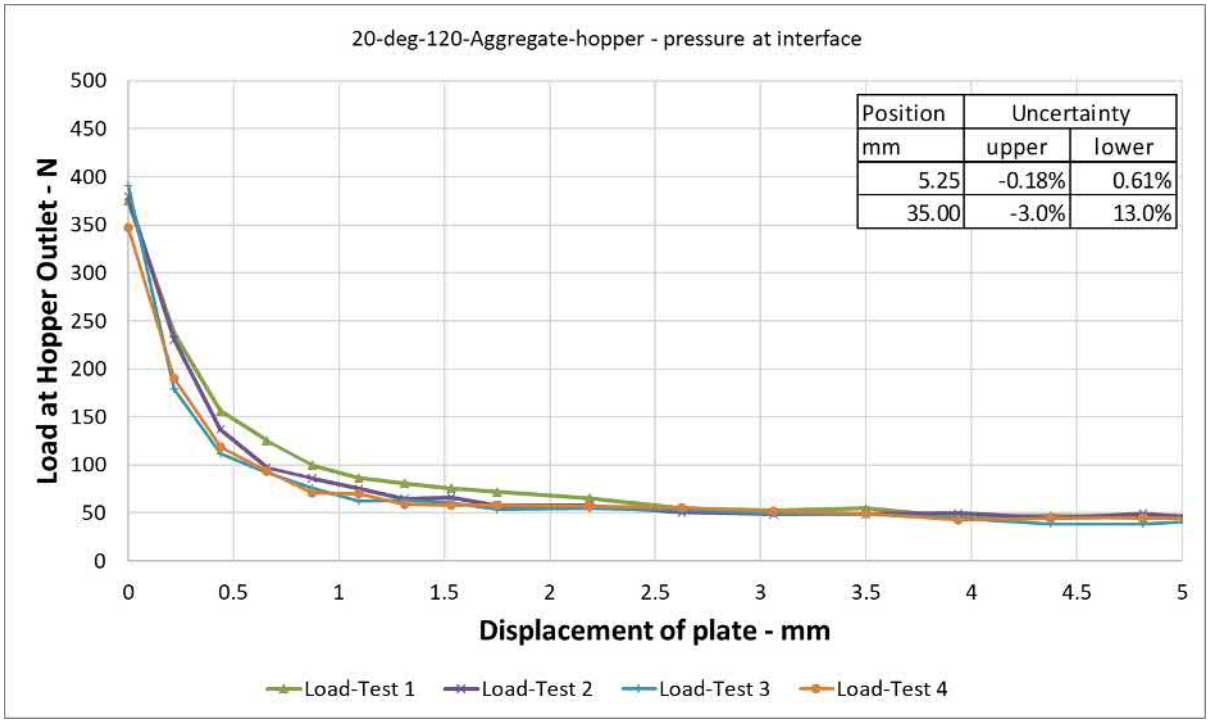


Figure 3-10 Result curves on Set 9 test repetitions

Chapter 4 Observations

4.1 Introduction

During testing, observations were made relating to the variations of loads on the feeder plate (recorded as voltage). These include the effects of time delay between nut adjustment and voltage reading, and also consideration of events occurring during a test that had the effect of presenting anomalies in the recorded data. Examples are incorrect rotation direction of a nut, a delay between adjustment and reading, or accidental bumping of the test rig.

Observations of the test result include how the loads encountered relate to analytical calculated values, and how various test cases compare to each other. These are explored in the discussion section. However, it is noted in this section (prior to presentation of the full set of results) how test parameters fall acceptably within the design range of the test rig.

4.2 Range of pressures encountered during testing, compared to design

Comparing the loading capacity of the test rig, as listed in Section 3.2.2, which includes selection of the loadcells to be accurate in the range of 20 N to 1000 N, the range of measured tensions onto the loadcells across all tests performed, ranged from 52 N to 337 N. These extremes were all within the range of the loads calibrated for the loadcells.

Also described in Section 3.2.2 was the intent that the test pressures be in the range of several kPa in order to reliably expect that cohesive properties present in the material were suitably demonstrated.

The range of expected initial (high) pressures in the lower portions of the hopper were analytically calculated as between 4.5 kPa and 11.3 kPa using the method of Roberts [4]. Corresponding actual maximum measured pressures were in the range of 3.9 kPa and 7.4 kPa. Based on this, the requirement that the maximum working pressures be in the range of several kPa (as noted in Section 3.2.2) was satisfied, and this implies that the test results will present some conclusions relating to material cohesion and pressure consolidation which does typically present in the range of several kPa.

4.3 Behaviours noted during testing action

Due to the time requirements, it was not feasible to wait an average of five minutes between recording data collection points. As a result, all the pressure recordings were taken immediately after lowering the plate or within about 20 seconds. This ensured a consistent basis of comparison between readings. In some cases, when the measurements were interrupted by a minute or more, it was apparent in the pressure graphs that a reading was observably higher than measurements immediately before or after. The magnitude of this pressure increase was small and did not present a significant influence on the overall results, but it does demonstrate that time effects are at play in the seconds after plate lowering,

It was noticeable from careful inspection through the Perspex wall at the back of the hopper, that several seconds after the screw loosening actions, some particles would make small, localised movements while the bed stabilised. This was consistent with the observed load increase. This leads to a conclusion that small-scale movements, mostly not visible, occur during the time after turning the nut, gradually taking the hopper into a stabilised state.

In other test cases, when due to human error, a wing nut was turned the wrong way, or by the wrong amount, the effects on the measured pressures were clear. Tightening the nuts led to the plate being raised instead of lowered, compressing the bed of material and resulting in a steep increase in pressure. This pressure increase was observable on both loadcell sides due to prying action, although the most significant effect was on the loadcell where the error was made. This event only occurred a small number of times and the effect on the data was noted. Once corrected, it did not impact on subsequent measurements within that particular test.

Converse to the above, over-loosening the nuts led to faster pressure reduction. Those tests were informative in terms of validating similarity of other tests performed on the same configuration, but in terms of basic data analysis, they were omitted from the analysis because sufficient tests were performed to establish the relative behaviours. In one case, the test data was retained and processed by smoothing between values before and after, in order to ensure sufficient number of tests to present reliability of data for comparative purposes.

4.4 Initial observations in test result data

4.4.1 Comparisons between calculated and measured initial and flow pressures

In Figure 3-7 and Figure 3-8, representing the test case using dry Quartz aggregate, it is apparent that the maximum and minimum pressures are similar to, but slightly lower, than those calculated by the analytical method. Based on the full composite average results for test case 10 (Set 9), pressure was measured as 92% of the calculated value and flow pressures at 59% of the calculated values. It is not the scope of this present study to identify and define reasons for the deviations between analytically calculated and experimentally measured pressure results. The calculated values are used for reference and comparison purposes only, but they are used for comparative ratios and to support discussion as to why some material sets behave differently from others.

Bulk density is a significant determinant of actual load, however with the characterisation testing performed, and the considerations to use a 25% consolidated density inside the bin for dry materials, there is limited uncertainty relating to bulk density. Rather than considering full theoretical extent of density range (from 0% to 100% consolidated), it can be reasonably assumed that deviations from the 25% consolidated state may be approximately 10% higher or lower than the selected value. Therefore, if the density range is selected as 15% to 35% consolidated, this implies a density variation of 1486 kg/m^3 to 1522 kg/m^3. This represents a variation of only 1.23% above or below the assumed density. By contrast the deviation from calculated initial and flow pressures are larger than this. In both states the pressures that occurred were lower (92% and 59% respectively).

4.4.2 Rate of pressure reduction

Referring to Figure 3-8 it is apparent that within a distance of about 1 mm, the majority of the pressure reduction from initial to flow pressure was complete.

Especially relevant to this test case was the rapid rate of pressure reduction from the initial case. The first one eighth rotation (vertical drop of 0.219 mm, or 0.182% of the 120.3 mm opening width) resulted in a reduction from 380 N to 230 N. This reduction of 150 N or 39% of the initial pressure represented a very rapid reduction of pressure from the initial filling case. Further discussion on results from other test sets is included in Chapter 6.

4.4.3 Effects of experimental events and anomalies.

The method described in Section 3.4 required that test readings be taken soon after nuts were adjusted. In some cases, there was a delay between nut adjustment and taking a reading, or other events occurred which affected results. These occurrences were not widespread, and the affected data were retained or corrected as noted below. The data sets that were selected for comparative analysis did not include these anomalies.

- Nut turned incorrect direction
  - This compressed the material back upwards into the hopper and led to a sharp increase in the load. The load increase was observed most significantly on the loadcell side where the nut was turned upward, but also the opposite side recorded an increase in pressure due to the effect of prying over material which had already been lowered with the feeder plate.
  - One occasion when data was smoothed after incorrect direction turn was recorded in the test 2 of set 3 as per Table 4-1. The selected value was selected as the average between prior and subsequent readings.

Table 4-1 Error correction on nut turn direction

Test Record Sheet		Hopper base plate lowering force curve					
Set Number		3					
Test Name		20 degrees, 120 mm slot, dry sand, hopper					
		Test 1		Test 2		Test 3	
Load record (screw turns)	Disp. (mm)	Volt 1	Volt 2	Volt 1	Volt 2	Volt 1	Volt 2
empty	empty	140.8	147.9	142.4	148.9	142.9	147.8
2.625	4.594			234	268	247	266
2.75	4.813	258	283				
2.875	5.031						
3	5.250	276	301				
3.125	5.469			245.5	268.5	246	262
3.25	5.688	251	286				
3.375	5.906						
3.5	6.125						
3.625	6.344					257	278
3.75	6.563	254	283				
3.875	6.781						
4	7.000						
4.125	7.219			257	269	268	296

Measured as 277

Measured as 337, nut turned wrong way

- Test rig bumped
  - A bump onto the test rig (during the time test, set 12) caused an upward step in the pressure, resulting from material consolidating faster than would be the case for time based consolidation this was recorded in test data as shown in Table 4-2. This data was retained, and it was observed that after the next lowering of the plate, the test pressures returned to overall trends.

Table 4-2 Error recording - rig bumped during time consolidation test

Time	Load record (screw turns)	Disp. (mm)	Volt 1	Volt 2	Load 1	Load
10:33	5	8.750	238	257	58.3	
10:34	6	10.500	220	241	53.9	
10:35	6	10.500	226	246	55.4	
10:36	6	10.500	229	249	56.1	
10:37	6	10.500	245	268	60	
10:38	6	10.500	248	270	60.7	
10:39	8	14.000	224	252	54.9	
10:40	8	14.000	228	255		
10:41	8	14.000	229	255	56.1	

bumps

stable

- Delay in taking reading
  - Some cases where the test parameters showed a significant deviation from norm were due to a delay in the readings after turning the nut. An example of this and the method to record is shown in Table 4-3 (example from test 1 from set 4). These were noted and recorded, but the data was processed as collected and was treated valid data although it deviates from normal data trends. This deviation also did not affect the overall comparative parameters of the test compared with a set of smoothed data.

Table 4-3 Step change in pressure due to Delayed reading

1.375	2.406	600	644	483	486
1.5	2.625	600	644	483	486
1.625	2.844	500	550		
1.75	3.063	500	550		
1.875	3.281	538	585	422	424
2	3.500	538	585	422	424

time response due to reading delay

Cases where a shorter variation in the delay from turning the nut to taking the measurement had the effect of flattening or steepening a curve occurred during normal experimental variation. These were not specifically recorded and were not treated differently from other small experimental variations that may have been present.

4.5 Dimensional scaling of calculated loads and test rig dimensional constraints

Some consideration was given towards scaling of the laboratory test rig. However, no suitable dimensionless variables were apparent which would facilitate such analysis, considering that there were no dynamic effects at play. Typical practice was assumed as valid for large scale facilities in that test results were performed on equivalent pressures in a test cell which informed the wall friction angle and flow function as inputs into the calculation.

No further consideration was made in terms of dimensional scaling of results, other than noting the ratios of material displacement (as a percentage of opening width) to percentage reduction from initial to flow pressures.

Chapter 5 Results

5.1 Introduction

In this Chapter, the Results of all the tests are presented according to the different configurations (sets) as laid out in Table 3-3. A listing of the full set of results is tabulated and presented in graphical form in included in Appendix G.

The graphical representation of each data set includes the calculated initial and flow loads for comparison.

A graph of each results set is presented in Section 5.2 to Section 5.12:

5.2 Test Set 2, 20-degree, 120 mm, dry sand, bin filled (levelled)

Figure 5-1 shows that in this this test set, the initial pressure did not reach the calculated load, but that the flow case was relatively closely predicted by the calculation and that the load was consistent after the shift to flow load.

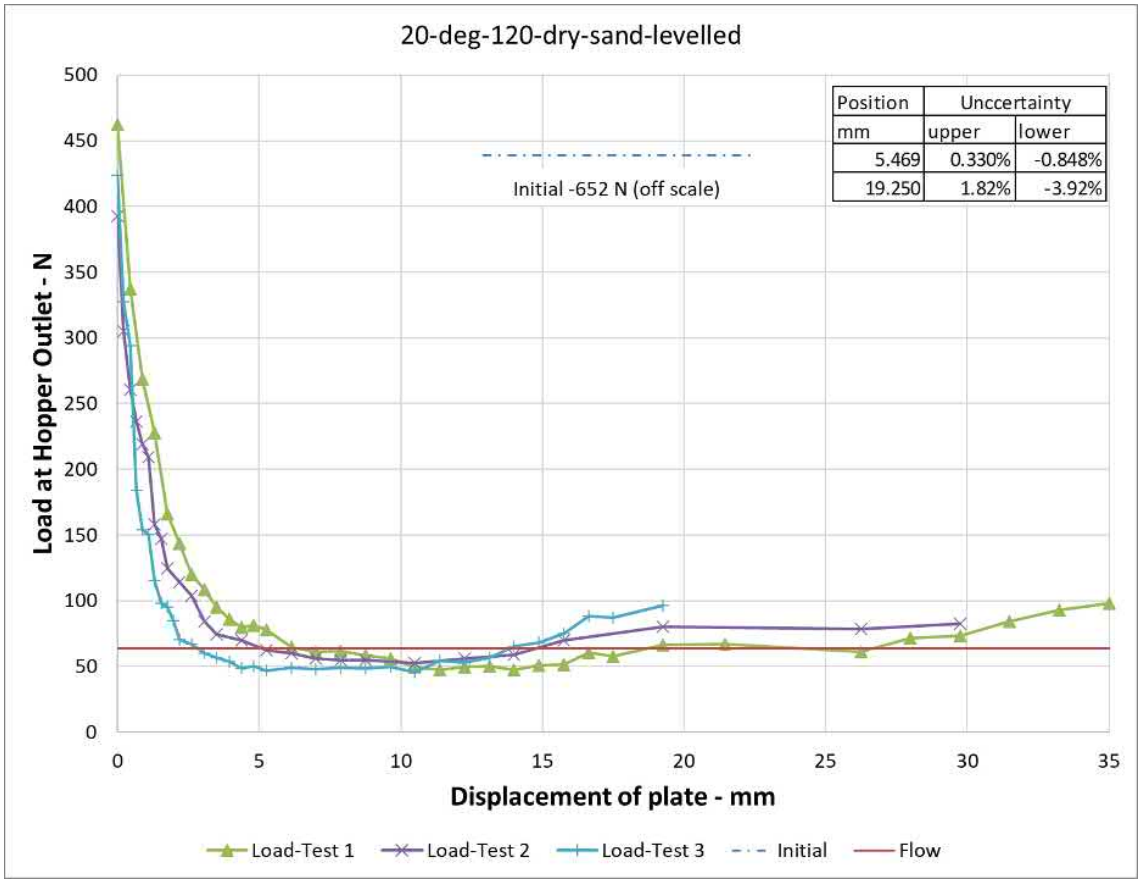


Figure 5-1 Set 2, 20-degree, 120 mm, dry sand, Levelled

5.3 *Test Set 3, 20-degree, 120 mm, dry sand, hopper filled*

Figure 5-2 presents the test results with a 20-degree slope and 120 mm opening with only the hopper loaded.

It is notable that the rate of load reduction is rapid initially, and that after the pressure reaches its minimum, the load at the hopper outlet rebounds to a load slightly higher than the flow load.

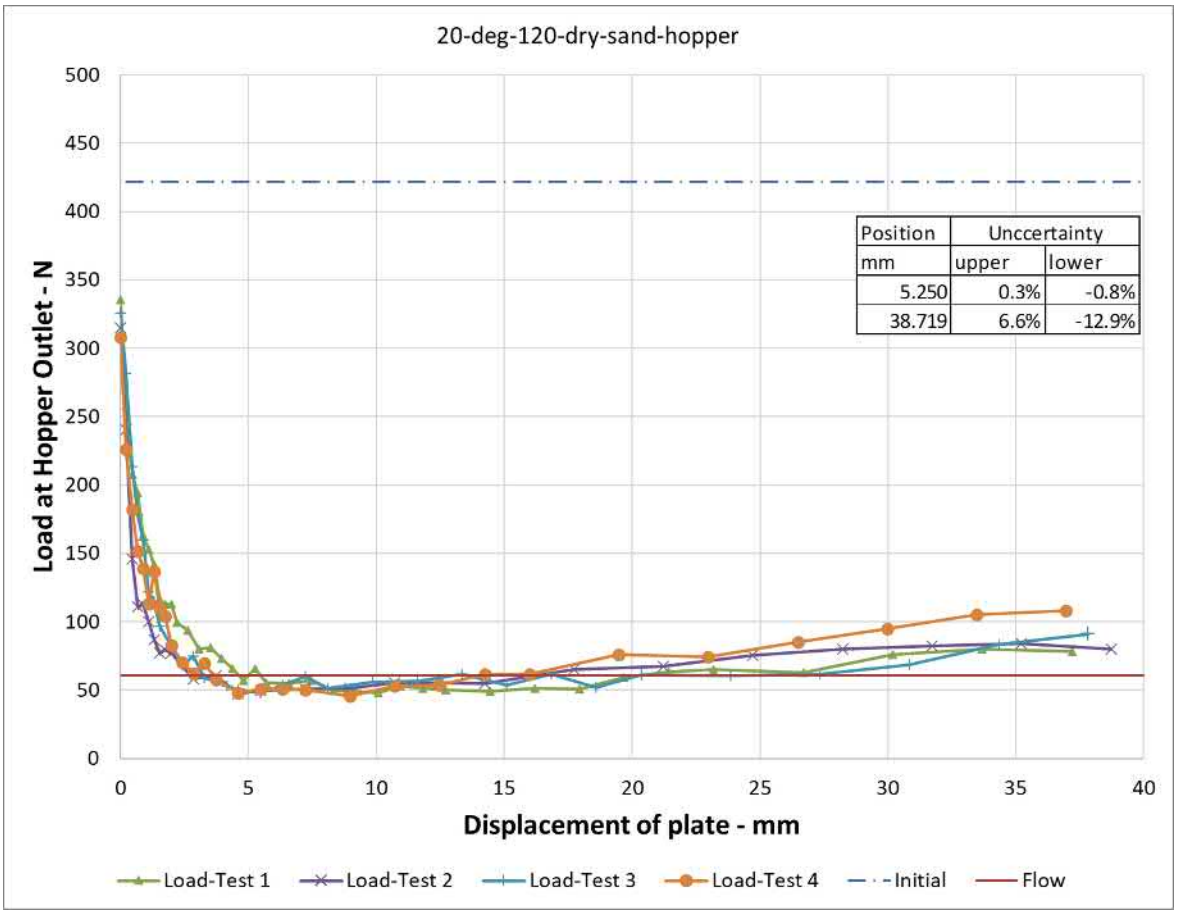


Figure 5-2 Set 3, 20-degree, 120 mm, dry sand, Hopper filled

5.4 Test Set 4, 20-degree, 150 mm, dry sand, bin filled (levelled)

Figure 5-3 presents the case with a levelled bin with dry sand on 120 mm wide and 20-degree hopper slope.

Each of the test curves indicated a test reading that indicated an increase in load during the portion of the drawdown when it would normally be expected that each reading with reduce load. These relate to experimental anomalies cause by delay or incorrect rotation direction.

Besides this, it is apparent that the material load did not reach the calculated load value, and that the flow load was similar to the value as calculated analytically.

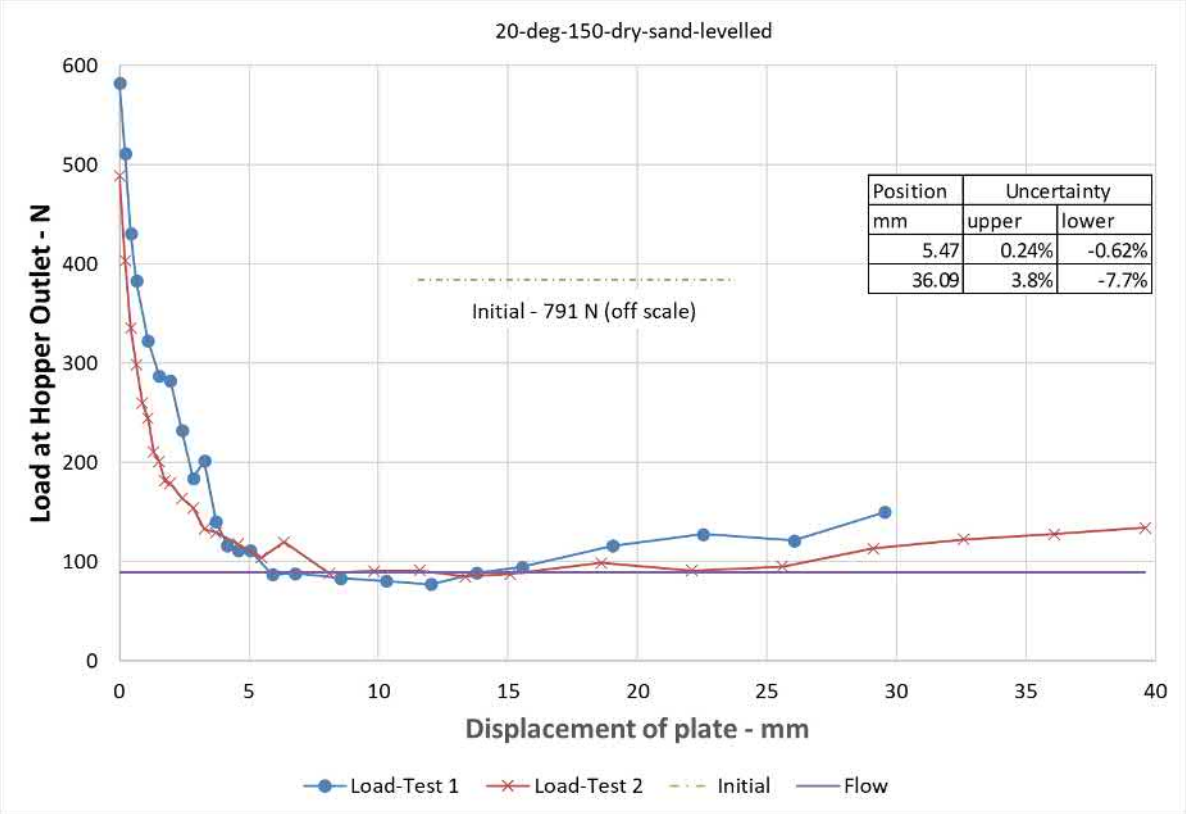


Figure 5-3 Set 4, 20-degree, 150 mm, dry sand, Levelled

5.5 *Test Set 5, 30-degree, 150 mm, dry sand, hopper filled*

Figure 5-4 presents the results for the 30-degree wall angle with 150 mm wide opening and hopper filled.

It is notable that after completion of the test, the load at hopper appears to increase again to a magnitude significantly higher than the calculated flow load.

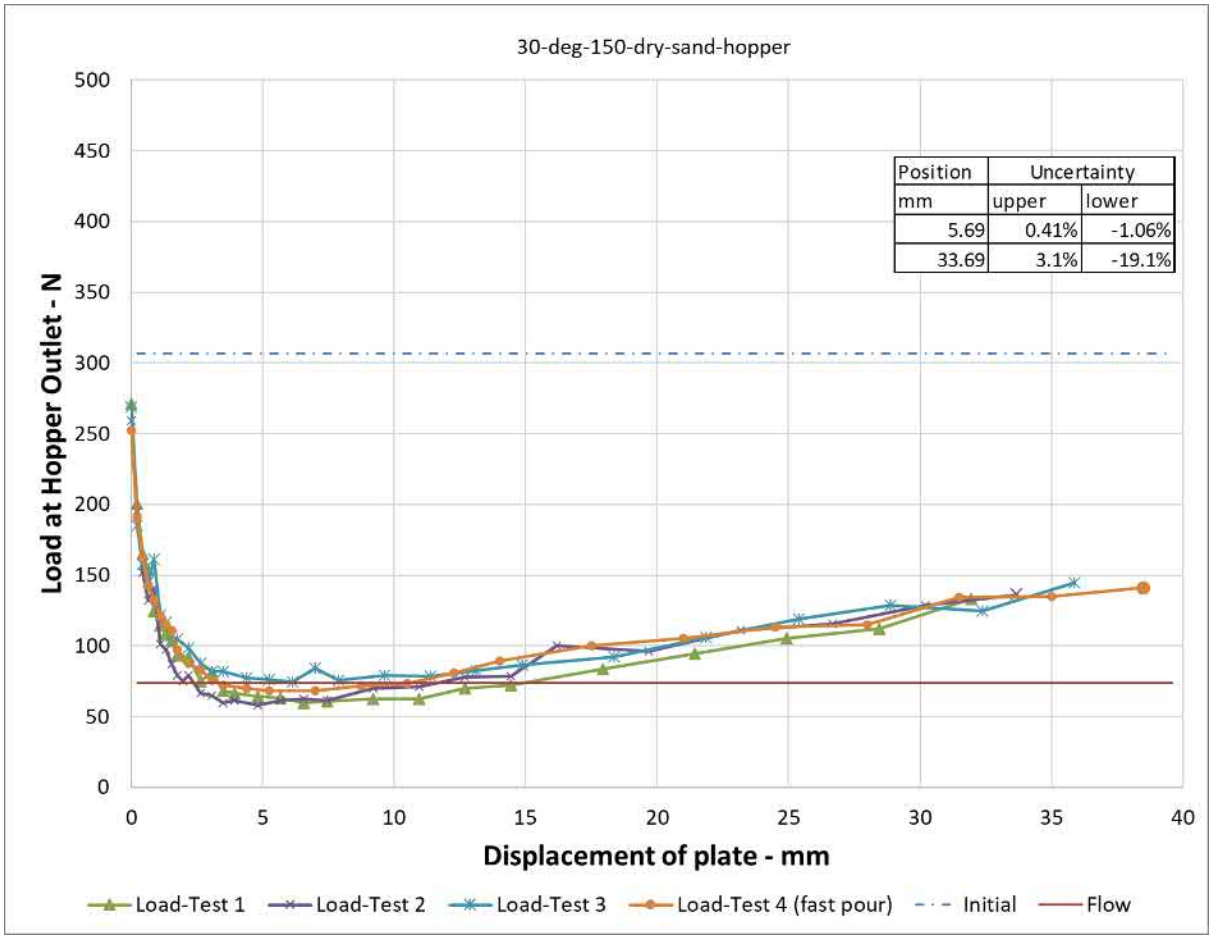


Figure 5-4 Set 5, 30-degree, 150 mm, dry sand, Hopper filled

5.6 Test Set 6, 30-degree, 120 mm, dry sand, bin filled (levelled)

Figure 5-5 presents the flow profile of the case with entire bin filled (levelled to the top) with 120 mm wide opening and 30-degree slope angle.

The initial pressure did not reach a large percentage of the calculated initial load. The flow load calculation appeared to be a relatively reliable predictor of the actual load during withdrawal.

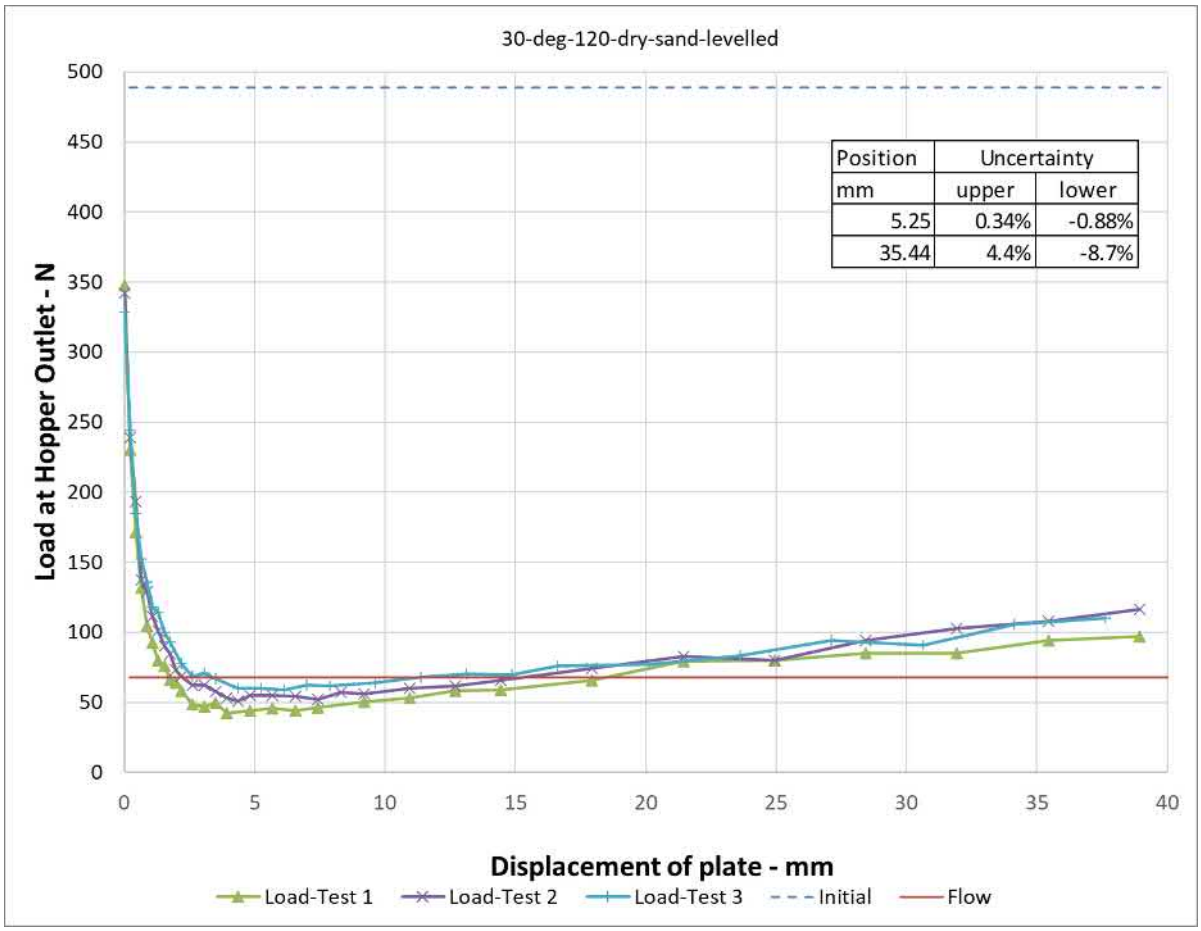


Figure 5-5 Set 6, 30-degree, 120 mm, dry sand, Levelled

5.7 Test Set 7, 30-degree, 120 mm, dry sand, hopper filled

Figure 5-6 presents the results for 120 mm wide hopper opening with a full hopper loading.

Similar to Test Set 5, the load at hopper appears to increase again to a magnitude greater than the calculated flow load.

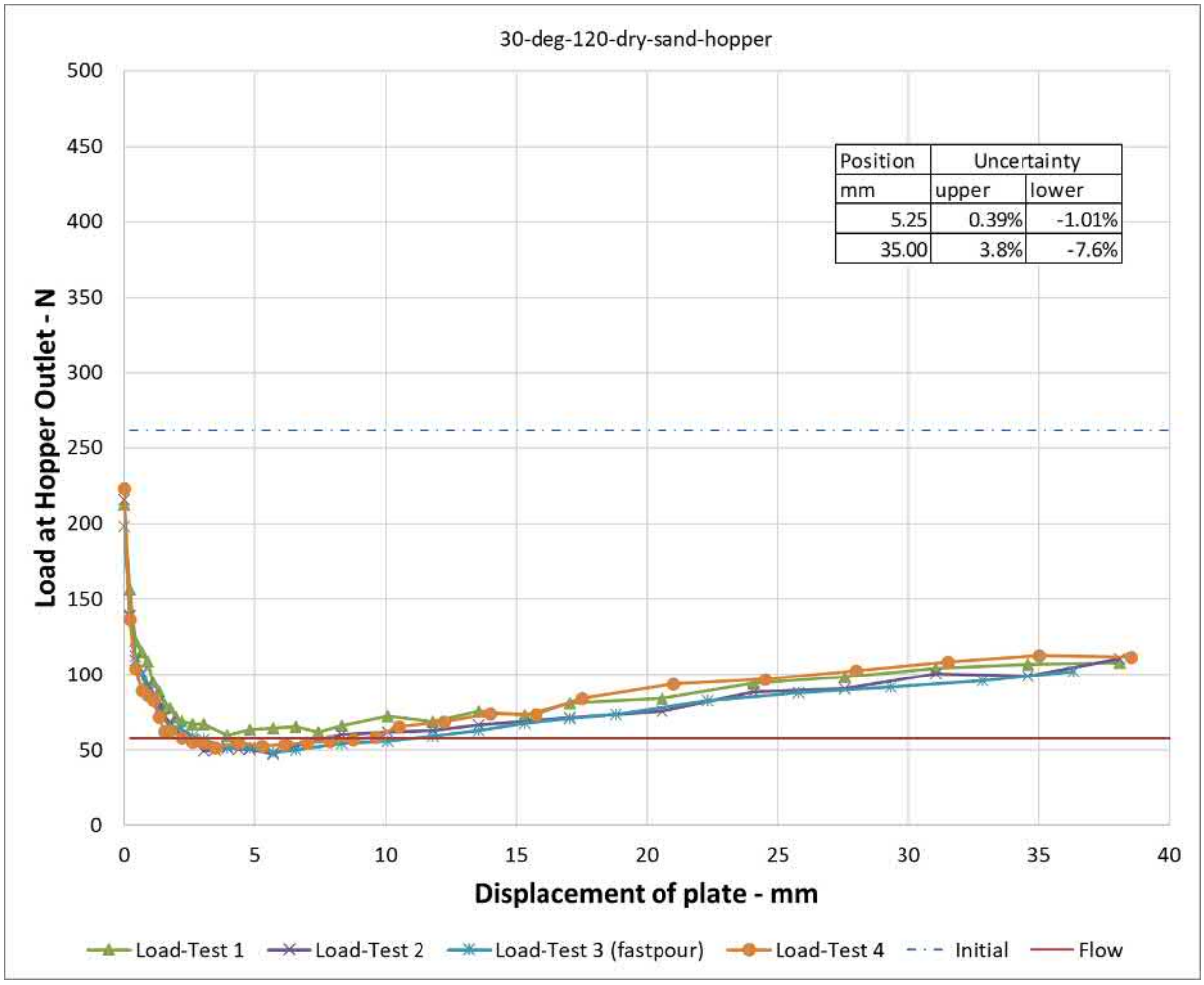


Figure 5-6 Set 7, 30-degree, 120 mm, dry sand, Hopper filled

5.8 Test Set 8, 20-degree, 150 mm, dry sand, hopper filled

Figure 5-7 presents the behaviour of the dry sand with a 150 mm wide hopper opening. The load reduced at a relatively high rate, and the profile after lowering of the plate was relatively consistent, and close to the theoretically calculated flow load.

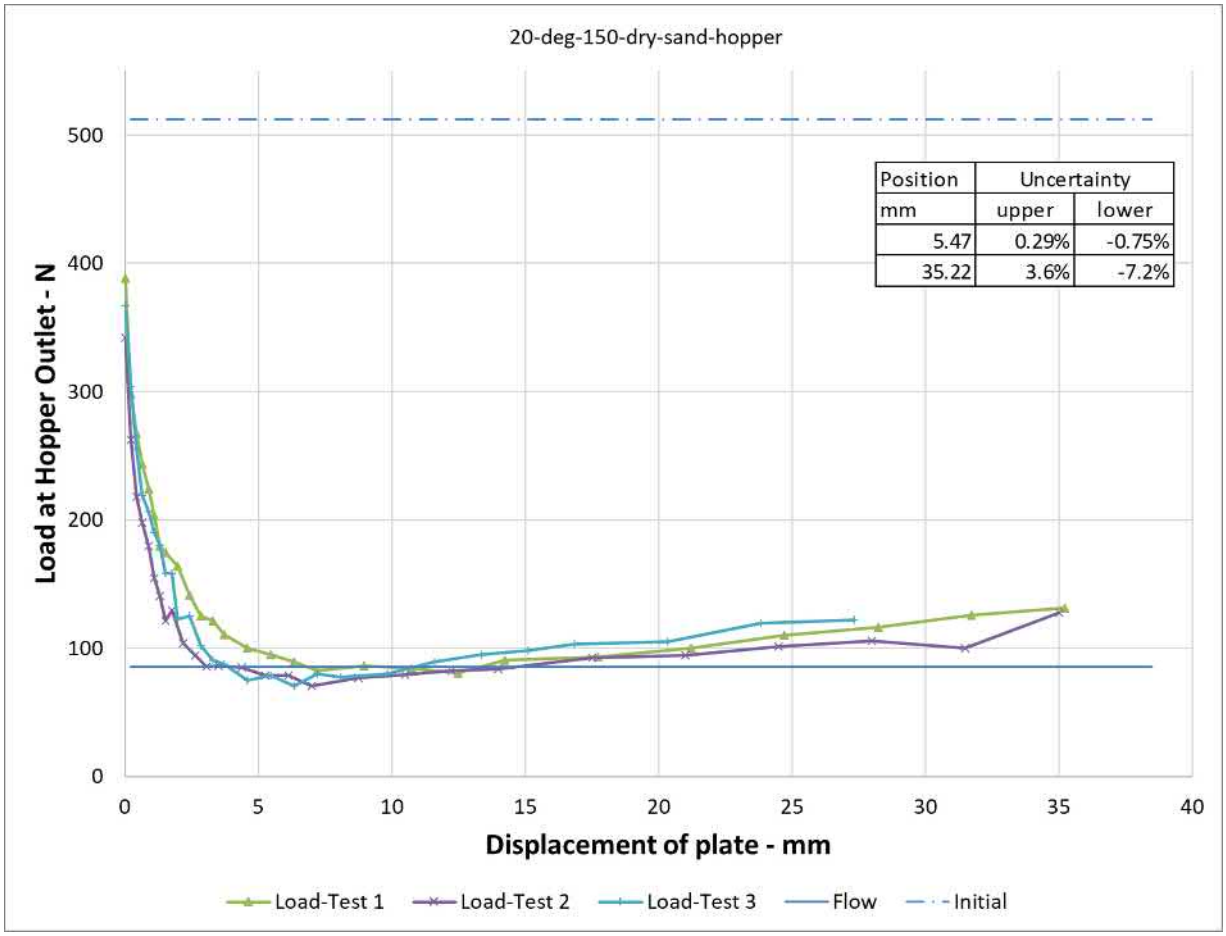


Figure 5-7 Set 8, 20-degree, 150 mm, dry sand, Hopper filled

5.9 Test Set 9, 20-degree, 120 mm, dry aggregate, hopper filled

Figure 5-8 presents the test results from aggregate. It is notable that the initial load approached quite closely to the calculated initial load, and that the rate of reduction in load was very rapid initially.

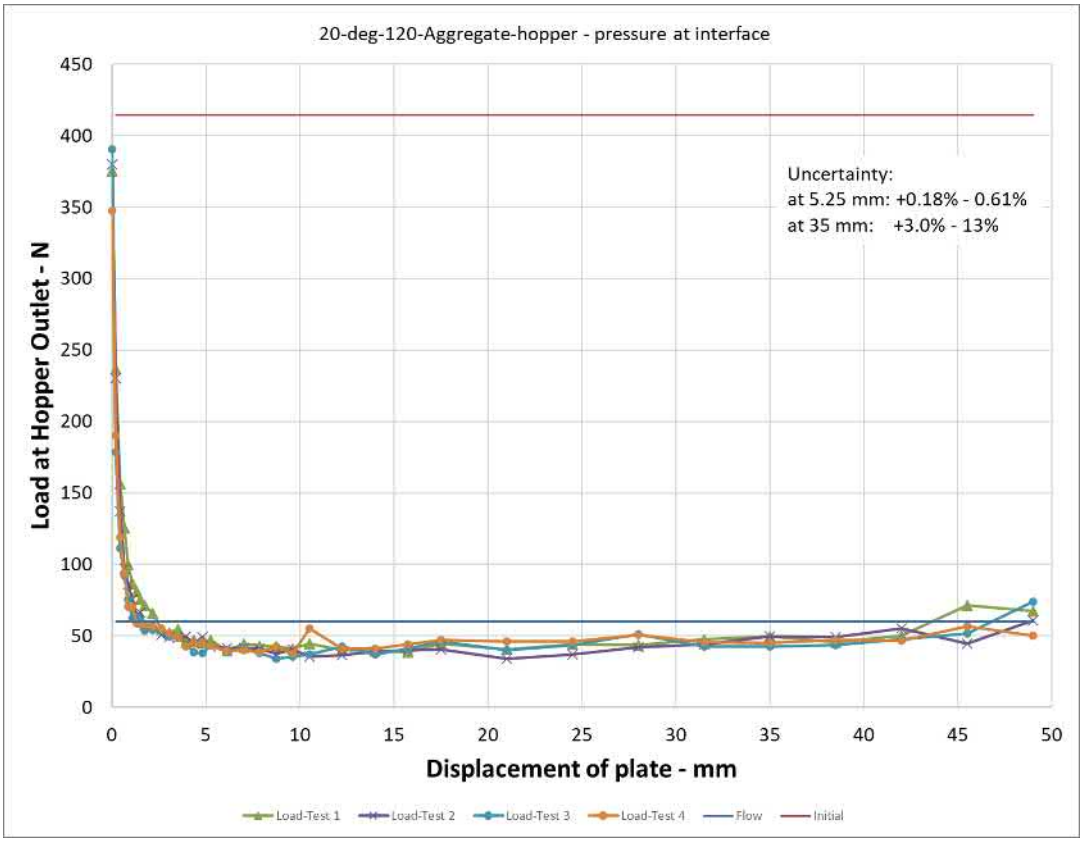


Figure 5-8 Set 9, 20-degree, 120 mm, dry aggregate, Hopper filled

5.10 Test Set 10, 20-degree, 120 mm, moist sand, hopper filled

Figure 5-9 presents moist sand material in a 120 mm wide hopper. One test iteration was performed using the fast filling method to develop inertial compaction of the material.

The balance of the tests, which are slow filling cases, do not present a consistent unloading profile, possibly because of some variation in the filling process between tests.

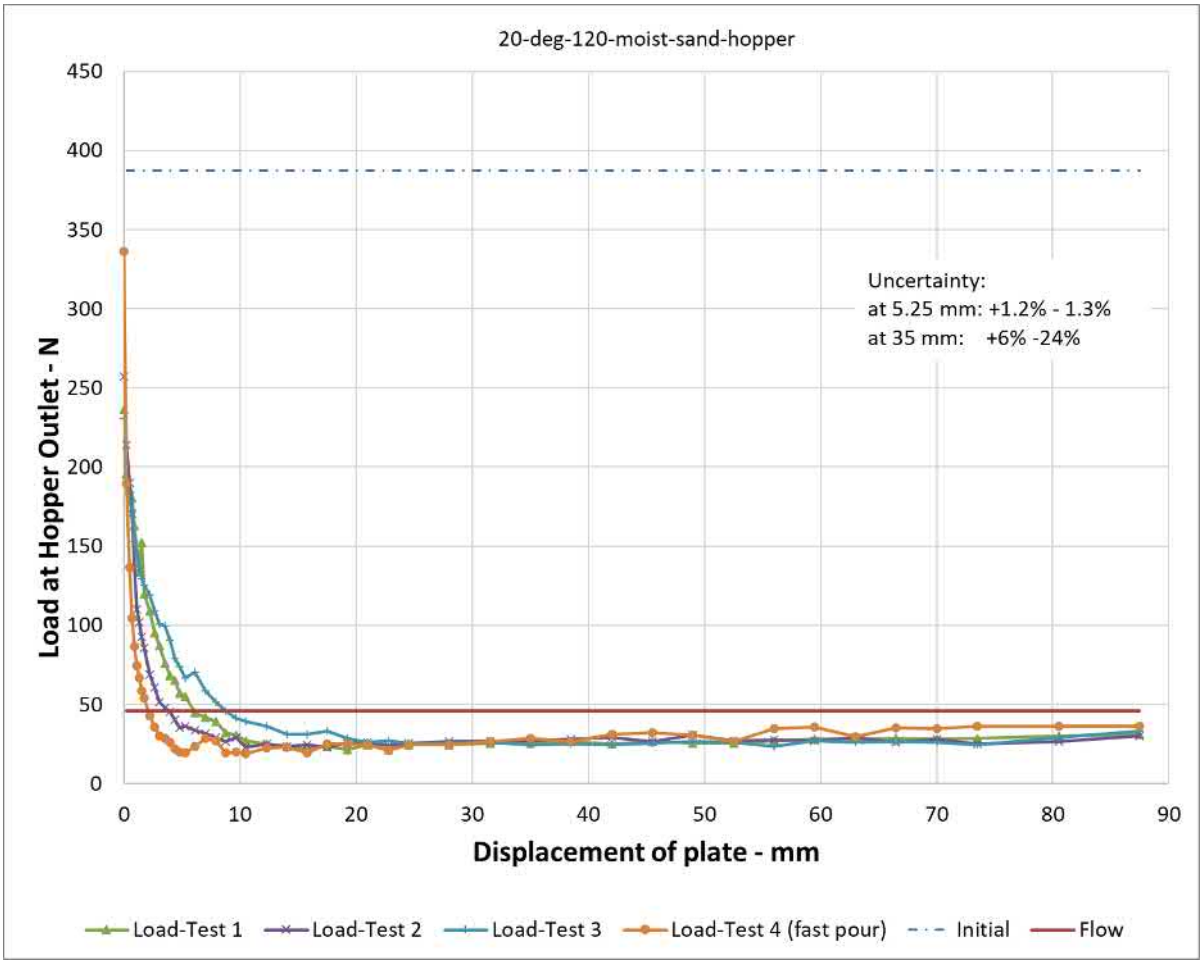


Figure 5-9 Set 10, 20-degree, 120 mm, moist sand, Hopper filled

5.11 Test Set 11, 20-degree, 120 mm, moist sand, hopper filled – PVC lined

Figure 5-10 presents the effects of PVC lined side walls on the hopper. One test iteration was performed using the fast filling method in order to develop inertial compaction of the material.

The PVC lined side walls had the effect of increasing wall friction angle.

It is notable that the relative rate of load reduction is slower than was the case for Test Set 10, besides this, the behaviour is very similar to Test Set 10.

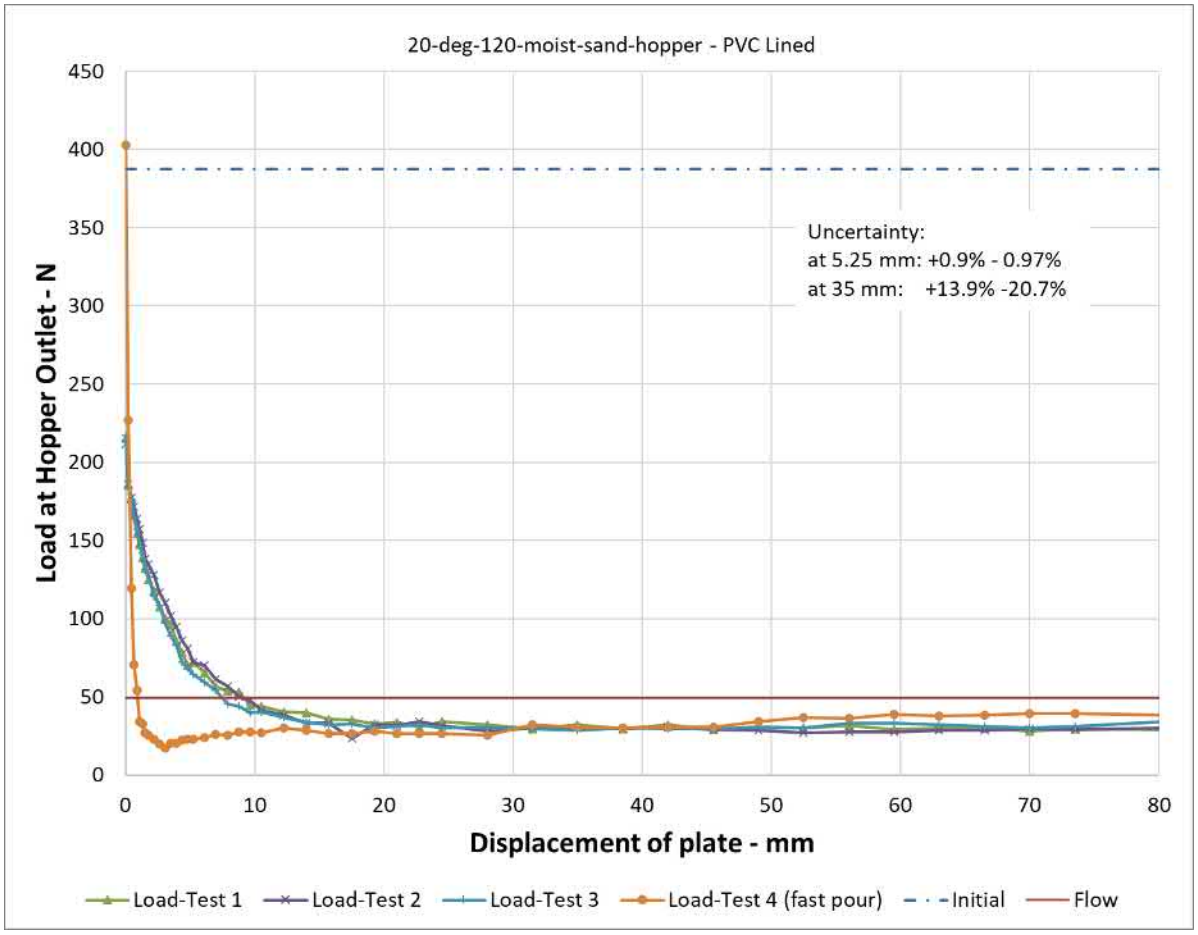


Figure 5-10 Set 11, 20-degree, 120 mm, moist sand, Hopper filled – PVC Lined

5.12 Test Set 12, Time response test

Figure 5-11 and Figure 5-12 present the time effects on load that occur when the load is allowed to settle for several minutes after each lowering of the feeder plate. It is notable that after each lowering, the load begins to recover as the materials settle and re-orient, and the load stabilises after several minutes.

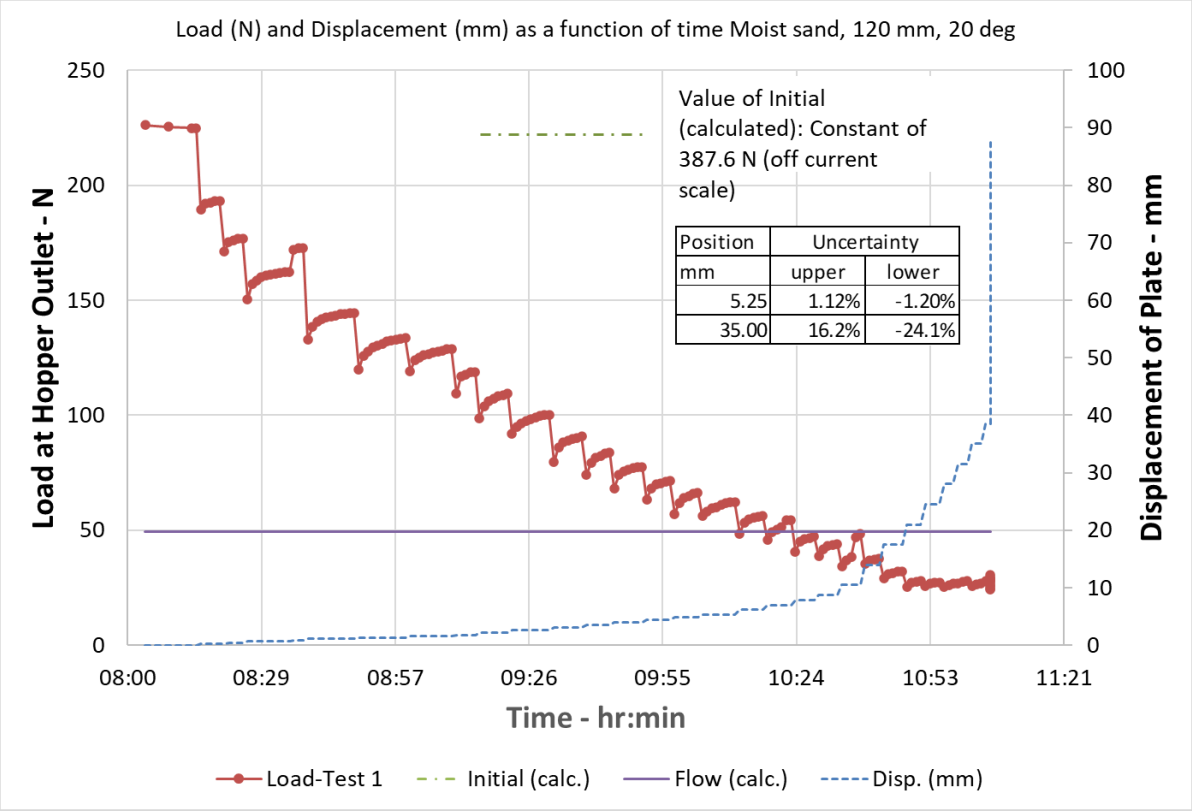


Figure 5-11 Set 12, 20-degree, 120 mm, moist sand, hopper filled – PVC wall – time tesponse test

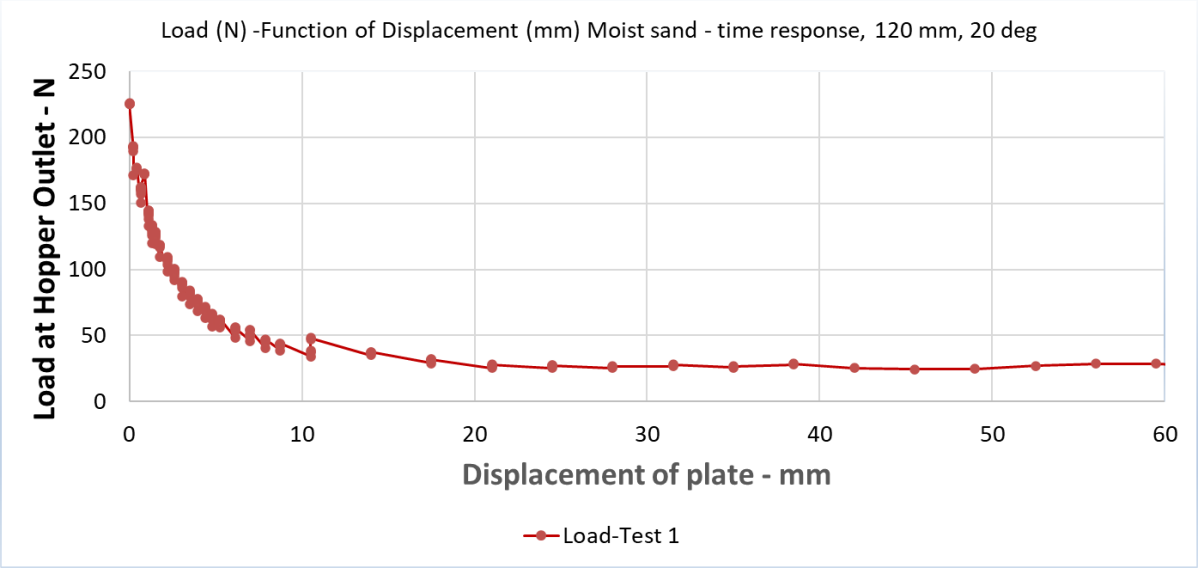


Figure 5-12 Set 12, plot of load to plate displacement – time response test

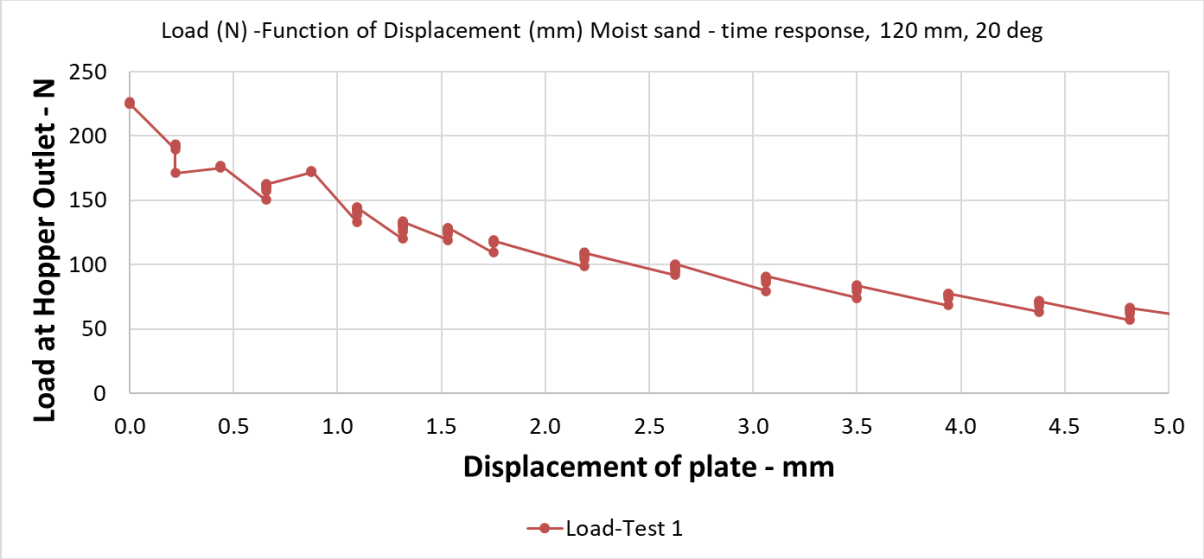


Figure 5-13 Load-displacement function of time response test – first 5 mm of deflection

5.13 Summary of test data

The test sets listed above, are separated into distinct analysis cases, and tabulated in terms of their main parameters. The cases denoted as 'fast pour' are separated from the standard 'slow pour' cases in the same set.

The tabulated parameters relate to the initial and flow pressures measured vs. calculated, and also to the rate at which the pressure changes are effected as a function of feeder plate displacement.

The comparison is based on average pressure curves for each valid evaluated test iteration, which are averaged into the parameters for each analysis case.

The key parameters relating to each test set are the required displacement (as a percentage of opening width) to achieve a 50% or an 80% reduction from measured initial pressures to measured flow (minimum) pressures. This is the parameter that is useful for informing the strength design of a feeder.

The summary is presented in Table 5-1.

Table 5-1 - Summary of material drawdown per test set

Case N	Set N	Description	chosen tes	Max Load		Min Load		Min /M	Load after reduction t		Displacement to cause reduced load to:			Displacement as % of width	
				(N)	% of calc	(N)	% of calc	(%)	50% (N)	80% (N)	min (mm)	50% (mm)	80% (mm)	50% load	80% load
	1	not used													
1	2	20 degrees, 120 mm slot, dry sand, levelled	3	393	60%	52	82%	13%	223	121	10.5	0.8	2.2	0.69%	1.83%
2	3	20 degrees, 120 mm slot, dry sand, hopper	3	326	77%	48	79%	15%	187	104	5.5	0.6	1.4	0.50%	1.20%
3	4	20 degrees, 150 mm slot, dry sand, levelled	1	583	74%	77	87%	13%	330	179	12.0	1.1	3.0	0.76%	2.04%
4	5	30 degrees, 150 mm slot, dry sand, hopper	1	271	88%	60	81%	22%	165	102	6.6	0.4	1.6	0.31%	1.12%
5	5 - fast pour		4	253	52%	68	101%	27%	160	105	5.3	0.5	1.6	0.33%	1.16%
6	6	30 degrees, 120 mm slot, dry sand, levelled	2	342	70%	51	75%	15%	197	109	4.4	0.4	1.1	0.35%	0.95%
7	7	30 degrees, 120 mm slot, dry sand, hopper	2	216	82%	47	82%	22%	132	81	5.7	0.3	1.3	0.23%	1.11%
8	7 - fast pour		3	199	76%	48	84%	24%	123	78	5.7	0.3	1.2	0.28%	1.04%
9	8	20 degrees, 150 mm slot, dry sand, hopper	3	367	72%	71	83%	19%	219	130	6.3	0.7	1.9	0.45%	1.32%
	Average - dry sand				69%		85%							**0.42%**	**1.28%**
10	9	20 degrees, 120 mm slot, 13mm aggregate, hopper only	2	380	92%	34	57%	9%	207	103	21.0	0.3	0.6	0.23%	0.52%
11	10	20 degrees, 120 mm slot, moist sand,	3	231	60%	23	51%	10%	127	65	56.0	1.6	5.4	1.34%	4.46%
12	10 - fast pour		4	337	87%	19	41%	6%	178	82	10.5	0.3	0.9	0.22%	0.79%
13	11	20 degrees, 120 mm slot, moist sand, hopper only-pvc	2	212	55%	23	47%	11%	117	61	17.5	2.6	7.1	2.15%	5.87%
14	11- fast pour		4	403	104%	17	34%	4%	210	94	3.1	0.3	0.6	0.21%	0.46%
15	12	20 degrees, 120 mm slot, moist sand, hopper -time response	1	226	58%	24	49%	11%	125	65	45.5	1.3	3.9	1.09%	3.27%
	Average - Moist Sand				79%		43%							**0.8%**	**2.4%**

The following parameters are tabulated

- Measured maximum (initial) and flow (maximum) loads that occurred during the test
- Measured initial load as a percentage of the analytically calculated initial load
- Measured flow load as a percentage of the analytically calculated initial load
- Minimum measured load as a percentage of maximum measured load
- Calculated loads that correspond with load reduction of 50% and 80% from measured initial to measured flow state, which are metrics of the degree of transition from initial to flow load condition. These are based on an interpolation of data between the noted percentages of reduction.
- Displacement of the plate required to reach the minimum load, load reduced by 50% of the difference between initial and flow load, load reduced by 80% of the difference between initial and flow load.
- Displacement required to achieve significant reduction in loads, 50% and 80% respectively, presented as a percentage of the opening width.
- Average of the main parameters per material type for overall comparison.
- The cells highlighted provide a comparative summary of the average across the material sets for the parameters of displacement required to achieve 50% or 80% reduction for each material set. This makes it possible to draw a conclusion that the aggregate displays

the fastest pressure reduction, followed by dry sand, and that moist sand displays the slowest reduction of pressure as a function of feeder plate displacement.

The ratios presented provide insight into which material sets experience the largest percentage of their calculated load (aggregate) the load at the fastest rates after initiation of flow (aggregate and dry sand), and the percentages of opening width that are required for the various configurations.

The effects of fast filling are seen to be significant for the moist material, in that a high initial pressure occurs and a more rapid reduction of pressure takes place after onset of flow. Withdrawal from bins filled fast with dry material filling by contrast did not indicate any demonstrable difference from the slow filled case.

5.14 Comparative presentation of test data

When comparing test results from differing test sets, including with differing bin outlet width (and therefore differing area), comparison is made on the basis of calculated pressure at the hopper outlet rather than loads. All comparative graphs are therefore presented in units of pressure, kilopascals (kPa).

5.14.1 Variation of material types (fixed configuration)

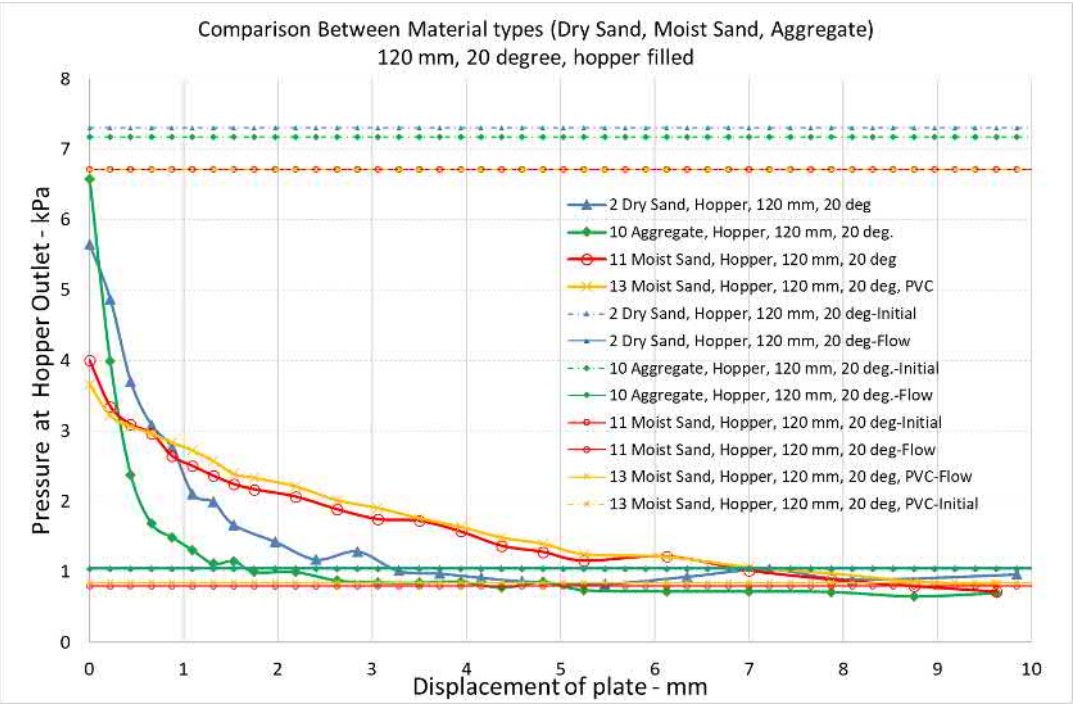


Figure 5-14 Comparative behaviours of materials with varying properties

5.14.2 Variation of wall angle (fixed materials, width and fill configuration)

Figure 5-15 shows comparative pressure relieving behaviour of the 20-degree and 30-degree hopper wall slope angles based on dry sand and a filled hopper and bin vertical section and a 120 mm opening width

Figure 5-16 shows the comparison for a hopper only filled configuration with dry sand and with 120 mm opening width, and Figure 5-17 shows the comparison for hopper only filled, with dry sand, and 150 mm opening width.

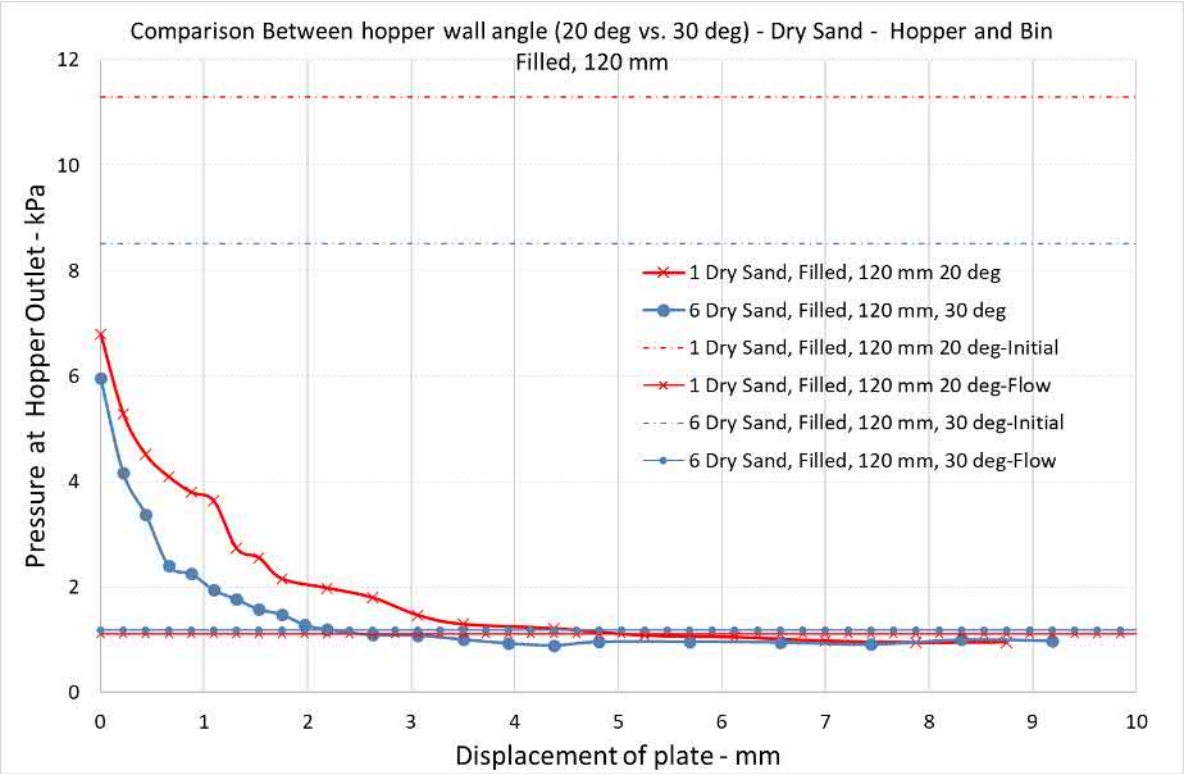


Figure 5-15 Comparative behaviours resulting from angle variation 20-degree to 30-degree - filled 120 mm

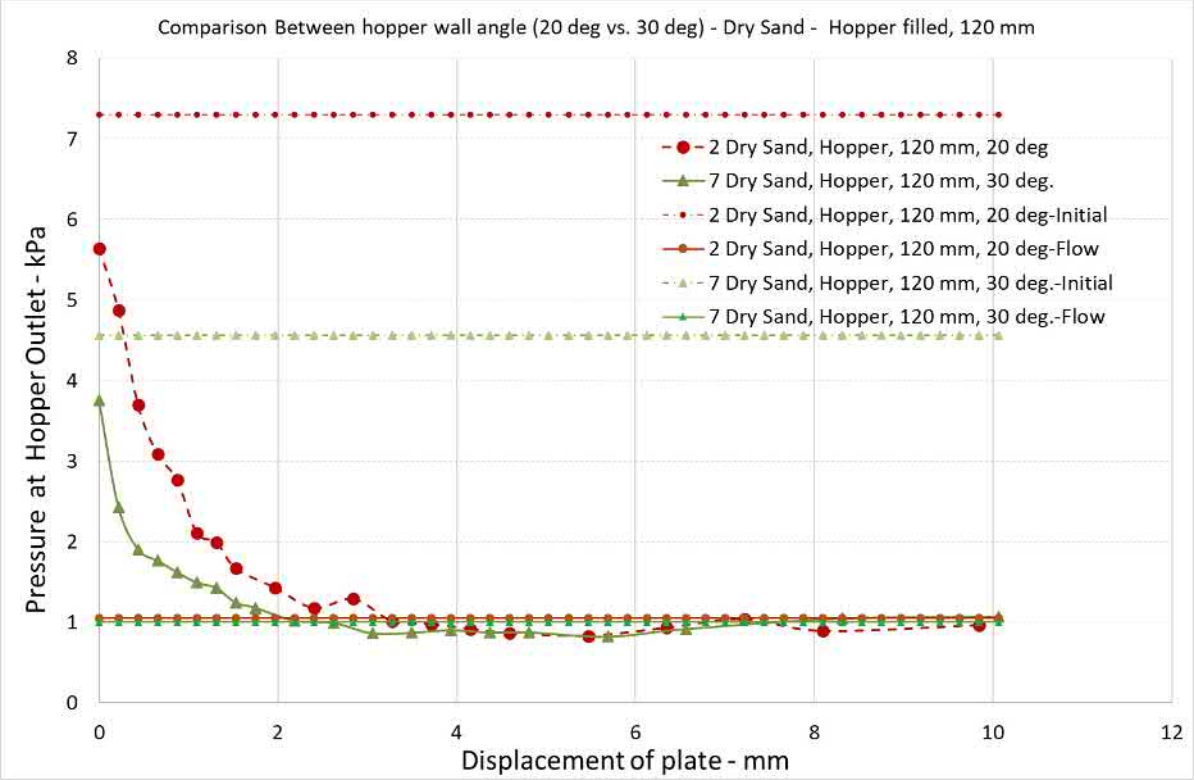


Figure 5-16 Comparative behaviours resulting from angle variation 20-degree to 30-degree – hopper, 120 mm

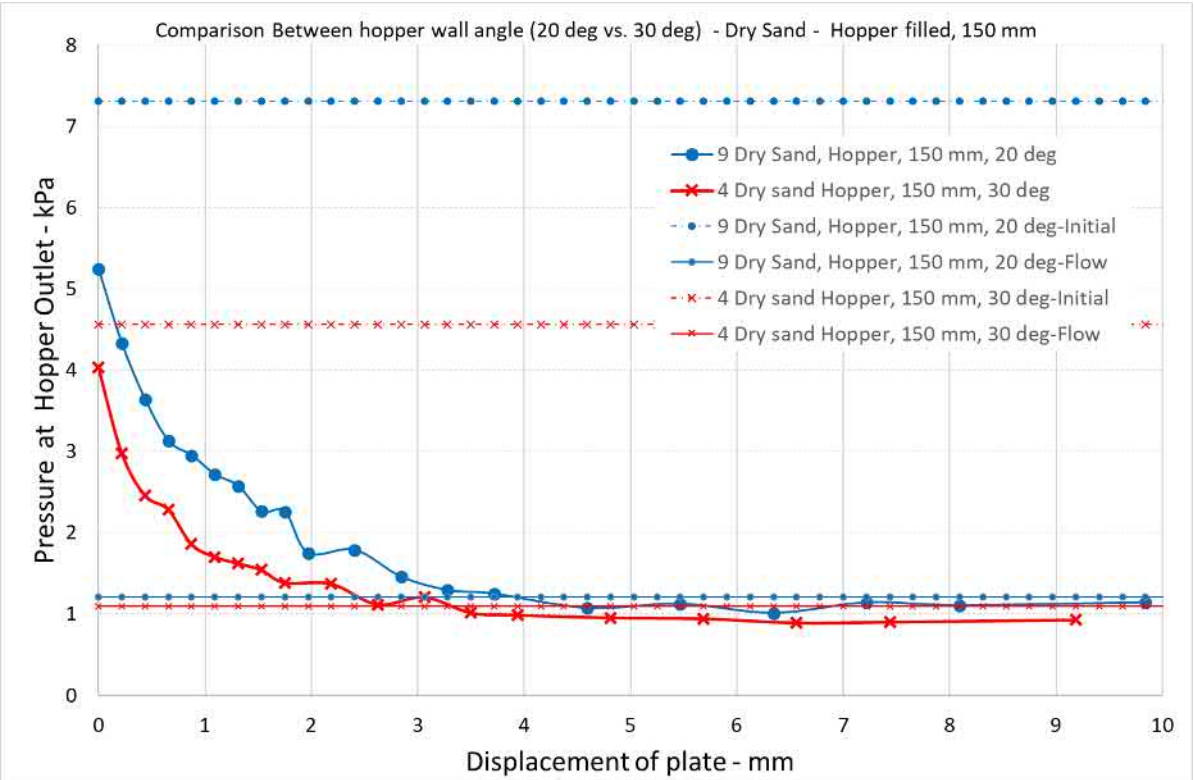


Figure 5-17 Comparison of behaviours from angle variation, 20-degree to 30-degree - Hopper 150 mm

5.14.3 Variation of opening width (fixed materials, angle and fill configuration)

Comparisons of the effects of variations to opening width are shown in Figure 5-18, Figure 5-19, and Figure 5-20 for the bin filled cases, and for the hopper filled cases (20-degree wall angle and 30-degree wall angle), respectively.

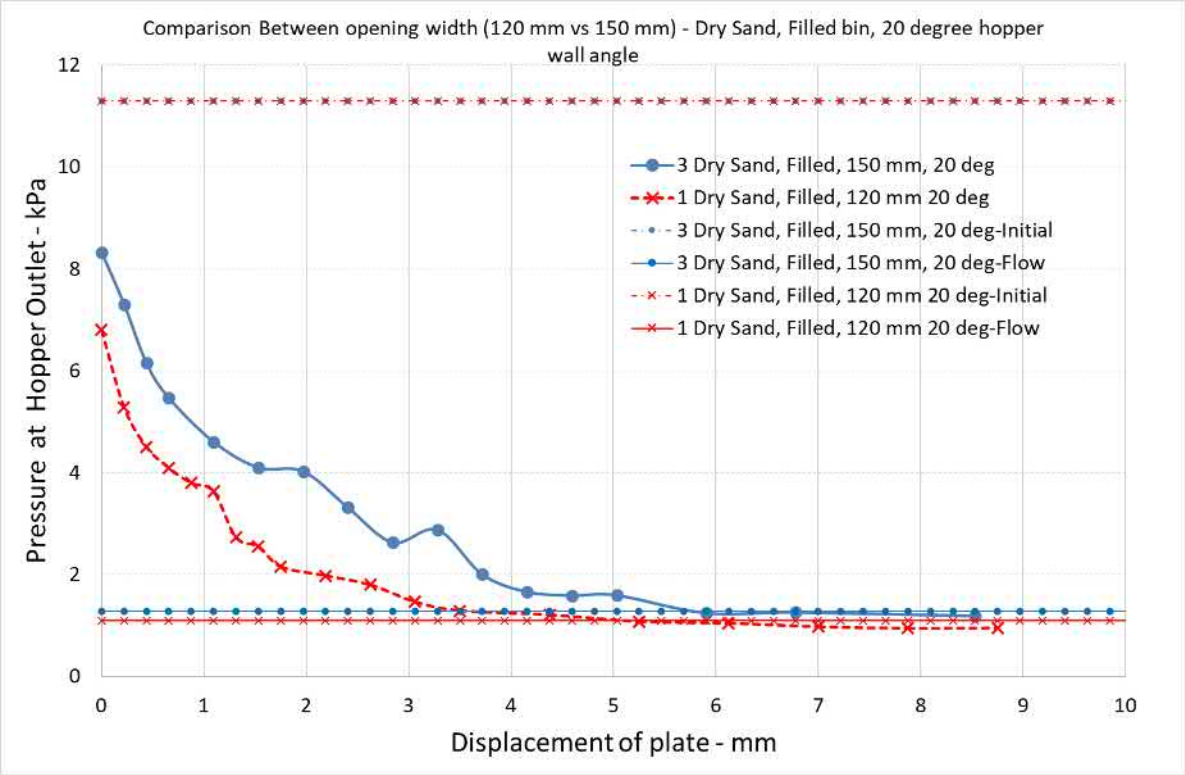


Figure 5-18 Comparison of the effect of outlet opening width - dry sand, filled bin, 20-degree hopper

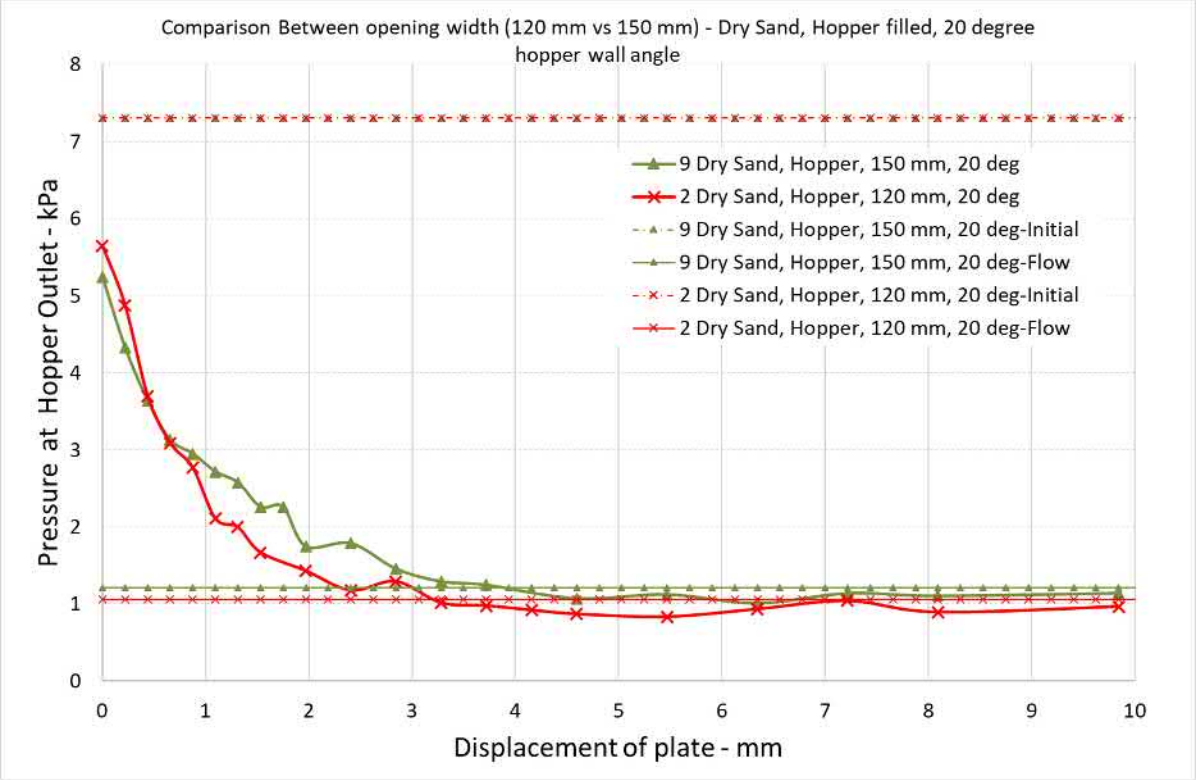


Figure 5-19 Comparison of the effect of outlet opening width - dry sand, hopper filled, 20-degree hopper

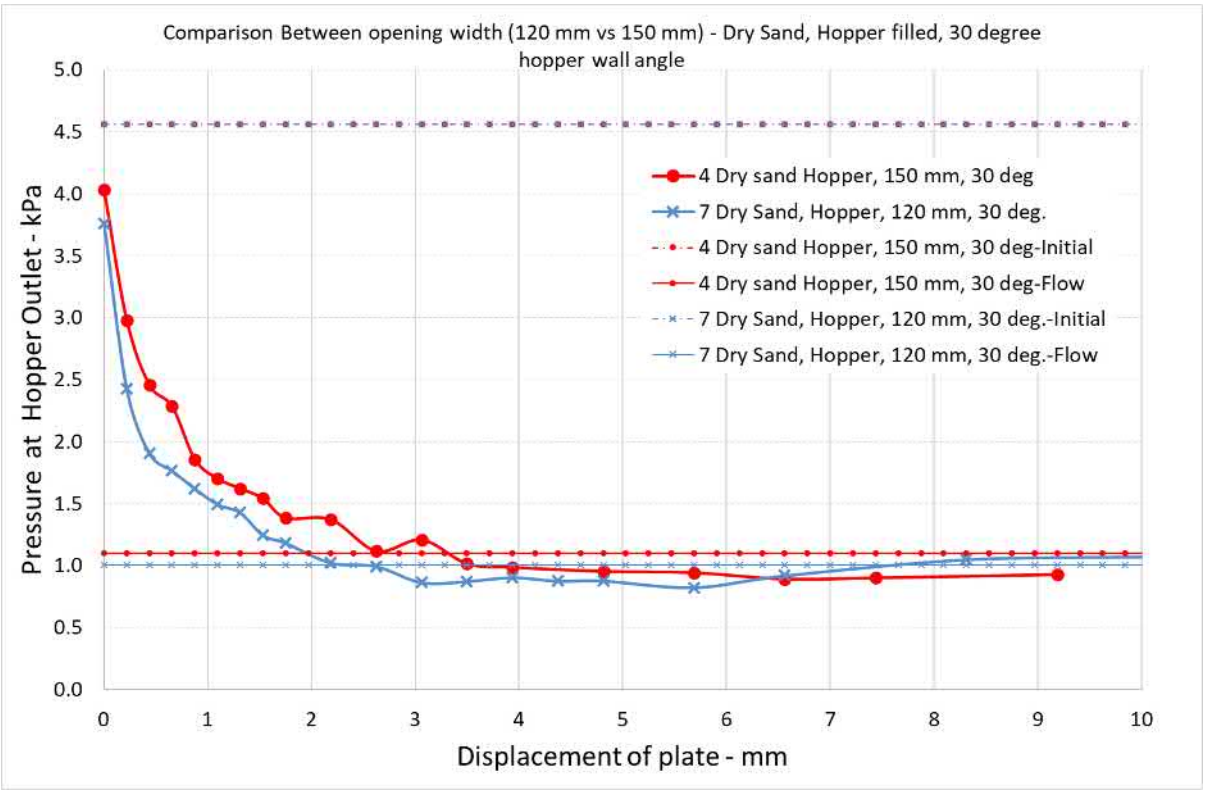


Figure 5-20 Comparison of the effect of outlet opening width - dry sand, hopper filled, 30-degree hopper

5.14.4 Variation of fill configuration (fixed materials, angle, and opening width)

The comparisons between behaviours of variation in bin fill configuration are shown in Figure 5-21, Figure 5-22, and Figure 5-23. The configurations are based on 120 mm, and 20-degrees, 150 mm, and 20-degrees, and 12o mm and 30-degrees respectively, in all cases with dry sand,

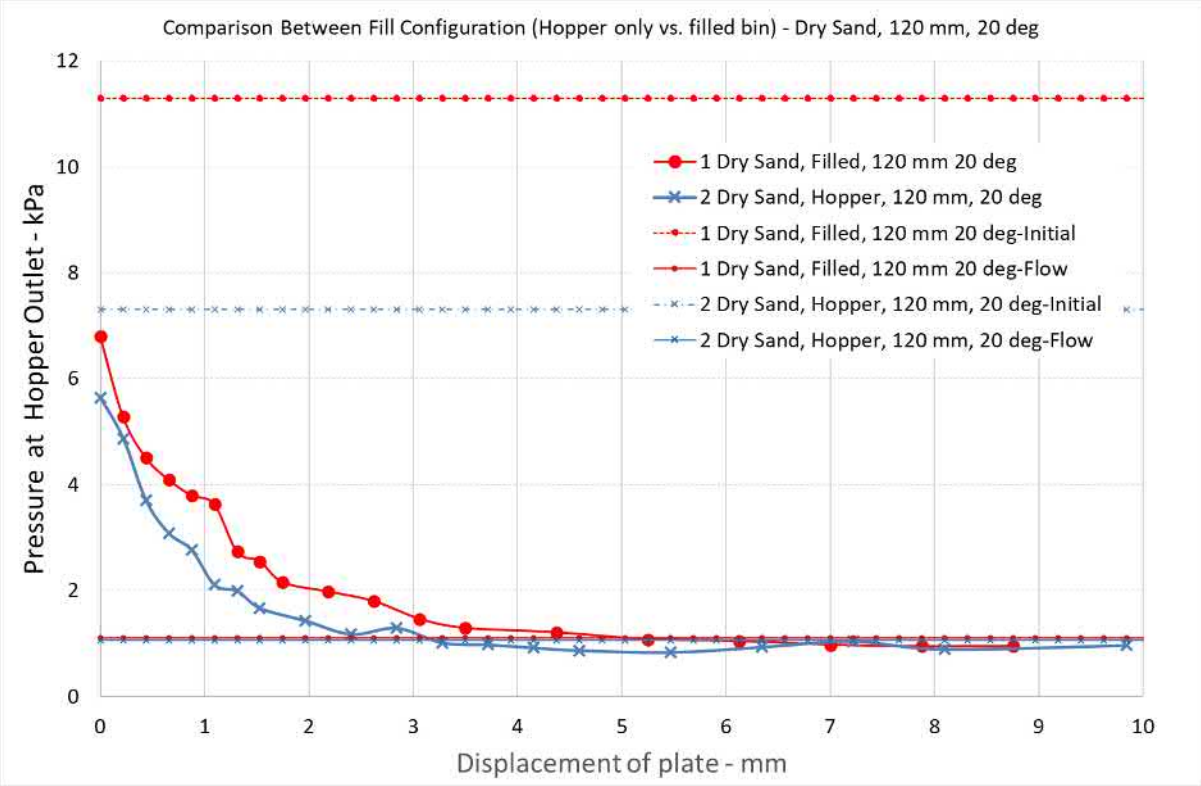


Figure 5-21 Effect of fill configuration, hopper only vs. filled bin, dry sand, 120 mm, 20-deg

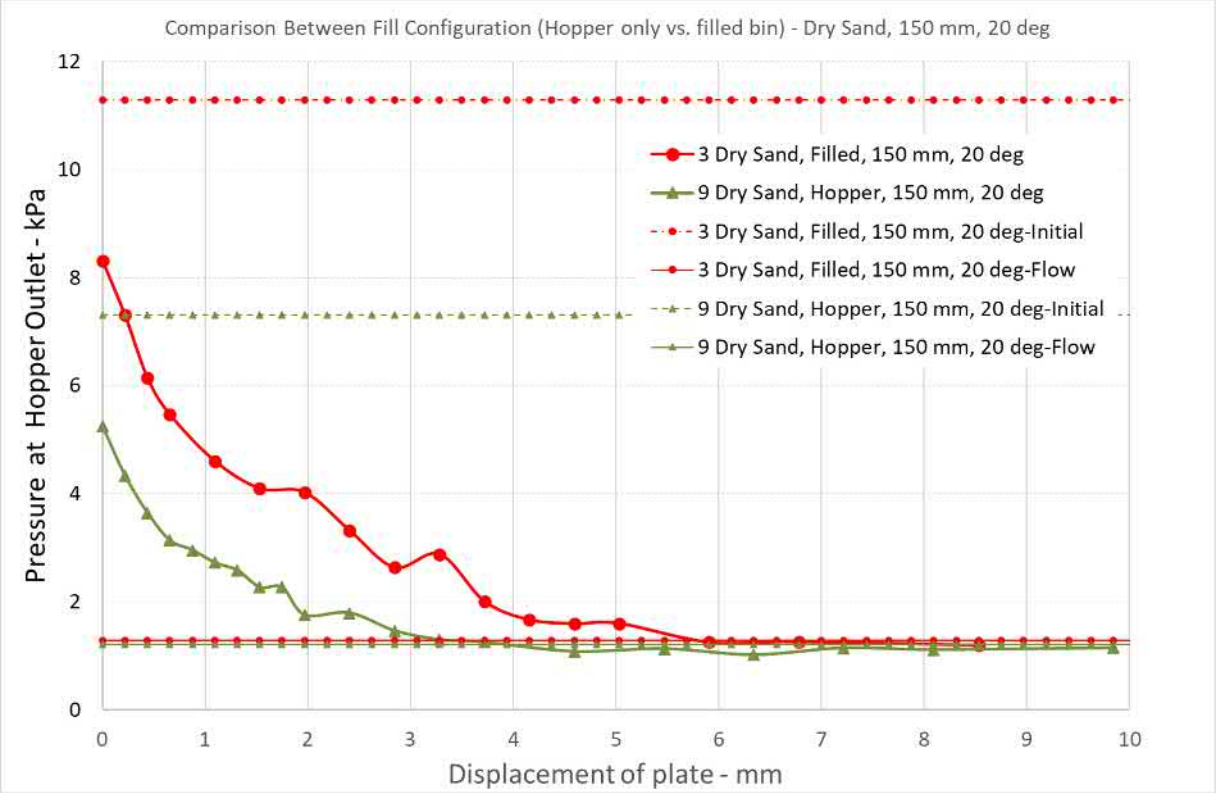


Figure 5-22 Effect of fill configuration, hopper only vs. filled bin, dry sand, 120 mm, 20-deg

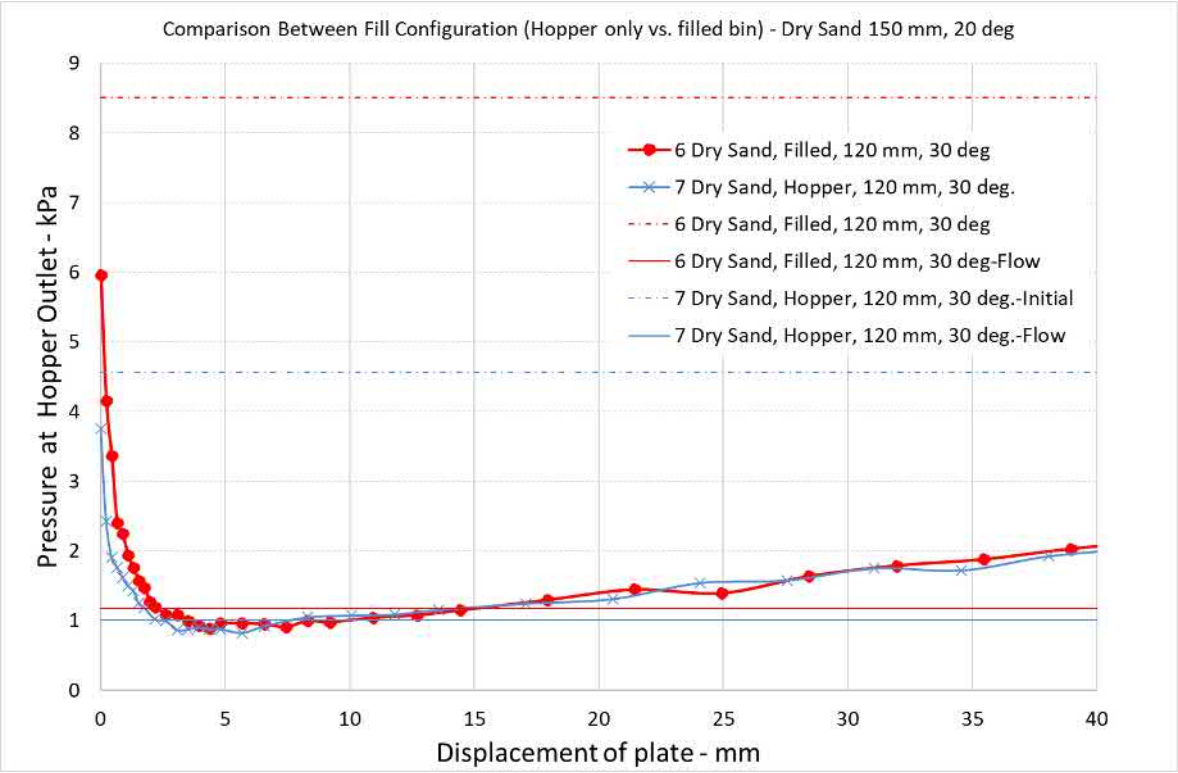


Figure 5-23 Effect of fill configuration, hopper only vs. filled bin, dry sand, 120 mm, 20-deg

5.14.5 Variation of wall friction (fixed materials, angle, fill configuration and opening width)

The comparative graph of wall friction materials is apparent as shown in Figure 5-24.

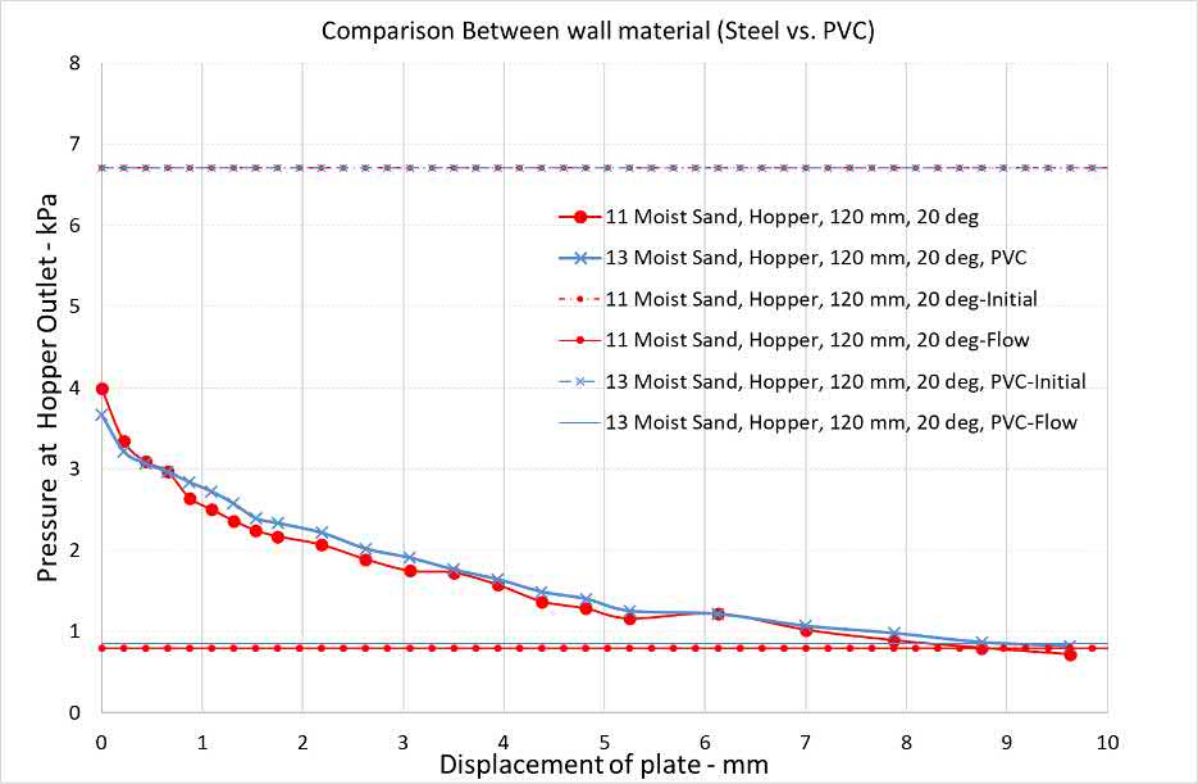


Figure 5-24 Effect of wall friction at hopper surface

5.14.6 Variation of rate of filling (fixed all other parameters)

Figure 5-25, shows the effect on dry sand of compaction during filling for two configurations 150 mm opening width and 120 mm opening width.

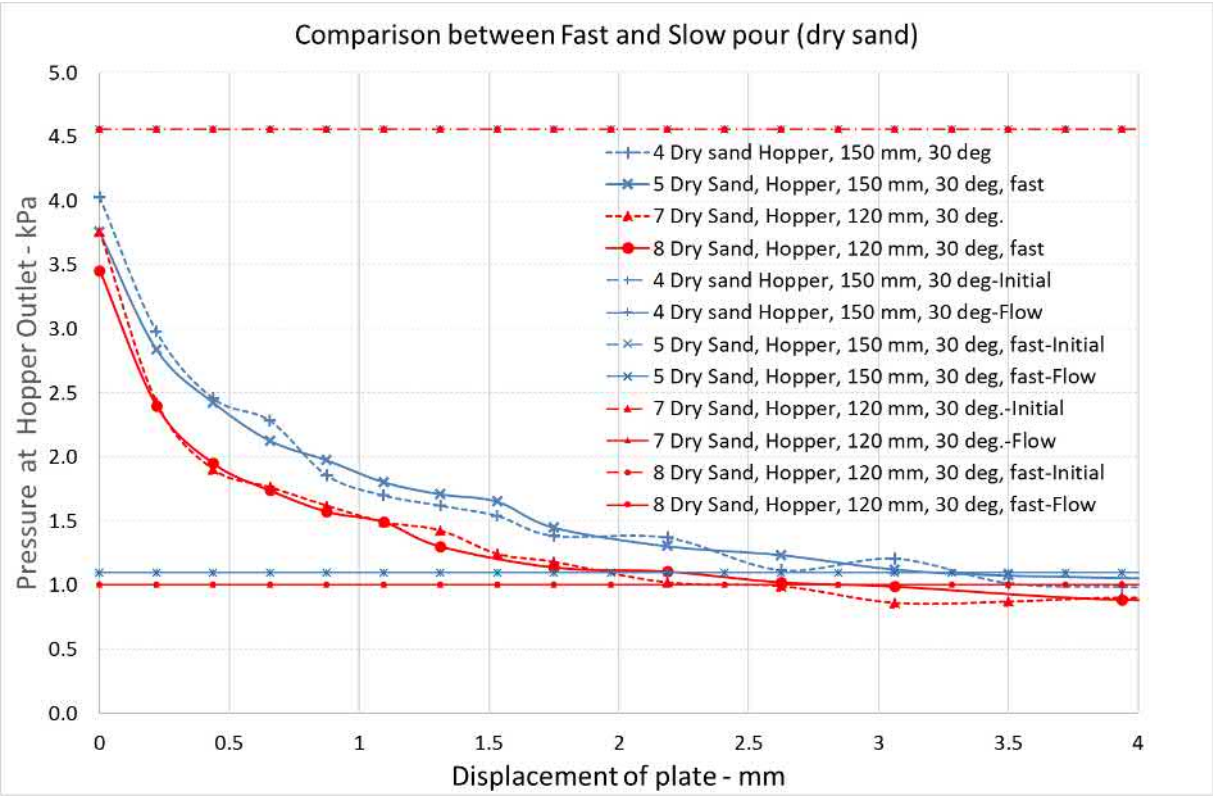


Figure 5-25 Fast-pour compaction effects - dry materials

Figure 5-26 shows the same consideration for moist sand.

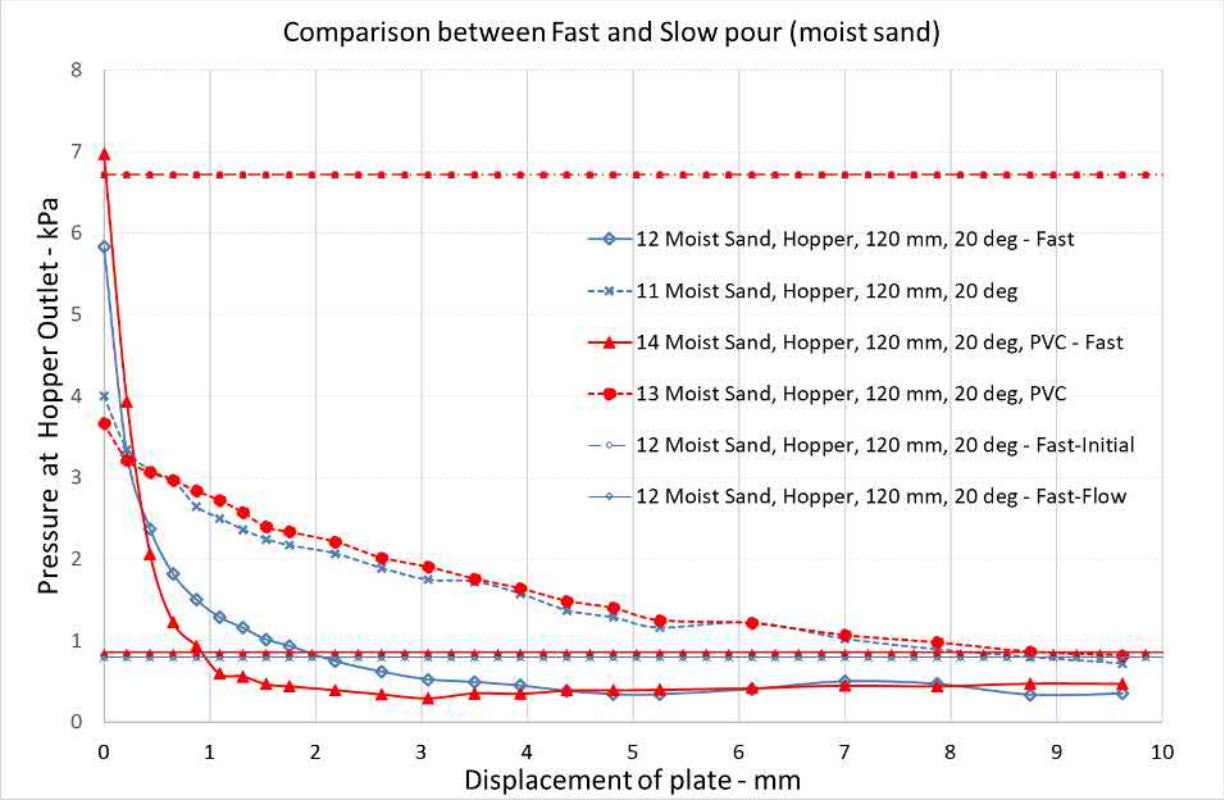


Figure 5-26 Fast-pour compaction effects - moist (cohesive) materials

5.15 Overall summary of pressure reduction rates, all cases

An overall view of the behaviour of each test case, in terms of rate of pressure reduction to 50% and to 80% from measured to initial flow case is shown in Figure 5-27. In each data set, the first data point represents the feeder plate deflection to 50% and the second, to 80%.

The vertical axis shows the averaged rate of pressure reduction from the measured initial pressure to the measured flow pressure. The horizontal axis shows the deflection of the feeder plate, as a function of the hopper opening width.

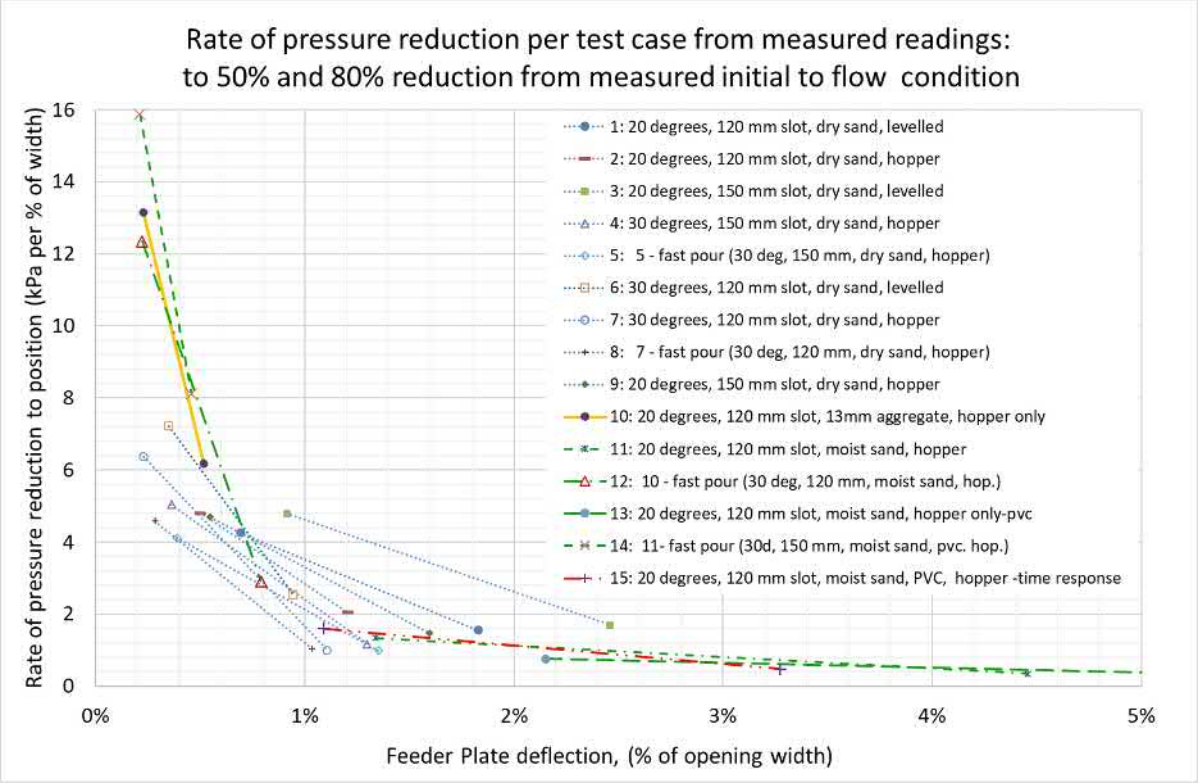


Figure 5-27 Rate of pressure reduction per test case, to 50% and 80% reduced

Overall trends per material type as noted in the above sections, are observable. For example, aggregate, with reduction of 50% at and 80% at 0.23% and 0.52% of opening width respectively. It is also observable that this case showed a rapid rate of pressure reduction as a percentage of opening width, of 13.2 kPa per percentage of opening width to the 50% reduced pressure state. The dry sand cases showed moderate rate of pressure reduction, whereas the moist sand (dashed lines at bottom of graph) showed low rates of pressure reduction. The two fast-fill cases for moist sand (case 12 and 14) showed very steep rate of pressure reduction due to the compacted state at the outlet.

Chapter 6 Discussion

6.1 Introduction

This chapter presents a basis for interpreting the results in terms of theoretical understanding. The discussion includes development on the reasonings behind expected behaviours of each test and explores possible reasons for the deviations from calculated loads.

Comparisons between various test sets are made in order to isolate the behaviours relating to each major parameter in order to characterise these.

6.2 Effects of material properties

Bulk material flow properties affect the forces and flow behaviour in any bulk handling system to a significant extent. Especially, the compressibility, internal friction, wall friction, and cohesiveness are expected to predominate.

Materials with high friction properties (both internal and against wall surfaces) will tend to limit the transfer of loads to the lower portions of a bin and will instead transfer a larger portion of their loads onto the bin and hopper walls with the result that loads onto the lower areas of the hopper, and onto the feeder will be lower than would be the case for low friction properties.

Internal strength due to cohesion and pressure-induced consolidation has the effect of presenting a high internal friction angle, which has the same effect of limiting the pressures.

All the above properties are included in the methods defined by Roberts [4] and [6] for initial and flow pressures (also as described in Appendix A). Compressibility is, however, not included in any of the calculations because they are all based on a fixed density parameter.

Jenike and Johanson's method [3] uses the compressibility coefficient to predict behaviour in a hopper as a result of compressibility, which causes the position of the maximum initial pressure to shift higher into a the hopper. This same mechanism has the effect of lowering the pressure at the hopper outlet, because the relevant loads resolve to a position higher in the hopper. No basis is presented for calculating the consequent reduction in the feeder initial pressures, but it is expected from this analysis that compressible materials will achieve a

lower initial pressure at the outlet than would be the case for an incompressible material with similar friction properties.

A highly compressible bulk solid will have a greater effect of cushioning the material above, by yielding to pressures from above, and allowing a partial transition to an arched stress field, even without movement of the feeder or plate underneath.

Based on the above, it is reasonable to expect that low friction, free-flowing materials with low compressibility would show high initial pressures onto the feeder.

This leads to an expectation that the three material properties chosen would present properties and behaviours as listed in Table 6-1

Table 6-1 – Expected behaviours of the selected materials

Property or Behaviour	**Quartz Aggregate**	**Dry Sand**	**Moist Sand**
Compressibility	Very low	Low, but higher than Quartz aggregate	High
Cohesion property	Zero cohesion	Zero cohesion	Notable cohesion effects
Initial pressure (expectation)	High, near to theoretical	High	Relatively low
Rate of pressure reduction (expectation)	High	High	Relatively low

On consideration of material lump size, it is essential that firstly the opening dimension is at least four times the maximum lump size in order to avoid mechanical arching as noted by Roberts [4]. Comparing the minimum hopper opening width (120 mm) to the nominal maximum lump size of the aggregate (13 mm), it is apparent that mechanical arching is not possible (120 / 13 = 9.2, and 9.2 > 4). Cohesive arching or funnel flow within the bin may have been possible, depending on the cohesive properties. These effects were however not observed and in all cases, material drew out from the bin without forming a stable cohesive arch (a blockage to the flow), and it was apparent from the clear Perspex side of the bin that material movement took place across the full width of the bin .

Common understanding of bulk flow properties, as outlined by Jenike [2], defines that cohesive flow properties are governed by the small particles (4 mm and smaller, and especially in the less than 250 um range). Materials that do not contain particles in this size

range would have minimal to zero cohesiveness at any moisture level and would, therefore, be free-flowing, with low internal friction.

Considering dry, cohesionless material, the expectation is that wall friction angle and internal friction angle will be relatively low compared with a moisture containing material with fine material present.

In considering which particle sizes would be more prone to a rapid switch between the peaked (initial) to the arched (flow) condition, consideration is necessary to determine the mechanism by which the direction of the principal stress is re-oriented. The rate of change of the loads relates directly to the rate at which the re-orientation of principal stress fields takes place.

If the mechanism requires that the particles must re-orient themselves, then it could be expected that large lumps would require more movement in the bed in order to re-orient or reposition themselves than would be the case with small lumps.

If however the re-orientation of the stress field is based on the particles remaining in their previous orientations, but that only the stress fields change orientation due to small movements of the overall material bulk, then this stress field orientation is not dependant on individual particle re-orientation. In that case then, larger particle size should not require larger movement of the material bulk than for the small lump size materials.

A comparison of how coarse and fine materials respond to material withdrawal (how quickly they effect the pressure switch) can provide insight into whether the load re-orientation is by particle re-orientation or by bulk movement without required particle re-orientation.

The behaviours of the various materials can be seen in Figure 5-14 where the pressure behaviour on the feeder plate is plotted against the feeder plate displacement for aggregate, dry sand, and moist sand, and an additional case of a PVC hopper wall material. These are also plotted against their analytically calculated initial and flow pressures.

Secondly, in relation to the internal material pressures, the quartz aggregate experienced the highest initial pressures, and this case also presented the fastest drop off in pressure.

After the concrete aggregate, the next highest loaded and fastest reducing pressure was that of the dry sand, which, due to no cohesion and low compressibility, as well as low friction properties, also demonstrated a high initial, and fast reducing, pressure.

The moist sand, with higher internal friction and compressibility, as well as the effects of cohesion which further increase the internal friction, demonstrated significantly lower initial pressure and slower transition to the flow condition as a result of induced flow.

Lastly, for the case of increased wall friction with lining by PVC, the initial pressure was lower than the equivalent case with the unlined steel surface, and the rate of pressure drop-off was slower than was the case for the lower-friction steel case.

The tests performed on moist sand that included compaction by momentum effects, resulted in high initial pressures and rapid reduction of pressure with onset of flow. Effects due to compaction were not observed with dry materials.

6.3 Comparison to theoretical calculations

The theoretical calculation of loads at the hopper outlet only provide reference loads for initial and flow pressures for each test set. These are useful for observing the actual pressures encountered and whether they are in general higher or lower than the predicted values. The measured values and their behaviour during feeder plate lowering, is the subject of the present research.

In terms of analysis of different material tests, and their pattern of pressure reduction during withdrawal it is only important to identify which material sets present more or less friction than each other. This is sufficient to make an appropriate comparison.

To give some insight into the selected material friction properties and the actual pressures encountered, as well as how these can affect the initial and flow pressures, a sensitivity analysis has been provided in Appendix E.

6.4 Hopper wall angle

Because of the nature of the test rig, which alters the angle by lifting up the outlet and sliding the wall angles upward, there is less hopper height present for the 30-degree wall slope case than for the 20-degree wall slope. Therefore, the differences observed between the pressure

behaviours of the two cases also relate to the system depth. It is therefore not straightforward to isolate the effect of the wall angle compared to the hopper depth dimension.

Although angle cannot be isolated without also introducing the height difference between test configurations, it is still interesting to see whether pressure reduction ratios and rates were significantly different as a function of the slope angle.

From Figure 5-15, Figure 5-16, and Figure 5-17, it can be observed, that the shallower angle (30°) hopper case displays a more rapid drop-off in pressure than does the steeper angle (20°) hopper. This is the case even though the steeper case has more initial pressure to disperse than the shallower angle case has. This may be contributed to by the effect that the 20-degrees hopper case does not reach as high a percentage of its calculated load (65%) than the 30-degrees hopper case does (69%). This is to be expected because it is typical for deep hoppers with narrow hopper width to transmit loads less effectively than wider hoppers due to the edge effects, which are expected to be more significant for a steeper hopper wall (as per discussion of Roberts [4] in Section 2.2). This 4% difference is, however, not sufficient to explain why the 30° hopper experiences faster drop-off than the 20° hopper does. The data suggests that the stress fields are re-oriented more rapidly for a shallower wall hopper than they are for a steep wall hopper.

To summarise the difference in rate of reduction in pressure of 20-degrees vs. 30-degrees, consider the parameters according to Table 5-1, which indicate for the required displacements, summarised in Table 6-2. This clarifies how in each case, the 20-degree example requires more displacement as a percentage of opening with to achieve 50% and 80% reduction than the corresponding 30-degree example does.

The hopper wall angle effects are summarised in Table 6-2.

Table 6-2 - Effects of variation to, hopper wall angle

		Displacement to cause reduced load to:			Displacement as % of width		Rate of load reduction
Case No	Description	min (mm)	50% (mm)	80% (mm)	50% load	80% load	
1	20-degrees, 120 mm slot, dry sand, levelled	10.5	0.8	2.2	0.69%	1.83%	Low
6	30-degrees, 120 mm slot, dry sand, levelled	4.4	0.4	1.1	0.35%	0.95%	High
9	20-degrees, 150 mm slot, dry sand, hopper	6.3	0.7	1.9	0.45%	1.32%	Low
4	30-degrees, 150 mm slot, dry sand, hopper	6.6	0.4	1.6	0.31%	1.12%	High
2	20-degrees, 120 mm slot, dry sand, hopper	5.5	0.6	1.4	0.50%	1.20%	Low
7	30-degrees, 120 mm slot, dry sand, hopper	5.7	0.3	1.3	0.23%	1.11%	High

6.5 Hopper opening width

From Figure 5-18, Figure 5-19, and Figure 5-20, it can be seem that results from the variations between hopper opening width are more closely comparable than wall angle variations. This is because overall height of the loading configuration is unchanged between cases, and initial loading is only a function of surcharge pressure and depth of the sloped hopper, as noted by Roberts [5].

It would have been expected to observe a higher initial pressure for the case of the wider gap opening case, because of reduced local and edge effects present with a wider opening. This effect was apparent for the 20-degree case with filled bin and is observable as being marginally the case for the 30-degree case with only hopper filled. The case of only hopper filled with 20-degree wall angle however, presented a deviation from this expectation and it was seen that the 120 mm case showed higher initial pressure. This deviation may be due to a small variation within the experimental method. Overall, however, it is expected that the pressures would be similar between the various cases because the overall height from the top of material to the outlet is a constant across the comparable cases.

It is apparent that for the case with filled bin (refer Figure 5-18), which applies greater surcharge pressure onto the hopper, that a wider hopper opening (150 mm) presented a higher initial pressure than the narrower (120 mm) opening did. This was to be expected due to reduced local effects and edge effects at the outlet of the 150 mm case compared to the 120 mm case. This is consistent with the discussion in Section 2.2 per Roberts [6].

By contrast, the cases with only hopper filled, (refer Figure 5-19, and Figure 5-20), indicated a closer similarity of initial pressure between the two cases. This may be related to the absence of loads from the hopper above which would provide necessary pressures to cause edge effects due to compressibility and local deflections at the bottom of the hopper. With those effects absent, or present to a lesser degree, it is feasible that the initial pressures would be more similar between the cases.

The feeder plate deflection needs to be considered in terms of the varied hopper opening width and not purely on the basis of the recorded distance of deflection. This is because for example, a plate displacement of 1 mm with a 120 mm bin opening width (where this is 0.83% of opening width) is more significant than for a 150 mm width, (where it is only 0.66% of the opening width). A set of data for a 150 mm opening gap may therefore show a higher rate of reduction on a linear basis, but not on an equivalent basis with deflection defined as percentage of opening width.

When comparing plate displacements on the basis of percentage of hopper opening width, it is apparent only for the case with full loaded bin, that the narrower opening led to a more rapid reduction in pressure as result of the plate displacement. The difference in the rate was however small, differing only by approximately a factor of 10% between the two cases.

The cases with the hopper filled were not significantly varied between the two cases, possibly due to less significant pressures forcing the development of the arched stress field.

The summary of the effects of hopper width variation is shown in Table 6-3.

Table 6-3 Effects of variation to hopper opening width

		Displacement to cause reduced load to:			Displacement as % of width		Rate of load reduction
Case No	Description	min (mm)	50% (mm)	80% (mm)	50% load	80% load	
1	20-degrees, 120 mm slot, dry sand, levelled	10.5	0.8	2.2	0.69%	1.83%	High
3	20-degrees, 150 mm slot, dry sand, levelled	12.0	1.1	3.0	0.76%	2.04%	Low
9	20-degrees, 150 mm slot, dry sand, hopper	6.3	0.7	1.9	0.45%	1.32%	Neutral
2	20-degrees, 120 mm slot, dry sand, hopper	5.5	0.6	1.4	0.50%	1.20%	Neutral
4	30-degrees, 150 mm slot, dry sand, hopper	6.6	0.4	1.6	0.31%	1.12%	Neutral
7	30-degrees, 120 mm slot, dry sand, hopper	5.7	0.3	1.3	0.23%	1.11%	Neutral

6.6 *Fill configuration (hopper only or filled bin)*

In comparing the level of fill in each bin configuration the expectation would be that the additional pressure from the upper portions of the bin will lead to an initial pressure at the outlet to be higher than the hopper only pressure, as is per the calculated case.

The effects of varying fill configuration for dry sand are shown in Figure 5-21, Figure 5-22, and Figure 5-23.

It is apparent that for the filled bin case, initial pressure was a lower percentage of calculated initial pressure than for the case with only the hopper filled. This was noted for all three comparisons. This was likely due to the higher pressure at the bottom of the hopper causing increased consolidation and deflections, thereby resulting in some load support from a partially formed arched stress field in the to the material in the hopper developing as per the description from Jenike & Johanson [3].

The slopes of the pressure curves as a function of the bottom plate lowering are very similar in each case regardless of the level of bin fill. This is likely due to the geometric effects that lead to re-orientation of the pressure fields in the lower portions of the hopper being constant as a function of the slope and opening width parameters.

The comparative results are shown in Table 6-4.

Table 6-4 Effects of variation to fill configuration

Case No.	Description	Displacement to cause reduced load to:			Displacement as % of width		Rate of load reduction
		min (mm)	50% (mm)	80% (mm)	50% load	80% load	
1	20-degrees, 120 mm slot, dry sand, levelled	10.5	0.8	2.2	0.69%	1.83%	Low
2	20-degrees, 120 mm slot, dry sand, hopper	5.5	0.6	1.4	0.50%	1.20%	High
3	20-degrees, 150 mm slot, dry sand, levelled	12.0	1.1	3.0	0.76%	2.04%	Low
9	20-degrees, 150 mm slot, dry sand, hopper	6.3	0.7	1.9	0.45%	1.32%	High
6	30-degrees, 120 mm slot, dry sand, levelled	4.4	0.4	1.1	0.35%	0.95%	Neutral
7	30-degrees, 120 mm slot, dry sand, hopper	5.7	0.3	1.3	0.23%	1.11%	Neutral

6.7 Wall material

The inclined chute test demonstrated that the wall friction angle for hopper walls lined with PVC sheeting was slightly higher than for plain steel. However, the test that was performed did not directly measure this wall friction angle.

From Figure 5-24 it can be seen that the minimum pressure (consistent with the flow case) is observed to be lower than for the higher friction case, which is consistent with the calculated parameters as a function of wall friction angle. The rate at which the pressure reduced from initial state, was seen to be less rapid when wall friction was higher. This is consistent with the expected behaviours from above sections where it is generally apparent that force retarding effects have the consequence of a slower reduction in pressures as a result of bottom plate displacement.

The comparative rate of reduction as a result of wall friction are shown in Table 6-5.

Table 6-5 Effects of variation to wall friction

Case No.	Description	Displacement to cause reduced load to:			Displacement as % of width		Rate of load reduction
		min (mm)	50% (mm)	80% (mm)	50% load	80% load	
11	20-degrees, 120 mm slot, moist sand, hopper	56.0	1.6	5.4	1.34%	4.46%	Low
13	20-degrees, 120 mm slot, moist sand, hopper only-PVC	17.5	2.6	7.1	2.15%	5.87%	Lowest

6.8 Rate of filling

From comparing Figure 5-25 and Figure 5-26, it is apparent that the cohesive effects of the moist sand result in higher initial pressures and more rapid reduction in pressures, whereas with dry sand there is negligible effect.

Pouring material into the hoppers at a high rate causes inertial forces due to the material deceleration as it lands onto the hopper surfaces and onto material already in place in the hopper. Materials with low cohesion are not affected significantly, whereas cohesive materials (mostly materials with moisture) undergo pressure induced consolidation which causes higher pressures and greater unconfined yield strength.

The large divergence between the fast poured PVC lined case compared to that of plain steel as shown in Figure 5-26 is not indicative specifically of effects from the wall friction properties, but is a consequence of the experimental procedure. In both cases, the buckets of test material were poured as fast as practicable, but in the case of the PVC test, this was done slightly faster and more effectively than for the plain steel case.

The result was that larger compaction pressures were present for the PVC- fast fill case, and the effect of the additional compaction is apparent from the test results: a significantly higher initial pressure, and more rapid pressure reduction as a function of plate deflection.

These results are summarised on Table 6-6.

Table 6-6 Effects of variation to filling rate (cohesive materials)

Case No.	Description	Displacement to cause reduced load to:			Displacement as % of width		Rate of load reduction
		min (mm)	50% (mm)	80% (mm)	50% load	80% load	
11	20-degrees, 120 mm slot, moist sand, hopper	56.0	1.6	5.4	1.34%	4.46%	Very low
12	20-degrees, 120 mm slot, moist sand, hopper - Fast Fill	10.5	0.3	0.9	0.22%	0.79%	Very high
13	20-degrees, 120 mm slot, moist sand, hopper only-PVC	17.5	2.6	7.1	2.15%	5.87%	Very low
14	20-degrees, 120 mm slot, moist sand, hopper only-PVC - Fast Fill	3.1	0.3	0.6	0.21%	0.46%	Very high

6.9 Time effects

The results from the time effect test are shown in Figure 5-11, Figure 5-12, and Figure 5-13.

It was apparent that on each occasion that the nut and plate were lowered, the initial load reduction was significant, but had not yet stabilised. In the seconds immediately after lowering the nut/plate, the load started to rise back up slightly, faster at first, and then slowing to a case where it was stable after approximately 5 minutes.

The magnitude of the load after stabilising was typically about 10% higher than the initial load measured immediately after adjustment of the nuts. The reason for this time effect was apparent when looking through the Perspex sheet at the mass flow hopper, in that small

material movements were observable while the material settled into a stable state as noted in Section 4.3. The transient state where the material has been withdrawn but not yet been replaced from the bin leads to a period where the material continues to gain additional pressure onto the bottom plate.

This analysis of the time effects demonstrates that the rate of withdrawal from a hopper has a relationship to the loads that are encountered and this manifests over a period of several minutes after material movement is stopped.

6.10 Increasing pressures on hopper

It was observed that the pressures of some material sets reached the minimum consistent with the flow case, but then started to increase significantly after passing the minimum pressure. As an example, see the results for test Set 7 in Figure 5-6.

It was verified that the data included in this set were calculated correctly, including the subtraction of the weight of material withdrawn from the hopper. It was also confirmed that the uncertainty related to bulk density and repose angle (+3.5% and -7.1%) was low compared to these measured values. It is not fully clear what was the cause for this pressure rise. It is apparent that this effect was most pronounced when:

- Material was dry sand (not aggregate, and not moist sand)
- Only the hopper section was filled (the bin vertical section was not filled)

In this example from Set 7, the increase in load was from an approximate minimum of 47 N, to a maximum of 122 N. With a bulk density of 1504 kg/m^3, (bulk weight of 14757 N/m^3) this represents a material volume increase of 3.39 dm^3. Considering that the measured slot width was 140 mm for test Set 7, with a length of 480 mm, this in turn represents an additional effective 50 mm of material head at the hopper outlet, in addition to the pressure noted from the minimum pressure noted as the flow state.

The author was not able to fully explain this effect from theory. However, it is feasible that the effect resulted from material above the outlet that was not supported by the arched stress field. A similar dynamic was observed by Guo [10]. Figure 6-1 below, depicts this effect.

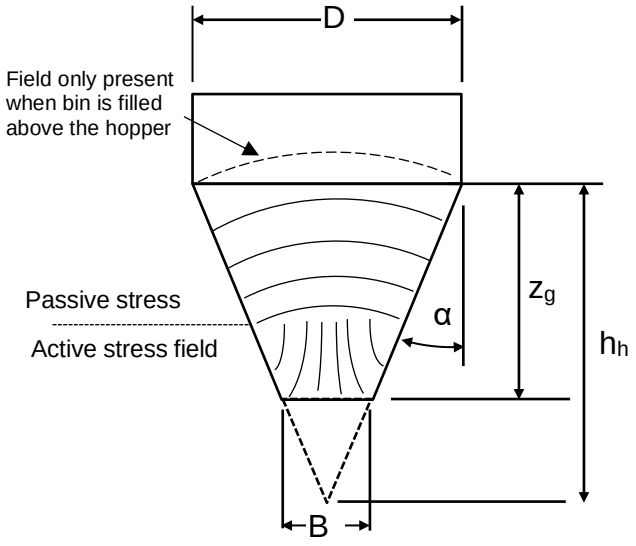


Figure 6-1 Stress field at hopper outlet, when presenting higher than expected loads [10]

It would be a reasonable expectation that this phenomenon would be more pronounced with free-flowing material than with cohesive material. This is because cohesive properties would limit the release of material from the arched zones.

There is not clear reasoning why the sand (and not the aggregate) would present the large, increasing pressures. A possibly consideration is that the aggregate is more able to form a steady arch than the dry sand due to the angular nature of the material, or that the lower compressibility forms a more steady arched stress field.

This bottom, unsupported portion of the material load as shown in Figure 6-1 is a likely configuration that may lead to such a scenario where the material draws out and subsequently leads to increasing pressure at the hopper interface.

6.11 Review of experimentation methods

After completion of the testing program and analysis, the following notes can be made relating to the experimental methods and equipment.

- It is essential to record the actual set up parameters of each test set, which will not exactly match the nominal slope angle and width parameters.
- The careful loading of the material into the hopper is critical when using cohesive materials, the method used was to use a small hand trowel, which is acceptable practice,

however a sufficient bed must be gently placed over the opening to a depth of at least two hopper opening widths.

- When taking measurements, it is important to ensure that a test set uses consistent number of rotations of each increment, and the change from one eighth to one quarter turns should be made after an integer number of full rotations, never at a partial rotation. This simplifies the processing of data by avoiding the need to fill in values not measured.
- The delay between turning the nuts and recording the voltage should be as short as practicable and should be a consistent time delay in order to result in clear, repeatable data. It is not necessary to wait for the pressure to stabilise prior to lowering the plate further.
- The repose angle of the material should be recorded as a useful reference to reduce uncertainty from data processing.
- Care should be taken to not bump the test rig during operations or to turn a nut in the incorrect direction or by the incorrect amount.
- The calibration range of the loadcells can be revisited in terms of the intended range of the test. Towards the range of less than 10% of the rated load, the accuracy reduces, but an appropriate calibration curve can improve the loadcell accuracy.

6.12 Summary and response to research questions.

Summarising the observations of the individual test results listed in Chapter 5 and in this chapter, it is apparent that it is feasible for a range of material sets and loading configurations, that small deflections of the feeder plate lead to significant reductions in the measured pressures. This is especially the case for the first few quarter turns of the adjustment nuts, which represents a small movement of less than a millimetre.

The rapid reduction of pressure is especially pronounced for the course dry material which behaves in a more elastic fashion than does the finer sized material.

It is notable from Table 5-1 that all but one case demonstrated a reduction in pressure by 80% of the difference between measured maximum (initial) and measured minimum (flow) pressures after lowering the feeder plate by less than 5% of the opening width. The exception, which required a displacement of 5.87% of opening width, displayed a comparatively low

initial pressure due to the cohesive properties of the material. This case is Case 14 – moist sand with PVC lined walls, 20-degree hopper, and 120 mm slot opening.

In all cases, the pressure reduction of 50% of the difference was completed after plate lowering of 5% of width or less. The slowest reducing case (also Case 14) required movement of 2.15% of the width to reach 50% reduction. This confirms the first research question.

This also provides insight into the design recommendation that lowering by 5% of width can allow a design load reduction of 80% of the difference between calculated initial and flow loads. This can be inferred also for the slowly filled cohesive material sets on the basis that actual loads, for the slowest responding cohesive materials, did not reach a large percentage of the calculated initial loads (Case 13 only reached 55% of the calculated initial load). Therefore, after movement of 5% of width, the load will be reduced to lower than a value corresponding to initial calculated load, less 80% of the difference between *calculated* initial and final loads. This will be true for cohesive, compressible materials even if the load has not yet reached 80% of difference between *measured* loads.

The average deflection for dry sand to reach the 80% reduction was 1.28% of opening width and the maximum case (Case 3) encountered the 80% reduction after deflection of 2.04%. in that case, the initial pressure was 84% of the calculated pressure, so on the basis of calculated pressure, this maximum case will reach 80% of calculated pressure reduction after less than 2% of deflection. Dry quartz aggregate reached an 80% reduction of total measured pressure reduction after deflection of 0.52% of opening width. These rates of reduction for dry material were significantly more rapid than anticipated prior to commencing the current research.

Therefore, an appropriate design recommendation can be made for start-up loads, with some conservatism. This is that the load state will be at least 80% transitioned from calculated initial load to calculated flow load after deflection corresponding with the material properties listed in Table 6-7.

Table 6-7 Required deflection to achieve 80% load reduction, per material type

Material properties description	Deflection (percentage of opening width)
Coarse material with low compressibility and no cohesion.	1%
Dry, fine material with no cohesion	2%
Moist material containing fines, with cohesive and compressibility properties	5%

This, therefore, confirms the first research question that deflection of 5% of the hopper opening width is sufficient to reduce pressure by the target 80% pressure difference.

To address the second research question, it is apparent from the analysis above that the effects of the nominated parameters were as follows:

- Particle size
  - It was apparent that larger particle size led to lower compressibility, which is likely the reason pressures reduced significantly faster for coarse than for fine material.
- Hopper half angle
  - It was apparent that steeper hopper half angle led to a more rapid transition from initial to flow pressures.
- Opening width
  - From comparative parameters it was apparent that narrower openings led to more rapid switching of the material pressures than wider openings.
- Internal friction
  - It was not conclusively determined that internal friction had a significant effect on the rate of pressure change, although it was apparent that cohesive properties are significant. Firstly, if the bin is softly loaded, the rate of pressure transition is relatively slow, but if loaded rapidly, thereby causing pressure induced compaction, then the rate of pressure reduction is very rapid.
- Wall friction
  - Wall friction was not conclusively noted as a factor affecting the rate of pressure transition.

Overall, it was apparent that compressibility and cohesion had the most pronounced effect relating to the transition of the pressures on the hopper from initial to flow condition.

6.13 Recommendations for operational sized installations

The test program was performed on a small sized test rig with less than 500 kg of material per test. Even so, many of the cohesive effects of bulk materials, which are significant also for larger scale applications have been shown to have an effect in this laboratory-scale example.

Any industrial applications making use of these methods should be validated against a similar application, but this is a preliminary guideline which may be considered for trial on non-critical production equipment, for example, stockpiles with multiple reclaim feeders.

It is recommended that the parameters as listed in Table 6-7 be adopted as a design basis for full operational sized feeders. Equipment should in all cases have sufficient mechanical strength to withstand the theoretically calculated initial loads, but after lowering by the recommended distances, the appropriate 80% reduced loads can be used for the selection of feeder driving equipment.

Chapter 7 Conclusion

A test rig was constructed and used to test a selection of materials in several differing layout and loading configurations, including variation of hopper angle, hopper opening width, height of bin filling and variation of wall slope angles. Three material sets were tested consisting of moist sand, dry sand, and dry aggregate.

The feeder plate underneath the hopper opening was lowered on a screw mechanism and loads measured from loadcells were recorded and analysed to demonstrate the reduction in the pressure onto the plate as a function of the displacement of the plate.

It is apparent that the reduction in pressures due to material drawdown takes place rapidly. Eighty percent of the reduction from measured Initial to measured Flow pressures was seen to take place after an average of 1.28% of hopper opening width for dry sand, and after 2.05% for the maximum case.

Dry aggregate showed an even more rapid reduction, requiring displacement of only 0.52% of opening width.

Cohesion in the sand, caused by moisture, required more displacement to achieve this 80% reduction, after an average of 2.4% of opening width, and maximum case value of 5.87%. 5% is an appropriate design recommendation for use for design considering that measured values are lower than calculated values for moist, cohesive materials.

When cohesive materials were compacted by the inertial forces associated with rapid filling, the initial pressures were significantly higher, but the pressure reduction during onset of flow was much more rapid than in gently loaded cases.

Mass flow feeder systems may be designed with provision to adjust vertically by a distance of 1% of opening width (for coarse, near-incompressible and free flowing materials), 2% of opening width (for fine, cohesionless materials with low compressibility) or up to 5% of opening width (for moderately cohesive, compressible materials). This design feature will make it acceptable to design the feeder mechanical components to withdraw at a load reduced by 80% of the difference between the calculated initial (active) and the flow (passive) loads. This recommendation excludes structural components, which must comply with statutory design codes based on maximum possible theoretical loads.

7.1 Recommendations for future work

It is appropriate to make the following recommendations for future work:

1. Further study may be performed to evaluate the effects of lowering the plate by a small amount during the loading of the hopper. This would present the effects of a ‘less than rigid’ feeder. Such arrangement may also provide suitable insight into the design to take consideration of flexibility in the feeder mounting arrangement.
2. An additional study may be to explore further the time consolidation effects on the material pressures (beyond approx. 5-10 minutes as done for the present study).
3. The study may be expanded using alternative materials frequently handled in industry, for example mined ores or coal material sets. This may assist to define operational parameters and verify the method for varied bulk density parameters.
4. A theory expanding the initial pressure calculation on the hopper outlet as a function of material compressibility, wall friction, internal friction and cohesive properties may be investigated.
5. The phenomenon described in Section 6.10, whereby pressure reduces during transition from initial state to flow state, but then increases again due to unsupported portions of material at the hopper outlet is interesting and is worth further investigation.
6. It would be useful to collate some similar test parameters (initial, running, and a time response of the torque on the drive), from full scale operational facilities which may give useful insights into the actual starting and running tensions of the belt feeder/hopper or gate system.

References

[1] Janssen, H.A. (1895). *Versuche über Getreiderdruck in Silozellen,* Verein Deutscher Ingenieure, Zeitschrift, V.39, Aug. 31 1895. 1045-1049

[2] Jenike, A.W. (1964). *Storage and flow of solids*. Bulletin no. 123 of the Utah Engineering Experiment Station, University of Utah, Salt Lake City, Utah.

[3] Jenike, A.W., Johanson, J.R. (1968). *Bin Loads* Journal or the Structural Division. Proceedings (American Society of Civil Engineers) 1011-1041

[4] Roberts, A.W. (2009). Characterisation for Hoppers and Stockpile design, The University of Newcastle, NSW, Australia.

[5] Roberts, A.W. (2009). *Bin Wall Loads*, The University of Newcastle, NSW, Australia.

[6] Roberts, A.W. (2009). *Feeding of Bulk Solids 2 – Feeder Interfacing, Loads, and Power focusing on Belt and Apron Feeders*, The University of Newcastle, NSW, Australia.

[7] Arnold, P.C, McLean, A.G, Roberts, A.W. (1982). *Bulk Solids Storage, Flow, and handling*, TUNRA, The university of Newcastle, NSW, Australia.

[8] Holmes, C.P.H. (2011). *Start-up and Running Loads Exerted by Bulk Materials on Belt Feeders – a Comparison between Experimental Results and Predictive Techniques.* Master's Thesis, University of Greenwich.

[9] Roberts, A.W., Beh, B., Shen, J., Chen, B., Donohue, T. (2019). *Investigation of Loads Acting on Flow Isolating Gates in Bulk Solids Storage Bins.* 13th International Conference on Bulk Materials Storage, Handling, and Transportation, July 2019, Queensland, Australia.

[10] Guo, J. (2014). *Investigation of Arching Behaviour Under Surcharge Pressure in Mass-Flow Bins and Stress States at Hopper/Feeder Interface*. PhD Thesis, The University of Newcastle Australia.

[11] Roberts, A.W. (2001). *An Overview of Feeder Design Focusing on Belt and Apron Feeders*, Bulk Solids Handling, Vol 21, Num 1, Jan/Feb 2001

[12] Standards Australia (1996). *AS3774-1996, Loads on Bulk Solids Containers*. Standards Association of Australia. Sydney

[13] Leech, J. (2012). *Belt Feeder Case Study – Application within the DBCT 7X Project*, Presentation at the 9th Bulk Materials Handling Conference, June 2012, Brisbane

[14] McGee, E., Bates, L. (2012). *Design Considerations for Loads on Feeders*, Presentation at the BulkSolids Europe conference, Berlin

[15] Hose, R.S. (2011). *RBCT Phase V Expansion Project Case Study and Focus on Belt Feeder Using DEM (Discrete Element Modelling)* – Presentation at Beltcon 16 conference, Johannesburg

[16] Hose, R.S. (2012). *RBCT Phase V, Belt Feeders and DEM* - Presentation at the 9th Bulk Materials Handling Conference, June 2012, Brisbane

[17] Haupt, C.L., Frangakis, T. (2019). *The displacement needed to transition from initial to flow pressure*, Presentation at Beltcon 20, International Material Handling Conference (IHMC), Pretoria

Appendix A Hopper and gate pressure calculation methodology

The Methodology used for the calculation of the hopper pressures follows the equations and derivation as proposed by Roberts [4] and [6] and the equations and methodologies are summarised and adapted in this section. These describe the basis of the calculation of expected initial and flow pressure for each case.

A.1 Initial Filling Case – Vertical bin Section

The vertical bin section (typically referred to as the cylinder) is the top part of the bin with vertical walls. It is not necessarily cylindrical but can be a square or rectangular prism. When the bin is filled from empty, and no material has yet been withdrawn, the initial filling load case is present.

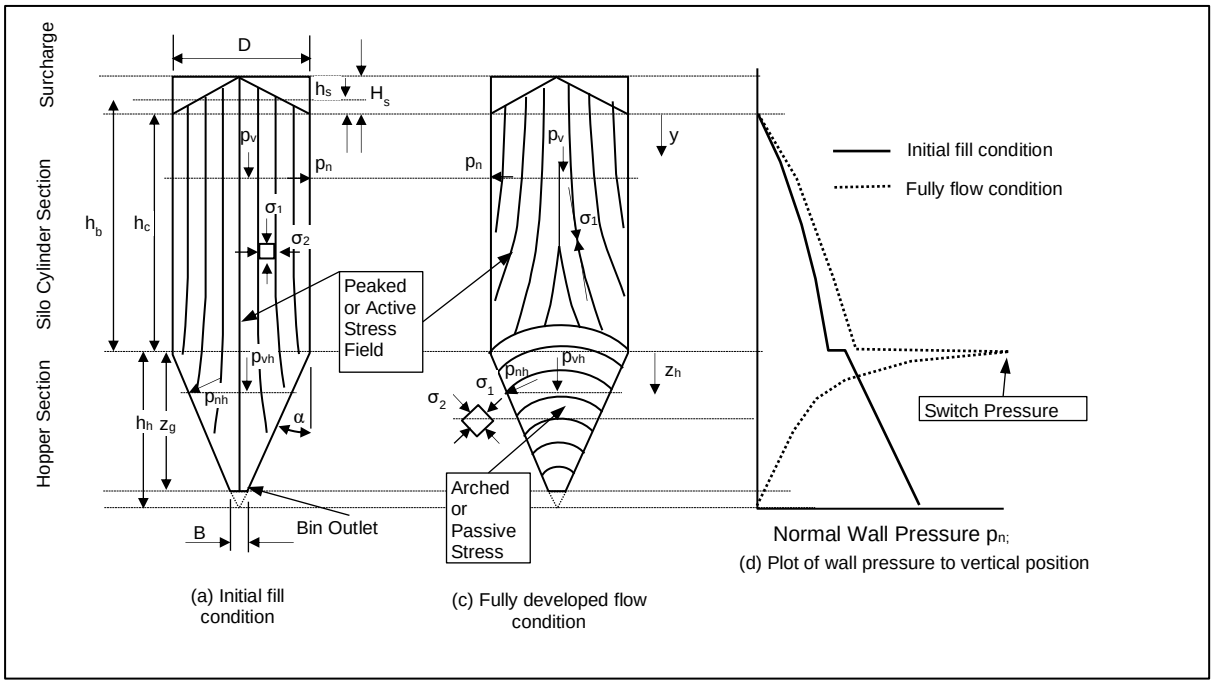


Figure A- 1 Silo principal stress (σ1) fields and normal wall pressures (p_n) based on Roberts [4] pp 3-1

At a depth y as shown in Figure A.1, the average vertical pressure p_v and normal wall pressure p_n are determined by a Janssen equation with an initial surcharge included. The solution to the governing differential equation is:

$$p_v = \frac{\gamma\, r_c}{\mu\, k}\left[1 - e^{-(\mu\, k\, y/r_c)}\right] + p_{vo}\, e^{-(\mu\, k\, y/r_c)} \qquad \text{(A.1)}$$

Where

r_c = Characteristic radius of container (m)

$\gamma = \rho \cdot g$ = Bulk specific weight (N/m^3)

ρ = bulk density (kg/m^3)

g = acceleration due to gravity (9.81 m/s^2)

$\mu = \tan\phi_w$ =coefficient of wall friction (dimensionless)

ϕ_w = wall friction angle (radians)

p_{vo} = average surcharge pressure due to natural surcharge of material (at position y = 0)

k = p_{ni} / p_v = lateral pressure ratio

The normal pressure p_{ni} acting on the wall is given by

$$P_{ni} = k\, p_v \qquad \text{(A.2)}$$

Hence from (A.1) and (A.2),

$$p_{ni} = \frac{\gamma\, r_c}{\mu}\left[1 - e^{-(\mu\, k\, y/r_c)}\right] + p_{vo}\, e^{-(\mu\, k\, y/r_c)} \qquad \text{(A.3)}$$

Where $p_{no} = k\, p_{vo}$ (A.4)

a) Characteristic Radius r_c

In the above, for circular and square containers, the characteristic radius r_c is calculated as:

$$r_c = D/4 \qquad \text{(A.5)}$$

where D = bin diameter or width

b) Pressure Ratio k

The coefficient k is the ratio between the normal pressure p_n and the vertical pressure p_v,

$$k = p_n / p_v \qquad \text{(A.6)}$$

This ratio depends on the geometry and properties of the walls and contained material, the relationship from AS3774 [12] is shown below with notation consistent with the current research.

$$k = \frac{1+\sin^2\delta - \sqrt{\sin^2\delta - \mu^2\cos^2\delta}}{4\,\mu^2 + \cos^2\delta} \quad \geq 0.35 \qquad \text{(A.7)}$$

Where,

δ = effective angle of internal friction (radians)

Practical values of δ and μ in most cases lead to a value of k less than 0.35. Therefore, in practice a constant is given for k = 0.35, which has also been used in the current research.

Initial Surcharge Pressure

According to the method of Roberts [4] it is appropriate to determine p_{vo} from

$$p_{vo} = \gamma h_s \qquad \text{(A.8)}$$

Where h_s = effective surcharge head.

The value of p_{no} is then,

$$p_{no} = k\, p_{vo} = k\, \gamma\, h_s \qquad \text{(A.9)}$$

h_s depends on the shape of the bin and its loading configuration. For a square or circular bin, a conical surcharge is assumed, and for a long, narrow bin, a surcharge with triangular prism shape is assumed. The dimension of h_s is therefore calculated from:

$$h_s = H_s / (m_s+2) \qquad \text{(A.10)}$$

Where m_s = 0 for triangular surcharge

m_s = 1 for conical surcharge

H_s = actual surcharge head, to top of pile

The surcharge head is given by

$$H_s = D \tan(\phi_r)/2 \qquad \text{(A.11)}$$

where D = diameter, or width of bin at top opening

ϕ_r = repose angle

A.2 Flow Case – Vertical Bin Section

Following the methodology noted in AS 3774-1996 [12], the method of Roberts [4] applies the same factors to determine the pressures in the flow case. The Janssen pressure is multiplied with the factor $c_{nf:}$

$$p_{nf} = c_{nf}\, p_{ni} \qquad \text{(A.12)}$$

where c_{nf} is the larger of

$$c_{nf} = [7.6\,(h_b/d_c)^n - 6.4]c_c \qquad \text{(A.13)}$$

and c_{nf} = 1.2 c_c (A.14)

In the above equations,

h_b = $h_c + h_s$ = total effective height of stored solid

c_c = 1 for axi-symmetric flow

= 1.2 for planar flow (the current research)

n = 0.06

d_c = D

p_{ni} = Janssen pressure given by equation (A4)

The basic profile of the flow pressures in the vertical bin section are as shown in Figure A.1

A.3 Mass-Flow Hopper Pressures

At the depth z_h from the top of the hopper, the normal pressure p_{nh} is related to the average vertical pressure at the depth h_h, through the parameter k_h.

$k_h = p_{nh} / p_{vh}$ (A.15)

Solution of the governing differential equation to this equation leads to:

$$p_{vh} = \gamma\left[\frac{h_h - z_h}{j-1}\right] + \left[\left(p_s - \frac{\gamma\, h_h}{(j-1)}\right)\left(\frac{h_h - z_h}{h_h}\right)^j\right] \quad \text{(A.16)}$$

The normal pressure on the hopper wall is

$p_{nf} = k_{hf}\, p_{vf}$ (A.17)

Where $$j = (m+1)\left\{k_h\left[1 + \frac{\tan\phi_w}{\tan\alpha}\right] - 1\right\} \quad \text{(A.18)}$$

α = hopper half angle

p_s = surcharge pressure at datum transition

h_h = distance from apex to transition

γ = bulk specific weight

ϕ_w = wall friction angle

m = symmetry factor

= 1 for axi-symmetric or conical hoppers

= 0 for plane-flow hoppers (the current research)

A.3.1 Hopper Initial pressures

For the initial filling case, the lower-limit of k_h (this being, k_{hi}) is used. In this case, j = 0 and the vertical pressure p_{vhi} is hydrostatic, which is an upper limit value. From equation (A.16) with j = 0,

$$p_{vhi} = p_s + \gamma z_h \qquad \text{(A.19)}$$

and the normal pressure p_{nhi} is

$$p_{nhi} = k_{hi}\, p_{vhi} = k_{hi}\,(p_s + \gamma\, z_h) \qquad \text{(A.20)}$$

and from (A.18) with j = 0,

$$k_{hi} = \tan\alpha / (\tan\phi_w + \tan\alpha) \qquad \text{(A.21)}$$

A.3.2 Hopper Flow pressures

Equations (A.16), (A.17) and (A.18) apply to the flow case also, so with notation referring to the flow case they become:

$$p_{vhf} = \gamma\left[\frac{h_h - z_h}{j-1}\right] + \left[\left(p_s - \frac{\gamma\, h_h}{(j-1)}\right)\left(\frac{h_h - z_h}{h_h}\right)^j\right] \qquad \text{(A.22)}$$

$$p_{nhf} = k_{hf}\, p_{vhf} \qquad \text{(A.23)}$$

and $$j = (m+1)\left\{k_{hf}\left[1 + \frac{\tan\phi_w}{\tan\alpha}\right] - 1\right\} \qquad \text{(A.24)}$$

The value of the pressure ratio k_{hf} is determined using modified values as recommended in [4] as the most accurate estimate for the flow pressures. This value is calculated as:

$$k_{hf} = \frac{2(1+sin\delta\ cos2\eta)}{2-sin\delta(1+\cos(\alpha+\eta))} \qquad \text{(A.25)}$$

where

$$\eta = 0.5\left(\phi_w + \sin^{-1}\left(\frac{\sin\phi_w}{\sin\delta}\right)\right) \qquad \text{(A.26)}$$

A.3.3 Surcharge pressure applied to the mass-flow hopper

The surcharge pressure p_s which acts downward onto the interface of the mass flow hopper is the vertical pressure from the vertical bin section, including mass contained in the vertical bin and any surcharge above this, subject to a Janssen equation resulting from the upper section.

Roberts [4] notes that surcharge pressure onto the hopper interface should be based on initial vertical bin section pressures always and, therefore, no adjustments should be made to consider flow condition pressures, this is due to design conservatism, as required from AS 3774 [12]. The surcharge pressure is given by adapting equation (A.1) to:

$$p_s = \frac{\gamma\, r_c}{\mu\, k}\left[1 - e^{-(\mu\, k\, h_b/r_c)}\right] + p_{vo}\, e^{-(\mu\, k\, h_b/r_c)} \qquad \text{(A.27)}$$

Where,

p_{vo} $= \gamma h_s$ (A.28)

h_c = height of material in contact with vertical walls

k ≥ 0.35

In this case, the dimension h_b is substituted for h_c (used in [4]) so as not to omit the effects of surcharge pressures, which can be significant in cases where the surcharge present as a material repose but does not present as material contacting the bin side walls.

A.4 Hopper loads on Feeder/Gate

The practical application of the hopper pressures onto the withdrawal equipment (either a feeder or a gate) is described by Roberts [6].

The loads acting on the feeder and corresponding power requirements vary according to the stress condition in the stored bulk mass. The general expression for the load V is

$$V = p_{vo}\, A_o \qquad \text{(A.29)}$$

Where,

p_{vo} = vertical pressure on the feeder surface and

A_o = Area of hopper outlet

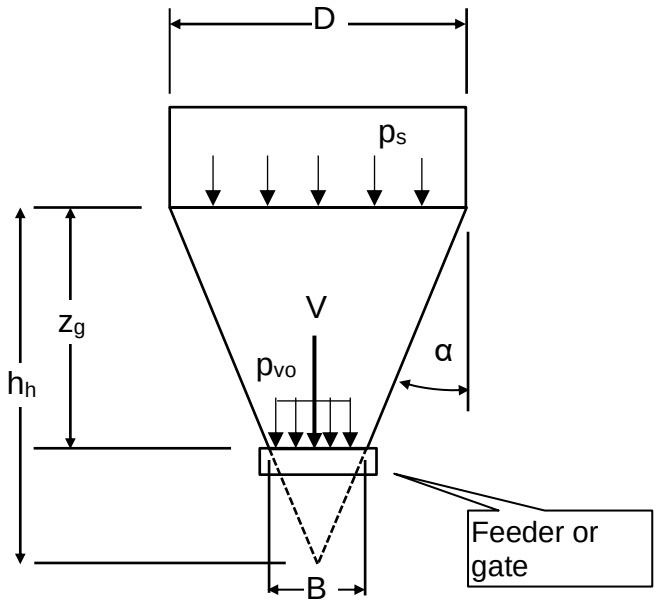


Figure A- 2 Loads on feeder

The load may be expressed in terms of a non-dimensional surcharge factor, as described by Arnold et al [7] as follows:

$$V = q\,\gamma\,L^{(1-m)}\,B^{(2+m)} \qquad (A.30)$$

Where,

q = non-dimensional surcharge factor

$\gamma = \rho.g$ = bulk specific weight

ρ = bulk density

L = Length of slotted opening

B = width of slot or diameter of circular/square opening

m = hopper symmetry factor:

= 0 for plane flow hopper

= 1 for conical or axi-symmetric hopper

from (A.29) and (A.30) the expression is determined,

$$q = (\pi/4)^m\,(p_{vo}/[\gamma B]) \qquad (A.31)$$

Analysing the pressures in the hopper, the overall pressure onto the hopper outlet can be calculated as:

$$P_{vo} = \frac{\gamma B}{2(j-1)\tan\alpha} + \left[p_s - \frac{\gamma D}{2(j-1)\tan\alpha}\right]\left[\frac{B}{D}\right]^j \qquad \text{(A.32)}$$

Where, p_s = surcharge pressure acting at the transition from vertical bin to hopper

The exponent 'j' in equation (A.29)32 is per equation (A.18)

From (A.32) and (A.18), an expression for the non-dimensional surcharge factor is:

$$q = \left(\frac{\pi}{4}\right)^m \frac{1}{2\,(j-1)\tan\alpha}\left\{1 + \left[\frac{2\,p_s(j-1)\,\tan\alpha}{\gamma} - D\right]\frac{B^{j-1}}{D^j}\right\} \qquad \text{(A.33)}$$

Whereas Roberts [6] provides analyses for both the initial and flow condition loads onto the feeder, the current research only makes reference to the initial condition at feeders and the range of recommend j values that are recommended to be used.

Flow conditions are only considered as far as predicted vertical pressures from the hopper outlet position, described in Sections A.1 to A.3, are concerned.

A.4.1 Initial Filling Condition

The initial filling condition is specifically relevant for the case when the bin is emptied completely and then filled from empty to full with the feeder not operating. As noted by Roberts [6], research has shown that the initial filling loads can vary substantially according to such factors as;

- Rate of filling and drop height
- Uniformity of filling over the length and breadth of the feed bin; asymmetric loading will produce a non-uniform pressure distribution along the feeder.
- Clearance between the hopper bottom and feeder surface.
- Degree of compressibility of bulk solid
- Rigidity of feeder surface

For the initial filling condition, the stress field in the hopper is peaked; that is, the major principal stress is almost vertical at any location. The determination of the initial surcharge factor q_i can be made by using an appropriate value of 'j' in equation (A.33).

a) For a totally uncompressible bulk solid and a rigid feeder with minimum clearance, the upper bound value of q_i may be approached. The upper bound value corresponds to j = 0,

for which the pressure in the hopper is 'hydrostatic'. In this case the ratio of normal pressure to vertical pressure is given by:

$$k_{hi} = \frac{\tan\alpha}{\tan\alpha + \tan\phi_w} \qquad \text{(A.34)}$$

With j = 0, the upper bound value of q_i is obtained from equation (A.33) which becomes

$$q_i = \left(\frac{\pi}{4}\right)^m \left\{\frac{1}{2\tan\alpha}\left[\frac{D}{B} + \left[\frac{2\,p_s\tan\alpha}{\gamma\,B}\right] - 1\right]\right\} \qquad \text{(A.35)}$$

This equation corresponds to the pressure at the outlet being 'hydrostatic'.

b) For a very incompressible bulk solid and a stiff feeder, j = 0.1.
c) For a very compressible bulk solid and a flexibly supported feeder, j = 0.9.
d) For a moderately compressible bulk solid stored above a flexibly supported feeder, j = 0.45.

Recommended value of q_i

Although using an appropriate value of j in equation (A.33) can give the value of q_i, from a practical point of view, it has been established that a suitable prediction of q_i may be obtained from,

$$q_i = \left(\frac{\pi}{4}\right)^m \left\{\frac{1}{2\tan\alpha}\left[\frac{D}{B} + \left[\frac{2\,p_s\tan\alpha}{\gamma\,D}\right] - 1\right]\right\} \qquad \text{(A.36)}$$

The vertical load V_i is given by

$$Vi = q_i\,\rho\,g\,L^{(1-m)}\,B^{(2+m)} \qquad \text{(A.37)}$$

Appendix B Calculation of withdrawn material mass

Conversion of measured weight on the bottom plate to average pressure at the hopper outlet requires an evaluation of the mass of the material withdrawn from the hopper.

As the plate is lowered, the vertical projection of the hopper outlet is filled, as a rectangular prism.

Additional material is also withdrawn so as to fill the repose angle of the material, around all points. The repose angle along the straight sections of the outlets forms a triangular prism, and around the corners forms a quarter cone. The geometry is as shown in Figure B- 2.

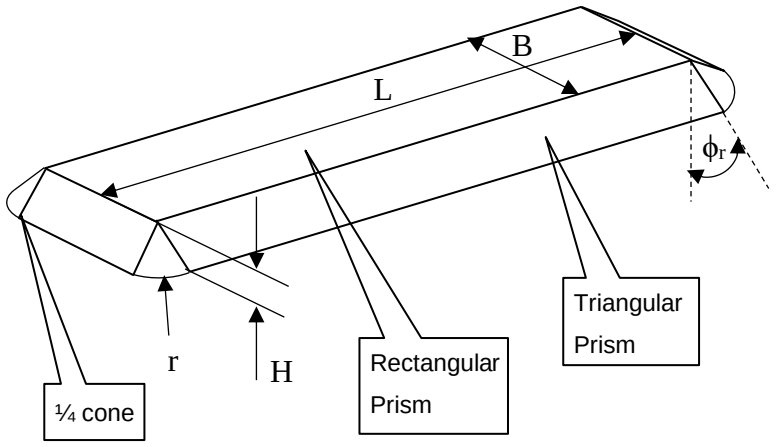


Figure B- 1 Geometry of withdrawn material pile

Defining,

V_w = Volume of all withdrawn material
V_r = Volume of rectangular prism
V_t = Volume of triangular prism composite
V_c = Volume of corner cones composite
ϕ_r = Repose angle
r = Radius of cone developed by material at repose angle

The volume is calculated as,

$$V_w = V_r + V_t + V_c \quad \text{(B.1)}$$

$$= L \cdot B \cdot H + 2 \cdot (L+B) \cdot H \cdot r/2 + \pi \cdot r^2 \cdot H/3$$

Noting that $r = H/\tan(\phi_r)$, the above can be written as:

$$= L \cdot B \cdot H + (L+B) \cdot H^2/\tan \phi_r + \pi \cdot H^3/(3 \cdot \tan^2 \phi_r) \quad \text{(B.2)}$$

The bulk density has been calculated based on assumed percentages of consolidation for dry and moist materials based on the reasoning as described in Section 3.3.3, and calculated according to (4) and (5), with dry materials consolidated by 25% and moist materials consolidated by 50%.

The bulk density of dry materials is assumed as a 25% consolidated density, therefore,

$$\rho = 0.75 \cdot \rho_{loose} + 0.25 \cdot \rho_{compact} \quad \text{(B.3)}$$

The moist sand (due to its more significant compressibility) is assumed as 50% consolidated, therefore,

$$\rho = 0.5 \cdot (\rho_{loose} + \rho_{compact}) \quad \text{(B.4)}$$

The mass of the material contained in the withdrawn material is,

$$M_{wd} = V_w \cdot \rho \quad \text{(B.5)}$$

For dry material that has no cohesive strength, the repose angles are as measured from poured tests. Drained repose angles are not applicable to material being withdrawn from the bin.

Moist material, or other material with sufficient cohesive strength to withdraw without failing, will maintain its shape as it is extruded from the hopper, and as a result the repose angle is 90 degrees. In this case the repose portion has a zero volume for the triangular prism and cone. Since the tan function cannot return a value for 90 degrees, the function for this case is altered by removing the second and third terms of (B.2) giving the functions,

$$V_{90} = H \cdot L \cdot B \quad \text{(B.6)}$$

$$M_{90} = V_{90} \cdot \rho \quad \text{(B.7)}$$

For a visual indication of the sloped repose angle of dry sand and the near-vertical slope of moist sand, see the photographs from tests in progress in Figure B- 2.



Figure B- 2 Sloped (dry) and near-vertical (moist) repose angles from dry and moist sand

Appendix C Loadcell calibration and tare weight evaluation

Each loadcell was configured with a signal amplifier and a voltmeter to provide an accurate, readable voltage output.

The two sets of loadcell and amplifier were calibrated on a bench with test weights. The minimum applied load was 238.5/239.2 g (for loadcell 1 and loadcell 2 respectively) for the mass of the rod, nut, wingnut, and washer.

Test weights of 5 kg were incrementally added up to a total combed mass of 60.2 kg, including the support rod/washer/ nut assembly. A mass excluding the washer was used in the calibration procedure (9.5 g for the washer) whereas mass including the washer was used for data collection during main testing.

A calibration curve was determined for each curve, ignoring values less than 5 kg, because the calibration readings indicated less stability for loads less than 5 kg and also considering that the configuration of the rig would see no values lower than 5 kg per loadcell in any test.

Additional to the mass of the rods, the mass of the plate was measured as 6.63 kg. This mass, together with the mass of the rods, was subtracted from all measured forces to give an appropriate tare weight in the evaluation calculations.

The two loadcells were calibrated together with their respective amplifiers. The calibration formulae were calculated from a line fit to measured readings taken of known loads. The formulae used in calculations are,

Loadcell 1: Mass = 24.739 (V) - 0.0532

Loadcell 2: Mass = 25.116 (V) - 0.323

In calculations, converting from mass to force, gravitation acceleration was taken as 9.81 m/s^2, which is sufficiently accurate for the purposes of the study although gravitational acceleration in Johannesburg is slightly lower than 9.81 m/s^2

The configuration of the loadcell for calibration is as shown in Figure C- 1, complete with wingnut, washer, locking nut, and threaded bar.

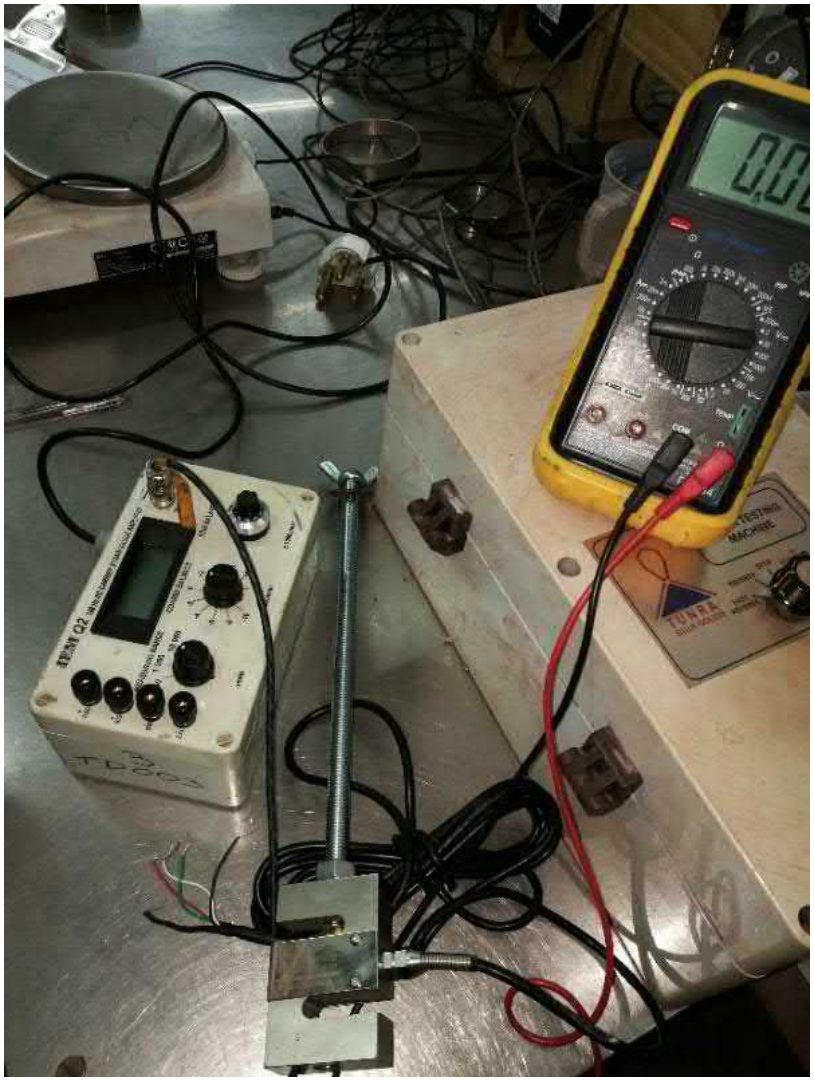


Figure C- 1 Loadcell and amplifier

The calibration worksheets for the two loadcells are shown in Table C- 1 and Table C- 2.

Table C- 1 Loadcell 1 calibration worksheet

Loadcell Calibration #1		Calibrated, 2017/06/29			C. Haupt	
Serial Number		5N11547				
Amplifier Number		TD004				
Tare mass		238.5	g	(rod plus wingnut plus washer)		
Tare mass		229	g	(excluding washer)		
Measuring range "5 - 100"						
Calibration Curve - Loadcell #1						
Volt (V)	Calibration Mass (kg)	kg/Volt	Indicated Mass (kg)	Error		
0.078	0.2385	3.0576923				
0.2091	5.2385	25.052606	5.2261	-0.24%		
0.4118	10.2385	24.862797	10.2407	0.02%		
0.614	15.2385	24.818404	15.2429	0.03%		
0.817	20.2385	24.771726	20.2650	0.13%		
1.017	25.2385	24.816618	25.2128	-0.10%		
1.22	30.2385	24.785656	30.2348	-0.01%		
1.422	35.2385	24.780942	35.2321	-0.02%		
1.624	40.2385	24.777401	40.2293	-0.02%		
1.826	45.2385	24.774644	45.2266	-0.03%		
2.029	50.2385	24.760227	50.2486	0.02%		
2.231	55.2385	24.759525	55.2459	0.01%		
2.433	60.2385	24.75894	60.2432	0.01%		
	Average	24.787898				
	SD	0.032211		0.06%		
	SD (%Av.)	0.13%				
Calibration Formula:	Mass=24.739 x (Volt) +0.0532					

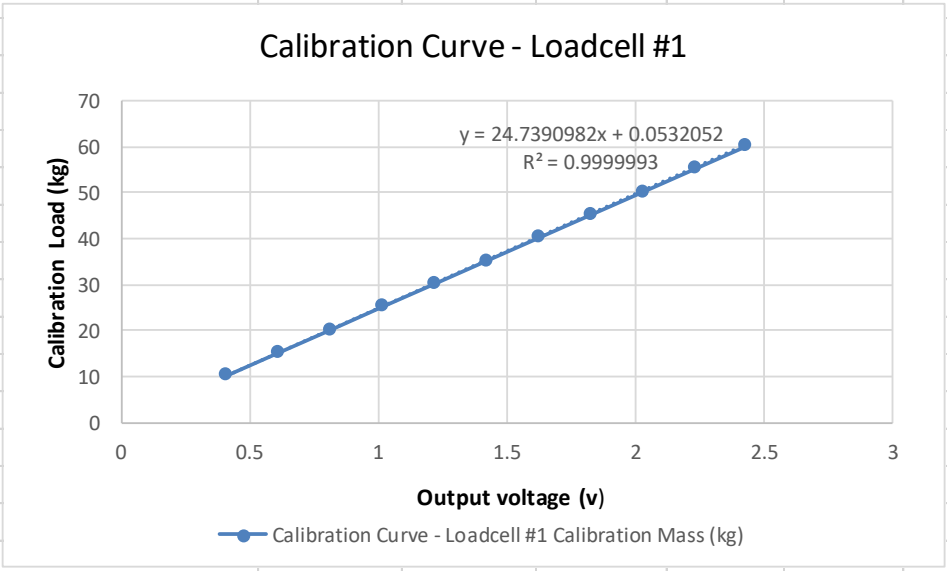
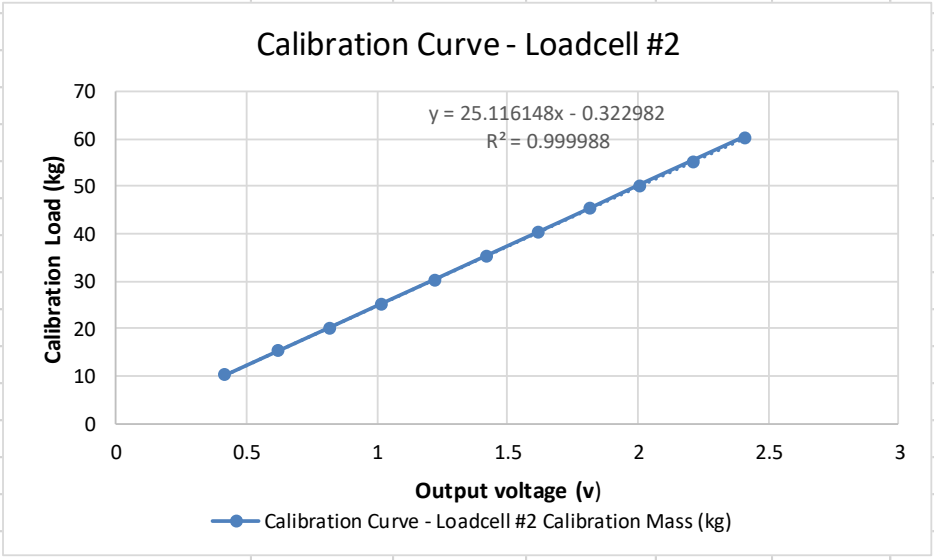


Table C- 2 Loadcell 2 calibration worksheet

Loadcell Calibration #2		Calibrated, 2017/06/29		C. Haupt		
Serial Number		5016586				
Amplifier Number		TD003				
Tare mass		239.2	g	(rod plus wingnut plus washer)		
Tare mass		229.6	g	(excluding washer)		
Measuring range "5 - 100"						
Calibration Curve - Loadcell #2						
Volt (V)	Calibration Mass (kg)	kg/Volt	Indicated Mass (kg)	Error		
0.018	0.2392	13.288889				
0.218	5.2392	24.033028	5.1523	-1.66%	Loadcell1	average
0.418	10.2392	24.495694	10.1755	-0.62%	0.02%	-0.30%
0.618	15.2392	24.6589	15.1987	-0.27%	0.03%	-0.12%
0.819	20.2392	24.712088	20.2470	0.04%	0.13%	0.08%
1.018	25.2392	24.792927	25.2451	0.02%	-0.10%	-0.04%
1.219	30.2392	24.806563	30.2934	0.18%	-0.01%	0.08%
1.418	35.2392	24.85134	35.2915	0.15%	-0.02%	0.07%
1.618	40.2392	24.869716	40.3147	0.19%	-0.02%	0.08%
1.817	45.2392	24.897744	45.3128	0.16%	-0.03%	0.07%
2.01	50.2392	24.994627	50.1602	-0.16%	0.02%	-0.07%
2.21	55.2392	24.995113	55.1834	-0.10%	0.01%	-0.04%
2.41	60.2392	24.995519	60.2066	-0.05%	0.01%	-0.02%
	Average	24.824566		-0.042%	0.004%	-0.019%
	SD	0.1564995		0.24%	0.06%	0.12%
	SD (%Av.)	0.63%				
Calibration Formula:	Mass=25.116 x (Volt) -0.323					



In the table for Loadcell 2, the calibration error for each test weight was placed alongside that for Loadcell 1. The average between the errors of the two loadcells are indicated. It is apparent that the errors of the two loadcells offset each other to a large degree and the resulting error from calibration is typically less than 0.1%.

In large part the loads under interest are in the range of 10 to 20 kg per loadcell. In this loading range the calibration error of the system is in the range of 0.3% to 0.1%.

Considering that most results are presented on the basis of 2 or 3 significant digits, this uncertainty is significant enough to be included into the processed data. – A constant calibration accuracy is therefore taken as median between these – at 0.2%, which is added to uncertainty of all processed results.

The calculation of the tare weight for the weighing assembly includes the consideration of the self-weight of the connecting rods and the bottom plate. The nut that was used for the calibration was not used for the testing operation, therefore 9 grams was subtracted from the measured tare weight of the threaded rod assembly, as shown in Table C- 3.

Table C- 3 Calculation of tare weight

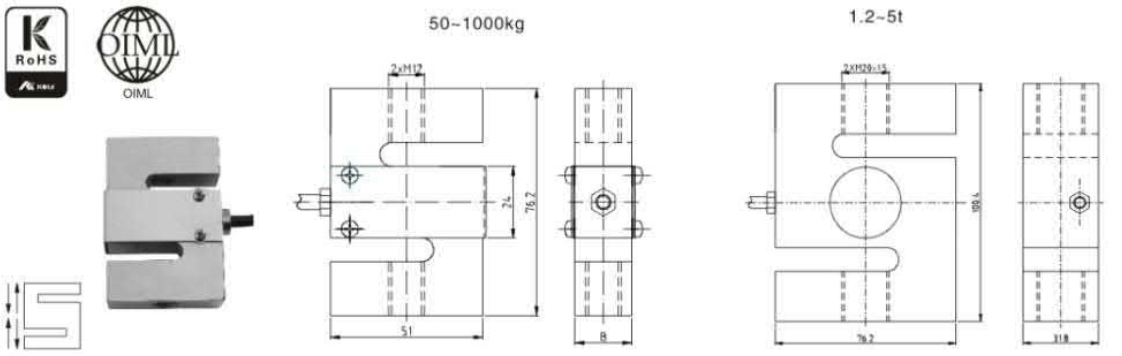
Tare Mass					
Loadcell 1	229	g	Rod+nut (excluding washer)		
Loadcell 2	229.6	g	Rod+nut (excluding washer)		
Plate	6630	g			
Total tare mass	7088.6	g			
	7.09	kg			
Tare Weight	69.54	N	g=	9.81	

Specific tare weight was noted for each test repetition (prior to loading of the bin). This tare was measured at values ranging from 64.8 N to 71.4 N, representing a range of 6.6 N. Tests performed on a single day varied by less than 2 N, indicating possible set-up or temperature effects. It was also noted that when testing moist material there was a higher tare weight which is understandable because it took more effort to clean the plate, with some moist sand and moisture adhering to the plate after being brushed clean.

The loadcell datasheet is indicated in Figure C- 2.

DEE/DEF-A/-SS/-ASS Loadcell

DEE/DEF-A/-SS/-ASS



额定载荷(kg) Rated Load	D	L	H	B
50~750	M12	51	76.2	19.1
1000	M12	51	76.2	25.4
1200~5000	M20x1.5	76.2	100.4	31.8

吊钩秤、皮带秤、配料系统
Crane scale,belt scale, blending system

TECHNICAL PARAMETER

4Wires:Exc+(红,Red);Exc-(黑,Black);Sig+(绿,Green);Sig-(白,White)

额定载荷 Rated capacities(Emax)	50,100,150,200,250,300,500,750kg;1,1.2,1.5,2,3,5t	温度补偿范围 Temperature range, compensated	-10℃~+40℃
灵敏度 Sensitivity	2.0±0.003mV/V(DEE);3.0±0.003mV/V(DEF)	工作温度范围 Temperature range, operating	-30~+70℃
精度等级 Accuracy class	C2~C3	安全过载 Maximum safe overload	120%F.S
		极限过载 Ultimate overload	150%F.S
零点平衡 Zero balance	±1%F.S	推荐激励电压 Excitation,recommend	10~12V DC
零点温度影响 TCO	±0.02%F.S/10℃	最大激励电压 Excitation,maximum	15V DC
输出温度影响 TC SPAN	±0.02%F.S/10℃	防封等级 Protection class	IP65(100~1000kg);IP67(1200~5000kg)
输入阻抗 Input impedance	400±20Ω (50~750kg)	材质 Construction	合金钢Alloy Steel, 不锈钢Stainless Steel
输出阻抗 Output impedance	352±3Ω	电缆 Cable	Length:3m
绝缘电阻 Insulation impedance	≥5000MΩ		Diameter: ϕ 5mm

Figure C- 2 Loadcell datasheet

Appendix D Test material properties

The following material properties were measured for the dry sand, moist sand, and 13 mm quartz aggregate:

- Bulk density – loose poured
- Bulk density – tapped
- Moisture content – as received
- Saturation moisture content
- Moisture content – test moisture
- Particle size distribution
- Repose angle, poured
- Repose angle, drained
- Inclined chute angle (moist sand on mill scale mild steel)
- Inclined chute angle (moist sand on PVC covered plate)

Material properties tests were performed several times and the average of all valid results were used as the selected test property.

The physical properties were used as an input to:

- Calculated feeder load pressures for comparison to measured loads
- Data processing to subtract mass of withdrawn material, to give a basis for calculated load at the hopper outlet.
- Preparation of a suitable sample of moist sand, with appropriate moisture content of approximately 50% of saturation

Results are as tabulated in the following sections.

D.1 Bulk density

The summary of the measured bulk densities (loose poured, and tapped) are as listed in Table D- 1 and Table D- 1.

Table D- 1 Bulk density, sand (dry and moist)

Sand - Dry						Sand - (50% saturation)				
Mass(water)	5.25	Kg				Mass(water)	5.25	Kg		
Volume(Bucket)	0.00525	m3				Volume(Bucket)	0.00525	m3		
Loose Poured Density						**Loose Poured Density**				
				Averages						Averages
	m1	m2	m3	m			m1	m2	m3	m
Mass(Kg)	7.67	7.65	7.645	7.655		Mass(Kg)	6.1	6.055	6.295	6.15
Density(kg/m3)	1461	1457	1456	**1458**		Density(kg/m3)	1162	1153	1199	**1171**
Tapped Density						**Tapped Density**				
				Averages						Averages
	m1	m2	m3	m			m1	m2	m3	m
Mass(Kg)	8.665	8.56	8.66	8.628333		Mass(Kg)	8.24	8.335	8.52	8.365
Density(kg/m3)	1650	1630	1650	**1643**		Density(kg/m3)	1570	1588	1623	**1593**
Density used for calculation						**Density used for calculation**				
Loose + 25% of difference to tapped density				1504		Loose + 50% of difference to tapped density				1382

Table D- 2 Bulk density, 13 mm quartz aggregate

13 mm Quartz aggregate - full size fraction				
Mass(water)	5.25	Kg		
Volume(Bucket)	0.00525	m3		
Loose Poured Density				
				Average
	m1	m2	m3	m
Mass(Kg)	7.555	7.705	7.72	7.66
Density(kg/m3)	1439	1468	1470	**1459**
Tapped Density				
				Average
	m1	m2	m3	m
Mass(Kg)	7.945	7.975	8.27	8.063333
Density(kg/m3)	1513	1519	1575	**1536**
Density used for calculation:				
loose + 25% density increase from Tapped				1478

D.2 Moisture content

The record of the sand initial moisture content testis listed in Table D- 3. This indicated 0.45% as the result.

Table D- 3 Sand – initial moisture content test record

TUNRA BULK SOLIDS AFRICA

Material Flow Property Testing
Moisture Content (Total)

Material type	River sand		
Sample fraction	Full size fraction		Input cell
Moisture content	Air dried		Locked output cell
Date	04.07.2017		Drop down menu

Test data

Tray ID	S1		Initial material mass	516.4	g (damp)
Empty tray mass	933.0	g	Variation limit	0.3	g
Tray + material mass	1449.4	g	Variation limit	0.06	%
Measurement uncertainty	0.05	g			

Time (min)	Tray + matl mass (g)	Material mass (g)	Change in mass (g)	Change %	Instruction
0	1449.4	516.4	-	-	Conduct another reading after 15 mins.
15	1447.5	514.5	1.9	0.13	Conduct another reading after 15 mins.
30	1447.1	514.1	0.4	0.03	Conduct another reading after 15 mins.
45	1447.1	514.1	0.0	0.00	Limit reached. Stop reading
60					
75					
90					
105					
120					

Initial dry material	514.1	g
Mass of moisture driven off	2.3	g
Initial moisture content	0.45	%, wet mass basis
Uncertainty	2.17	%

Notes

Wet mass basis % is (100*mw)/mw+ms), where mw is mass of water and ms is mass of dry solids.

Revision no 3 : 20.02.20

Revision history

1 Minor changes to include scale precision, accuracy etc.

2 Modified saturated moisture content sheet, finalised reconstituting moisture sheet, minor changes to text boxes.

The sand saturation moisture content test record is shown in Table D- 4 – this indicates 16.3% as the measured saturation moisture content test.

Table D- 4 Sand – saturation moisture content test record

TUNRA BULK SOLIDS AFRICA

Material Flow Property Testing
Moisture Content (Saturated)

Material type	River sand		
Sample fraction	Full size fraction		Input cell
Moisture content	Air dried		Locked output cell
Date	04.07.2017		Drop down menu

Test data

Cone ID	large	-	Damp sample mass	701.7	g
Cone mass (dry, empty)	333.0	g	Dry material mass	698.5	g
Cone + material mass (AD MC)	1034.7	g	Initial water mass	3.14	g
Cone + material mass (wet)	1215.0	g	Variation limit (mass)	0.3	g
Initial moisture content	0.45	% wet basis	Variation limit (%)	0.04	%

Time (min)	Total wet mass (g)	Material plus water mass (g)	Change in mass (g)	Moisture %, wb	Instruction
0	1215.0	882.0	-	20.80	Conduct another reading after 15 mins.
15	1169.2	836.2	45.8	16.46	Conduct another reading after 15 mins.
30	1168.2	835.2	1.0	16.36	Conduct another reading after 15 mins.
45	1167.8	834.8	0.4	16.32	Conduct another reading after 15 mins.
60	1167.7	834.7	0.1	16.31	Limit reached. Stop reading
75					
90					
105					
120					

Total mass of moisture in sample	136.2	g
Saturated moisture content	16.3	%, wet basis
Uncertainty %	0.04	%, based on meas. uncertainty of 0.05g and final water mass

% of total saturation	10	20	30	40	50	60	70	80	90	100
Material moisture %	1.6	3.3	4.9	6.5	8.2	9.8	11.4	13.0	14.7	16.3

Revision no 3 : 20.02.2017

Moist sand was reconstituted to 8.2% water by mass. 50% of saturation moisture was selected on the basis of experience which shows that maximum cohesive properties of a mineral bulk solid typically occurs in the range from about 50% to 60% of saturation moisture.

After completion of test work, the moisture content was re-measured, and had reduced to 7.3%, which represents 45% of saturation moisture.

The calculation sheet for the moisture make-up is listed in Table D- 5.

Table D- 5 Summary of water addition to give selected moisture content (50% saturation)

TUNRA BULK SOLIDS AFRICA

Material Flow Property Testing

Reconstituting Moisture in Material Sample

Material type	River Sand	
Sample fraction	Full size fraction	Input cell
Moisture content	Air dried (0.45%)	Locked output cell
Date	8/29/2017	Drop down menu

Equipment and material

1. Material sample.
2. Calibrated scale.
3. Bucket or material container, and jug.
4. Water.

Procedure

1. Place an empty bucket or container on the scale and tare the scale so that it reads zero.
2. Add required mass of moist material to the container and record the mass in the table below.
3. Record the existing material moisture content % in the table below.
4. Enter the desired moisture % (wet basis).
5. The calculation will determine how much water to add to sample to reconstitute the required moisture content.
6. Remove the container with material from the scale. Place the jug on the scale and tare so that it reads zero.
7. Add water to the jug to the required mass as calculated below.
8. Add the water to the material while thoroughly stirring the material in order to evenly distribute the moisture.

Initial state			
Material mass*, g or kg	2575.90	* dry material + existing moisture	
Existing material moisture, % wb	0.45		
Dry material mass, g or kg	2564.31		
Existing water mass, g or kg	11.59		
Final state			
Desired material moisture, % wb	8.20		
Total mass of water required, g or kg	229.06		
Amount of water to add, g or kg	217.46	<-	**Add this amount of water to sample**
Total wet mass at desired moisture, g or	2793.36		

Revision no 3 : 20.02.2017

The test report for the initial moisture of Quartz aggregate (0.2%) is shown in Table D- 6.

Table D- 6 Quartz aggregate – initial moisture content test record

TUNRA BULK SOLIDS AFRICA

Material Flow Property Testing

Moisture Content (Total)

Material type	Quartz aggregate		
Sample fraction	Other :	+6.3 -16 mm	Input cell
Moisture content	Air dried		Locked output cell
Date	05.07.2017		Drop down menu

Test data

Tray ID	S1		Initial material mass	1095.1	g (damp)
Empty tray mass	932.8	g	Variation limit	0.3	g
Tray + material mass	2027.9	g	Variation limit	0.03	%
Measurement uncertainty	0.05	g			

Time (min)	Tray + matl mass (g)	Material mass (g)	Change in mass (g)	Change %	Instruction
0	2027.9	1095.1	-	-	Conduct another reading after 15 mins.
15	2025.8	1093.0	2.1	0.10	Conduct another reading after 15 mins.
30	2025.7	1092.9	0.1	0.00	Limit reached. Stop reading
45					
60					
75					
90					
105					
120					

Initial dry material	1092.9	g
Mass of moisture driven off	2.2	g
Initial moisture content	0.20	%, wet mass basis
Uncertainty	2.27	%

Notes

Wet mass basis % is (100*mw)/mw+ms), where mw is mass of water and ms is mass of dry solids.

Revision no 3 : 20.02.2017

Revision history

1 Minor changes to include scale precision, accuracy etc.

2 Modified saturated moisture content sheet, finalised reconstituting moisture sheet, minor changes to text boxes.

The Quartz Aggregate saturation moisture is (1.3%) record is shown in Table D- 7.

Table D- 7 Quartz aggregate saturation moisture test record

TUNRA BULK SOLIDS AFRICA

Material Flow Property Testing
Moisture Content (Saturated)

Material type	Quartz aggregate		
Sample fraction	Other :	+6.3-16	Input cell
Moisture content	Air dried		Locked output cell
Date	05.07.2017		Drop down menu

Test data

Cone ID	large	-	Damp sample mass	807.9	g
Cone mass (dry, empty)	334.3	g	Dry material mass	806.3	g
Cone + material mass (AD MC)	1142.2	g	Initial water mass	1.62	g
Cone + material mass (wet)	1169.8	g	Variation limit (mass)	0.3	g
Initial moisture content	0.20	% wet basis	Variation limit (%)	0.04	%

Time (min)	Total wet mass (g)	Material plus water mass (g)	Change in mass (g)	Moisture %, wb	Instruction
0	1169.8	835.5	-	3.50	Conduct another reading after 15 mins.
15	1160.4	826.1	9.4	2.40	Conduct another reading after 15 mins.
30	1156.5	822.2	3.9	1.94	Conduct another reading after 15 mins.
45	1154.4	820.1	2.1	1.69	Conduct another reading after 15 mins.
60	1153.1	818.8	1.3	1.53	Conduct another reading after 15 mins.
75	1152.2	817.9	0.9	1.42	Conduct another reading after 15 mins.
90	1151.7	817.4	0.5	1.38	Conduct another reading after 15 mins.
105	1151.4	817.1	0.3	1.34	Limit reached. Stop reading
120	1151.2	816.9	0.2	1.32	Limit reached. Stop reading

Total mass of moisture in sample	10.6	g
Saturated moisture content	1.3	%, wet basis
Uncertainty %	0.47	%, based on meas. uncertainty of 0.05g and final water mass

% of total saturation	10	20	30	40	50	60	70	80	90	100
Material moisture %	0.1	0.3	0.4	0.5	0.7	0.8	0.9	1.0	1.2	1.3

Revision no 3 : 20.02.2017

D.3 Particle size distribution

The particle size distribution of the sand is as listed in Table D- 8.

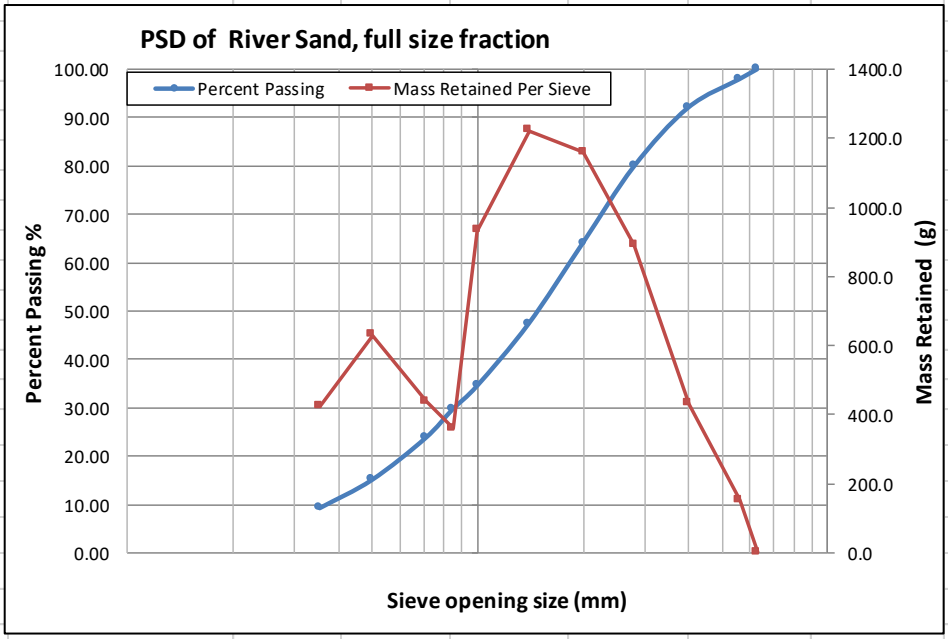
Table D- 8 Particle size distribution of sand

TUNRA BULK SOLIDS AFRICA

Particle Size Distribution

Material type	River Sand		
Sample fraction	full size fraction		
Date		**Moisture content**	0.5%

Action	Sieve size (mm)	Mass retained (g)	Cumulative mass (g)	Percent retained (%)	Cumulative retained (%)	Percent Passing (%)
Add data for the mass	6.30	0.0	0.000	0.00	0.00	100.00
retained per sieve	5.60	151.5	7326.100	2.07	2.07	97.93
aperture size, starting	4.00	431.8	7174.600	5.89	7.96	92.04
from the pan and	2.80	891.3	6742.800	12.17	20.13	79.87
working upwards. For	2.00	1159.8	5851.500	15.83	35.96	64.04
non-standard sieve	1.40	1222.4	4691.700	16.69	52.64	47.36
sizes (yellow) indicate	1.00	932.9	3469.300	12.73	65.38	34.62
zero if not used and	0.850	359.7	2536.400	4.91	70.29	29.71
hide the row so that it	0.710	437.4	2176.700	5.97	76.26	23.74
will not show on the	0.500	629.8	1739.300	8.60	84.86	15.14
graph. Have one row of	0.355	425.1	1109.500	5.80	90.66	9.34
zeros for the upper	Pan	684.4	684.40	9.34	100.00	0.00
limit and hide all other	Sum (g)	7326.1				



Template revision 3 : 2017.06.19

The particle size distribution of the sand is as listed in Table D- 9.

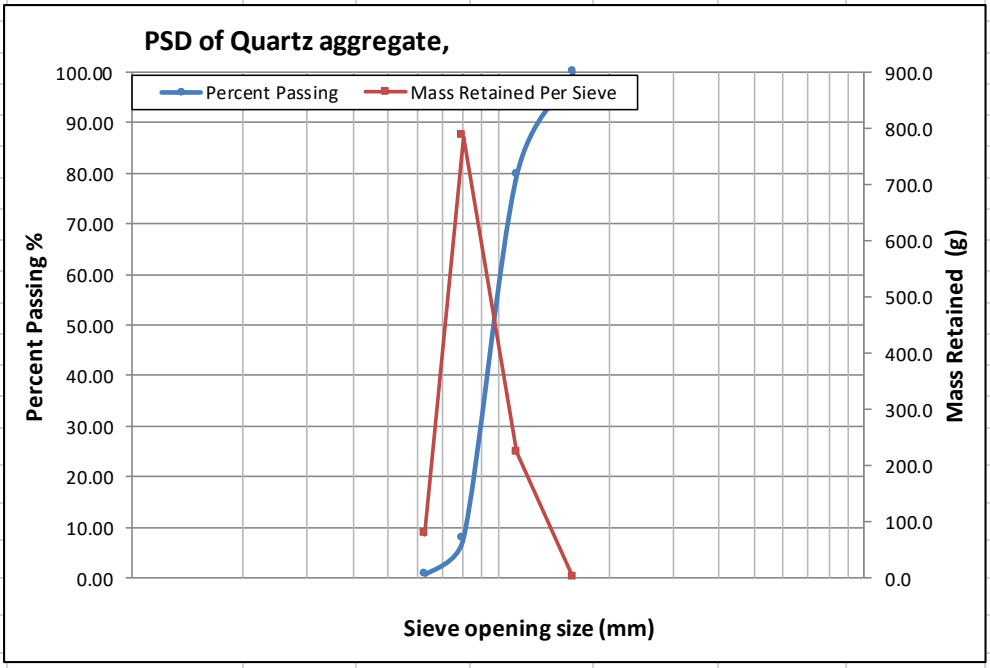
Table D- 9 Quartz aggregate particle size distribution

TUNRA BULK SOLIDS AFRICA

Particle Size Distribution

Material type	Quartz aggregate		
Sample fraction	Other :		
Date		**Moisture content**	AD, 0.20

Action	Sieve size (mm)	Mass retained (g)	Cumulative mass (g)	Percent retained (%)	Cumulative retained (%)	Percent Passing (%)
Add data for the mass	16.00	0.0	1091.500	0.00	0.00	100.00
retained per sieve	11.20	222.5	1091.500	20.38	20.38	79.62
aperture size, starting	8.00	786.0	869.000	72.01	92.40	7.60
from the pan and	6.30	77.0	83.000	7.05	99.45	0.55
working upwards. For	Pan	6.0	6.00	0.55	100.00	0.00
non-standard sieve	Sum (g)	1091.5				

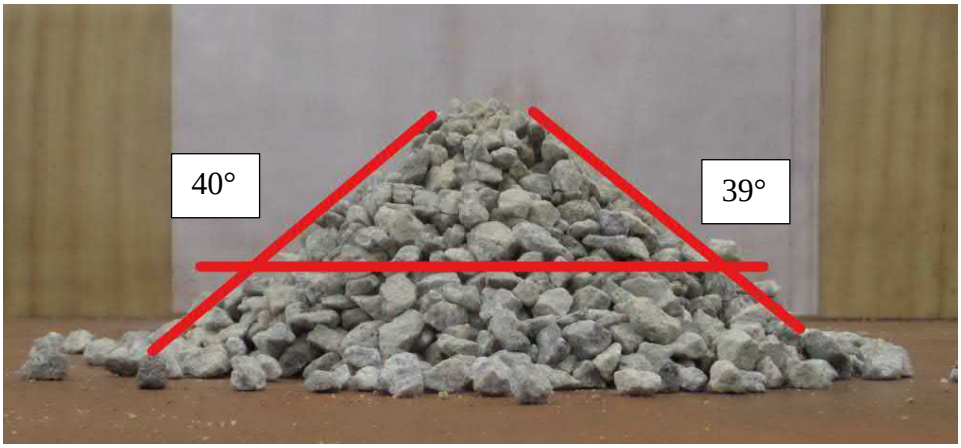
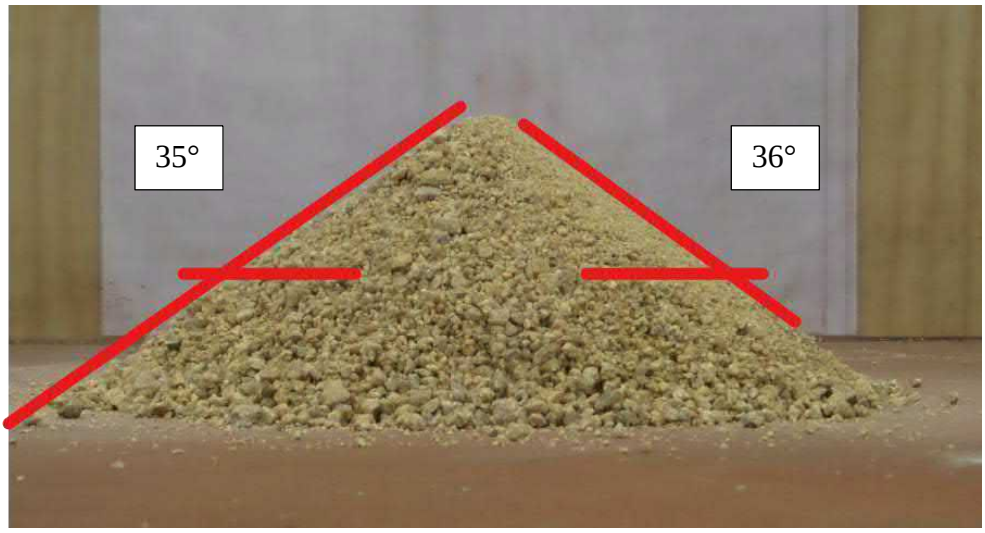


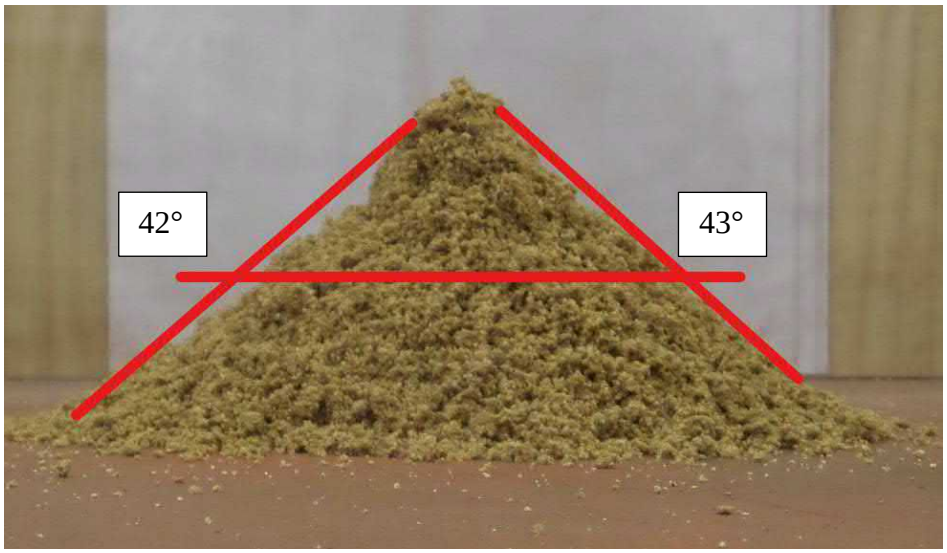
Template revision 3 : 2017.06.19

D.4 Poured angle of repose

Poured angle of repose was measured by placing a pile on a flat surface and taking measurement from a photograph of the material repose angle. The relevant photographs, with their indicated angles are shown in Table D-10.

Table D-10 Poured angle of repose - photographic record

Material	**Photograph**
Dry Aggregate 40 degrees	
Dry Sand 35 degrees	

Moist Sand 43 degrees	

D.5 Inclined chute test

An incline chute test was performed with two material combinations only – moist sand on steel (Inclination angle notes as 35 degrees), and moist sand on PVC sheeting (38 degrees).

The test method, shown in Figure D- 1 includes placing a consolidating weight onto the material to press it onto the chute wall, and then removing the consolidating weight. The plate is inclined slowly until sliding is initiated down the slope, at which position the inclination of the plate is measured. A test example (PVC lined wall material) is shown in

The inclined chute angle does not directly indicate wall friction angle but instead provides insight into the comparative friction properties of the various material sets.



Figure D- 1 Inclined chute test

Appendix E Friction Angle Sensitivity Analysis

Comparing the selected friction angles to alternative friction angles provides variation to the expected (calculated) pressures onto the bottom plate, both for the initial condition and for the flow condition.

This section presents a comparison of the calculated results as a function of flow properties. All the cases presented here are based on a hopper wall angle of 20-degrees and an opening width of 120 mm. This configuration was used to perform tests on bulk material types used in the present research. This corresponds to the following test parameters:

- Quartz aggregate –Set 9
- Dry sand – Set 3
- Moist sand – Set 10

Quartz aggregate with wall friction angle ϕ_w of 28 degrees as listed in Table E- 1.

Table E- 1 Quartz aggregate, internal friction sensitivity (ϕ_w = 28°)

Internal Friction δ (degrees)	**30**	**35**	**40**	**45**	**47**	**50**	**55**	**Measured (47)**
Initial Load (N)	414	415	415	415	415	415	415	380
Flow Load (N)	142	102	80	65	60	60	46	34
Flow/Initial (%)	34%	25%	19%	16%	14%	13%	11%	9%

Quartz aggregate with internal friction angle δ of 47 degrees as listed in Table E- 2.

Table E- 2 Quartz aggregate, wall friction sensitivity (δ= 47°)

Wall Friction ϕ_w (degrees)	**20**	**25**	**28**	**30**	**35**	**40**	**Measured (28)**
Initial Load (N)	415	415	415	415	415	415	380
Flow Load (N)	48	55	60	64	77	100	34
Flow/Initial (%)	12%	13%	14%	15%	19%	24%	9%

The sensitivity analysis data for quartz aggregate are shown graphically in Figure E- 1.

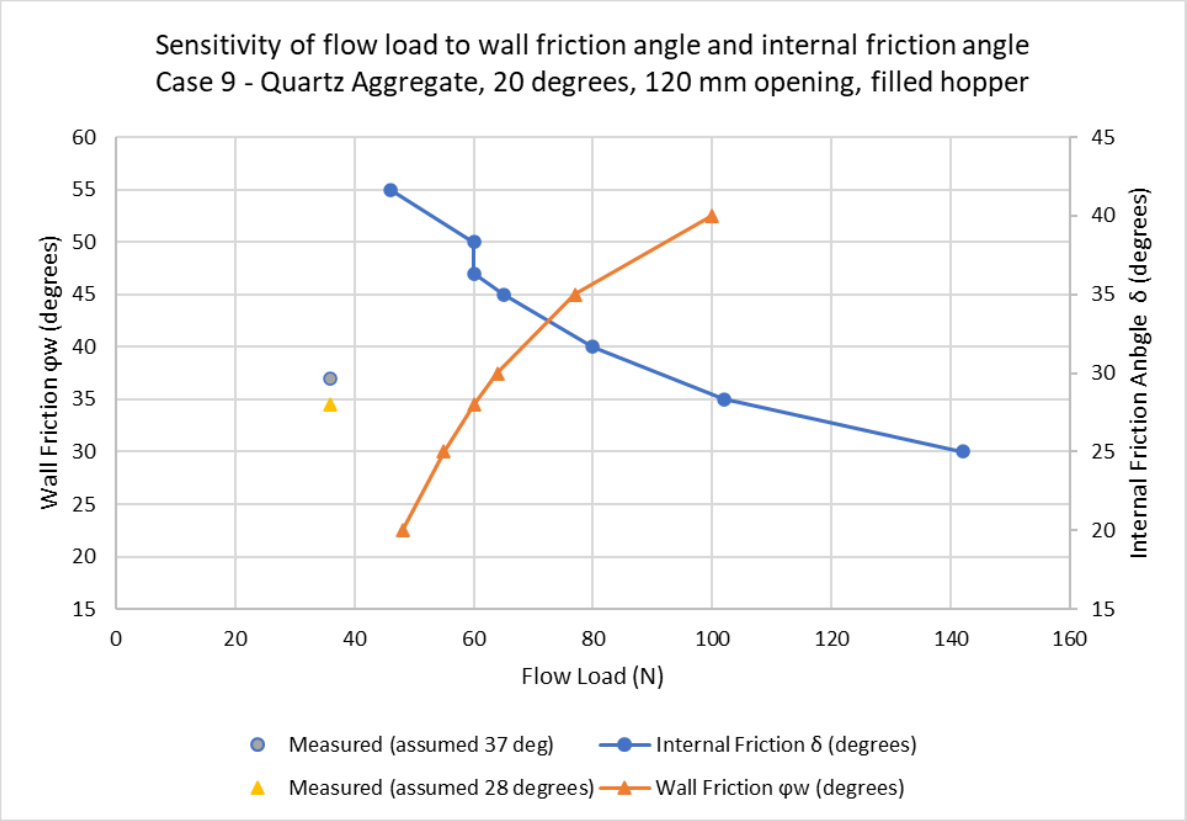


Figure E- 1 Friction properties sensitivity – quartz aggregate

It is apparent that initial pressure is not a function of either wall friction or internal friction. It is only a function of density and material height and as such it is a calculated hydrostatic condition.

The flow pressure is strongly dependent on both the internal friction and the wall friction. The flow pressure decreases with increasing internal friction and it increases with increasing wall friction. These are all related to how the weight of the contained material resolves onto the bin walls, as a function of wall friction angle and bin wall pressures.

It is apparent that additional internal friction in the material $\delta > 47°$ leads to additional material load being retained at the upper sections of the hopper. The result is that, in the lower portions of the hopper there is a lower magnitude of pressure.

It is plausible that the internal friction of the quartz aggregate may have been lower than assumed, possibly between 25 degrees and 20-degrees.

Dry Sand with wall friction angle of 28 degrees as listed in Table E- 3.

Table E- 3 Dry sand, internal friction sensitivity

Internal Friction δ (degrees)	**30**	**35**	**40**	**45**	**47**	**50**	**55**	**Measured (47)**
Initial Load (N)	422	422	422	422	422	422	422	326
Flow Load (N)	145	104	81	66	61	60	47	48
Flow/Initial (%)	34%	25%	19%	16%	14%	13%	11%	15%

Dry Sand with internal friction angle of 47 degrees as listed in Table E- 4.

Table E- 4 Dry sand, wall friction sensitivity

Wall Friction ϕ_w (degrees)	**20**	**25**	**28**	**30**	**35**	**40**	**Measured (28)**
Initial Load (N)	422	422	422	422	422	422	326
Flow Load (N)	49	56	61	65	79	102	48
Flow/Initial (%)	12%	13%	14%	15%	19%	24%	15%

The sensitivity data as for dry sand is shown graphically in Figure E- 2.

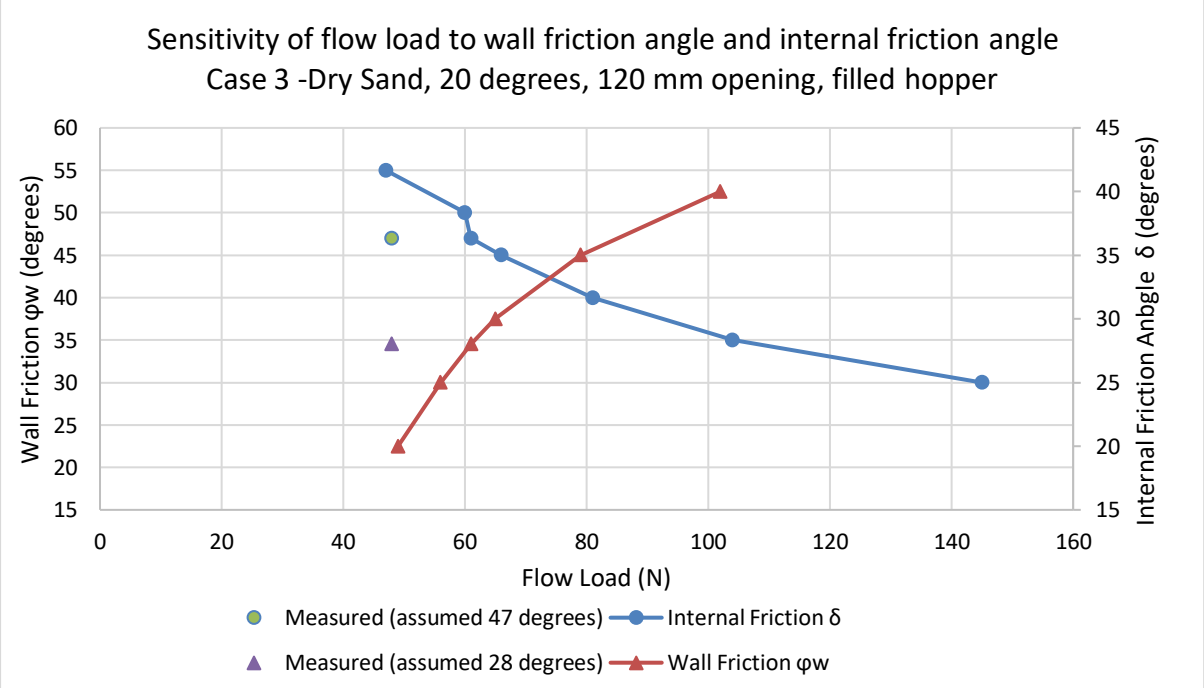


Figure E- 2 Friction properties sensitivity – dry sand

The calculated pressures for aggregate and dry sand were very similar due to only the density parameter being varied between the two cases.

It is apparent that whereas the aggregate was effective at transferring a large percentage of its initial theoretical calculated load onto the bottom plate (380 N compared to 415 N, or 92%), the sand only reached 326 N of 422 N, or 77%). This is expected due to the slightly higher compressibility of the sand (which relieves initial load during filling) and also due to higher friction. The flow load is not a function of compressibility because it presents after material has fully transitioned into flow, therefore it is feasible that the actual wall friction of the dry sand is lower than 28 degrees, possibly it is between 20-degrees and 25 degrees.

Moist Sand with wall friction angle of 30-degrees as listed in Table E- 5.

Table E- 5 Moist sand, internal friction sensitivity

Internal Friction δ (degrees)	**35**	**40**	**45**	**50**	**55**	**60**	**65**	**Measured (47)**
Initial Load (N)	388	388	388	388	388	388	388	320
Flow Load (N)	105	80	65	54	46	40	36	23
Flow/Initial (%)	27%	21%	17%	14%	12%	10%	9%	12%

Moist Sand with internal friction angle of 55 degrees as listed in Table E- 6 .

Table E- 6 Moist sand, wall friction sensitivity

Wall Friction ϕ_w (degrees)	**20**	**25**	**30**	**35**	**40**		**Measured (28)**
Initial Load (N)	388	388	388	388	388		321
Flow Load (N)	34	39	46	55	68		46
Flow/Initial (%)	9%	10%	12%	14%	17%		14%

The sensitivity data as for dry sand is shown graphically in Figure E- 3.

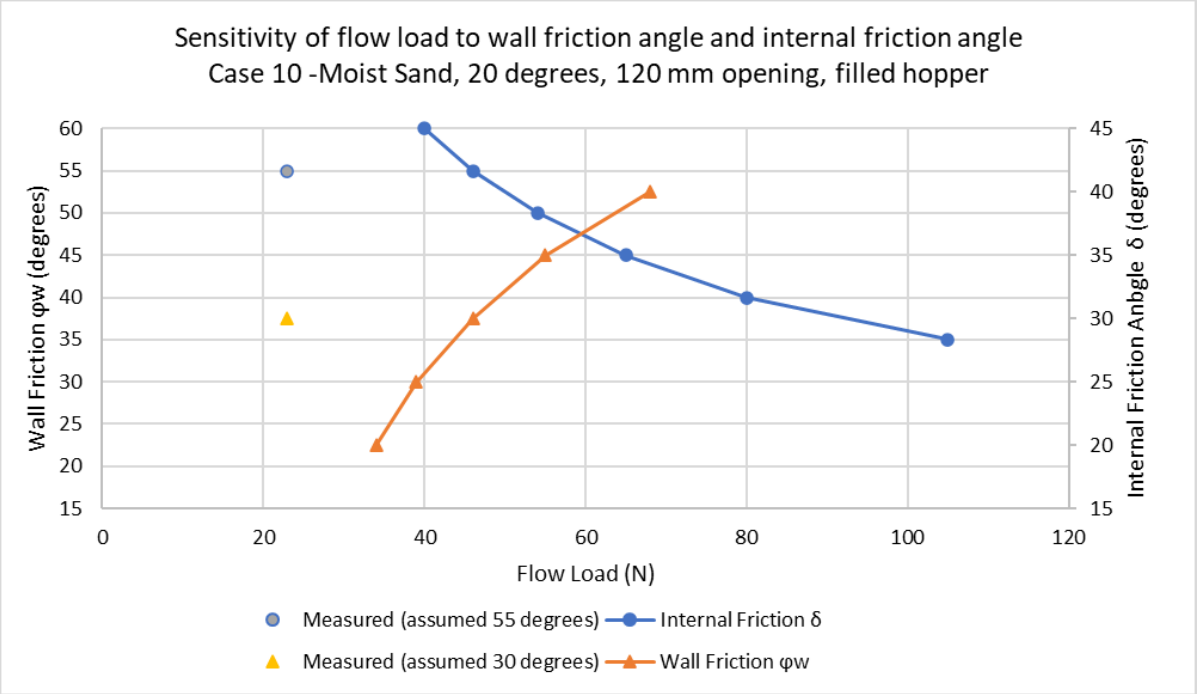


Figure E- 3 Friction properties sensitivity – moist sand

The moist sand represented a relatively small percentage of its calculated initial load onto the feeder plate (231 N compared to 388 N, or 60%), This is expected due to the slightly higher compressibility and higher internal friction of the moist sand due to cohesion. The flow load is not a function of compressibility because it presents after material has fully transitioned into flow, therefore it is feasible that the actual wall friction of the dry sand is lower than 30-degrees, possibly it is between 25 degrees and 30-degrees.

In conclusion, although it is apparent that the measured initial and flow properties do not match with the calculated values. A portion of the difference is due to variation of the wall friction angles and internal friction angles, as well as some uncertainty within both the calculation methodology (followed as per generally accepted theory per Roberts [6]) and the experimental methodology. There are also other effects present which are not reflected in the calculation methodology.

The following can affect the measured vs. calculated pressures:

- Compressibility, following effects as noted by Jenike and Johanson [3] and by Roberts [6] – affects initial pressures
- Flexibility of the system components – affects initial pressures
- Wall friction angle – affect flow pressures
- Internal friction angle – affect flow pressures

As it is, the intention of the present research is to compare between sample sets, with regard to their rates of transition from initial to flow properties are and demonstrate qualitative effects. Numerical comparison between calculated and measured values are useful only in terms of comparison between test sets.

Appendix F Sample Calculations

F.1 Calculation of hopper initial and flow pressures

Using the theory presented in Appendix A and Appendix B, a sample calculation is presented for the analytical calculation of initial pressures, flow pressures, and the data processing to establish a calculated actual pressure at the hopper outlet on the basis of from raw experimental readings.

The configuration of test Set 2 is used, which represents the nominal 120 mm hopper width, 20-degree wall angle, dry sand, and the bin filled to the high level, and levelled off.

The input parameters of the case are:

B = Hopper opening width = 120.33 mm
D = Width of vertical wall bin vertical bin section = 480 mm
L = Hopper opening length = 480 mm
h_c = Vertical bin section height (filled portion = 350 mm)
ρ = Bulk Density = 1504.25 kg/m^3
$\gamma = \rho \cdot g$ = Bulk specific weight = 14,757 N/m^3
δ = Angle of effective internal friction = 47°
ϕ_w = Wall friction angle = 28°
μ = tan(ϕ_w) = coefficient of wall friction = 0.5317..
α = Hopper half angle = 19.97°
z_g = Hopper height = 495 mm
z_h = Distance from top of hopper to position of interest.
h_h = Projected height of the hopper to its intersection point = 660 mm
h_s = Effective surcharge head = 0 m (for levelled off top surface)
m = symmetry factor for plane flow hoppers = 0

To calculate initial pressure, firstly the pressure at the interface from vertical bin to hopper is calculated using (A.1), repeated here for ease of reference:

$$p_v = \frac{\gamma\, r_c}{\mu\, k}\left[1 - e^{-(\mu\, k\, y/r_c)}\right] + p_{vo}\, e^{-(\mu\, k\, y/r_c)} \qquad \text{(F.1)}$$

Specifying the input parameters calculated as:

r_c = D/4 = 480/4 = 120 mm (from calc. A.5)

k = 0.35 (selected value for all materials in the current research)

P_{v0} = γ . h_s = γ . 0 = 0 kPa

for ease of calculation, and considering practicality in calculation, factor is applied as "Jansen exponent factor", calculated as:

$$J_{ansexp} = e^{-\left(\mu\, k\frac{y}{r_c}\right)} = e^{-\left(0.5317..\times 0.35\times\frac{0.35}{0.12}\right)} = 0.581126562.. \quad \text{(F.2)}$$

Therefore, (F.1) is evaluated as:

$$p_v = \frac{14.756..\cdot 0.1203..}{0.05317..\cdot 0.35}[1 - 0.581126562..] + 0 \cdot 0.581126562.. = 3.985..\text{kPa}$$

The initial load on the hopper is evaluated from (A.19), with z_h substituted for z_g, which as, 845 mm,

$p_{vhi} = p_s + \gamma z_h$ = 3.985.. + 14,756..(0.845) = 11.290 kPa (F.3)

for flow pressure,

$$p_{vhf} = \gamma\left[\frac{h_h - z_h}{j-1}\right] + \left[\left(p_s - \frac{\gamma\, h_h}{(j-1)}\right)\left(\frac{h_h - z_h}{h_h}\right)^j\right] \quad \text{(F.4)}$$

In this term, p_s is equal to p_{vo} from (F.1)

Calculating for (A.26),

$$\eta = 0.5\left(\phi_w + \sin^{-1}\left(\frac{\sin\phi_w}{\sin\delta}\right)\right)$$

$$= 0.5\left(47° + \sin^{-1}\left(\frac{\sin 47}{\sin 28}\right)\right) = 0.592846..Radians = 33.9° \quad \text{(F.5)}$$

Calculating for (A.25),

$$k_{hf} = \frac{2(1+sin\delta\, cos2\eta)}{2-sin\delta(1+\cos(\alpha+\eta))}$$

$$= \frac{2(1+sin47\, cos2(33.9))}{2-sin47(1+\cos(19.97+33.9))} = 1.7075.. \quad \text{(F.6)}$$

Calculating for (A.24),

With $j = (m+1)\left\{k_{hf}\left[1+\frac{\tan\phi_w}{\tan\alpha}\right]-1\right\}$

$$= (0+1)\left\{1.7075..\left[1+\frac{0.5317..}{\tan 19.97}\right]-1\right\} = 3.2067\ldots \qquad \text{(F.7)}$$

Calculating for (F.4),

$$p_{vhf} = 14.756\left[\frac{0.66-0.495}{3.2067\ldots-1}\right] + \left[\left(3.985\ldots-\frac{14.756\cdot 0.66}{(3.2067\ldots-1)}\right)\left(\frac{0.66-0.495}{0.66}\right)^{3.2067\ldots}\right]$$

$$= 1.1023\ldots \qquad \text{(F.8)}$$

F.2 Calculation of material withdrawal volume

Using the methodology described in Appendix B, an example calculation is presented to evaluate the material withdrawal angle.

The configuration of test Set 9 is used, which represents the nominal 120 mm hopper width, 20-degree wall angle, quartz aggregate, and only the hopper filled.

The example dimension of the comparison is a feeder plate displacement of 35 mm (20 rotations of the nut).

The input parameters of the example are:

B = Hopper opening width = 120.33 mm
L = Hopper opening length = 480 mm
H = Height of material pile = 35 mm
ρ = Bulk Density = 1478.3 kg/m^3 (consolidated 25% as noted in Section 3.3.3)
ϕ_r = Repose angle = 43°

Calculating for (B.2):

$$V_w = L \cdot B \cdot H + (L+B) \cdot H^2 / \tan \phi_r + \pi \cdot H^3 / (3 \cdot \tan^2 \phi_r)$$

$$= (0.48 \cdot 0.12033 \cdot 0.035) + (0.48 + 0.12033) \cdot 0.035^2 / \tan(43°) + \pi \cdot 0.035^3 / (3 \cdot \tan^2(43°))$$

$$= 0.002862\ldots \text{ m}^3$$

Calculating for (B.6):

$$M_{wd} = V_w \cdot \rho = 0.002862 \cdot 1478.3 = 4.229\ldots$$

The load applied onto the loadcell is:

$$\text{Load} = M_{wd} \cdot g = 4.229\ldots \cdot 9.81 = 41.5 \text{ N} \qquad \text{(F.9)}$$

Appendix G Test Results

The full set of test results tabulated, and graphed, is contained in this Appendix.

Where tabulated tables are long, only the upper portion of the table is shown for ease of usage, this on the basis that the majority of the information of interest is at the deflections less than 8 mm. The full data sets are tabulated.

Cells highlighted in green represent tests with some observed method inconsistencies but which still provide useful reference information in the context of the study. The data records of accepted errors or record of corrections are made in the relative sections listed here.

Set 1 – was not used because data was discarded due to the case being a preliminary test run.

G.1 Set 2, 20-degrees, 120 mm slot, dry sand, bin levelled full

Table G- 1 Test Set 2, 20-degrees, 120 mm, dry sand, bin filled

Test Record Sheet		Hopper base plate lowering force curve																	
Set Number		2																	
Test Name		20 degrees, 120 mm slot, dry sand, levelled																	
											Calculated loads								
Max Lump		mm	P80 Lump		mm	Moisture		%			Initial:	652.1	N						
Width	120.33	mm	Length	480	mm	Angle	19.4435	degrees			Flow:	63.7	N						
Tare	7.09	kg	Spec. wt	14756.7	N/m3	(loose density +25% of difference to tapped density)													
Screw Pitch M1	1.75	mm	repose	35	degrees														
		Test 1		Test 2		Test 3		Test 4 (kg)		t 1 (Repose)	Test 2 (Repose)		Test 3 (Repose)				Initial	Flow	Average
Load record (screw turns)	Disp. (mm)	Volt 1	Volt 2	Volt 1	Volt 2	367	Volt 2	Load 1	Load 2	Draw Load	Load-Test 1	Draw Load	Load-Test 2	Draw Load	Load-Test 3	DISP.	(calc)	(calc)	
empty																			
max	392.804										462.2		392.8		423.6				
min	52.4494										47.5		52.4		45.8				
50% reduction	222.626										254.9		222.6		234.7				
80% reduction	120.52										130.5		120.5		121.4				
displacement -	10.5										11.4		10.5		10.5				
displacement -	0.83339										1.3384		0.8334		0.5556				
50% red displ a	0.69%										1.112%		0.693%		0.462%				
displacement -	2.19941										1.7033		2.1994		1.2747				
80% red displ a	1.83%										1.415%		1.828%		1.059%				
0	0	1060	1125	914	987	926	1100			0.00	462.2	0.00	392.8	0.00	423.6	0	652.1	63.7	426.2
0.125	0.219			745	799	683	950			0.19		0.19	305.3	0.19	327.4	0.21875	652.1	63.7	316.4
0.25	0.438	723	952	638	723	677	821			0.38	337.5	0.38	260.4	0.38	294.0	0.4375	652.1	63.7	297.3
0.375	0.656			590	674	480	570			0.56		0.56	236.5	0.56	184.2	0.65625	652.1	63.7	210.3
0.5	0.875	645	751	570	625	420	507			0.76	268.6	0.76	219.4	0.76	153.9	0.875	652.1	63.7	214.0
0.625	1.094			555	601	426	489			0.95		0.95	209.6	0.95	150.7	1.09375	652.1	63.7	180.2
0.75	1.313	561	670	465	480	371	400			1.14	227.9	1.14	157.8	1.14	115.3	1.3125	652.1	63.7	167.0
0.875	1.531			439	464	335	367			1.33		1.33	147.3	1.33	98.2	1.53125	652.1	63.7	122.8
1	1.750	487	493	380	430	327	364			1.53	165.9	1.53	124.4	1.53	95.3	1.75	652.1	63.7	128.6
1.125	1.969					304	345			1.73		1.73		1.73	84.9	1.96875	652.1	63.7	84.9
1.25	2.188	413	478	350	420	276	315			1.93	143.9	1.93	114.3	1.93	70.5	2.1875	652.1	63.7	109.5
1.375	2.406									2.12		2.12		2.12		2.40625	652.1	63.7	
1.5	2.625	370	426	345	384	274	304			2.33	120.2	2.33	103.8	2.33	66.9	2.625	652.1	63.7	97.0
1.625	2.844									2.53		2.53		2.53		2.84375	652.1	63.7	
1.75	3.063	366	383	317	335	265	287			2.73	108.3	2.73	84.5	2.73	60.1	3.0625	652.1	63.7	84.3
1.875	3.281									2.93		2.93		2.93		3.28125	652.1	63.7	
2	3.500	340	357	290	323	245	294			3.14	95.1	3.14	74.6	3.14	56.6	3.5	652.1	63.7	75.4
2.125	3.719									3.35		3.35		3.35		3.71875	652.1	63.7	
2.25	3.938	310	350			249	280			3.55	85.7	3.55		3.55	53.7	3.9375	652.1	63.7	69.7
2.375	4.156									3.76		3.76		3.76		4.15625	652.1	63.7	
2.5	4.375	295	341	285	312	246	263			3.97	79.4	3.97	69.9	3.97	48.3	4.375	652.1	63.7	65.9
2.625	4.594									4.19		4.19		4.19		4.59375	652.1	63.7	
2.75	4.813	318	328			250	268			4.40	81.4	4.40		4.40	50.1	4.8125	652.1	63.7	65.7
2.875	5.031									4.61		4.61		4.61		5.03125	652.1	63.7	
3	5.250	301	332	267	302	241	266			4.83	77.8	4.83	62.2	4.83	47.0	5.25	652.1	63.7	62.3
3.125	5.469									5.0		5.0		5.0		5.46875	652.1	63.7	
3.25	5.688									5.3		5.3		5.3		5.6875	652.1	63.7	
3.375	5.906									5.5		5.5		5.5		5.90625	652.1	63.7	
3.5	6.125	278	305	270	295	253	267			5.7	64.7	5.7	60.3	5.7	49.3	6.125	652.1	63.7	58.1
3.625	6.344									5.9		5.9		5.9		6.34375	652.1	63.7	
3.75	6.563									6.1		6.1		6.1		6.5625	652.1	63.7	
3.875	6.781									6.4		6.4		6.4		6.78125	652.1	63.7	
4	7.000	272	300	260	292	248	270			6.6	61.1	6.6	56.2	6.6	47.9	7	652.1	63.7	55.1
4.125	7.219									6.8		6.8		6.8		7.21875	652.1	63.7	
4.25	7.438									7.1		7.1		7.1		7.4375	652.1	63.7	
4.375	7.656									7.3		7.3		7.3		7.65625	652.1	63.7	
4.5	7.875	284	294	265	284	256	271			7.5	61.7	7.5	54.6	7.5	49.2	7.875	652.1	63.7	55.1
4.625	8.094									7.7		7.7		7.7		8.09375	652.1	63.7	
4.75	8.313									8.0		8.0		8.0		8.3125	652.1	63.7	
4.875	8.531									8.2		8.2		8.2		8.53125	652.1	63.7	
5	8.750	273	295	265	289	252	275			8.4	58.3	8.4	54.9	8.4	48.3	8.75	652.1	63.7	53.8
5.125	8.969									8.7		8.7		8.7		8.96875	652.1	63.7	
5.25	9.188									8.9		8.9		8.9		9.1875	652.1	63.7	
5.375	9.406									9.2		9.2		9.2		9.40625	652.1	63.7	
5.5	9.625	270	292			260	276			9.4	55.9	9.4		9.4	49.5	9.625	652.1	63.7	52.7
5.625	9.844									9.6		9.6		9.6		9.84375	652.1	63.7	
5.75	10.063									9.9		9.9		9.9		10.0625	652.1	63.7	
5.875	10.281									10.1		10.1		10.1		10.28125	652.1	63.7	
6	10.500	265	275	264	288	251	274			10.4	49.5	10.4	52.4	10.4	45.8	10.5	652.1	63.7	49.3
6.125	10.719									10.6		10.6		10.6		10.71875	652.1	63.7	
6.25	10.938									10.9		10.9		10.9		10.9375	652.1	63.7	
6.375	11.156									11.1		11.1		11.1		11.15625	652.1	63.7	
6.5	11.375	258	278			269	295			11.4	47.5	11.4		11.4	54.4	11.375	652.1	63.7	51.0
6.625	11.594									11.6		11.6		11.6		11.59375	652.1	63.7	
6.75	11.813									11.9		11.9		11.9		11.8125	652.1	63.7	
6.875	12.031									12.1		12.1		12.1		12.03125	652.1	63.7	
7	12.250	264	285	275	299	271	291			12.4	49.7	12.4	55.8	12.4	52.9	12.25	652.1	63.7	52.8
7.125	12.469									12.7		12.7		12.7		12.46875	652.1	63.7	
7.25	12.688									12.9		12.9		12.9		12.6875	652.1	63.7	
7.375	12.906									13.2		13.2		13.2		12.90625	652.1	63.7	
7.5	13.125	264	292			282	300			13.4	50.4	13.4		13.4	56.7	13.125	652.1	63.7	53.5

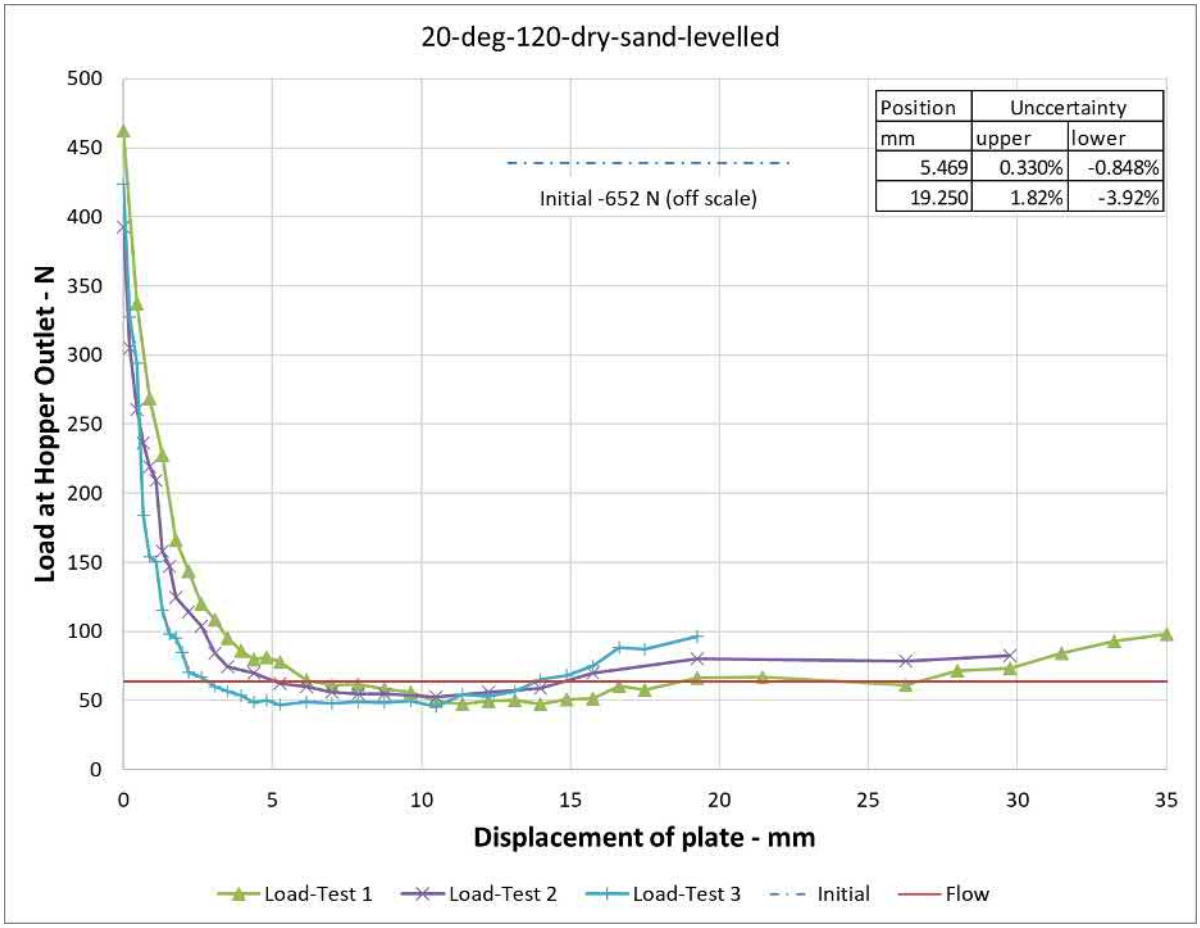


Figure G- 1 Test Set 2, 20-degrees, 120 mm, dry sand, bin filled to top level

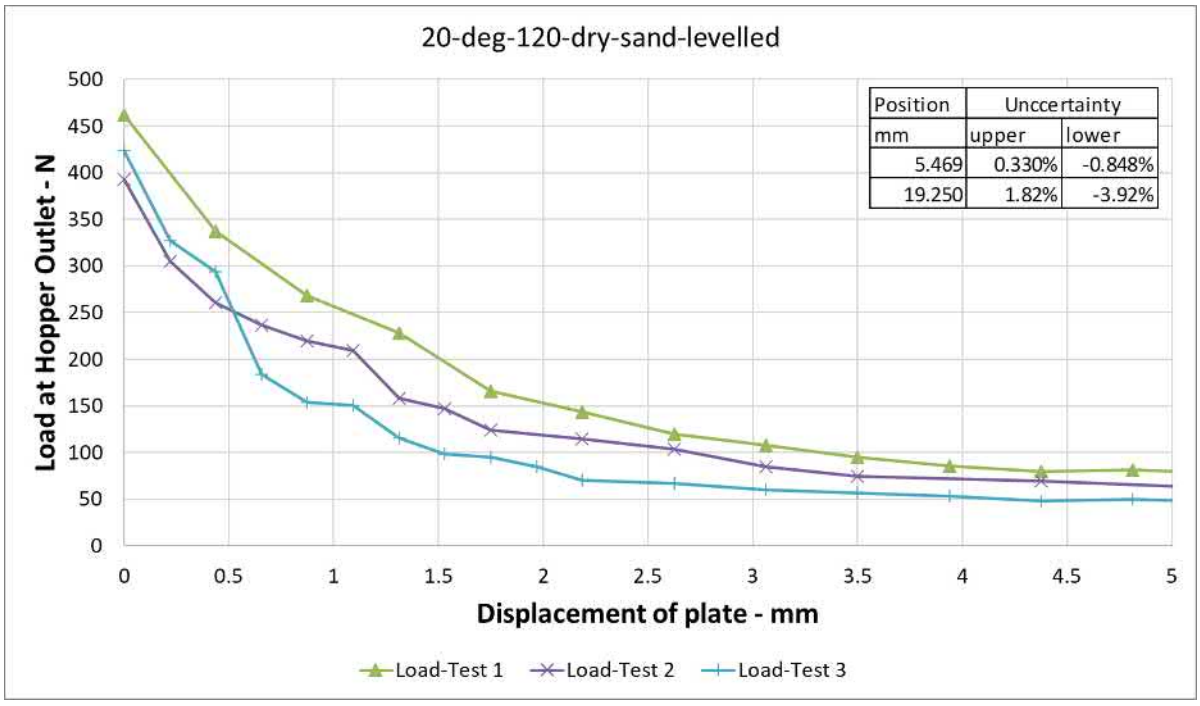


Figure G- 2 Test Set 2, 20-degrees, 120 mm, dry sand, bin filled to top level – 1-5 mm range

G.2 Set 3, 20-degrees, 120 mm, dry sand, hopper only filled

The second test included a method inconsistency, which was corrected in the data to maintain its consistency with other data.

Table G- 2 Test Set 3, 20-degrees, 120 mm, dry sand, hopper filled

Test Record Sheet		Hopper base plate lowering force curve																			
Set Number		3																			
Test Name		20 degrees, 120 mm slot, dry sand, hopper																			
											Calculated loads										
Max Lump		mm	P80 Lump		mm	Moisture		%	(air dry)		Initial:	421.9	N								
Width	120.33	mm	Length	480	mm	Angle	19.4435	degrees			Flow:	60.9	N								
Tare	7.09	kg	Spec. wt	14756.7	N/m3	(loose density +25% of difference to tapped density)															
Screw Pitch M12	1.75	mm	repose	35	degrees																
		Test 1		Test 2		Test 3		Test 4		t 1 (Repose)		Test 2 (Repose)		Test 3 (Repose)		Test 4 (Repose)			Initial	Flow	Average
Load record (screw turns)	Disp. (mm)	Volt 1	Volt 2	Volt 1	Volt 2	Volt 1	Volt 2	Volt 1	Volt 2	Draw Load	Load-Test 1	Draw Load	Load-Test 2	Draw Load	Load-Test 3	Draw Load	Load-Test 4	DISP.	(calc)	(calc)	
empty	empty	140.8	147.9	142.4	148.9	142.9	147.8	137	147												
max	326.064										335.7		315.0		326.1		307.9				
min	48.1141										47.7		47.4		48.1		45.4				
50% reduction	187.089										191.7		181.2		187.1		176.6				
80% reduction	103.704										105.3		100.9		103.7		97.9				
displacement - min	5.46875										10.1		4.6		5.5		9.0				
displacement - 50% rec	0.60151										0.6716		0.3560		0.6015		0.4765				
50% red displ as % of ga	0.500%										0.558%		0.296%		0.500%		0.396%				
displacement - 80% rec	1.44567										2.0889		1.0825		1.4457		1.8118				
80% red displ as % of ga	1.201%										1.736%		0.900%		1.201%		1.506%				
0	0	797	864	766	813	804	820	771	772	0.00	335.7	0.00	315.0	0.00	326.1	0.00	307.9	0			321.1
0.125	0.219	615	729	598	676	686	756	605	605	0.19	258.1	0.19	240.3	0.19	281.5	0.19	226.2	0.21875	421.9	60.9	251.5
0.25	0.438	513	625	421	469	594	572	504	526	0.38	207.5	0.38	146.1	0.38	213.6	0.38	182.1	0.4375	421.9	60.9	187.3
0.375	0.656	494	589	349	397	517	505	463	443	0.56	193.8	0.56	110.7	0.56	178.2	0.56	151.5	0.65625	421.9	60.9	158.6
0.5	0.875	442	517	347	408	469	478	413	443	0.76	163.3	0.76	112.7	0.76	159.7	0.76	139.2	0.875	421.9	60.9	143.7
0.625	1.094	429	487	337	368	383	409	377	375	0.95	152.6	0.95	100.3	0.95	121.7	0.95	113.5	1.09375	421.9	60.9	122.0
0.75	1.313	421	453	312	340	364	402	427	420	1.14	142.0	1.14	87.1	1.14	115.1	1.14	136.5	1.3125	421.9	60.9	120.2
0.875	1.531	365	407	293	320	332	358	374	365	1.33	116.9	1.33	77.4	1.33	96.3	1.33	109.9	1.53125	421.9	60.9	100.1
1	1.750	355	401	295	326			350	365	1.53	112.8	1.53	79.1	1.53		1.53	103.9	1.75	421.9	60.9	98.6
1.125	1.969	355	401	291	322	303	332	307	322	1.73	112.6	1.73	77.0	1.73	82.5	1.73	82.6	1.96875	421.9	60.9	88.7
1.25	2.188	317	385							1.93	99.3	1.93		1.93		1.93		2.1875	421.9	60.9	99.3
1.375	2.406					276	301	286	295	2.12		2.12		2.12	67.9	2.12	70.5	2.40625	421.9	60.9	69.2
1.5	2.625	314	367							2.33	93.7	2.33		2.33		2.33		2.625	421.9	60.9	93.7
1.625	2.844			257	282	291	315	271	277	2.53		2.53	58.1	2.53	74.6	2.53	62.0	2.84375	421.9	60.9	64.9
1.75	3.063	295	332							2.73	80.1	2.73		2.73		2.73		3.0625	421.9	60.9	80.1
1.875	3.281					262	280	286	296	2.93		2.93		2.93	58.5	2.93	69.9	3.28125	421.9	60.9	64.2
2	3.500	301	331							3.14	80.9	3.14		3.14		3.14		3.5	421.9	60.9	80.9
2.125	3.719			260	293	255	280	257	277	3.35		3.35	60.7	3.35	56.4	3.35	57.8	3.71875	421.9	60.9	58.3
2.25	3.938	278	325							3.55	73.4	3.55		3.55		3.55		3.9375	421.9	60.9	73.4
2.375	4.156					249	274			3.76		3.76		3.76	53.1	3.76		4.15625	421.9	60.9	53.1
2.5	4.375	270	304							3.97	65.9	3.97		3.97		3.97		4.375	421.9	60.9	65.9
2.625	4.594			234	268	247	266	245	252	4.19		4.19	47.4	4.19	50.2	4.19	47.9	4.59375	421.9	60.9	48.5
2.75	4.813	258	283							4.40	57.3	4.40		4.40		4.40		4.8125	421.9	60.9	57.3
2.875	5.031									4.61		4.61		4.61		4.61		5.03125	421.9	60.9	
3	5.250	276	301							4.83	65.7	4.83		4.83		4.83		5.25	421.9	60.9	65.7
3.125	5.469			245.5	268.5	246	262	242	269	5.0		5.0	49.4	5.0	48.1	5.0	50.5	5.46875	421.9	60.9	49.4
3.25	5.688	251	286							5.3	55.5	5.3		5.3		5.3		5.6875	421.9	60.9	55.5
3.375	5.906			Measured as 277		Measured as 337, nut turned wrong way				5.5		5.5		5.5		5.5		5.90625	421.9	60.9	
3.5	6.125									5.7		5.7		5.7		5.7		6.125	421.9	60.9	
3.625	6.344					257	278	255	260	5.9		5.9		5.9	53.8	5.9	50.6	6.34375	421.9	60.9	52.2
3.75	6.563	254	283							6.1	54.6	6.1		6.1		6.1		6.5625	421.9	60.9	54.6
3.875	6.781									6.4		6.4		6.4		6.4		6.78125	421.9	60.9	
4	7.000									6.6		6.6		6.6		6.6		7	421.9	60.9	
4.125	7.219			257	269	268	296	247	270	6.8		6.8	50.6	6.8	60.1	6.8	50.2	7.21875	421.9	60.9	53.6
4.25	7.438	260	291							7.1	57.1	7.1		7.1		7.1		7.4375	421.9	60.9	57.1
4.375	7.656									7.3		7.3		7.3		7.3		7.65625	421.9	60.9	
4.5	7.875									7.5		7.5		7.5		7.5		7.875	421.9	60.9	
4.625	8.094					256	277			7.7		7.7		7.7	51.5	7.7		8.09375	421.9	60.9	51.5
4.75	8.313	250	274							8.0	49.6	8.0		8.0		8.0		8.3125	421.9	60.9	49.6
4.875	8.531									8.2		8.2		8.2		8.2		8.53125	421.9	60.9	
5	8.750									8.4		8.4		8.4		8.4		8.75	421.9	60.9	
5.125	8.969			264	273			241	264	8.7		8.7	51.4	8.7		8.7	45.4	8.96875	421.9	60.9	48.4
5.25	9.188	246	279							8.9	48.9	8.9		8.9		8.9		9.1875	421.9	60.9	48.9
5.375	9.406									9.2		9.2		9.2		9.2		9.40625	421.9	60.9	
5.5	9.625									9.4		9.4		9.4		9.4		9.625	421.9	60.9	
5.625	9.844					269	289			9.6		9.6		9.6	55.7	9.6		9.84375	421.9	60.9	55.7
5.75	10.063	251	273							9.9	47.7	9.9		9.9		9.9		10.0625	421.9	60.9	47.7
5.875	10.281									10.1		10.1		10.1		10.1		10.28125	421.9	60.9	
6	10.500									10.4		10.4		10.4		10.4		10.5	421.9	60.9	
6.125	10.719			275	287			261	283	10.6		10.6	55.6	10.6		10.6	53.0	10.71875	421.9	60.9	54.3
6.25	10.938	262	289							10.9	53.3	10.9		10.9		10.9		10.9375	421.9	60.9	53.3
6.375	11.156									11.1		11.1		11.1		11.1		11.15625	421.9	60.9	
6.5	11.375									11.4		11.4		11.4		11.4		11.375	421.9	60.9	
6.625	11.594					267	301			11.6		11.6		11.6	56.2	11.6		11.59375	421.9	60.9	56.2
6.75	11.813	264	283							11.9	51.3	11.9		11.9		11.9		11.8125	421.9	60.9	51.3
6.875	12.031									12.1		12.1		12.1		12.1		12.03125	421.9	60.9	
7	12.250									12.4		12.4		12.4		12.4		12.25	421.9	60.9	
7.125	12.469			277	293			272	284	12.7		12.7	55.5	12.7		12.7	53.9	12.46875	421.9	60.9	54.7
7.25	12.688	254	292							12.9	50.1	12.9		12.9		12.9		12.6875	421.9	60.9	50.1
7.375	12.906									13.2		13.2		13.2		13.2		12.90625	421.9	60.9	
7.5	13.125									13.4		13.4		13.4		13.4		13.125	421.9	60.9	
7.625	13.344					289	309			13.7		13.7		13.7	61.5	13.7		13.34375	421.9	60.9	61.5

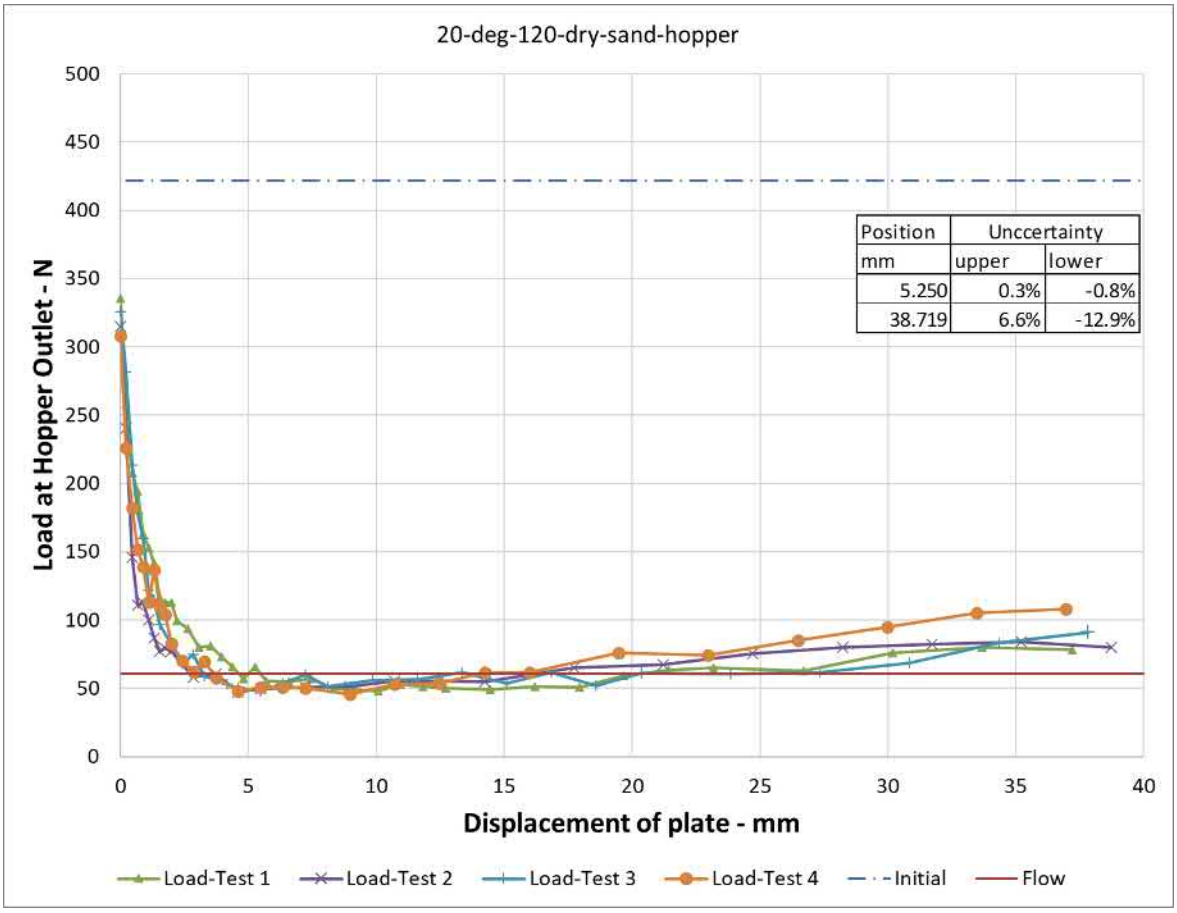


Figure G- 3 Test Set 3, 20-deg, 120 mm, dry sand, hopper filled

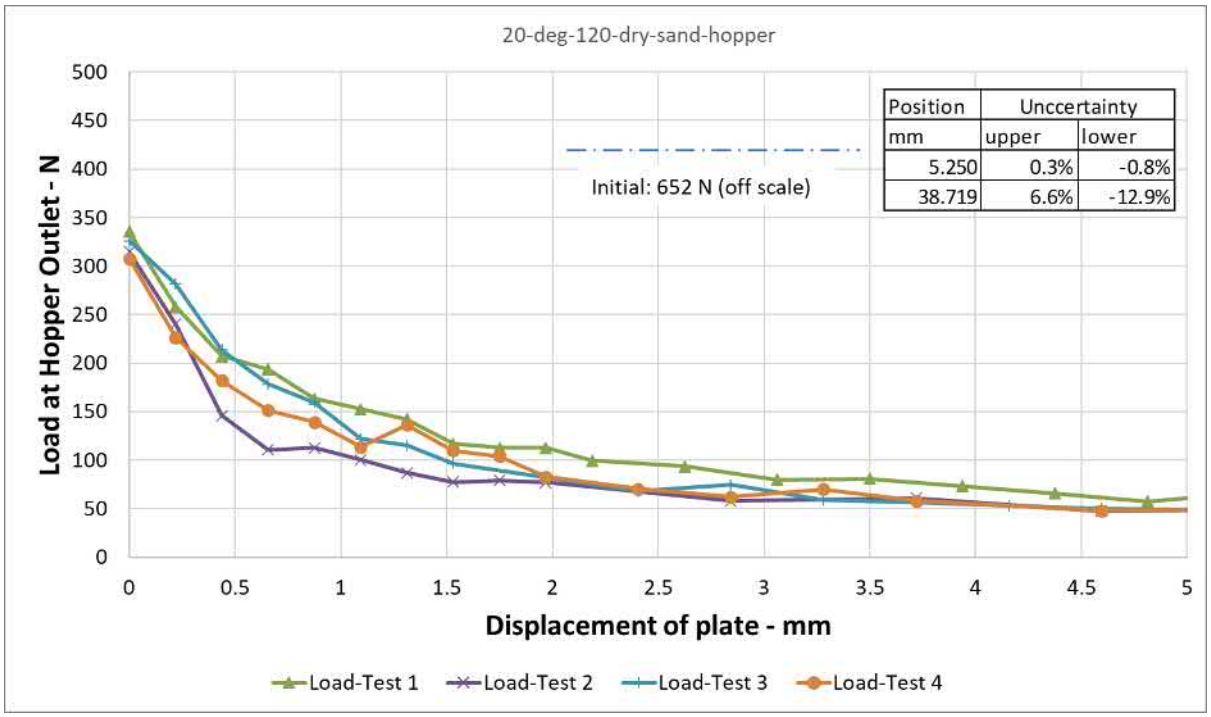


Figure G- 4 Test Set 3, 20-deg, 120 mm, dry sand, hopper filled

G.3 Set 4, 20-degrees, 150 mm, dry sand, bin levelled full

Table G- 3 Test Set 4, 20-degrees, 150 mm, dry sand, bin levelled full

Test Record Sheet		Hopper base plate lowering force curve															
Set Number		4															
Test Name		20 degrees, 150 mm slot, dry sand, levelled															
											Calculated loads						
Max Lump		mm	P80 Lump		mm	Moisture		%	(air dry)		Initial:	791.2	N				
Width	145	mm	Length	480	mm	Angle	18.3171	degrees			Flow:	89.4	N				
Tare	7.09	kg	Spec. wt	14756.7	N/m3	(loose density +25% of difference to tapped density)											
Screw Pitch M12	1.75	mm	repose	35	degrees												
		Test 1		Test 2		Test 3		Test 4		t 1 (Repose)	Test 2 (Repose)				Initial	Flow	Average
Load record (screw turns)	Disp. (mm)	Volt 1	Volt 2	Volt 1	Volt 2	Volt 1	Volt 2	Volt 1	Volt 2	Draw Load	Load-Test 1	Draw Load	Load-Test 2	DISP.	(calc)	(calc)	
empty		137	147	138	149												
max	582.89										582.9		488.9				
min	77.411										77.4		85.1				
50% reduction	330.15										330.2		287.0				
80% reduction	178.51										178.5		165.9				
displacement - min	12.031										12.0		13.3				
displacement - 50% red.	1.0989										1.0989		0.7207				
50% red displ as % of gap	0.76%										0.758%		0.497%				
displacement - 80% red.	2.9601										2.9601		2.4084				
80% red displ as % of gap	2.04%										2.041%		1.661%				
0	0	1286	1381	1124	1162					0.00	582.9	0.00	488.9	0	791.2	89.4	535.9
0.125	0.219	1100	1277	985	954					0.23	511.9	0.23	403.7	0.21875	791.2	89.4	457.8
0.25	0.438	956	1091	815	847					0.45	430.9	0.45	335.8	0.4375	791.2	89.4	383.4
0.375	0.656	925	928	728	782					0.68	383.0	0.68	298.5	0.65625	791.2	89.4	340.7
0.5	0.875			673	679					0.91		0.91	259.5	0.875	791.2	89.4	259.5
0.625	1.094	815	793	643	648					1.14	322.6	1.14	244.4	1.09375	791.2	89.4	283.5
0.75	1.313			575	579					1.37		1.37	210.6	1.3125	791.2	89.4	210.6
0.875	1.531	734	731	556	558					1.60	287.2	1.60	200.6	1.53125	791.2	89.4	243.9
1	1.750			518	518					1.84		1.84	181.3	1.75	791.2	89.4	181.3
1.125	1.969	722	724	505	522					2.07	282.1	2.07	178.9	1.96875	791.2	89.4	230.5
1.25	2.188									2.31		2.31		2.1875	791.2	89.4	
1.375	2.406	600	644	483	486					2.55	232.3	2.55	164.2	2.40625	791.2	89.4	198.2
1.5	2.625									2.79		2.79		2.625	791.2	89.4	
1.625	2.844	500	550	461	470					3.03	184.4	3.03	154.5	2.84375	791.2	89.4	169.4
1.75	3.063									3.27		3.27		3.0625	791.2	89.4	
1.875	3.281	538	585	422	424					3.51	201.7	3.51	133.2	3.28125	791.2	89.4	167.4
2	3.500									3.76		3.76		3.5	791.2	89.4	
2.125	3.719	417	457	413	420					4.00	140.3	4.00	129.5	3.71875	791.2	89.4	134.9
2.25	3.938									4.25		4.25		3.9375	791.2	89.4	
2.375	4.156	372	406							4.50	116.3	4.50		4.15625	791.2	89.4	116.3
2.5	4.375									4.75		4.75		4.375	791.2	89.4	
2.625	4.594	361	399	388	401					5.00	111.5	5.00	117.8	4.59375	791.2	89.4	114.6
2.75	4.813									5.25		5.25		4.8125	791.2	89.4	
2.875	5.031	365	398							5.50	111.7	5.50		5.03125	791.2	89.4	111.7
3	5.250									5.76		5.76		5.25	791.2	89.4	
3.125	5.469			367	370					6.0		6.0	104.0	5.46875	791.2	89.4	104.0
3.25	5.688									6.3		6.3		5.6875	791.2	89.4	
3.375	5.906	313	354							6.5	87.2	6.5		5.90625	791.2	89.4	87.2
3.5	6.125									6.8		6.8		6.125	791.2	89.4	
3.625	6.344			384	421					7.1		7.1	119.7	6.34375	791.2	89.4	119.7
3.75	6.563									7.3		7.3		6.5625	791.2	89.4	
3.875	6.781	322	353							7.6	88.1	7.6		6.78125	791.2	89.4	88.1
4	7.000									7.8		7.8		7	791.2	89.4	
4.125	7.219									8.1		8.1		7.21875	791.2	89.4	
4.25	7.438									8.4		8.4		7.4375	791.2	89.4	
4.375	7.656									8.6		8.6		7.65625	791.2	89.4	
4.5	7.875									8.9		8.9		7.875	791.2	89.4	
4.625	8.094			338	348					9.2		9.2	88.4	8.09375	791.2	89.4	88.4
4.75	8.313									9.5		9.5		8.3125	791.2	89.4	
4.875	8.531	316	348							9.7	83.2	9.7		8.53125	791.2	89.4	83.2
5	8.750									10.0		10.0		8.75	791.2	89.4	
5.125	8.969									10.3		10.3		8.96875	791.2	89.4	
5.25	9.188									10.6		10.6		9.1875	791.2	89.4	
5.375	9.406									10.9		10.9		9.40625	791.2	89.4	
5.5	9.625									11.1		11.1		9.625	791.2	89.4	
5.625	9.844			348	357					11.4		11.4	90.8	9.84375	791.2	89.4	90.8
5.75	10.063									11.7		11.7		10.0625	791.2	89.4	
5.875	10.281	314	349							12.0	80.7	12.0		10.28125	791.2	89.4	80.7
6	10.500									12.3		12.3		10.5	791.2	89.4	
6.125	10.719									12.6		12.6		10.71875	791.2	89.4	
6.25	10.938									12.9		12.9		10.9375	791.2	89.4	
6.375	11.156									13.1		13.1		11.15625	791.2	89.4	
6.5	11.375									13.4		13.4		11.375	791.2	89.4	
6.625	11.594			356	359					13.7		13.7	90.9	11.59375	791.2	89.4	90.9
6.75	11.813									14.0		14.0		11.8125	791.2	89.4	
6.875	12.031	317	342							14.3	77.4	14.3		12.03125	791.2	89.4	77.4

time response due to reading delay

(volt 2 turned wrong way) affects volt 1 also

Volt 2 turned wrong way

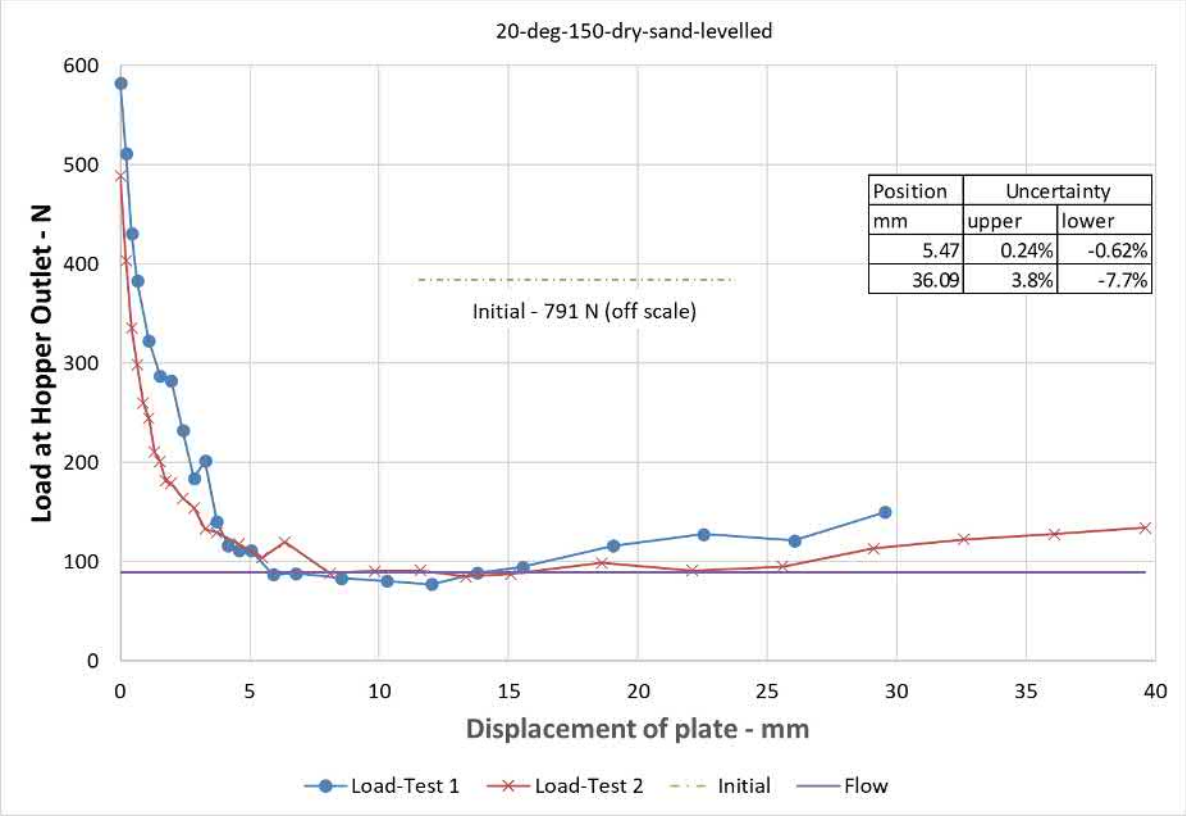


Figure G- 5 Test Set 4, 20deg, 150 mm, dry sand levelled full

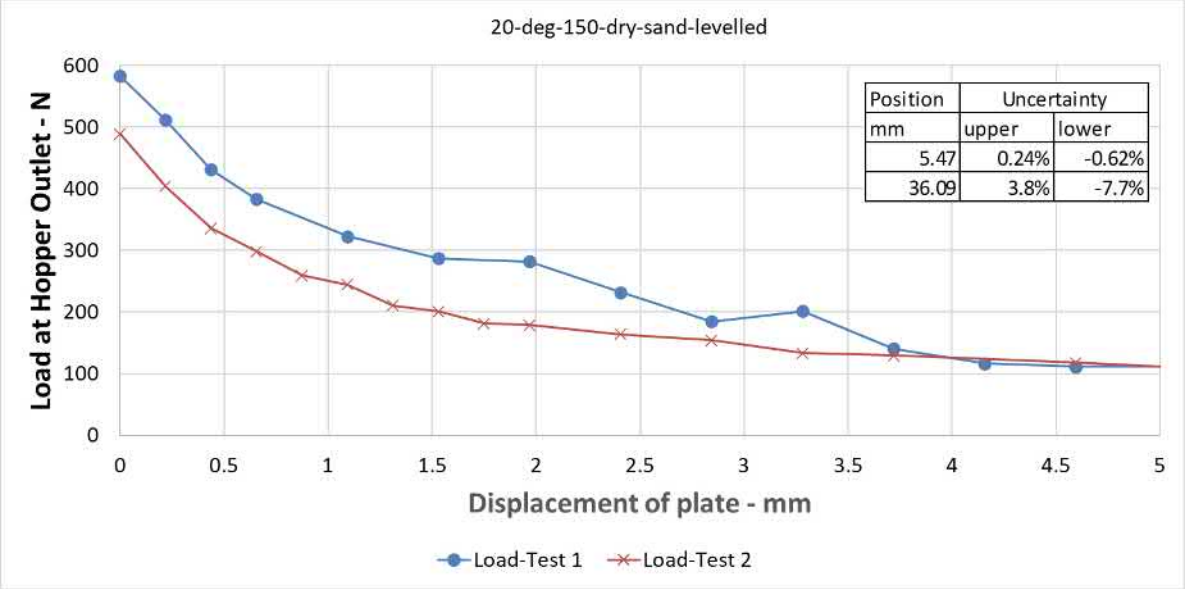


Figure G- 6 Test Set 4, 20-deg, 150 mm, dry sand, levelled full

G.4 Set 5, 30-degrees, 150 mm, dry sand, hopper filled

Table G- 4 Test Set 5, 30-degrees, 150 mm, dry sand, hopper filled

Test Record Sheet		Hopper base plate lowering force curve																			
Set Number		5																			
Test Name		30 degrees, 150 mm slot, dry sand, hopper																			
											Calculated loads										
Max Lump		mm	P80 Lump		mm	Moisture		%	(air dry)		Initial:	306.5	N								
Width	140	mm	Length	480	mm	Angle	27.9719	degrees			Flow:	73.9	N								
Tare	7.09	kg	Spec. wt	14756.7	N/m3	(loose density +25% of difference to tapped density)															
Screw Pitch M12	1.75	mm	repose	35	degrees																
		Test 1		Test 2		Test 3		Test 4 (fastpour)		t 1 (Repose)	Test 2 (Repose)		Test 3 (Repose)		Test 4 (Repose)				Initial	Flow	Average
Load record (screw turns)	Disp. (mm)	Volt 1	Volt 2	Volt 1	Volt 2	Volt 1	Volt 2	Volt 1	Volt 2	Draw Load	Load-Test 1	Draw Load	Load-Test 2	Draw Load	Load-Test 3	Draw Load	Load-Test 4 (fast pour)	DISP.	(calc)	(calc)	
empty		146	148	148.5	148.3	147.7	148.8	135	149												
max	270.904582										270.9		259.0		268.6		252.6				
min	59.9538818										60.0		58.1		74.5		68.3				
50% reduction	165.429232										165.4		158.5		171.6		160.4				
80% reduction	102.144022										102.1		98.3		113.3		105.1				
displacement - min	6.5625										6.6		4.8		6.1		5.3				
displacement - 50% red.	0.43611686										0.4361		0.4045		0.3276		0.4668				
50% red displ as % of gap	0.31%										0.312%		0.289%		0.234%		0.333%				
displacement - 80% red.	1.56223758										1.5622		1.2737		1.3864		1.6270				
80% red displ as % of gap	1.12%										1.116%		0.910%		0.990%		1.162%				
0	0	712	690	684	672	709	686	658	659	0.00	270.9	0.00	259.0	0.00	268.6	0.00	252.6	0			264.9
0.125	0.219	543	571	542	554	521	534	534	532	0.22	200.4	0.22	195.2	0.22	185.3	0.22	191.0	0.21875	306.5	73.9	197.8
0.25	0.438	460	511	442	478	459	484	481	472	0.44	165.2	0.44	152.0	0.44	157.7	0.44	163.1	0.4375	306.5	73.9	158.6
0.375	0.656	435	489	398	441	431	461	441	431	0.66	153.5	0.66	132.0	0.66	145.0	0.66	143.1	0.65625	306.5	73.9	142.8
0.5	0.875	383	425	467	408	405	552	419	412	0.88	124.9	0.88	140.4	0.88	160.9	0.88	132.8	0.875	306.5	73.9	132.6
0.625	1.094	359	407	338	378	384	415	397	388	1.10	114.4	1.10	101.5	1.10	121.8	1.10	121.4	1.09375	306.5	73.9	107.9
0.75	1.313	357	388	333	368	374	404	384	376	1.32	109.0	1.32	97.6	1.32	116.5	1.32	115.0	1.3125	306.5	73.9	103.3
0.875	1.531	353	371	320	339	357	384	389	356	1.55	103.6	1.55	87.1	1.55	107.2	1.55	111.1	1.53125	306.5	73.9	95.3
1	1.750	334	348	303	324	349	382	341	349	1.78	93.1	1.78	79.0	1.78	104.5	1.78	97.5	1.75	306.5	73.9	86.1
1.125	1.969			295	318					2.00		2.00	75.4	2.00		2.00		1.96875	306.5	73.9	75.4
1.25	2.188	334	346	301	328	341	368	327	325	2.23	92.2	2.23	79.1	2.23	98.7	2.23	87.7	2.1875	306.5	73.9	85.6
1.375	2.406									2.46		2.46		2.46		2.46		2.40625	306.5	73.9	
1.5	2.625	293	319	277	304	322	344	317	318	2.69	75.1	2.69	66.9	2.69	87.7	2.69	83.1	2.625	306.5	73.9	71.0
1.625	2.844									2.93		2.93		2.93		2.93		2.84375	306.5	73.9	
1.75	3.063	311	328	277	298	308	336	303	303	3.16	81.2	3.16	64.9	3.16	81.9	3.16	75.6	3.0625	306.5	73.9	73.1
1.875	3.281									3.40		3.40		3.40		3.40		3.28125	306.5	73.9	
2	3.500	288	300	272	285	315	331	296	299	3.63	68.3	3.63	60.0	3.63	81.9	3.63	72.4	3.5	306.5	73.9	64.2
2.125	3.719									3.87		3.87		3.87		3.87		3.71875	306.5	73.9	
2.25	3.938	283	299	272	293					4.11	66.3	4.11	61.5	4.11		4.11		3.9375	306.5	73.9	63.9
2.375	4.156									4.35		4.35		4.35		4.35		4.15625	306.5	73.9	
2.5	4.375					307	324	293	297	4.59		4.59		4.59	77.2	4.59	70.2	4.375	306.5	73.9	
2.625	4.594									4.83		4.83		4.83		4.83		4.59375	306.5	73.9	
2.75	4.813	279	298	268	287					5.08	64.2	5.08	58.1	5.08		5.08		4.8125	306.5	73.9	61.1
2.875	5.031									5.32		5.32		5.32		5.32		5.03125	306.5	73.9	
3	5.250					308	324	286	300	5.57		5.57		5.57	76.5	5.57	68.3	5.25	306.5	73.9	
3.125	5.469									5.8		5.8		5.8		5.8		5.46875	306.5	73.9	
3.25	5.688	281	297	279	294					6.1	63.4	6.1	61.5	6.1		6.1		5.6875	306.5	73.9	62.5
3.375	5.906									6.3		6.3		6.3		6.3		5.90625	306.5	73.9	
3.5	6.125					304	324			6.6		6.6		6.6	74.5	6.6		6.125	306.5	73.9	
3.625	6.344									6.8		6.8		6.8		6.8		6.34375	306.5	73.9	
3.75	6.563	275	293	282	300					7.1	60.0	7.1	62.7	7.1		7.1		6.5625	306.5	73.9	61.3
3.875	6.781									7.3		7.3		7.3		7.3		6.78125	306.5	73.9	
4	7.000						347	287	308	7.6		7.6		7.6	84.3	7.6	68.5	7	306.5	73.9	
4.125	7.219									7.9		7.9		7.9		7.9		7.21875	306.5	73.9	
4.25	7.438	281	294	282	300					8.1	60.6	8.1	61.7	8.1		8.1		7.4375	306.5	73.9	61.1
4.375	7.656									8.4		8.4		8.4		8.4		7.65625	306.5	73.9	
4.5	7.875					312	329			8.6		8.6		8.6	75.6	8.6		7.875	306.5	73.9	
4.625	8.094									8.9		8.9		8.9		8.9		8.09375	306.5	73.9	
4.75	8.313									9.2		9.2		9.2		9.2		8.3125	306.5	73.9	
4.875	8.531									9.4		9.4		9.4		9.4		8.53125	306.5	73.9	
5	8.750							299	318	9.7		9.7		9.7		9.7	71.7	8.75	306.5	73.9	
5.125	8.969									10.0		10.0		10.0		10.0		8.96875	306.5	73.9	
5.25	9.188	287	304	302	322					10.2	62.4	10.2	69.8	10.2		10.2		9.1875	306.5	73.9	66.1
5.375	9.406									10.5		10.5		10.5		10.5		9.40625	306.5	73.9	
5.5	9.625					323	340			10.8		10.8		10.8	78.9	10.8		9.625	306.5	73.9	
5.625	9.844									11.1		11.1		11.1		11.1		9.84375	306.5	73.9	
5.75	10.063									11.3		11.3		11.3		11.3		10.0625	306.5	73.9	
5.875	10.281									11.6		11.6		11.6		11.6		10.28125	306.5	73.9	
6	10.500							307	325	11.9		11.9		11.9		11.9	73.2	10.5	306.5	73.9	
6.125	10.719									12.2		12.2		12.2		12.2		10.71875	306.5	73.9	
6.25	10.938	297	304	306	333					12.5	62.6	12.5	71.3	12.5		12.5		10.9375	306.5	73.9	67.0
6.375	11.156									12.7		12.7		12.7		12.7		11.15625	306.5	73.9	
6.5	11.375					327	344			13.0		13.0		13.0	78.6	13.0		11.375	306.5	73.9	
6.625	11.594									13.3		13.3		13.3		13.3		11.59375	306.5	73.9	
6.75	11.813									13.6		13.6		13.6		13.6		11.8125	306.5	73.9	
6.875	12.031									13.9		13.9		13.9		13.9		12.03125	306.5	73.9	
7	12.250							324	349	14.2		14.2		14.2		14.2	81.0	12.25	306.5	73.9	
7.125	12.469									14.5		14.5		14.5		14.5		12.46875	306.5	73.9	
7.25	12.688	312	328	330	345					14.7	69.9	14.7	77.8	14.7		14.7		12.6875	306.5	73.9	73.8
7.375	12.906									15.0		15.0		15.0		15.0		12.90625	306.5	73.9	
7.5	13.125					339	357			15.3		15.3		15.3	82.4	15.3		13.125	306.5	73.9	
7.625	13.344									15.6		15.6		15.6		15.6		13.34375	306.5	73.9	
7.75	13.563									15.9		15.9		15.9		15.9		13.5625	306.5	73.9	
7.875	13.781									16.2		16.2		16.2		16.2		13.78125	306.5	73.9	
8	14.000							346	370	16.5		16.5		16.5		16.5	89.1	14	306.5	73.9	
8.125	14.219									16.8		16.8		16.8		16.8		14.21875	306.5	73.9	
8.25	14.438	317	343	337	350					17.1	72.4	17.1	78.3	17.1		17.1		14.4375	306.5	73.9	75.4

posible incorrect direction Data not used

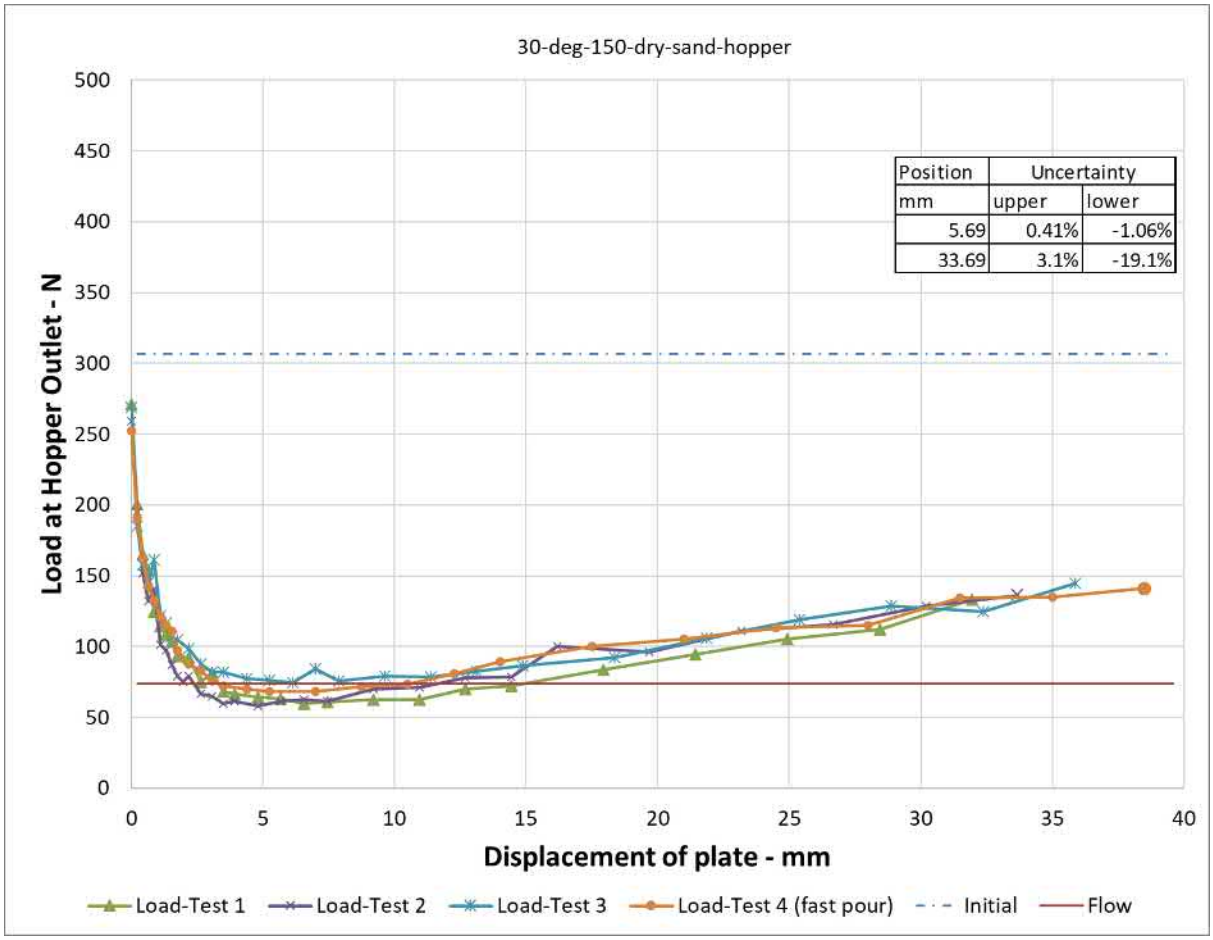


Figure G- 7 Test Set 5, 30-degrees, 150 mm, dry sand, hopper filled

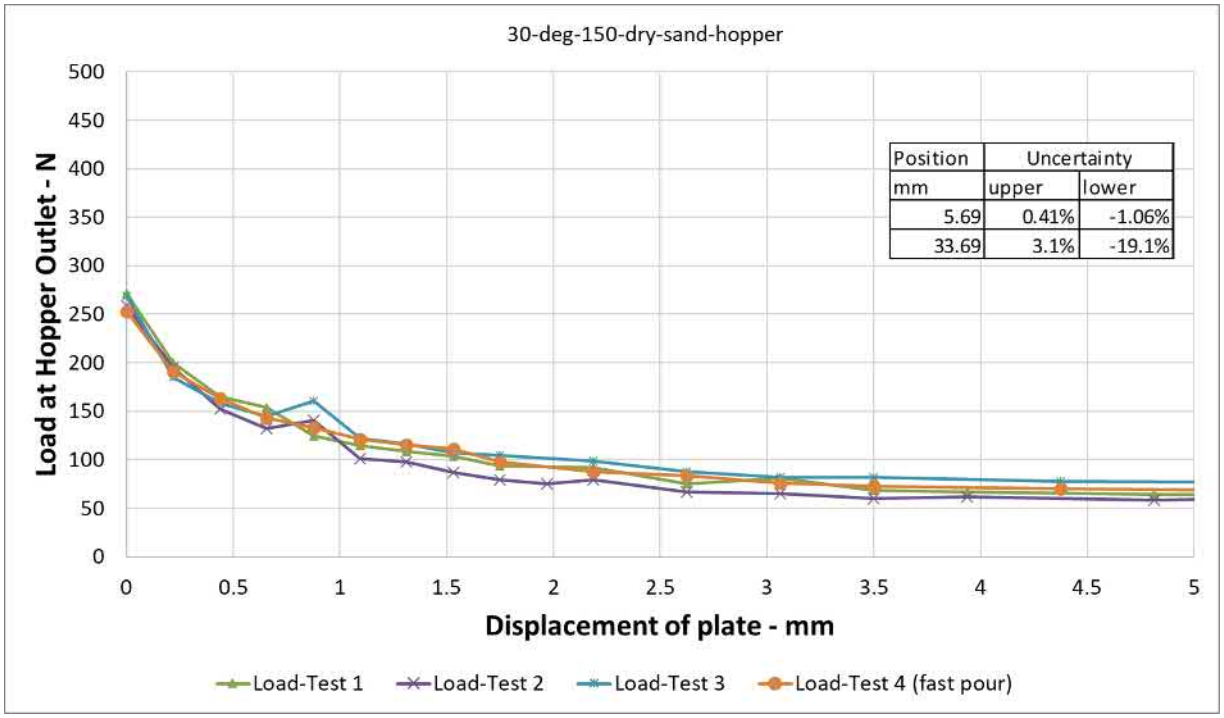


Figure G- 8 Test Set 5, 30-degrees, 150 mm, dry sand, hopper filled, 1-5 mm range

G.5 Set 6, 30-degrees, 120 mm, dry sand, bin levelled full

Table G- 5 Test Set 6, 30-degrees, 120 mm, dry sand, bin levelled full

Test Record Sheet		Hopper base plate lowering force curve																			
Set Number		6																			
Test Name		30 degrees, 120 mm slot, dry sand, levelled																			
											Calculated loads										
Max Lump		mm	P80 Lump		mm	Moisture		%	(air dry)		Initial:	488.7	N								
Width	120	mm	Length	480	mm	Angle	29.2195	degrees			Flow:	67.7	N								
Tare	7.09	kg	Spec. wt	14756.7	N/m3	(loose density +25% of difference to tapped density)															
Screw Pitch M12	1.75	mm	repose	35	degrees																
		Test 1		Test 2		Test 3		Test 4		t 1 (Repose)		Test 2 (Repose)		Test 3 (Repose)		Test 4 (Repose)			Initial	Flow	Average
Load record (screw turns)	Disp. (mm)	Volt 1	Volt 2	Volt 1	Volt 2	Volt 1	Volt 2	Volt 1	Volt 2	Draw Load	Load-Test 1	Draw Load	Load-Test 2	Draw Load	Load-Test 3	Draw Load	Load-Test 4	DISP.	(calc)	(calc)	
empty		152	149	145	148	143	146														
max	342.295										347.9		342.3		328.4						
min	51.1146										42.2		51.1		58.7						
50% reduction	196.705										195.1		196.7		193.5						
80% reduction	109.351										103.4		109.4		112.6						
displacement - min	4.375										3.9		4.4		6.1						
displacement - 50% red.	0.42045										0.3497		0.4204		0.4053						
50% red displ as % of gap	0.35%										0.292%		0.351%		0.339%		0.000%				
displacement - 80% red.	1.13684										0.8950		1.1368		1.3354						
80% red displ as % of gap	0.95%										0.748%		0.950%		1.116%		0.000%				
0	0	884	840	861	832	813	819			0.00	347.9	0.00	342.3	0.00	328.4	0.00	0.0	0			339.5
0.125	0.219	638	605	620	650	632	656			0.19	230.1	0.19	238.8	0.19	244.1	0.19	-0.2	0.21875	488.7	67.7	237.7
0.25	0.438	495	509	516	568	499	547			0.37	171.6	0.37	193.1	0.37	184.8	0.37	-0.4	0.4375	488.7	67.7	183.2
0.375	0.656	410	433	452	407	431	484			0.56	132.0	0.56	137.8	0.56	152.6	0.56	-0.6	0.65625	488.7	67.7	140.8
0.5	0.875	354	377	391	432	399	447			0.75	104.4	0.75	128.9	0.75	135.5	0.75	-0.8	0.875	488.7	67.7	123.0
0.625	1.094	325	358	356	396	362	413			0.94	92.5	0.94	111.4	0.94	118.0	0.94	-0.9	1.09375	488.7	67.7	107.3
0.75	1.313	301	332	344	367	362	398			1.13	80.1	1.13	101.1	1.13	114.1	1.13	-1.1	1.3125	488.7	67.7	98.4
0.875	1.531	295	322	326	341	342	361			1.33	76.0	1.33	90.2	1.33	99.9	1.33	-1.3	1.53125	488.7	67.7	88.7
1	1.750	280	299	317	329	327	348			1.52	66.5	1.52	84.8	1.52	92.9	1.52	-1.5	1.75	488.7	67.7	81.4
1.125	1.969	282	288	295	305					1.72	64.1	1.72	73.4	1.72		1.72	-1.7	1.96875	488.7	67.7	68.7
1.25	2.188	265	282	282	299	300	314			1.91	58.3	1.91	68.5	1.91	77.6	1.91	-1.9	2.1875	488.7	67.7	68.1
1.375	2.406									2.11		2.11		2.11		2.11	-2.1	2.40625	488.7	67.7	
1.5	2.625	245	265	266	292	279	300			2.31	48.8	2.31	62.5	2.31	68.6	2.31	-2.3	2.625	488.7	67.7	60.0
1.625	2.844									2.51		2.51		2.51		2.51	-2.5	2.84375	488.7	67.7	
1.75	3.063	238	266	271	287	290	300			2.72	47.0	2.72	62.1	2.72	70.9	2.72	-2.7	3.0625	488.7	67.7	60.0
1.875	3.281									2.92		2.92		2.92		2.92	-2.9	3.28125	488.7	67.7	
2	3.500	250	267	264	277	282	294			3.12	49.7	3.12	57.5	3.12	67.1	3.12	-3.1	3.5	488.7	67.7	58.1
2.125	3.719									3.33		3.33		3.33		3.33	-3.3	3.71875	488.7	67.7	
2.25	3.938	238	250	257	269					3.54	42.2	3.54	53.5	3.54		3.54	-3.5	3.9375	488.7	67.7	47.8
2.375	4.156									3.74		3.74		3.74		3.74	-3.7	4.15625	488.7	67.7	
2.5	4.375			245	273	267	283			3.95		3.95	51.1	3.95	59.9	3.95	-4.0	4.375	488.7	67.7	55.5
2.625	4.594									4.16		4.16		4.16		4.16	-4.2	4.59375	488.7	67.7	
2.75	4.813	239	259	261	275					4.38	43.8	4.38	55.1	4.38		4.38	-4.4	4.8125	488.7	67.7	49.5
2.875	5.031									4.59		4.59		4.59		4.59	-4.6	5.03125	488.7	67.7	
3	5.250					273	282			4.80		4.80		4.80	60.3	4.80	-4.8	5.25	488.7	67.7	60.3
3.125	5.469									5.0		5.0		5.0		5.0	-5.0	5.46875	488.7	67.7	
3.25	5.688	251	258	265	275					5.2	45.6	5.2	55.2	5.2		5.2	-5.2	5.6875	488.7	67.7	50.4
3.375	5.906									5.5		5.5		5.5		5.5	-5.5	5.90625	488.7	67.7	
3.5	6.125					266	286			5.7		5.7		5.7	58.7	5.7	-5.7	6.125	488.7	67.7	58.7
3.625	6.344									5.9		5.9		5.9		5.9	-5.9	6.34375	488.7	67.7	
3.75	6.563	245	262	262	279					6.1	44.3	6.1	54.6	6.1		6.1	-6.1	6.5625	488.7	67.7	49.4
3.875	6.781									6.3		6.3		6.3		6.3	-6.3	6.78125	488.7	67.7	
4	7.000					282	288			6.6		6.6		6.6	62.2	6.6	-6.6	7	488.7	67.7	62.2
4.125	7.219									6.8		6.8		6.8		6.8	-6.8	7.21875	488.7	67.7	
4.25	7.438	256	264	262	273					7.0	46.6	7.0	52.2	7.0		7.0	-7.0	7.4375	488.7	67.7	49.4
4.375	7.656									7.2		7.2		7.2		7.2	-7.2	7.65625	488.7	67.7	
4.5	7.875					277	295			7.5		7.5		7.5	61.8	7.5	-7.5	7.875	488.7	67.7	61.8
4.625	8.094									7.7		7.7		7.7		7.7	-7.7	8.09375	488.7	67.7	
4.75	8.313			276	284					7.9		7.9	57.4	7.9		7.9	-7.9	8.3125	488.7	67.7	57.4
4.875	8.531									8.2		8.2		8.2		8.2	-8.2	8.53125	488.7	67.7	
5	8.750									8.4		8.4		8.4		8.4	-8.4	8.75	488.7	67.7	
5.125	8.969									8.6		8.6		8.6		8.6	-8.6	8.96875	488.7	67.7	
5.25	9.188	269	275	273	286					8.9	50.6	8.9	56.2	8.9		8.9	-8.9	9.1875	488.7	67.7	53.4
5.375	9.406									9.1		9.1		9.1		9.1	-9.1	9.40625	488.7	67.7	
5.5	9.625					288	302			9.4		9.4		9.4	64.3	9.4	-9.4	9.625	488.7	67.7	64.3
5.625	9.844									9.6		9.6		9.6		9.6	-9.6	9.84375	488.7	67.7	
5.75	10.063									9.8		9.8		9.8		9.8	-9.8	10.0625	488.7	67.7	
5.875	10.281									10.1		10.1		10.1		10.1	-10.1	10.28125	488.7	67.7	
6	10.500									10.3		10.3		10.3		10.3	-10.3	10.5	488.7	67.7	
6.125	10.719									10.6		10.6		10.6		10.6	-10.6	10.71875	488.7	67.7	
6.25	10.938	277	285	285	297					10.8	53.0	10.8	59.9	10.8		10.8	-10.8	10.9375	488.7	67.7	56.4
6.375	11.156									11.1		11.1		11.1		11.1	-11.1	11.15625	488.7	67.7	
6.5	11.375					297	316			11.3		11.3		11.3	67.9	11.3	-11.3	11.375	488.7	67.7	67.9
6.625	11.594									11.6		11.6		11.6		11.6	-11.6	11.59375	488.7	67.7	
6.75	11.813									11.8		11.8		11.8		11.8	-11.8	11.8125	488.7	67.7	
6.875	12.031									12.1		12.1		12.1		12.1	-12.1	12.03125	488.7	67.7	
7	12.250									12.3		12.3		12.3		12.3	-12.3	12.25	488.7	67.7	
7.125	12.469									12.6		12.6		12.6		12.6	-12.6	12.46875	488.7	67.7	
7.25	12.688	291	300	296	303					12.9	58.1	12.9	62.0	12.9		12.9	-12.9	12.6875	488.7	67.7	60.0

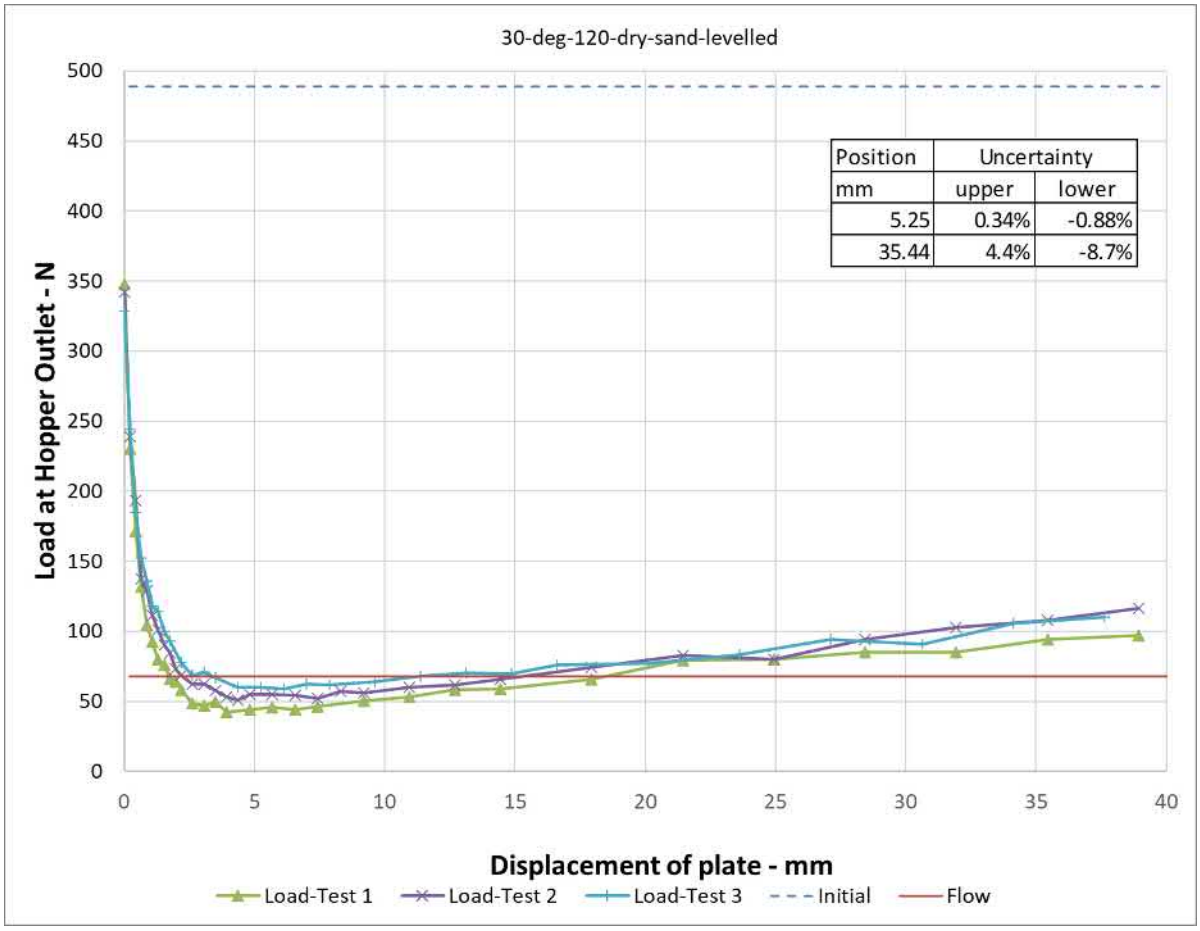


Figure G- 9 Test Set 6, 30-degrees, 120 mm, dry sand, bin levelled full

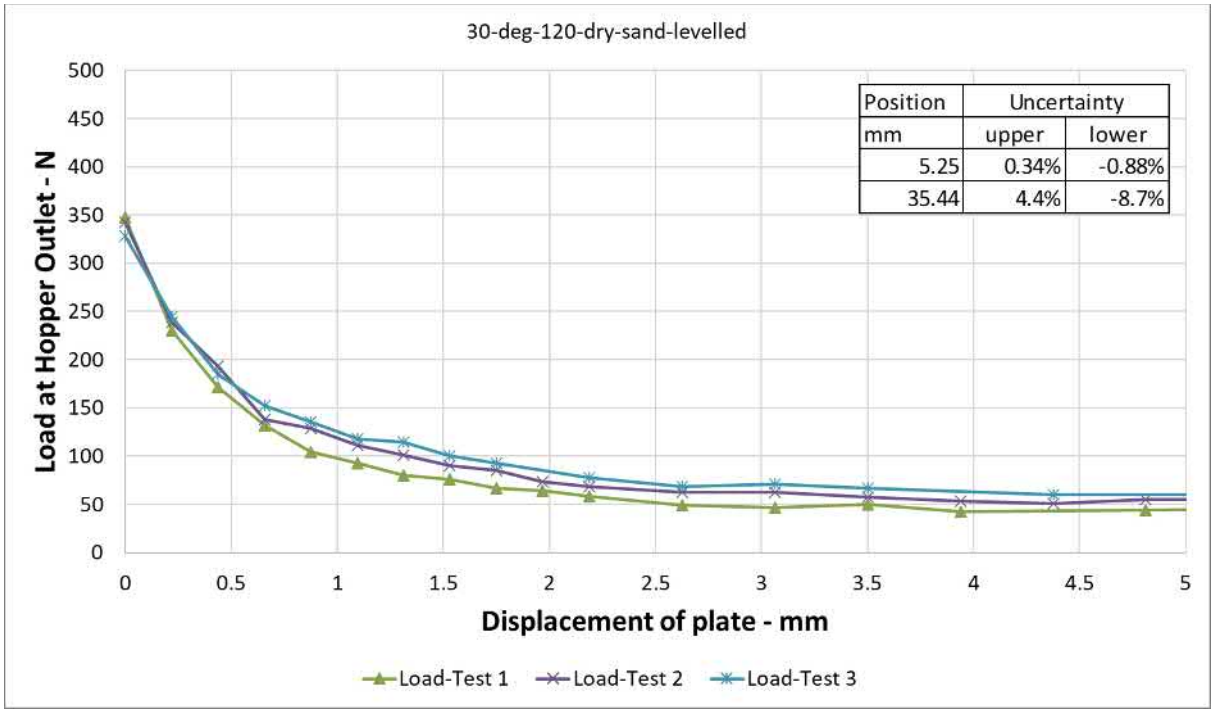


Figure G- 10 Test Set 6, 30-degrees, 120 mm, dry sand, bin levelled full, 1-5 mm range

G.6 Set 7, 30-degrees, 120 mm, dry sand, hopper filled

Table G- 6 Test Set 7, 30-degrees, 120 mm, dry sand, hopper filled

Test Record Sheet		Hopper base plate lowering force curve																			
Set Number		7																			
Test Name		30 degrees, 120 mm slot, dry sand, hopper																			
											Calculated loads										
Max Lump		mm	P80 Lump		mm	Moisture		%	(air dry)		Initial:	262.0	N								
Width	119.7	mm	Length	480	mm	Angle	29.22	degrees			Flow:	57.6	N								
Tare	7.09	kg	Spec. wt	14756.7	N/m3	(loose density +25% of difference to tapped density)															
Screw Pitch M12	1.75	mm	repose	35	degrees																
		Test 1		Test 2		Test 3 (fastpour)		Test 4		t 1 (Repose)		Test 2 (Repose)		Test 3 (Repose)		Test 4 (Repose)			Initial	Flow	Average
Load record (screw turns)	Disp. (mm)	Volt 1	Volt 2	Volt 1	Volt 2	Volt 1	Volt 2	Volt 1	Volt 2	Draw Load	Load-Test 1	Draw Load	Load-Test 2	Draw Load	Load-Test 3 (fastpour)	Draw Load	Load-Test 4	DISP.	(calc)	(calc)	
empty		146	157	146	158	146	161	145	159												
max	215.9333										212.5		215.9		198.6		223.5				
min	47.33482										59.3		47.3		48.3		51.4				
50% reduction	131.6341										135.9		131.6		123.4		137.5				
80% reduction	81.05452										89.9		81.1		78.4		85.8				
displacement - min	5.6875										3.9		5.7		5.7		3.5				
displacement - 50% red.	0.27573										0.3494		0.2757		0.3418		0.2169				
50% red displ as % of gap	0.230%										0.292%		0.230%		0.286%		0.181%				
displacement - 80% red.	1.332331										1.2626		1.3323		1.2431		0.9024				
80% red displ as % of gap	1.113%										1.055%		1.113%		1.039%		0.754%				
0	0	582	590	586	601	553	566	596	622	0.00	212.5	0.00	215.9	0.00	198.6	0.00	223.5	0			217.3
0.125	0.219	471	472	429	446	425	447	430	434	0.19	156.3	0.19	139.5	0.19	138.0	0.19	136.7	0.21875	262.0	57.6	144.2
0.25	0.438	397	407	369	384	376	391	364	368	0.37	122.1	0.37	109.4	0.37	112.1	0.37	104.3	0.4375	262.0	57.6	111.9
0.375	0.656	385	391	355	366	354	364	335	337	0.56	115.1	0.56	101.4	0.56	99.9	0.56	89.4	0.65625	262.0	57.6	102.0
0.5	0.875	366	386	341	347	339	341	329	331	0.75	109.1	0.75	93.1	0.75	90.4	0.75	86.3	0.875	262.0	57.6	96.2
0.625	1.094	340	353	325	334	334	328	318	328	0.94	94.4	0.94	85.9	0.94	85.8	0.94	82.7	1.09375	262.0	57.6	87.7
0.75	1.313	327	343	318	326	310	308	295	306	1.13	88.6	1.13	82.0	1.13	74.9	1.13	71.5	1.3125	262.0	57.6	80.7
0.875	1.531	311	325	292	310			278	286	1.33	80.1	1.33	71.6	1.33		1.33	62.2	1.53125	262.0	57.6	71.3
1	1.750	307	319	285	303	285	296	278	288	1.52	77.5	1.52	67.9	1.52	65.5	1.52	62.5	1.75	262.0	57.6	69.3
1.125	1.969	298	305							1.72	71.6	1.72		1.72		1.72		1.96875	262.0	57.6	71.6
1.25	2.188	291	302	269	283	281	294	270	278	1.91	69.0	1.91	58.7	1.91	63.6	1.91	57.7	2.1875	262.0	57.6	61.8
1.375	2.406									2.11		2.11		2.11		2.11		2.40625	262.0	57.6	
1.5	2.625	289	297	269	278	276	281	267	273	2.31	66.9	2.31	57.1	2.31	58.8	2.31	55.4	2.625	262.0	57.6	59.8
1.625	2.844									2.51		2.51		2.51		2.51		2.84375	262.0	57.6	
1.75	3.063	287	302	253	265	273	278	262	276	2.72	67.2	2.72	49.6	2.72	56.9	2.72	54.5	3.0625	262.0	57.6	57.1
1.875	3.281									2.92		2.92		2.92		2.92		3.28125	262.0	57.6	
2	3.500			255	267			257	270	3.12		3.12	50.2	3.12		3.12	51.4	3.5	262.0	57.6	50.8
2.125	3.719									3.33		3.33		3.33		3.33		3.71875	262.0	57.6	
2.25	3.938	275	285	262	269	259	271			3.54	59.3	3.54	52.0	3.54	51.0	3.54		3.9375	262.0	57.6	55.6
2.375	4.156									3.74		3.74		3.74		3.74		4.15625	262.0	57.6	
2.5	4.375			257	269			266	277	3.95		3.95	50.3	3.95		3.95	54.5	4.375	262.0	57.6	52.4
2.625	4.594									4.16		4.16		4.16		4.16		4.59375	262.0	57.6	
2.75	4.813	282	297	258	270	265	271			4.38	63.1	4.38	50.4	4.38	51.6	4.38		4.8125	262.0	57.6	56.8
2.875	5.031									4.59		4.59		4.59		4.59		5.03125	262.0	57.6	
3	5.250							264	274	4.80		4.80		4.80		4.80	52.4	5.25	262.0	57.6	52.4
3.125	5.469									5.0		5.0		5.0		5.0		5.46875	262.0	57.6	
3.25	5.688	287	301	255	264	259	267			5.2	64.5	5.2	47.3	5.2	48.3	5.2		5.6875	262.0	57.6	55.9
3.375	5.906									5.5		5.5		5.5		5.5		5.90625	262.0	57.6	
3.5	6.125							265	281	5.7		5.7		5.7		5.7	53.5	6.125	262.0	57.6	53.5
3.625	6.344									5.9		5.9		5.9		5.9		6.34375	262.0	57.6	
3.75	6.563	292	303	268	277	267	270			6.1	65.3	6.1	52.8	6.1	50.1	6.1		6.5625	262.0	57.6	59.1
3.875	6.781									6.3		6.3		6.3		6.3		6.78125	262.0	57.6	
4	7.000							269	286	6.6		6.6		6.6		6.6	54.8	7	262.0	57.6	54.8
4.125	7.219									6.8		6.8		6.8		6.8		7.21875	262.0	57.6	
4.25	7.438	285	298							7.0	61.5	7.0		7.0		7.0		7.4375	262.0	57.6	61.5
4.375	7.656									7.2		7.2		7.2		7.2		7.65625	262.0	57.6	
4.5	7.875							276	286	7.5		7.5		7.5		7.5	55.6	7.875	262.0	57.6	55.6
4.625	8.094									7.7		7.7		7.7		7.7		8.09375	262.0	57.6	
4.75	8.313	296	308	289	294	279	283			7.9	65.7	7.9	60.3	7.9	54.4	7.9		8.3125	262.0	57.6	63.0
4.875	8.531									8.2		8.2		8.2		8.2		8.53125	262.0	57.6	
5	8.750							281	290	8.4		8.4		8.4		8.4	56.9	8.75	262.0	57.6	56.9
5.125	8.969									8.6		8.6		8.6		8.6		8.96875	262.0	57.6	
5.25	9.188									8.9		8.9		8.9		8.9		9.1875	262.0	57.6	
5.375	9.406									9.1		9.1		9.1		9.1		9.40625	262.0	57.6	
5.5	9.625							285	296	9.4		9.4		9.4		9.4	58.4	9.625	262.0	57.6	58.4
5.625	9.844									9.6		9.6		9.6		9.6		9.84375	262.0	57.6	
5.75	10.063	313	325	292	304	285	291			9.8	72.1	9.8	61.6	9.8	55.9	9.8		10.0625	262.0	57.6	66.8
5.875	10.281									10.1		10.1		10.1		10.1		10.28125	262.0	57.6	
6	10.500							301	313	10.3		10.3		10.3		10.3	65.5	10.5	262.0	57.6	65.5
6.125	10.719									10.6		10.6		10.6		10.6		10.71875	262.0	57.6	
6.25	10.938									10.8		10.8		10.8		10.8		10.9375	262.0	57.6	
6.375	11.156									11.1		11.1		11.1		11.1		11.15625	262.0	57.6	
6.5	11.375									11.3		11.3		11.3		11.3		11.375	262.0	57.6	
6.625	11.594									11.6		11.6		11.6		11.6		11.59375	262.0	57.6	
6.75	11.813	316	316	299	309	296	301			11.8	68.6	11.8	62.5	11.8	59.1	11.8		11.8125	262.0	57.6	65.6
6.875	12.031									12.1		12.1		12.1		12.1		12.03125	262.0	57.6	
7	12.250							312	323	12.3		12.3		12.3		12.3	68.6	12.25	262.0	57.6	68.6
7.125	12.469									12.6		12.6		12.6		12.6		12.46875	262.0	57.6	
7.25	12.688									12.9		12.9		12.9		12.9		12.6875	262.0	57.6	

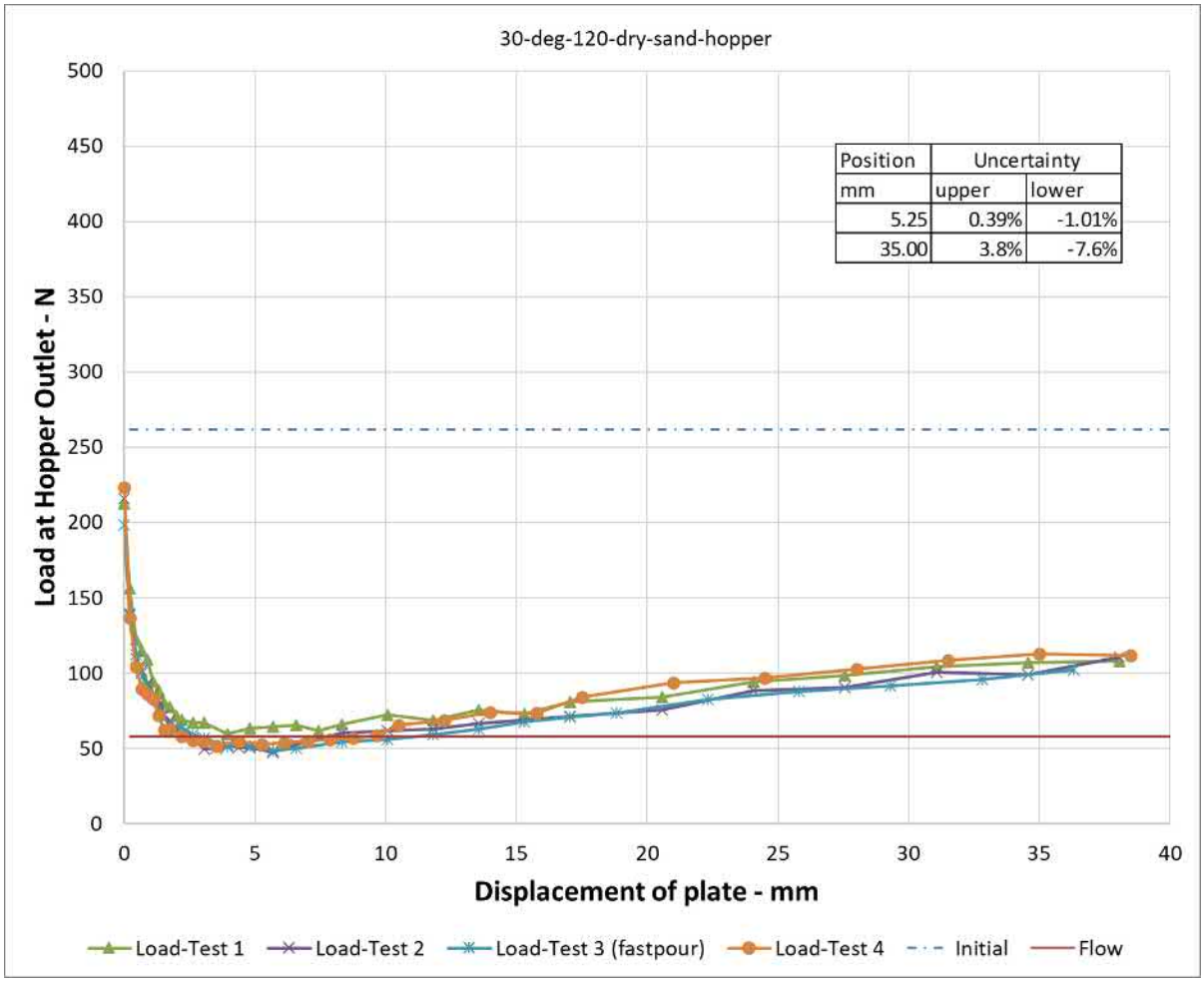


Figure G- 11 Test Set 7, 30-degrees, 120 mm, dry sand, hopper filled

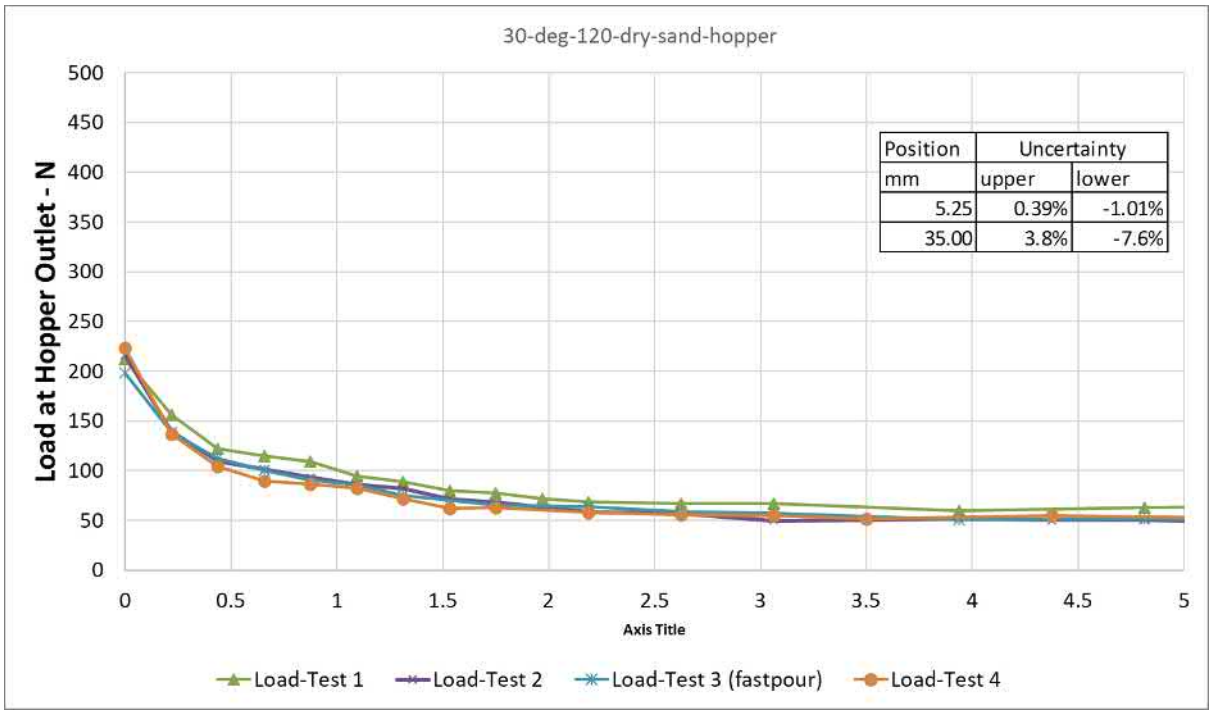


Figure G- 12 Test Set 7, 30-degrees, 120 mm, dry sand, hopper filled, 1-5 mm range

G.7 Set 8, 20-degrees, 150 mm slot, dry sand, hopper filled

Table G- 7 Test Set 8, 20-degrees, 150 mm, dry sand, hopper filled

Test Record Sheet		Hopper base plate lowering force curve																	
Set Number		8																	
Test Name		20 degrees, 150 mm slot, dry sand, hopper																	
											Calculated loads								
Max Lump		mm	P80 Lump		mm	Moisture		%	(air dry)		Initial:	511.9	N						
Width	146	mm	Length	480	mm	Angle	**18.32**	degrees			Flow:	85.0	N						
Tare	7.09	kg	Spec. wt	14756.7	N/m3	(loose density +25% of difference to tapped density)													
Screw Pitch M12	1.75	mm	repose	35	degrees														
		Test 1		Test 2		Test 3		Test 4		t 1 (Repose)		Test 2 (Repose)		Test 3 (Repose)			Initial	Flow	Average
Load record (screw turns)	Disp. (mm)	Volt 1	Volt 2	Volt 1	Volt 2	Volt 1	Volt 2	Volt 1	Volt 2	Draw Load	Load-Test 1	Draw Load	Load-Test 2	Draw Load	Load-Test 3	DISP.	(calc)	(calc)	
empty	0	138	148	138	152	137	147												
max	367.316										388.6		342.2		367.3				
min	70.9252										80.4		70.8		70.9				
50% reduction	219.12										234.5		206.5		219.1				
80% reduction	130.203										142.0		125.1		130.2				
displacement - min	6.34375										12.5		7.0		6.3				
displacement - 50% red.	0.6582										0.7570		0.5621		0.6582				
50% red displ as % of gap	0.45%										0.518%		0.385%		0.451%				
displacement - 80% red.	1.92277										2.4071		1.6862		1.9228				
80% red displ as % of gap	1.32%										1.649%		1.155%		1.317%				
0	0	916	959	826	863	883	903			0.00	388.6	0.00	342.2	0.00	367.3	0			378.0
0.125	0.219	729	776	664	700	754	772			0.23	297.9	0.23	262.4	0.23	303.5	0.21875	511.9	85.0	300.7
0.25	0.438	653	727	581	602	659	670			0.45	267.2	0.45	217.9	0.45	255.1	0.4375	511.9	85.0	261.1
0.375	0.656	629	655	551	551	577	607			0.68	243.4	0.68	197.9	0.68	219.4	0.65625	511.9	85.0	231.4
0.5	0.875	588	618	509	519	565	569			0.92	224.1	0.92	179.5	0.92	206.9	0.875	511.9	85.0	215.5
0.625	1.094	551	573	457	469	527	531			1.15	203.8	1.15	154.4	1.15	190.5	1.09375	511.9	85.0	197.2
0.75	1.313	494	533	424	448	478	498			1.38	179.9	1.38	141.0	1.38	180.6	1.3125	511.9	85.0	180.2
0.875	1.531	491	515	387	406	427	454			1.61	174.5	1.61	121.4	1.61	158.6	1.53125	511.9	85.0	166.5
1	1.750			397	431	427	512			1.85		1.85	129.7	1.85	158.5	1.75	511.9	85.0	158.5
1.125	1.969	472	492			377	417			2.09	163.7	2.09		2.09	122.7	1.96875	511.9	85.0	143.2
1.25	2.188			344	380					2.33		2.33	103.8	2.33		2.1875	511.9	85.0	
1.375	2.406	429	446			388	419			2.57	141.5	2.57		2.57	125.4	2.40625	511.9	85.0	133.4
1.5	2.625			338	349					2.81		2.81	94.3	2.81		2.625	511.9	85.0	
1.625	2.844	395	416			344	370			3.05	125.4	3.05		3.05	102.1	2.84375	511.9	85.0	113.7
1.75	3.063			316	337					3.29		3.29	85.5	3.29		3.0625	511.9	85.0	
1.875	3.281	389	407			322	347			3.54	121.2	3.54		3.54	90.6	3.28125	511.9	85.0	105.9
2	3.500			314	345					3.78		3.78	86.5	3.78		3.5	511.9	85.0	
2.125	3.719	365	391			316	342			4.03	110.9	4.03		4.03	87.5	3.71875	511.9	85.0	99.2
2.25	3.938									4.28		4.28		4.28		3.9375	511.9	85.0	
2.375	4.156									4.53		4.53		4.53		4.15625	511.9	85.0	
2.5	4.375			318	338					4.78		4.78	84.7	4.78		4.375	511.9	85.0	
2.625	4.594	350	365			292	320			5.03	99.9	5.03		5.03	75.2	4.59375	511.9	85.0	87.5
2.75	4.813									5.29		5.29		5.29		4.8125	511.9	85.0	
2.875	5.031									5.54		5.54		5.54		5.03125	511.9	85.0	
3	5.250			302	333					5.80		5.80	78.6	5.80		5.25	511.9	85.0	
3.125	5.469	337	362			303	328			6.1	95.0	6.1		6.1	78.8	5.46875	511.9	85.0	86.9
3.25	5.688									6.3		6.3		6.3		5.6875	511.9	85.0	
3.375	5.906									6.6		6.6		6.6		5.90625	511.9	85.0	
3.5	6.125			313	326					6.8		6.8	78.5	6.8		6.125	511.9	85.0	
3.625	6.344	333	347			292	311			7.1	89.3	7.1		7.1	70.9	6.34375	511.9	85.0	80.1
3.75	6.563									7.4		7.4		7.4		6.5625	511.9	85.0	
3.875	6.781									7.6		7.6		7.6		6.78125	511.9	85.0	
4	7.000			299	313					7.9		7.9	70.8	7.9		7	511.9	85.0	
4.125	7.219	318	338			311	333			8.2	82.3	8.2		8.2	79.9	7.21875	511.9	85.0	81.1
4.25	7.438									8.4		8.4		8.4		7.4375	511.9	85.0	
4.375	7.656									8.7		8.7		8.7		7.65625	511.9	85.0	
4.5	7.875									9.0		9.0		9.0		7.875	511.9	85.0	
4.625	8.094					308	331			9.3		9.3		9.3	77.6	8.09375	511.9	85.0	77.6
4.75	8.313									9.5		9.5		9.5		8.3125	511.9	85.0	
4.875	8.531									9.8		9.8		9.8		8.53125	511.9	85.0	
5	8.750			313	332					10.1		10.1	76.7	10.1		8.75	511.9	85.0	
5.125	8.969	333	349							10.4	86.5	10.4		10.4		8.96875	511.9	85.0	86.5
5.25	9.188									10.6		10.6		10.6		9.1875	511.9	85.0	
5.375	9.406									10.9		10.9		10.9		9.40625	511.9	85.0	
5.5	9.625									11.2		11.2		11.2		9.625	511.9	85.0	
5.625	9.844					320	338			11.5		11.5		11.5	80.0	9.84375	511.9	85.0	80.0
5.75	10.063									11.8		11.8		11.8		10.0625	511.9	85.0	
5.875	10.281									12.1		12.1		12.1		10.28125	511.9	85.0	
6	10.500			324	340					12.3		12.3	79.1	12.3		10.5	511.9	85.0	
6.125	10.719	336	346							12.6	84.2	12.6		12.6		10.71875	511.9	85.0	84.2
6.25	10.938									12.9		12.9		12.9		10.9375	511.9	85.0	
6.375	11.156									13.2		13.2		13.2		11.15625	511.9	85.0	
6.5	11.375									13.5		13.5		13.5		11.375	511.9	85.0	
6.625	11.594					340	367			13.8		13.8		13.8	89.7	11.59375	511.9	85.0	89.7
6.75	11.813									14.1		14.1		14.1		11.8125	511.9	85.0	
6.875	12.031									14.4		14.4		14.4		12.03125	511.9	85.0	
7	12.250			335	352					14.7		14.7	82.4	14.7		12.25	511.9	85.0	
7.125	12.469	328	348							15.0	80.4	15.0		15.0		12.46875	511.9	85.0	80.4
7.25	12.688									15.3		15.3		15.3		12.6875	511.9	85.0	
7.375	12.906									15.6		15.6		15.6		12.90625	511.9	85.0	
7.5	13.125									15.9		15.9		15.9		13.125	511.9	85.0	
7.625	13.344					363	377			16.2		16.2		16.2	95.3	13.34375	511.9	85.0	95.3

pressure rise unexplained Discard set

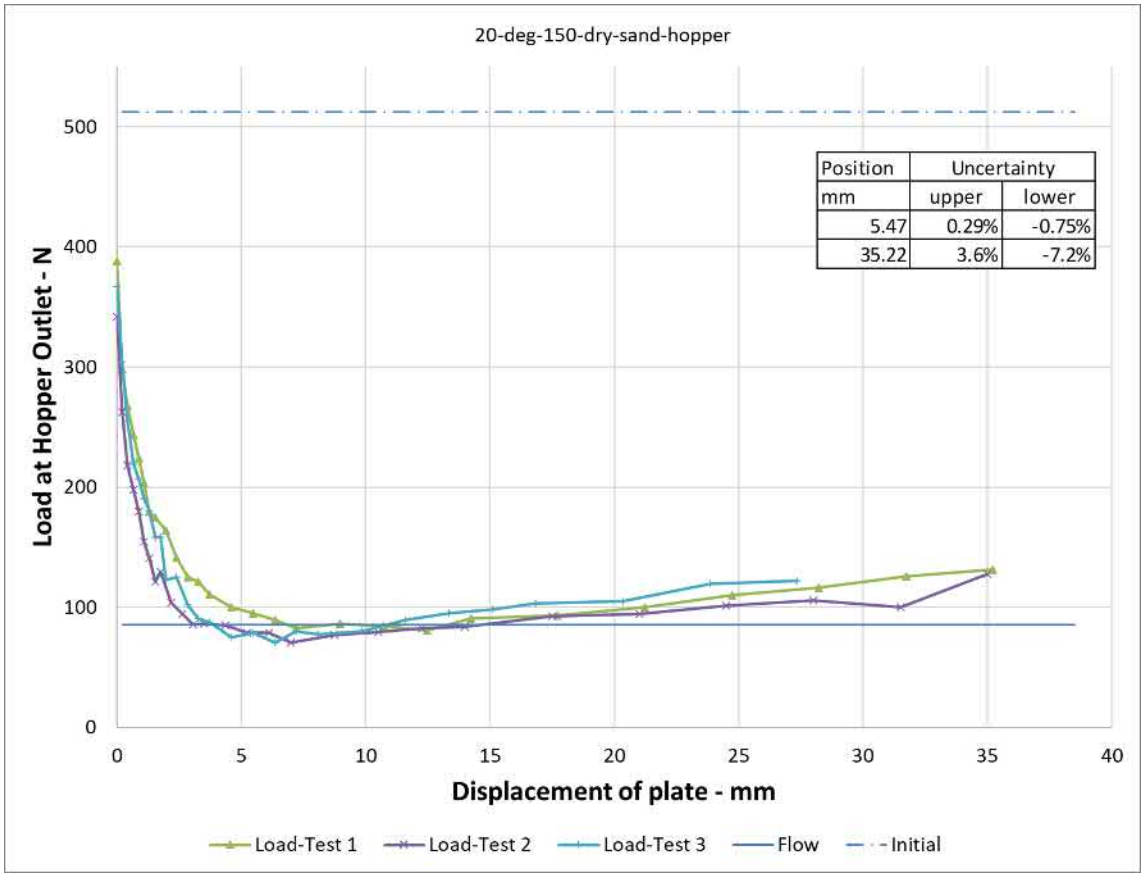


Figure G- 13 Test Set 8, 20-degrees, 150 mm, dry sand, hopper filled

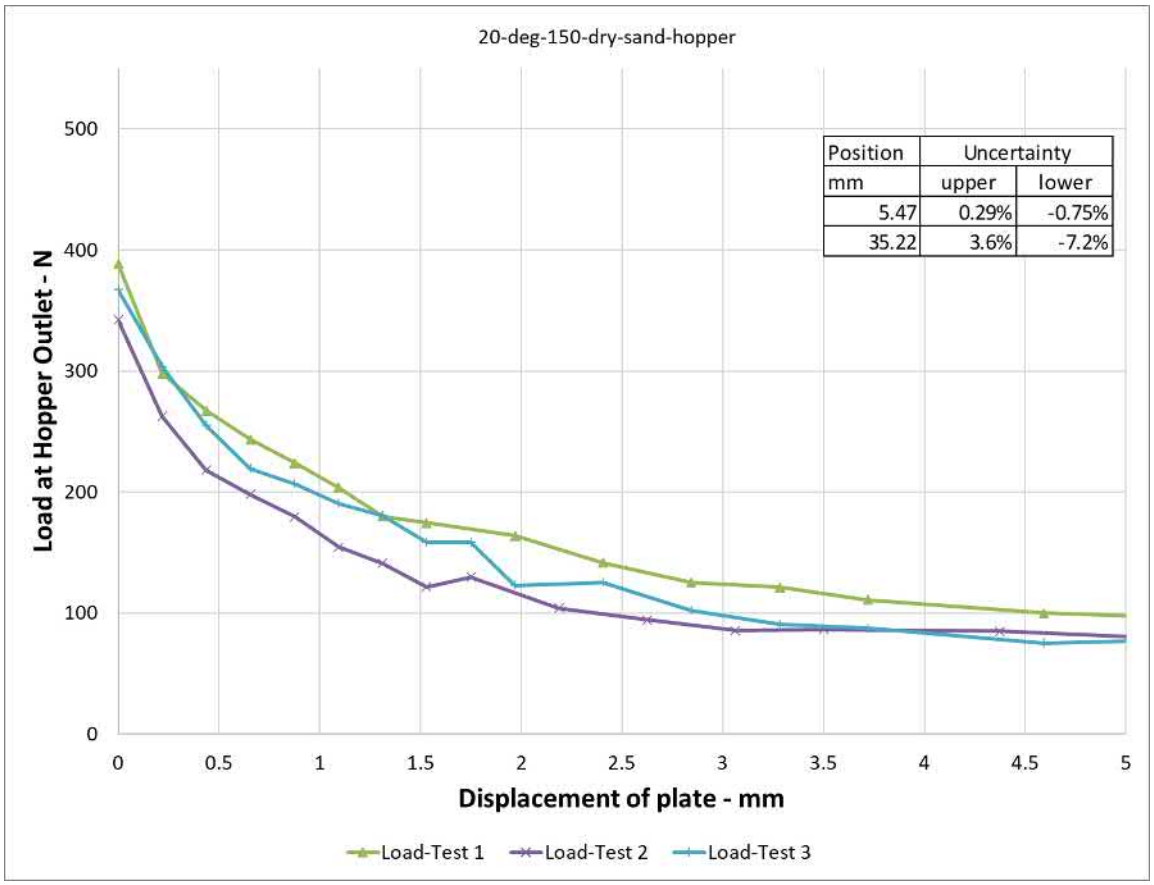


Figure G- 14 Test Set 8, 20-degrees, 150 mm, dry sand, hopper filled, 1-5 mm range

G.8 Set 9, 20-degrees, 120 mm, aggregate, hopper only

Table G- 8 Test Set 9, 20-degrees, 10 mm, Aggregate, hopper filled

Test Record Sheet		Hopper base plate lowering force curve																				
Set Number		9																				
Test Name		20 degrees, 120 mm slot, 13mm aggregate, hopper only																				
											Calculated loads						0.3935				
Max Lump	13	mm	P80 Lum	11.2	mm	Moisture	0.20%		(air dry)		Initial:	414.6	N									
Width	120.33333	mm	Length	480	mm	Angle	19.4435	degrees			Flow:	59.9	N									
Tare	7.09	kg	Spec. wt	14501.6	N/m3	(loose density +25% of difference to tapped density)																
Screw Pitch M12	1.75	mm	repose	43	degrees																	
		Test 1		Test 2		Test 3		Test 4		t 1 (Repose)		Test 2 (Repose)		Test 3 (Repose)		Test 4 (Repose)			Initial	Flow	Average
Load record (screw turns)	Disp. (mm)	Volt 1-1	Volt 1-2	Volt 2-1	Volt 2-2	Volt 3-1	Volt 3-2	Volt 4-1	Volt 4-2	Draw Load	Load-Test 1	Draw Load	Load-Test 2	Draw Load	Load-Test 3	Draw Load	Load-Test 4	DISP.	(calc)	(calc)	
0		128	157	128	157	127	159	127	153												
max	379.73728										375.1		379.7		390.3						
min	34.147285										38.5		34.1		34.3		37.5				
50% reduction	206.94228										206.8		206.9		212.3						
80% reduction	103.26528										105.8		103.3		105.5						
displacement - min	21										15.8		21.0		8.8		9.6				
displacement - 50% red.	0.2736099										0.3005		0.2736		0.1841						
50% red displ as % of gap	0.23%										0.250%		0.227%		0.153%		0.000%				
displacement - 80% red.	0.6236624										0.8230		0.6237		0.5049						
80% red displ as % of gap	0.52%										0.684%		0.518%		0.420%		0.000%				
0	0	913	906	913	925	923	959	835	865	0.00	375.1	0.00	379.7	0.00	390.3	0.00	347.3	0			381.7
0.125	0.219	616	638	566	661	503	515	518	541	0.18	236.8	0.18	230.3	0.18	178.8	0.18	190.3	0.21875	414.6	59.9	215.3
0.25	0.438	427	499	377	470	354	389	369	399	0.37	156.5	0.37	137.2	0.37	111.4	0.37	119.0	0.4375	414.6	59.9	135.0
0.375	0.656	352	449	310	375	311	354	319	346	0.55	125.8	0.55	97.3	0.55	92.1	0.55	93.6	0.65625	414.6	59.9	105.1
0.5	0.875	317	378	300	340	277	321	270	301	0.74	99.6	0.74	86.1	0.74	75.6	0.74	70.4	0.875	414.6	59.9	87.1
0.625	1.094	294	348	280	317	249	295	269	302	0.93	86.4	0.93	75.4	0.93	62.2	0.93	70.2	1.09375	414.6	59.9	74.7
0.75	1.313	285	335	261	292	257	291	247	278	1.12	80.8	1.12	64.4	1.12	63.0	1.12	58.8	1.3125	414.6	59.9	69.4
0.875	1.531	275	324	261	301	258	281	248	276	1.30	75.5	1.30	66.5	1.30	60.5	1.30	58.4	1.53125	414.6	59.9	67.5
1	1.750	267	317	246	281	245	266	249	275	1.49	71.7	1.49	57.7	1.49	53.5	1.49	58.2	1.75	414.6	59.9	61.0
1.25	2.188	261	300	247	281	241	275	239	281	1.88	65.6	1.88	57.6	1.88	54.4	1.88	56.8	2.1875	414.6	59.9	59.2
1.5	2.625	240	279	231	270	237	275	244	271	2.26	55.0	2.26	50.6	2.26	53.0	2.26	55.2	2.625	414.6	59.9	52.9
1.75	3.063	239	271	231	265	232	268	238	265	2.65	52.4	2.65	49.0	2.65	49.7	2.65	51.9	3.0625	414.6	59.9	50.3
2	3.500	246	276	231	266	229	268	232	262	3.05	54.9	3.05	48.8	3.05	48.6	3.05	49.3	3.5	414.6	59.9	50.8
2.25	3.938	227	258	239	263	224	256	218	251	3.44	45.5	3.44	49.6	3.44	44.0	3.44	42.8	3.9375	414.6	59.9	46.4
2.5	4.375	229	264	223	261	212	247	223	255	3.84	47.0	3.84	44.8	3.84	38.5	3.84	44.6	4.375	414.6	59.9	43.4
2.75	4.813	228	259	231	273	214	246	223	260	4.25	45.2	4.25	49.3	4.25	38.3	4.25	45.4	4.8125	414.6	59.9	44.3
3	5.250	233	264	223	256	226	256	227	248	4.66	47.2	4.66	42.8	4.66	43.3	4.66	43.0	5.25	414.6	59.9	44.4
3.5	6.125	218	251	226	252	214	255	217	247	5.48	39.5	5.48	41.7	5.48	39.3	5.48	39.5	6.125	414.6	59.9	40.2
4	7.000	231	263	228	253	224	257	218	252	6.33	44.8	6.33	41.6	6.33	41.4	6.33	40.2	7	414.6	59.9	42.6
4.5	7.875	227	263	223	260	218	252	220	247	7.18	43.0	7.18	41.2	7.18	37.8	7.18	38.5	7.875	414.6	59.9	40.7
5	8.750	227	266	221	251	213	246	231	256	8.06	42.8	8.06	37.7	8.06	34.3	8.06	42.6	8.75	414.6	59.9	38.3
5.5	9.625	231	259	230	257	217	250	222	248	8.94	41.2	8.94	40.5	8.94	35.3	8.94	37.5	9.625	414.6	59.9	39.0
6	10.500	237	270	221	249	223	255	245	300	9.84	44.5	9.84	35.4	9.84	37.1	9.84	55.0	10.5	414.6	59.9	39.0
7	12.250	232	264	227	255	236	271	236	260	11.69	39.9	11.69	36.5	11.69	42.4	11.69	41.1	12.25	414.6	59.9	39.6
8	14.000	234	268	237	263	228	265			13.60	39.5	13.60	39.0	13.60	37.0	13.60	40.9	14	414.6	59.9	38.5
9	15.750	234	272	242	270	239	278			15.6	38.5	15.6	39.9	15.6	40.9	15.6	44.3	15.75	414.6	59.9	39.8
10	17.500	256	283	245	278	259	288	257	287	17.6	44.5	17.6	40.6	17.6	46.2	17.6	47.0	17.5	414.6	59.9	43.8
12	21.000	252	288	238	276	252	288	268	291	21.9	40.5	21.9	34.1	21.9	40.3	21.9	46.4	21	414.6	59.9	38.3
14	24.500	269	305	253	292	270	303	271	305	26.4	44.3	26.4	37.2	26.4	43.8	26.4	46.0	24.5	414.6	59.9	41.8
16	28.000	280	311	274	310	293	329	291	323	31.2	43.7	31.2	42.0	31.2	51.0	31.2	50.5	28	414.6	59.9	45.6
18	31.500	299	328	288	325	288	320	295	319	36.2	47.4	36.2	44.0	36.2	42.5	36.2	45.5	31.5	414.6	59.9	44.7
20	35.000	315	342	315	343	298	332	307	327	41.5	49.5	41.5	49.7	41.5	42.6	41.5	45.1	35	414.6	59.9	47.3
22	38.500	314	351	323	355	312	345	320	346	47.1	45.9	47.1	49.0	47.1	43.6	47.1	47.3	38.5	414.6	59.9	46.2
24	42.000	336	371	350	377	331	367	328	360	52.9	50.3	52.9	55.1	52.9	47.8	52.9	46.8	42	414.6	59.9	51.1
26	45.500	395	424	327	382	344	395	361	393	59.1	71.5	59.1	44.6	59.1	51.7	59.1	56.8	45.5	414.6	59.9	56.0
28	49.000	365	462	384	417	407	450	361	393	65.5	67.2	65.5	60.7	65.5	74.1	65.5	50.4	49	414.6	59.9	67.3

unexplained, Dicard set

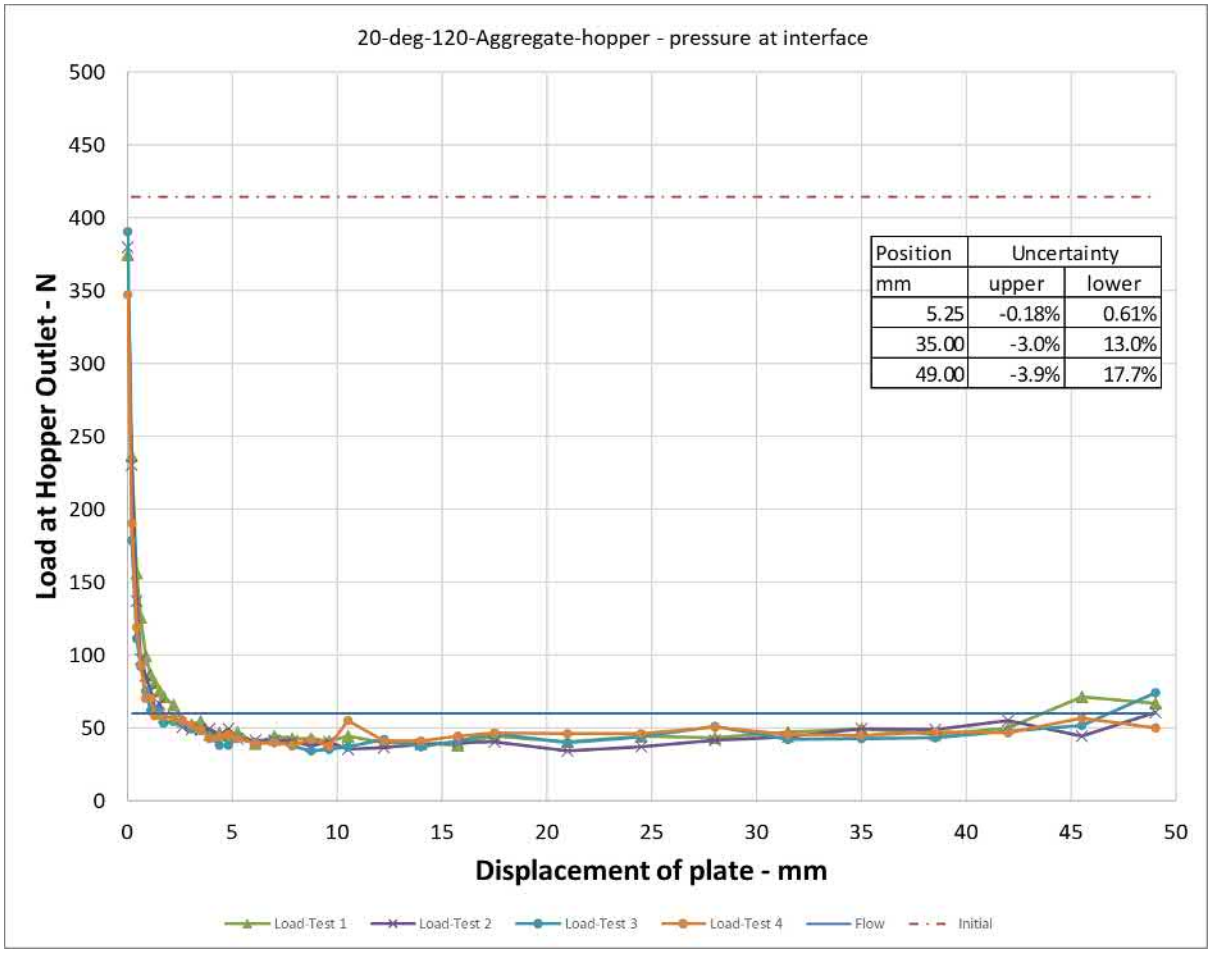


Figure G- 15 Test Set 9, 20-degrees, 10 mm, Aggregate, hopper filled

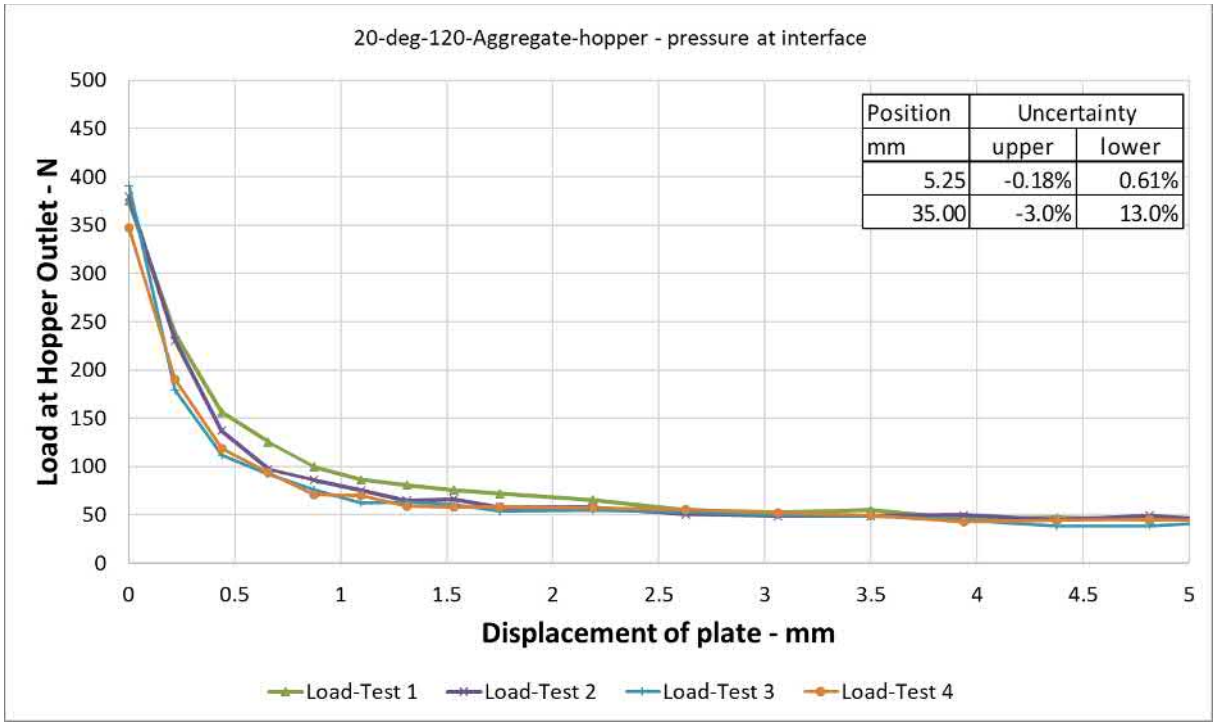


Figure G- 16 Test Set 9, 20-degrees, 10 mm, Aggregate, hopper filled, 1-5 mm range

G.9 Set 10, 20-degrees, 120 mm slot, moist sand, hopper filled

data anomalies on test 1 and test 2 were are noted but the associated causes were not identified, this test data was not used for analysis.

Test Record Sheet		Hopper base plate lowering force curve																			
Set Number		10																			
Test Name		20 degrees, 120 mm slot, moist sand, hopper																			
											Calculated loads										
Max Lump		mm	P80 Lump		mm	Moisture	8.20%				Initial:	387.6	N								
Width	120.33	mm	Length	480	mm	Angle	19.4435	degrees			Flow:	46.0	N								
Tare	7.09	kg	Spec. wt	13557	N/m3	(loose density +50% of difference tc`															
Screw Pitch M12	1.75	mm	repose	90	degrees	(compacted, so no additional flow-down)															
		Test 1		Test 2		Test 3		Test 4 (fastpour)		t 1 (Repose)	Test 2 (Repose)		Test 3 (Repose)		Test 4 (Repose)			Initial	Flow	Average	
Load record (screw turns)	Disp. (mm)	Volt 1	Volt 2	Volt 1	Volt 2	Volt 1	Volt 2	Volt 1	Volt 2	Draw Load	Load-Test 1	Draw Load	Load-Test 2	Draw Load	Load-Test 3	Draw Load	Load-Test 4 (fast pour)	DISP.	(calc)	(calc)	
empty		127	157	130	156	128	156	127	159												
max	230.84										236.4		257.2		230.8		336.5				
min	23.413										21.3		22.7		23.4		18.9				
50% reduction	127.13										128.9		140.0		127.1		177.7				
80% reduction	64.899										64.3		69.6		64.9		82.4				
displacement - min	56										22.8		17.5		56.0		10.5				
displacement - 50% red.	1.6116										1.6886		0.8516		1.6116		0.2679				
50% red displ as % of gap	1.34%										1.403%		0.708%		1.339%		0.223%				
displacement - 80% red.	5.3654										4.4683		2.1698		5.3654		0.9494				
80% red displ as % of gap	4.46%										3.713%		1.803%		4.459%		0.789%				
0	0	620	631	661	677	600	628	811	851	0.00	236.4	0.00	257.2	0.00	230.8	0.00	336.5	0			241.5
0.125	0.219	541	543	568	593	522	553	509	553	0.17	195.4	0.17	213.8	0.17	193.3	0.17	189.6	0.21875	387.6	46.0	200.8
0.25	0.438	513	533	505	559	488	527	394	452	0.34	186.0	0.34	190.0	0.34	178.4	0.34	136.6	0.4375	387.6	46.0	184.8
0.375	0.656	509	515	471	515	469	517	331	385	0.51	180.4	0.51	170.7	0.51	171.2	0.51	104.7	0.65625	387.6	46.0	174.1
0.5	0.875	473	481	396	450	435	476	294	349	0.69	163.1	0.69	136.3	0.69	152.7	0.69	86.7	0.875	387.6	46.0	150.7
0.625	1.094	431	458	350	389	421	457	270	323	0.86	147.1	0.86	109.9	0.86	144.4	0.86	74.3	1.09375	387.6	46.0	133.8
0.75	1.313	409	426	328	379	406	440	258	305	1.03	133.7	1.03	102.0	1.03	136.4	1.03	66.7	1.3125	387.6	46.0	124.0
0.875	1.531	491	422	318	353	397	422	246	284	1.20	152.4	1.20	93.0	1.20	129.6	1.20	58.5	1.53125	387.6	46.0	125.0
1	1.750	375	404	305	337	390	412	236	276	1.37	119.7	1.37	85.7	1.37	125.3	1.37	53.9	1.75	387.6	46.0	110.2
1.25	2.188	357	381	272	303	377	402	216	253	1.71	109.3	1.71	69.0	1.71	119.3	1.71	43.0	2.1875	387.6	46.0	99.2
1.5	2.625	333	350	251	292	347	391	202	238	2.06	95.5	2.06	60.8	2.06	109.0	2.06	35.6	2.625	387.6	46.0	88.4
1.75	3.063	313	338	237	269	337	369	193	226	2.40	87.3	2.40	51.4	2.40	100.8	2.40	30.1	3.0625	387.6	46.0	79.9
2	3.500	283	322	231	263	337	365	191	222	2.74	75.8	2.74	48.1	2.74	99.5	2.74	28.3	3.5	387.6	46.0	74.5
2.25	3.938	273	303	226	258	319	349	187	217	3.08	68.3	3.08	45.3	3.08	90.8	3.08	25.8	3.9375	387.6	46.0	68.2
2.5	4.375	268	296	215	249	295	326	178	212	3.43	65.0	3.43	40.1	3.43	79.0	3.43	22.0	4.375	387.6	46.0	61.4
2.75	4.813	252	281	206	239	287	315	176	206	3.77	57.1	3.77	35.1	3.77	74.0	3.77	19.7	4.8125	387.6	46.0	55.4
3	5.250	247	279	209	242	275	299	176	207	4.11	55.1	4.11	36.3	4.11	66.8	4.11	19.6	5.25	387.6	46.0	52.7
3.5	6.125	231	257	205	239	277	314	185	216	4.80	45.1	4.80	33.9	4.80	70.3	4.80	23.3	6.125	387.6	46.0	49.7
4	7.000	221	256	202	235	259	288	182	244	5.48	41.7	5.48	31.5	5.48	58.8	5.48	28.8	7	387.6	46.0	44.0
4.5	7.875	220	249	198	233	245	274	177	244	6.17	39.1	6.17	29.3	6.17	51.3	6.17	26.9	7.875	387.6	46.0	39.9
5	8.750	206	238	195	227	237	263	181	212	6.85	32.3	6.85	26.4	6.85	46.0	6.85	19.3	8.75	387.6	46.0	34.9
5.5	9.625	206	233	199	236	226	258	182	217	7.54	30.4	7.54	28.9	7.54	41.4	7.54	20.1	9.625	387.6	46.0	33.6
6	10.500	197	231	192	221	227	251	182	215	8.22	27.0	8.22	22.8	8.22	39.2	8.22	18.9	10.5	387.6	46.0	29.7
7	12.250	197	228	193	235	223	248	192	225	9.59	24.9	9.59	25.2	9.59	36.1	9.59	22.4	12.25	387.6	46.0	28.7
8	14.000	196	229	196	230	216	241	198	227	10.96	23.5	10.96	23.3	10.96	31.3	10.96	23.0	14	387.6	46.0	26.0
9	15.750	197	228	197	240	218	244	193	223	12.3	22.1	12.3	24.6	12.3	31.2	12.3	19.5	15.75	387.6	46.0	26.0
10	17.500	200	235	201	234	225	250	205	240	13.7	23.2	13.7	22.7	13.7	33.0	13.7	25.2	17.5	387.6	46.0	26.3
11	19.250	200	234	209	243	216	246	207	242	15.1	21.6	15.1	25.5	15.1	28.5	15.1	24.8	19.25	387.6	46.0	25.2
12	21.000	209	243	212	247	215	243	208	246	16.4	24.6	16.4	25.9	16.4	26.1	16.4	24.6	21	387.6	46.0	25.5
13	22.750	205	239	211	245	219	248	208	237	17.8	21.3	17.8	23.8	17.8	26.9	17.8	21.1	22.75	387.6	46.0	24.0
14	24.500	214	248	218	250	219	247	216	248	19.2	24.3	19.2	25.3	19.2	25.3	19.2	24.3	24.5	387.6	46.0	25.0
16	28.000	222	251	226	258	223	254	224	252	21.9	24.3	21.9	26.5	21.9	25.3	21.9	24.5	28	387.6	46.0	25.4
18	31.500	230	259	232	264	232	259	232	263	24.7	25.5	24.7	26.7	24.7	26.0	24.7	26.4	31.5	387.6	46.0	26.0
20	35.000	236	265	238	271	233	264	239	275	27.4	25.7	27.4	27.1	27.4	24.7	27.4	28.4	35	387.6	46.0	25.8
22	38.500	242	274	245	279	241	269	242	276	30.1	26.6	30.1	28.1	30.1	25.1	30.1	26.6	38.5	387.6	46.0	26.6
24	42.000	244	277	252	287	242	276	254	293	32.9	25.1	32.9	29.0	32.9	24.3	32.9	30.9	42	387.6	46.0	26.1
26	45.500	253	285	253	287	250	284	262	302	35.6	26.5	35.6	26.5	35.6	25.5	35.6	32.4	45.5	387.6	46.0	26.2
28	49.000	258	288	266	301	258	291	266	303	38.4	25.7	38.4	30.4	38.4	26.4	38.4	30.8	49	387.6	46.0	27.5
30	52.500	262	295	267	297	263	295	245	317	41.1	25.7	41.1	26.9	41.1	25.9	41.1	26.5	52.5	387.6	46.0	26.1
32	56.000	270	303	271	306	261	298	282	326	43.9	26.8	43.9	27.3	43.9	23.4	43.9	34.9	56	387.6	46.0	25.9
34	59.500	279	311	276	310	277	308	288	334	46.6	28.2	46.6	26.8	46.6	27.0	46.6	35.6	59.5	387.6	46.0	27.3
36	63.000	285	316	286	321	281	311	298	310	49.3	28.2	49.3	29.2	49.3	26.0	49.3	29.4	63	387.6	46.0	27.8
38	66.500	294	320	287	318	286	319	299	344	52.1	28.6	52.1	25.9	52.1	26.4	52.1	35.2	66.5	387.6	46.0	27.0
40	70.000	296	326	295	329	292	323	304	347	54.8	27.8	54.8	27.9	54.8	26.1	54.8	34.5	70	387.6	46.0	27.3
42	73.500	304	332	297	327	301	319	314	356	57.6	28.5	57.6	25.1	57.6	24.6	57.6	36.4	73.5	387.6	46.0	26.1
46	80.500	320	344	308	345	316	344	324	368	63.0	29.9	63.0	26.7	63.0	28.9	63.0	36.3	80.5	387.6	46.0	28.5
50	87.500	332	359	326	363	333	367	336	378	68.5	31.0	68.5	30.1	68.5	33.2	68.5	36.2	87.5	387.6	46.0	31.4

Table G- 9 Test Set 10, 20-degrees, 120 mm, moist sand, hopper filled

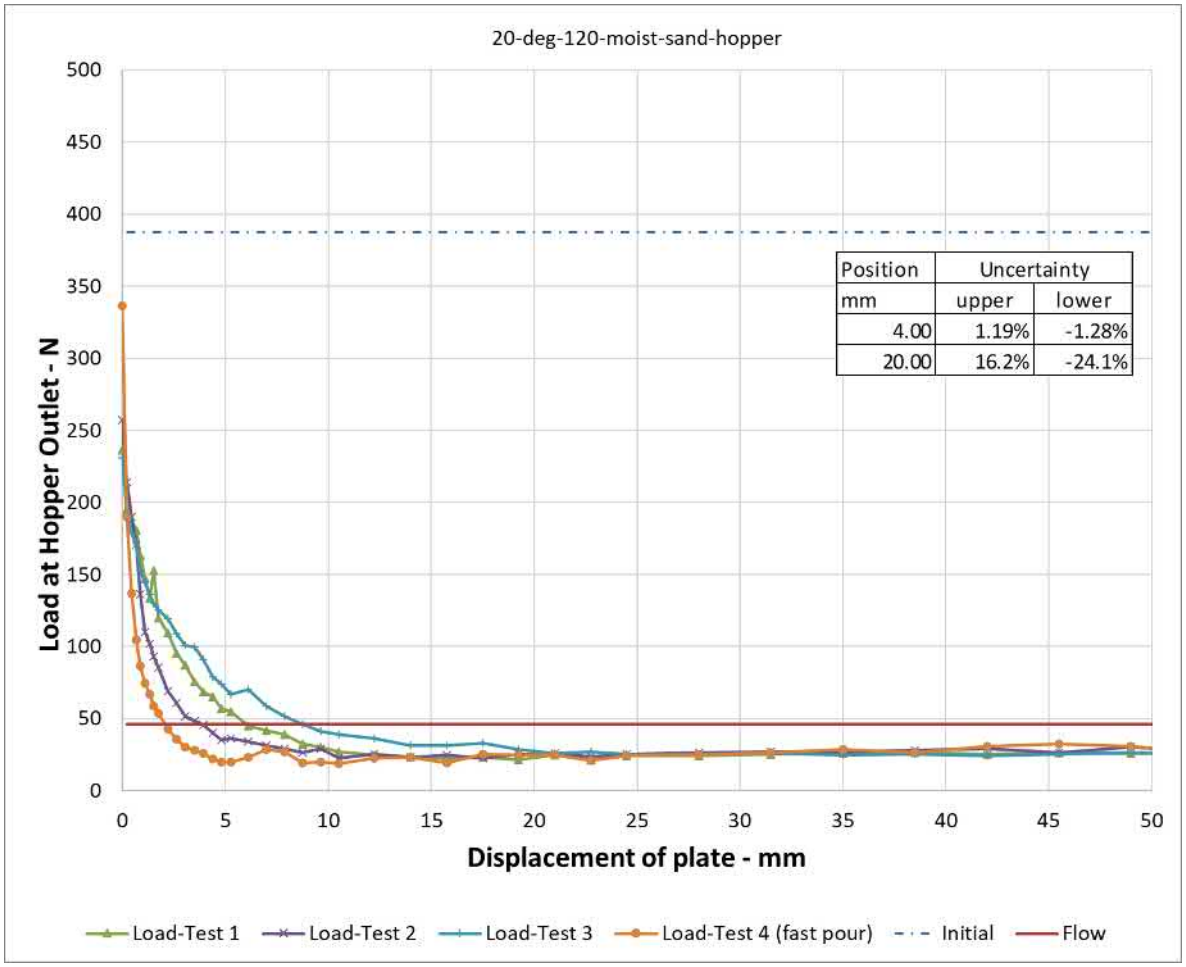


Figure G- 17 Test Set 10, 20-degrees, 120 mm, moist sand, hopper filled

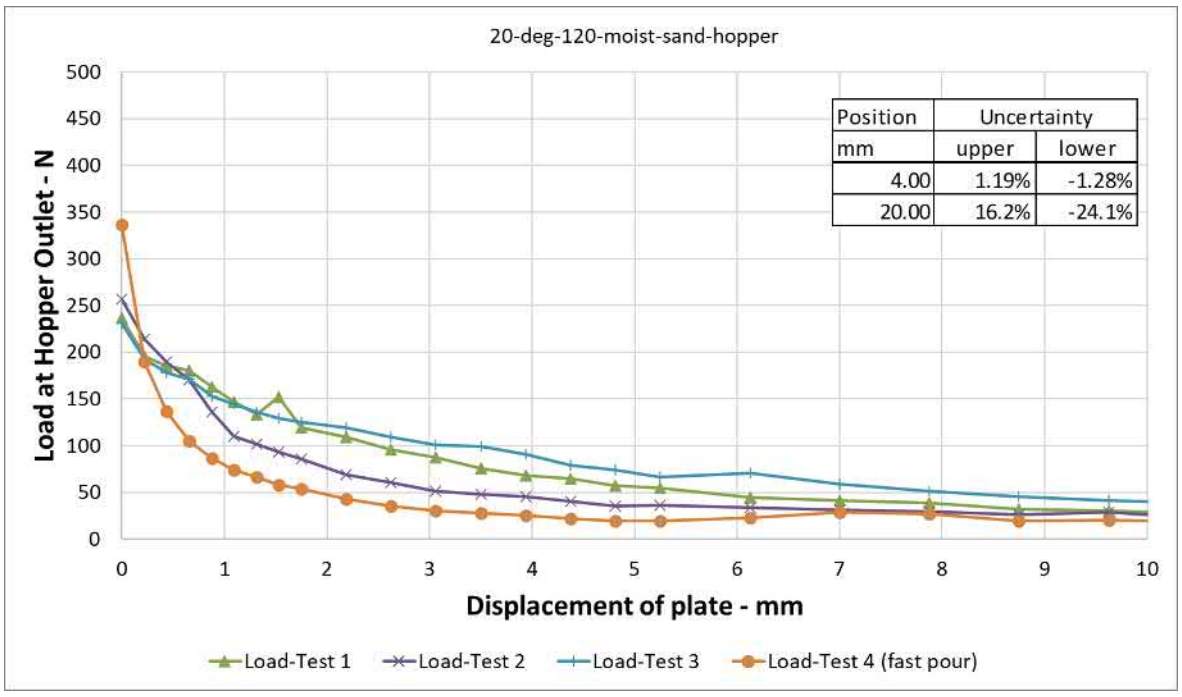


Figure G- 18 Test Set 10, 20-degrees, 120 mm, moist sand, hopper filled, 1-5 mm range

G.10 Set 11, 20-degrees, 120 mm, moist sand, hopper filled, PVC lined

Table G- 10 Test Set 11, 20-degrees, 120 mm, moist sand, hopper filled, PVC lined

Test Record Sheet		Hopper base plate lowering force curve																		
Set Number		11																		
Test Name		20 degrees, 120 mm slot, moist sand, hopper only-pvc																		
											Calculated loads									
Max Lump		mm	P80 Lump		mm	Moisture	8.20%				Initial:	387.6	N							
Width	120.333	mm	Length	480	mm	Angle	19.4435	degrees			Flow:	49.2	N							
Tare	7.09	kg	Spec. wt	13557	N/m3	(loose density +50% of difference to tapped density)														
Screw Pitch M12	1.75	mm	repose	90	degrees	(compacted, so no additional flow-down)														
		Test 1		Test 2		Test 3		Test 4 (fastpour)		t 1 (Repose)	Test 2 (Repose)		Test 3 (Repose)		Test 4 (Repose)			Initial	Flow	Average
Load record (screw turns)	Disp. (mm)	Volt 1	Volt 2	Volt 1	Volt 2	Volt 1	Volt 2	Volt 1	Volt 2	Draw Load	Load-Test 1	Draw Load	Load-Test 2	Draw Load	Load-Test 3	Draw Load	Load-Test 4 (fast pour)	DISP.	(calc)	(calc)	
empty		127	157	127	160	127	158	128	156												
max	211.748										215.4		211.7		217.4		402.8				
min	23.2049										27.8		23.2		28.4		16.9				
50% reduction	117.477										121.6		117.5		122.9		209.9				
80% reduction	60.9136										65.4		60.9		66.2		94.1				
displacement - min	17.5										70.0		17.5		35.0		3.1				
displacement - 50% red.	2.58857										1.8596		2.5886		1.9272		0.2532				
50% red displ as % of gap	2.15%										1.545%		2.151%		1.602%		0.210%				
displacement - 80% red.	7.06469										5.0734		7.0647		5.1240		0.5505				
80% red displ as % of gap	5.87%										4.216%		5.871%		4.258%		0.458%				
0	0	573	592	566	587	573	601	931	1000	0.00	215.4	0.00	211.7	0.00	217.4	0.00	402.8	0			214.9
0.125	0.219	520	524	511	537	507	532	570	642	0.17	185.6	0.17	185.9	0.17	184.2	0.17	226.8	0.21875	387.6	49.2	185.2
0.25	0.438	501	507	492	521	488	519	368	405	0.34	176.7	0.34	177.2	0.34	176.2	0.34	119.3	0.4375	387.6	49.2	176.7
0.375	0.656	472	493	486	504	460	499	282	293	0.51	166.0	0.51	171.4	0.51	164.3	0.51	70.6	0.65625	387.6	49.2	167.2
0.5	0.875	443	476	465	495	449	482	224	283	0.69	154.6	0.69	163.9	0.69	157.3	0.69	53.9	0.875	387.6	49.2	158.6
0.625	1.094	431	459	456	478	429	458	198	230	0.86	147.3	0.86	157.3	0.86	146.4	0.86	34.4	1.09375	387.6	49.2	150.3
0.75	1.313	421	437	430	469	420	449	193	228	1.03	139.3	1.03	148.6	1.03	141.8	1.03	32.5	1.3125	387.6	49.2	143.2
0.875	1.531	404	424	403	454	402	425	185	214	1.20	131.8	1.20	138.2	1.20	131.3	1.20	26.9	1.53125	387.6	49.2	133.8
1	1.750	393	408	406	438	396	422	186	208	1.37	125.0	1.37	134.8	1.37	129.0	1.37	25.5	1.75	387.6	49.2	129.6
1.25	2.188	379	394	388	429	370	388	180	204	1.71	117.8	1.71	127.9	1.71	113.9	1.71	22.7	2.1875	387.6	49.2	119.9
1.5	2.625	350	381	374	398	351	385	171	202	2.06	107.3	2.06	116.5	2.06	108.2	2.06	19.7	2.625	387.6	49.2	110.7
1.75	3.063	341	363	354	393	331	361	162	201	2.40	100.3	2.40	110.1	2.40	97.1	2.40	16.9	3.0625	387.6	49.2	102.5
2	3.500	330	358	337	377	319	342	174	205	2.74	96.0	2.74	101.7	2.74	89.2	2.74	20.5	3.5	387.6	49.2	95.6
2.25	3.938	311	334	325	362	305	332	173	206	3.08	85.2	3.08	94.7	3.08	83.0	3.08	20.2	3.9375	387.6	49.2	87.6
2.5	4.375	294	323	314	338	282	312	179	211	3.43	78.0	3.43	85.8	3.43	72.1	3.43	22.5	4.375	387.6	49.2	78.7
2.75	4.813	278	308	295	338	273	307	179	213	3.77	70.1	3.77	80.9	3.77	68.4	3.77	22.7	4.8125	387.6	49.2	73.1
3	5.250	282	313	267	332	270	296	182	213	4.11	71.9	4.11	72.2	4.11	64.6	4.11	23.0	5.25	387.6	49.2	69.6
3.5	6.125	270	300	283	310	251	295	185	217	4.80	65.1	4.80	70.0	4.80	59.1	4.80	24.1	6.125	387.6	49.2	64.7
4	7.000	254	285	259	302	252	277	191	222	5.48	56.9	5.48	61.5	5.48	54.2	5.48	26.1	7	387.6	49.2	57.5
4.5	7.875	247	281	256	287	227	269	189	224	6.17	53.5	6.17	56.4	6.17	45.5	6.17	25.4	7.875	387.6	49.2	51.8
5	8.750	248	282	240	279	232	261	196	228	6.85	53.3	6.85	49.9	6.85	44.0	6.85	27.4	8.75	387.6	49.2	49.1
5.5	9.625	232	267	239	272	225	254	194	232	7.54	45.0	7.54	47.2	7.54	39.9	7.54	27.2	9.625	387.6	49.2	44.1
6	10.500	232	264	209	281	229	255	199	229	8.22	43.6	8.22	41.5	8.22	40.4	8.22	27.0	10.5	387.6	49.2	41.8
7	12.250	229	259	221	262	223	251	208	237	9.59	40.3	9.59	38.4	9.59	36.6	9.59	29.8	12.25	387.6	49.2	38.4
8	14.000	229	263	206	262	218	250	207	239	10.96	39.9	10.96	33.3	10.96	33.8	10.96	28.7	14	387.6	49.2	35.7
9	15.750	223	257	210	263	216	251	204	239	12.3	35.6	12.3	33.2	12.3	32.2	12.3	26.6	15.75	387.6	49.2	33.7
10	17.500	223	261	207	231	218	256	210	238	13.7	35.2	13.7	23.2	13.7	32.5	13.7	26.4	17.5	387.6	49.2	30.3
11	19.250	221	257	214	266	219	250	215	245	15.1	32.4	15.1	32.2	15.1	29.9	15.1	28.0	19.25	387.6	49.2	31.5
12	21.000	226	263	222	262	226	253	215	244	16.4	33.7	16.4	31.7	16.4	31.0	16.4	26.4	21	387.6	49.2	32.1
13	22.750	229	253	229	270	228	260	219	245	17.8	30.6	17.8	34.0	17.8	31.8	17.8	26.2	22.75	387.6	49.2	32.2
14	24.500	237	265	229	266	227	259	223	247	19.2	34.1	19.2	31.7	19.2	30.0	19.2	26.3	24.5	387.6	49.2	31.9
16	28.000	238	266	219	271	237	263	229	249	21.9	31.9	21.9	27.8	21.9	30.6	21.9	25.5	28	387.6	49.2	30.1
18	31.500	238	268	234	277	240	267	245	271	24.7	29.6	24.7	30.1	24.7	29.6	24.7	32.1	31.5	387.6	49.2	29.8
20	35.000	245	282	244	278	239	274	247	273	27.4	32.0	27.4	30.1	27.4	28.4	27.4	30.3	35	387.6	49.2	30.1
22	38.500	249	278	246	285	246	285	252	279	30.1	29.3	30.1	29.5	30.1	30.0	30.1	30.3	38.5	387.6	49.2	29.6
24	42.000	262	288	255	291	254	287	256	288	32.9	32.2	32.9	30.5	32.9	29.7	32.9	30.7	42	387.6	49.2	30.8
26	45.500	258	290	258	294	257	294	262	293	35.6	28.9	35.6	29.2	35.6	29.4	35.6	30.6	45.5	387.6	49.2	29.2
28	49.000	268	298	262	299	265	302	273	307	38.4	30.6	38.4	28.6	38.4	30.6	38.4	34.0	49	387.6	49.2	29.9
30	52.500	274	301	261	304	271	305	281	322	41.1	30.0	41.1	26.9	41.1	30.1	41.1	36.9	52.5	387.6	49.2	29.0
32	56.000	285	307	268	310	284	315	285	327	43.9	31.5	43.9	27.3	43.9	32.9	43.9	36.4	56	387.6	49.2	30.6
34	59.500	283	311	276	313	289	321	292	340	46.6	29.2	46.6	27.3	46.6	32.9	46.6	38.5	59.5	387.6	49.2	29.8
36	63.000	291	317	285	320	293	325	295	345	49.3	29.9	49.3	28.4	49.3	32.1	49.3	37.8	63	387.6	49.2	30.1
38	66.500	295	324	290	326	298	327	303	351	52.1	29.8	52.1	28.4	52.1	31.1	52.1	38.4	66.5	387.6	49.2	29.8
40	70.000	295	327	297	335	300	331	312	357	54.8	27.8	54.8	29.6	54.8	29.8	54.8	39.4	70	387.6	49.2	29.1
42	73.500	306	334	300	340	309	339	316	363	57.6	29.5	57.6	28.8	57.6	31.2	57.6	39.1	73.5	387.6	49.2	29.8
46	80.500	316	345	315	353	329	353	327	370	63.0	29.2	63.0	30.1	63.0	34.0	63.0	38.0	80.5	387.6	49.2	31.1
50	87.500	330	359	328	366	336	368	356	387	68.5	30.5	68.5	31.0	68.5	33.9	68.5	43.7	87.5	387.6	49.2	31.8

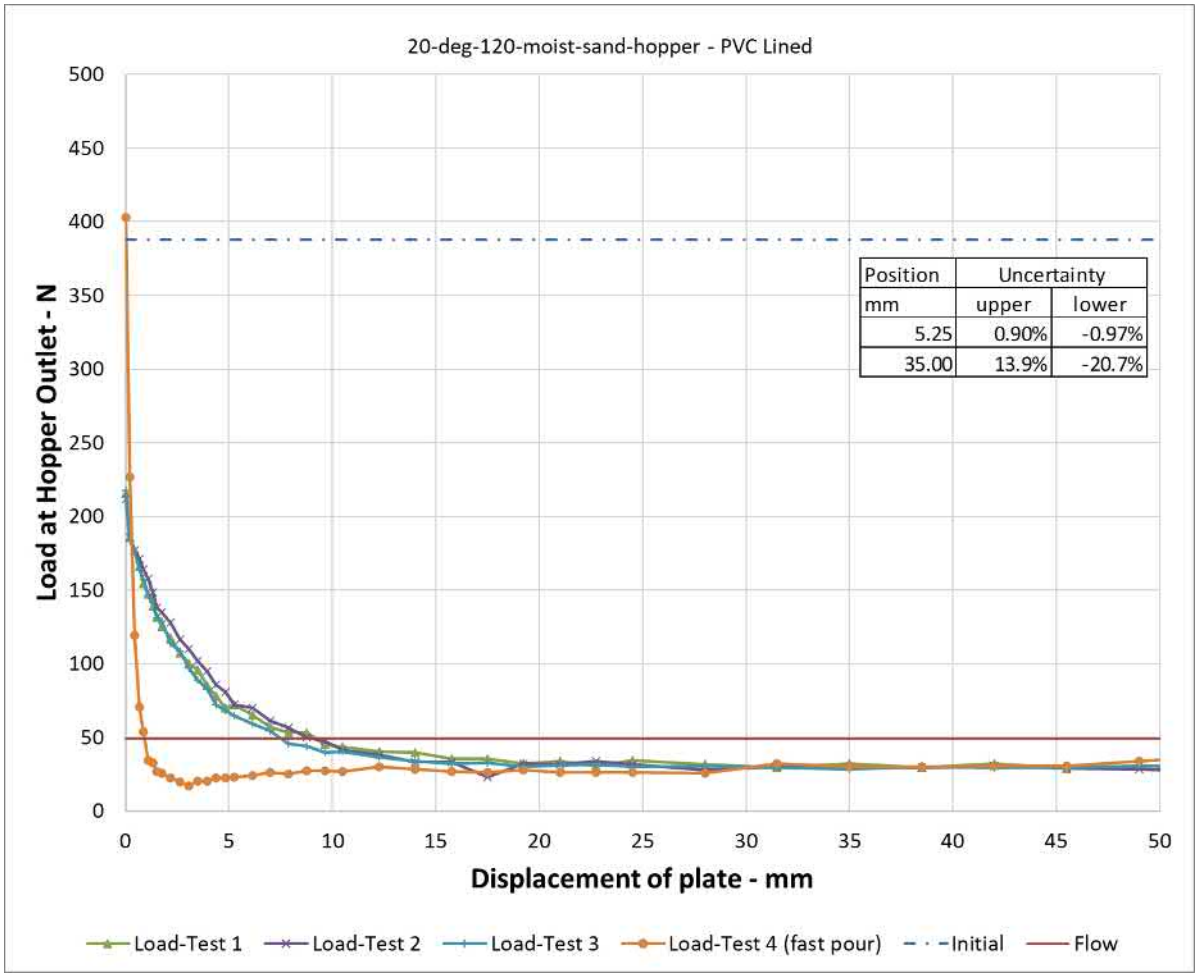


Figure G- 19 Test Set 11, 20-degrees, 120 mm, moist sand, hopper filled

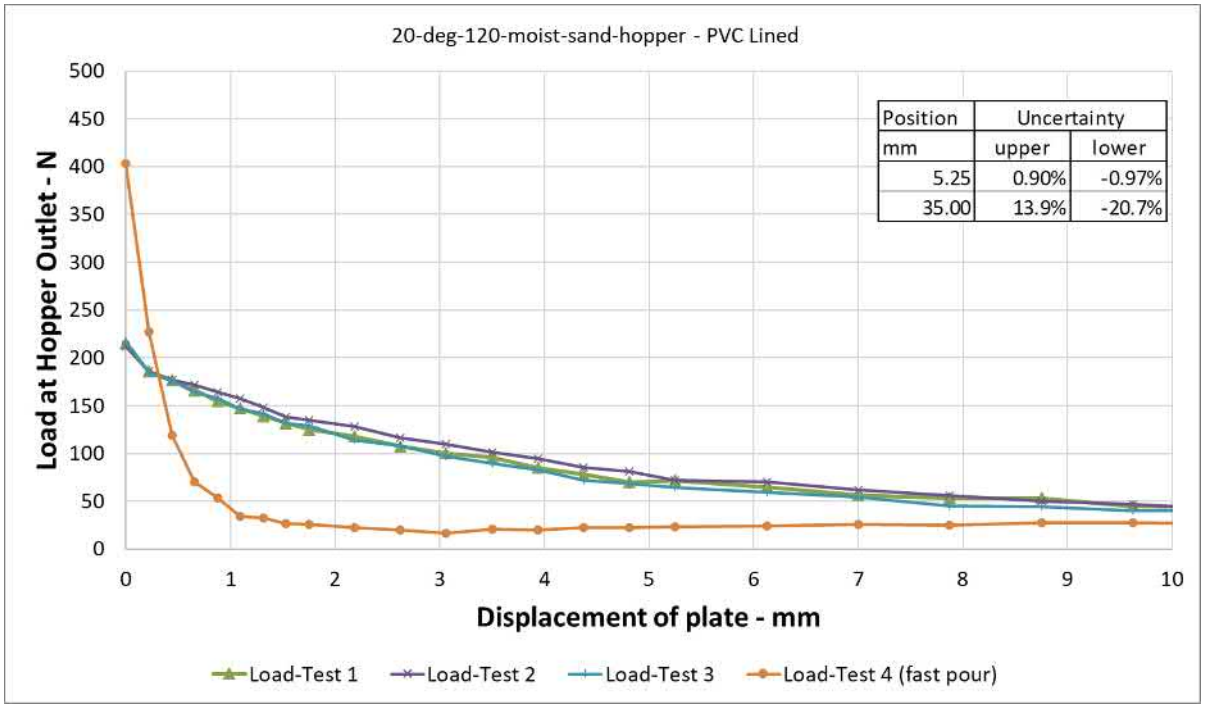


Figure G- 20 Test Set 11, 20-degrees, 120 mm, moist sand, hopper filled, 1-5 mm range

G.11 Set 12, Time response test

The time response test was performed with the same configuration as Test 11 (20-degrees, 120 mm, moist sand, hopper filled with PVC wall lining). Recorded data for the time response test is listed in Table G- 11.

The graph of load as a function of the time test is shown in Figure G- 21.

The plot of pressure to displacement, with the same data set, is shown in Figure G- 22 with view of the 1-5 mm range in Figure G- 23. This format compares to graphs from other tests performed for standard, non-time response tests.

Table G- 11 Set 12, Time response test. 20-degrees, 120 mm, moist sand, hopper filled, PVC lined

Test Record Sheet		Hopper base plate lowering force curve											
Set Number		12											
Test Name		20 degrees, 120 mm slot, moist sand, PVC, hopper -time response											
									Calculated loads				
Max Lump		mm	P80 Lump		mm	Moisture	8.20%	%	Initial:	387.6	N		
Width	120.3	mm	Length	480	mm	Angle	19.4	degrees	Flow:	49.2	N		
Tare	7.09	kg	Spec. wt	13557	N/m3	(loose density +50% of difference to tapped density)							
Screw Pitch M12	1.75	mm	repose	90	degrees	(compacted, so no additional flow-down)							
Time	Load record (screw turns)	Disp. (mm)	Volt 1	Volt 2	Load 1	Load 2	Load	Total N	Draw Load	Load-Test 1		Initial (calc.)	Flow (calc.)
max										226.19			
min										24.269			
50% reduction										125.23			
80% reduction										64.652			
displacement - min										45.5			
displacement - 50% red.										1.313			
50% displ as % of gap										1.09%			
displacement - 80% red.										3.938			
80% displ as % of gap										3.27%			
pre-load	0		128	159	31.6	36.0	67.6	0.0					
8:04	0	0.000	594	618	144.7	149.1	293.8	226.2	0.0	226.2	0.0	387.6	49.2
8:09	deleted the duplicate reading for 09:12	00	592	617	144.2	148.9	293.0	225.5	0.0	225.5	0.0	387.6	49.2
8:14		00	591	616	144.0	148.6	292.6	225.0	0.0	225.0	0.0	387.6	49.2
8:15	0	0.000	591	616	144.0	148.6	292.6	225.0	0.0	225.0	0.0	387.6	49.2
8:16	0.125	0.219	522	541	127.2	130.1	257.3	189.7	0.2	189.6	0.2	387.6	49.2
8:17	0.125	0.219	528	545	128.7	131.1	259.8	192.2	0.2	192.0	0.2	387.6	49.2
8:18	0.125	0.219	529	546	128.9	131.4	260.3	192.7	0.2	192.5	0.2	387.6	49.2
8:19	0.125	0.219	530	547	129.1	131.6	260.8	193.2	0.2	193.0	0.2	387.6	49.2
8:20	0.125	0.219	531	547	129.4	131.6	261.0	193.4	0.2	193.2	0.2	387.6	49.2
8:21	0.125	0.219	495	493	120.7	118.3	239.0	171.4	0.2	171.2	0.2	387.6	49.2
8:22	0.25	0.438	501	504	122.1	121.0	243.1	175.5	0.3	175.2	0.4	387.6	49.2
8:23	0.25	0.438	503	506	122.6	121.5	244.1	176.5	0.3	176.2	0.4	387.6	49.2
8:24	0.25	0.438	504	507	122.8	121.8	244.6	177.0	0.3	176.7	0.4	387.6	49.2
8:25	0.25	0.438	504	508	122.8	122.0	244.8	177.2	0.3	176.9	0.4	387.6	49.2
8:26	0.375	0.656	443	461	108.0	110.4	218.4	150.9	0.5	150.3	0.7	387.6	49.2
8:27	0.375	0.656	456	476	111.2	114.1	225.3	157.7	0.5	157.2	0.7	387.6	49.2
8:28	0.375	0.656	459	479	111.9	114.9	226.8	159.2	0.5	158.7	0.7	387.6	49.2
8:29	0.375	0.656	461	482	112.4	115.6	228.0	160.4	0.5	159.9	0.7	387.6	49.2
8:30	0.375	0.656	463	483	112.9	115.8	228.7	161.1	0.5	160.6	0.7	387.6	49.2
8:31	0.375	0.656	464	484	113.1	116.1	229.2	161.6	0.5	161.1	0.7	387.6	49.2
8:32	0.375	0.656	464	485	113.1	116.3	229.5	161.9	0.5	161.4	0.7	387.6	49.2
8:33	0.375	0.656	465	486	113.4	116.6	229.9	162.4	0.5	161.8	0.7	387.6	49.2
8:34	0.375	0.656	466	487	113.6	116.8	230.4	162.8	0.5	162.3	0.7	387.6	49.2
8:35	0.375	0.656	466	487	113.6	116.8	230.4	162.8	0.5	162.3	0.7	387.6	49.2
8:36	0.5	0.875	454	539	110.7	129.6	240.3	172.7	0.7	172.1	0.9	387.6	49.2
8:37	0.5	0.875	457	539	111.4	129.6	241.1	173.5	0.7	172.8	0.9	387.6	49.2
8:38	0.5	0.875	457	turned wrong way		129.6	241.1	173.5	0.7	172.8	0.9	387.6	49.2
8:39	0.625	1.094	389	445	94.9	bumps .5	201.4	133.8	0.9	133.0	1.1	387.6	49.2
8:40	0.625	1.094	402	454	98.1	108.7	206.8	139.2	0.9	138.3	1.1	387.6	49.2
8:41	0.625	1.094	407	45	stable 9.3	109.7	209.0	141.4	0.9	140.5	1.1	387.6	49.2
8:42	0.625	1.094	410	460	100.0	110.2	210.2	142.6	0.9	141.7	1.1	387.6	49.2
8:43	0.625	1.094	412	461	100.5	110.4	210.9	143.3	0.9	142.5	1.1	387.6	49.2
8:44	0.625	1.094	413	462	100.8	110.7	211.4	143.8	0.9	143.0	1.1	387.6	49.2
8:45	0.625	1.094	414	463	101.0	110.9	211.9	144.3	0.9	143.5	1.1	387.6	49.2
8:46	0.625	1.094	415	464	101.2	111.2	212.4	144.8	0.9	143.9	1.1	387.6	49.2
8:47	0.625	1.094	416	464	101.5	111.2	212.6	145.0	0.9	144.2	1.1	387.6	49.2
8:48	0.625	1.094	416	465	101.5	111.4	212.9	145.3	0.9	144.4	1.1	387.6	49.2
8:49	0.625	1.094	416	465	101.5	111.4	212.9	145.3	0.9	144.4	1.1	387.6	49.2
8:50	0.75	1.313	378	404	missed a reading, filled it in		188.6	121.0	1.0	120.0	1.3	387.6	49.2
8:51	0.75	1.313	390	416			194.5	126.9	1.0	125.9	1.3	387.6	49.2
8:52	0.75	1.313	394	420	96.1	100.3	196.5	128.9	1.0	127.8	1.3	387.6	49.2
8:53	0.75	1.313	397	424	96.9	101.3	198.2	130.6	1.0	129.5	1.3	387.6	49.2
8:54	0.75	1.313	399	425	97.4	101.5	198.9	131.3	1.0	130.3	1.3	387.6	49.2
8:55	0.75	1.313	400	427	97.6	102.0	199.6	132.0	1.0	131.0	1.3	387.6	49.2
8:56	0.75	1.313	402	429	98.1	102.5	200.6	133.0	1.0	132.0	1.3	387.6	49.2
8:57	0.75	1.313	403	430	98.3	102.8	201.1	133.5	1.0	132.5	1.3	387.6	49.2
8:58	0.75	1.313	404	431	98.6	103.0	201.6	134.0	1.0	133.0	1.3	387.6	49.2
8:59	0.75	1.313	404	432	98.6	103.3	201.8	134.2	1.0	133.2	1.3	387.6	49.2
9:00	0.75	1.313	405	432	98.8	103.3	202.1	134.5	1.0	133.5	1.3	387.6	49.2
9:01	0.875	1.531	374	405	91.3	96.6	187.9	120.3	1.2	119.1	1.5	387.6	49.2
9:02	0.875	1.531	384	414	93.7	98.8	192.6	125.0	1.2	123.8	1.5	387.6	49.2
9:03	0.875	1.531	387	417	94.4	99.6	194.0	126.4	1.2	125.2	1.5	387.6	49.2
9:04	0.875	1.531	389	419	94.9	100.1	195.0	127.4	1.2	126.2	1.5	387.6	49.2
9:05	0.875	1.531	390	420	95.2	100.3	195.5	127.9	1.2	126.7	1.5	387.6	49.2

Time	Load record (screw turns)	Disp. (mm)	Volt 1	Volt 2	Load 1	Load 2	Load	Total N	Draw Load	Load-Test 1		Initial (calc.)	Flow (calc.)
9:06	0.875	1.531	391	421	95.4	100.6	196.0	128.4	1.2	127.2	1.5	387.6	49.2
9:07	0.875	1.531	392	422	95.7	100.8	196.5	128.9	1.2	127.7	1.5	387.6	49.2
9:08	0.875	1.531	393	423	95.9	101.1	197.0	129.4	1.2	128.2	1.5	387.6	49.2
9:09	0.875	1.531	394	424	96.1	101.3	197.4	129.8	1.2	128.6	1.5	387.6	49.2
9:10	0.875	1.531	394	424	96.1	101.3	197.4	129.8	1.2	128.6	1.5	387.6	49.2
9:11	1	1.750	352	388	85.9	92.4	178.4	110.8	1.4	109.4	1.8	387.6	49.2
9:12	1	1.750	368	402	89.8	95.9	185.7	118.1	1.4	116.7	1.8	387.6	49.2
9:13	1	1.750	370	404	90.3	96.4	186.7	119.1	1.4	117.7	1.8	387.6	49.2
9:14	1	1.750	372	406	90.8	96.9	187.7	120.1	1.4	118.7	1.8	387.6	49.2
9:15	1	1.750	372	406	90.8	96.9	187.7	120.1	1.4	118.7	1.8	387.6	49.2
9:16	1.25	2.188	335	362	81.8	86.0	167.8	100.3	1.7	98.5	2.2	387.6	49.2
9:17	1.25	2.188	346	373	84.5	88.7	173.2	105.6	1.7	103.9	2.2	387.6	49.2
9:18	1.25	2.188	350	378	85.5	90.0	175.4	107.8	1.7	106.1	2.2	387.6	49.2
9:19	1.25	2.188	352	381	85.9	90.7	176.7	109.1	1.7	107.3	2.2	387.6	49.2
9:20	1.25	2.188	354	383	86.4	91.2	177.6	110.0	1.7	108.3	2.2	387.6	49.2
9:21	1.25	2.188	355	384	86.7	91.4	178.1	110.5	1.7	108.8	2.2	387.6	49.2
9:22	1.25	2.188	356	385	86.9	91.7	178.6	111.0	1.7	109.3	2.2	387.6	49.2
9:23	1.5	2.625	328	343	80.1	81.3	161.5	93.9	2.1	91.8	2.6	387.6	49.2
9:24	1.5	2.625	330	353	80.6	83.8	164.4	96.8	2.1	94.8	2.6	387.6	49.2
9:25	1.5	2.625	333	357	81.3	84.8	166.1	98.5	2.1	96.5	2.6	387.6	49.2
9:26	1.5	2.625	335	359	81.8	85.3	167.1	99.5	2.1	97.5	2.6	387.6	49.2
9:27	1.5	2.625	337	361	82.3	85.8	168.1	100.5	2.1	98.4	2.6	387.6	49.2
9:28	1.5	2.625	338	362	82.6	86.0	168.6	101.0	2.1	98.9	2.6	387.6	49.2
9:29	1.5	2.625	339	364	82.8	86.5	169.3	101.7	2.1	99.7	2.6	387.6	49.2
9:30	1.5	2.625	340	365	83.0	86.8	169.8	102.2	2.1	100.2	2.6	387.6	49.2
9:31	1.5	2.625	340	365	83.0	86.8	169.8	102.2	2.1	100.2	2.6	387.6	49.2
9:32	1.75	3.063	303	319	74.1	75.4	149.5	81.9	2.4	79.5	3.1	387.6	49.2
9:33	1.75	3.063	317	332	77.5	78.6	156.1	88.5	2.4	86.1	3.1	387.6	49.2
9:34	1.75	3.063	321	336	78.4	79.6	158.0	90.4	2.4	88.1	3.1	387.6	49.2
9:35	1.75	3.063	323	338	78.9	80.1	159.0	91.4	2.4	89.0	3.1	387.6	49.2
9:36	1.75	3.063	324	340	79.2	80.6	159.8	92.2	2.4	89.8	3.1	387.6	49.2
9:37	1.75	3.063	325	341	79.4	80.8	160.2	92.7	2.4	90.3	3.1	387.6	49.2
9:38	1.75	3.063	326	342	79.6	81.1	160.7	93.1	2.4	90.7	3.1	387.6	49.2
9:39	2	3.500	291	310	71.1	73.2	144.4	76.8	2.7	74.0	3.5	387.6	49.2
9:40	2	3.500	302	321	73.8	75.9	149.7	82.1	2.7	79.4	3.5	387.6	49.2
9:41	2	3.500	306	325	74.8	76.9	151.7	84.1	2.7	81.4	3.5	387.6	49.2
9:42	2	3.500	308	327	75.3	77.4	152.7	85.1	2.7	82.3	3.5	387.6	49.2
9:43	2	3.500	310	329	75.8	77.9	153.6	86.1	2.7	83.3	3.5	387.6	49.2
9:44	2	3.500	311	330	76.0	78.1	154.1	86.5	2.7	83.8	3.5	387.6	49.2
9:45	2.25	3.938	280	299	68.5	70.5	139.0	71.4	3.1	68.3	3.9	387.6	49.2
9:46	2.25	3.938	291	311	71.1	73.5	144.6	77.0	3.1	73.9	3.9	387.6	49.2
9:47	2.25	3.938	294	314	71.9	74.2	146.1	78.5	3.1	75.4	3.9	387.6	49.2
9:48	2.25	3.938	296	316	72.4	74.7	147.0	79.5	3.1	76.4	3.9	387.6	49.2
9:49	2.25	3.938	297	318	72.6	75.2	147.8	80.2	3.1	77.1	3.9	387.6	49.2
9:50	2.25	3.938	298	319	72.8	75.4	148.3	80.7	3.1	77.6	3.9	387.6	49.2
9:51	2.25	3.938	298	319	72.8	75.4	148.3	80.7	3.1	77.6	3.9	387.6	49.2
9:52	2.5	4.375	268	292	65.6	68.8	134.3	66.7	3.4	63.3	4.4	387.6	49.2
9:53	2.5	4.375	278	302	68.0	71.2	139.2	71.6	3.4	68.2	4.4	387.6	49.2
9:54	2.5	4.375	282	305	69.0	72.0	140.9	73.3	3.4	69.9	4.4	387.6	49.2
9:55	2.5	4.375	283	306	69.2	72.2	141.4	73.8	3.4	70.4	4.4	387.6	49.2
9:56	2.5	4.375	284	308	69.4	72.7	142.2	74.6	3.4	71.1	4.4	387.6	49.2
9:57	2.5	4.375	285	309	69.7	73.0	142.7	75.1	3.4	71.6	4.4	387.6	49.2
9:58	2.75	4.813	257	279	62.9	65.6	128.5	60.9	3.8	57.1	4.8	387.6	49.2
9:59	2.75	4.813	269	287	65.8	67.5	133.4	65.8	3.8	62.0	4.8	387.6	49.2
10:00	2.75	4.813	273	291	66.8	68.5	135.3	67.7	3.8	63.9	4.8	387.6	49.2
10:01	2.75	4.813	275	293	67.3	69.0	136.3	68.7	3.8	64.9	4.8	387.6	49.2
10:02	2.75	4.813	277	295	67.7	69.5	137.3	69.7	3.8	65.9	4.8	387.6	49.2
10:03	2.75	4.813	278	296	68.0	69.8	137.8	70.2	3.8	66.4	4.8	387.6	49.2
10:04	3	5.250	252	282	61.7	66.3	128.0	60.4	4.1	56.3	5.3	387.6	49.2
10:05	3	5.250	261	281	63.9	66.1	129.9	62.3	4.1	58.2	5.3	387.6	49.2
10:06	3	5.250	264	284	64.6	66.8	131.4	63.8	4.1	59.7	5.3	387.6	49.2
10:07	3	5.250	266	283	65.1	66.6	131.6	64.0	4.1	59.9	5.3	387.6	49.2
10:08	3	5.250	267	287	65.3	67.5	132.9	65.3	4.1	61.2	5.3	387.6	49.2
10:09	3	5.250	268	288	65.6	67.8	133.4	65.8	4.1	61.6	5.3	387.6	49.2
10:10	3	5.250	269	289	65.8	68.0	133.8	66.2	4.1	62.1	5.3	387.6	49.2

deleted the duplicate reading for 09:12

Time	Load record (screw turns)	Disp. (mm)	Volt 1	Volt 2	Load 1	Load 2	Load	Total N	Draw Load	Load-Test 1		Initial (calc.)	Flow (calc.)
10:11	3	5.250	269	289	65.8	68.0	133.8	66.2	4.1	62.1	5.3	387.6	49.2
10:12	3.5	6.125	239	266	58.5	62.4	120.9	53.3	4.8	48.5	6.1	387.6	49.2
10:13	3.5	6.125	248	277	60.7	65.1	125.8	58.2	4.8	53.4	6.1	387.6	49.2
10:14	3.5	6.125	251	279	61.4	65.6	127.0	59.4	4.8	54.6	6.1	387.6	49.2
10:15	3.5	6.125	252	281	61.7	66.1	127.7	60.2	4.8	55.4	6.1	387.6	49.2
10:16	3.5	6.125	253	282	61.9	66.3	128.2	60.6	4.8	55.8	6.1	387.6	49.2
10:17	3.5	6.125	254	282	62.2	66.3	128.5	60.9	4.8	56.1	6.1	387.6	49.2
10:18	4	7.000	239	258	58.5	60.4	118.9	51.3	5.5	45.8	7.0	387.6	49.2
10:19	4	7.000	246	265	60.2	62.1	122.3	54.8	5.5	49.3	7.0	387.6	49.2
10:20	4	7.000	248	267	60.7	62.6	123.3	55.7	5.5	50.3	7.0	387.6	49.2
10:21	4	7.000	250	269	61.2	63.1	124.3	56.7	5.5	51.2	7.0	387.6	49.2
10:22	4	7.000	251	280	61.4	65.8	127.3	59.7	5.5	54.2	7.0	387.6	49.2
10:23	4	7.000	251	280	61.4	65.8	127.3	59.7	5.5	54.2	7.0	387.6	49.2
10:24	4.5	7.875	227	252	55.6	58.9	114.5	46.9	6.2	40.8	7.9	387.6	49.2
10:25	4.5	7.875	236	260	57.8	60.9	118.7	51.1	6.2	44.9	7.9	387.6	49.2
10:26	4.5	7.875	239	262	58.5	61.4	119.9	52.3	6.2	46.1	7.9	387.6	49.2
10:27	4.5	7.875	240	263	58.8	61.6	120.4	52.8	6.2	46.6	7.9	387.6	49.2
10:28	4.5	7.875	241	264	59.0	61.9	120.9	53.3	6.2	47.1	7.9	387.6	49.2
10:29	5	8.750	227	247	55.6	57.7	113.3	45.7	6.9	38.9	8.8	387.6	49.2
10:30	5	8.750	234	252	57.3	58.9	116.2	48.6	6.9	41.8	8.8	387.6	49.2
10:31	5	8.750	236	255	57.8	59.7	117.5	49.9	6.9	43.0	8.8	387.6	49.2
10:32	5	8.750	237	257	58.0	60.2	118.2	50.6	6.9	43.7	8.8	387.6	49.2
10:33	5	8.750	238	257	58.3	60.2	118.4	50.8	6.9	44.0	8.8	387.6	49.2
10:34	6	10.500	220	241	53.9	56.2	110.1	42.5	8.2	34.3	10.5	387.6	49.2
10:35	6	10.500	226	246	55.4	57.4	112.8	45.2	8.2	37.0	10.5	387.6	49.2
10:36	6	10.500	229	249	56.1	58.2	114.3	46.7	8.2	38.5	10.5	387.6	49.2
10:37	6	10.500	245	268	60.0	62.9	122.8	55.3	8.2	47.0	10.5	387.6	49.2
10:38	6	10.500	248	270	60.7	63.4	124.1	56.5	8.2	48.2	10.5	387.6	49.2
10:39	8	14.000	224	252	54.4	58.9	113.8	46.2	11.0	35.2	14.0	387.6	49.2
10:40	8	14.000	228	255	55.9	59.7	115.5	47.9	11.0	37.0	14.0	387.6	49.2
10:41	8	14.000	229	255	56.1	59.7	115.8	48.2	11.0	37.2	14.0	387.6	49.2
10:42	8	14.000	229	256	56.1	59.9	116.0	48.4	11.0	37.4	14.0	387.6	49.2
10:43	10	17.500	219	243	53.7	56.7	110.4	42.8	13.7	29.1	17.5	387.6	49.2
10:44	10	17.500	222	247	54.4	57.7	112.1	44.5	13.7	30.8	17.5	387.6	49.2
10:45	10	17.500	223	248	54.6	57.9	112.6	45.0	13.7	31.3	17.5	387.6	49.2
10:46	10	17.500	225	249	55.1	58.2	113.3	45.7	13.7	32.0	17.5	387.6	49.2
10:47	10	17.500	225	249	55.1	58.2	113.3	45.7	13.7	32.0	17.5	387.6	49.2
10:48	12	21.000	216	242	52.9	56.5	109.4	41.8	16.4	25.4	21.0	387.6	49.2
10:49	12	21.000	220	245	53.9	57.2	111.1	43.5	16.4	27.1	21.0	387.6	49.2
10:50	12	21.000	221	246	54.2	57.4	111.6	44.0	16.4	27.6	21.0	387.6	49.2
10:51	12	21.000	222	247	54.4	57.7	112.1	44.5	16.4	28.1	21.0	387.6	49.2
10:52	14	24.500	222	248	54.4	57.9	112.3	44.7	19.2	25.6	24.5	387.6	49.2
10:53	14	24.500	225	250	55.1	58.4	113.6	46.0	19.2	26.8	24.5	387.6	49.2
10:54	14	24.500	226	251	55.4	58.7	114.0	46.5	19.2	27.3	24.5	387.6	49.2
10:55	14	24.500	226	251	55.4	58.7	114.0	46.5	19.2	27.3	24.5	387.6	49.2
10:56	16	28.000	228	253	55.9	59.2	115.0	47.4	21.9	25.5	28.0	387.6	49.2
10:57	16	28.000	229	255	56.1	59.7	115.8	48.2	21.9	26.2	28.0	387.6	49.2
10:58	16	28.000	230	256	56.3	59.9	116.2	48.7	21.9	26.7	28.0	387.6	49.2
10:59	18	31.500	235	262	57.6	61.4	118.9	51.3	24.7	26.7	31.5	387.6	49.2
11:00	18	31.500	237	263	58.0	61.6	119.7	52.1	24.7	27.4	31.5	387.6	49.2
11:01	18	31.500	238	264	58.3	61.9	120.2	52.6	24.7	27.9	31.5	387.6	49.2
11:02	20	35.000	240	265	58.8	62.1	120.9	53.3	27.4	25.9	35.0	387.6	49.2
11:03	20	35.000	241	266	59.0	62.4	121.4	53.8	27.4	26.4	35.0	387.6	49.2
11:04	20	35.000	242	267	59.3	62.6	121.9	54.3	27.4	26.9	35.0	387.6	49.2
11:05	22	38.500	251	274	61.4	64.3	125.8	58.2	30.1	28.0	38.5	387.6	49.2
11:06	22	38.500	252	275	61.7	64.6	126.3	58.7	30.1	28.5	38.5	387.6	49.2
11:06	24	42.000	251	275	61.4	64.6	126.0	58.4	32.9	25.5	42.0	387.6	49.2
11:06	26	45.500	254	278	62.2	65.3	127.5	59.9	35.6	24.3	45.5	387.6	49.2
11:06	28	49.000	260	285	63.6	67.1	130.7	63.1	38.4	24.7	49.0	387.6	49.2
11:06	30	52.500	271	295	66.3	69.5	135.8	68.2	41.1	27.1	52.5	387.6	49.2
11:06	32	56.000	280	303	68.5	71.5	140.0	72.4	43.9	28.5	56.0	387.6	49.2
11:06	34	59.500	286	309	69.9	73.0	142.9	75.3	46.6	28.7	59.5	387.6	49.2
11:06	38	66.500	293	314	71.6	74.2	145.8	78.2	52.1	26.2	66.5	387.6	49.2
11:06	42	73.500	308	329	75.3	77.9	153.2	85.6	57.6	28.0	73.5	387.6	49.2
11:06	46	80.500	322	348	78.7	82.6	161.2	93.6	63.0	30.6	80.5	387.6	49.2
11:06	50	87.500	334	354	81.6	84.1	165.6	98.0	68.5	29.5	87.5	387.6	49.2

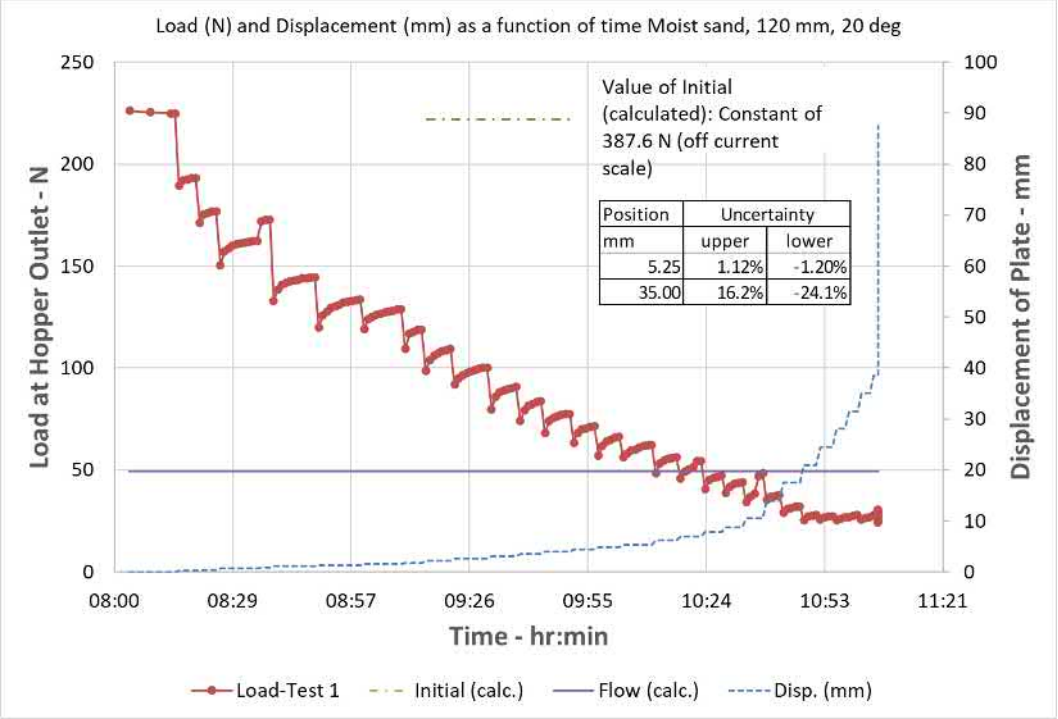


Figure G- 21 Results from Case 12, time response test

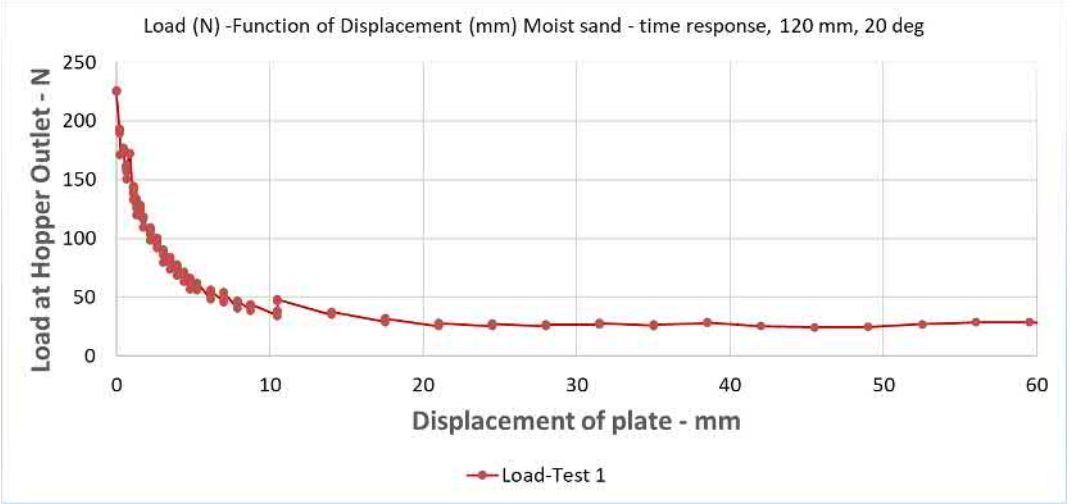


Figure G- 22 Case 12, time response test, load-displacement plot

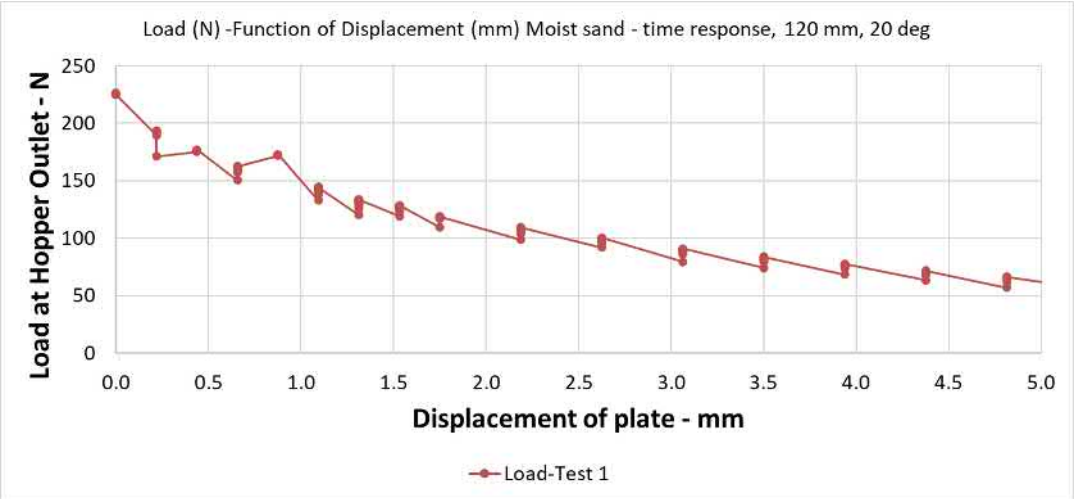
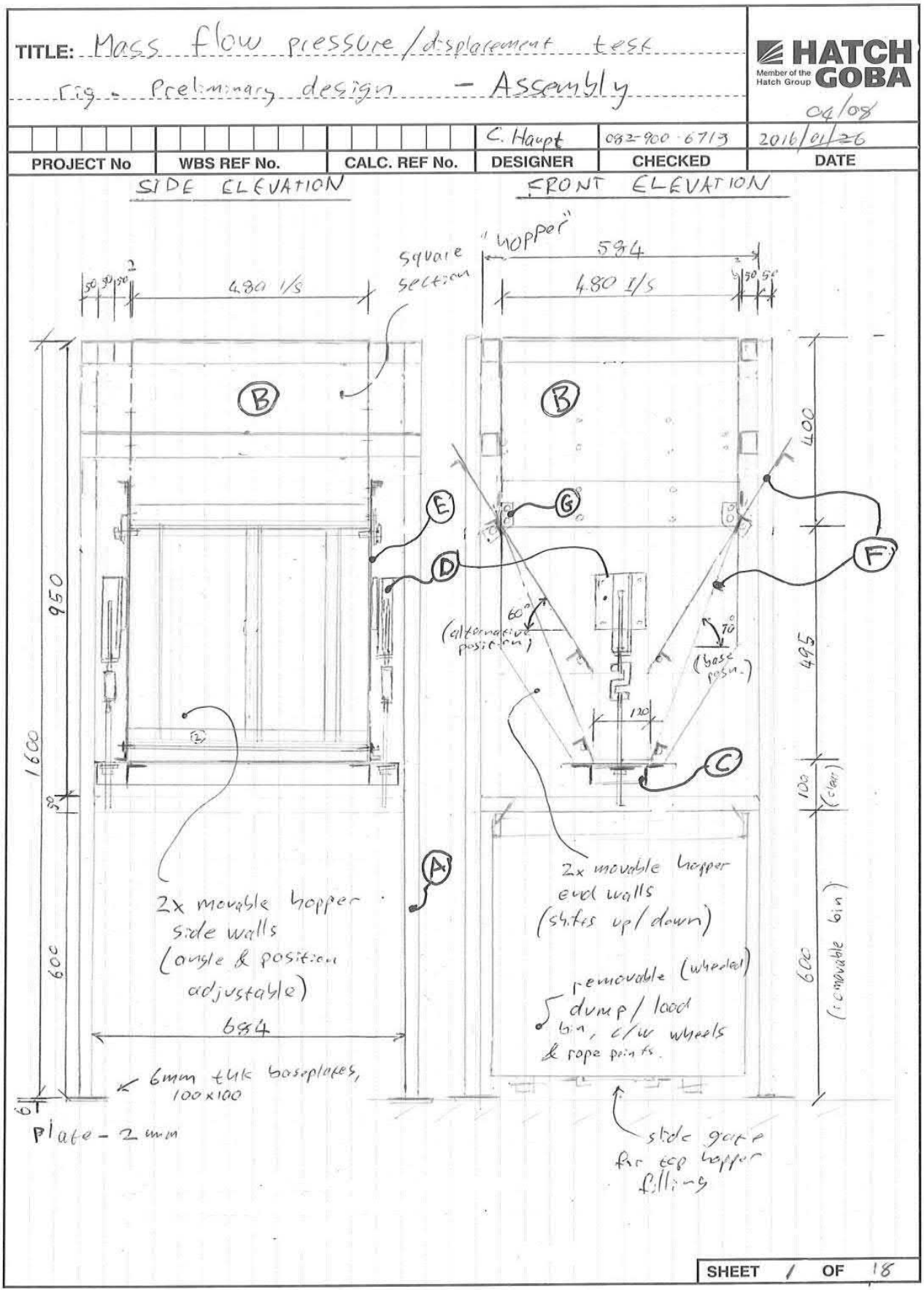


Figure G- 23 Case 12, time response test, load-displacement plot: 1-5 mm

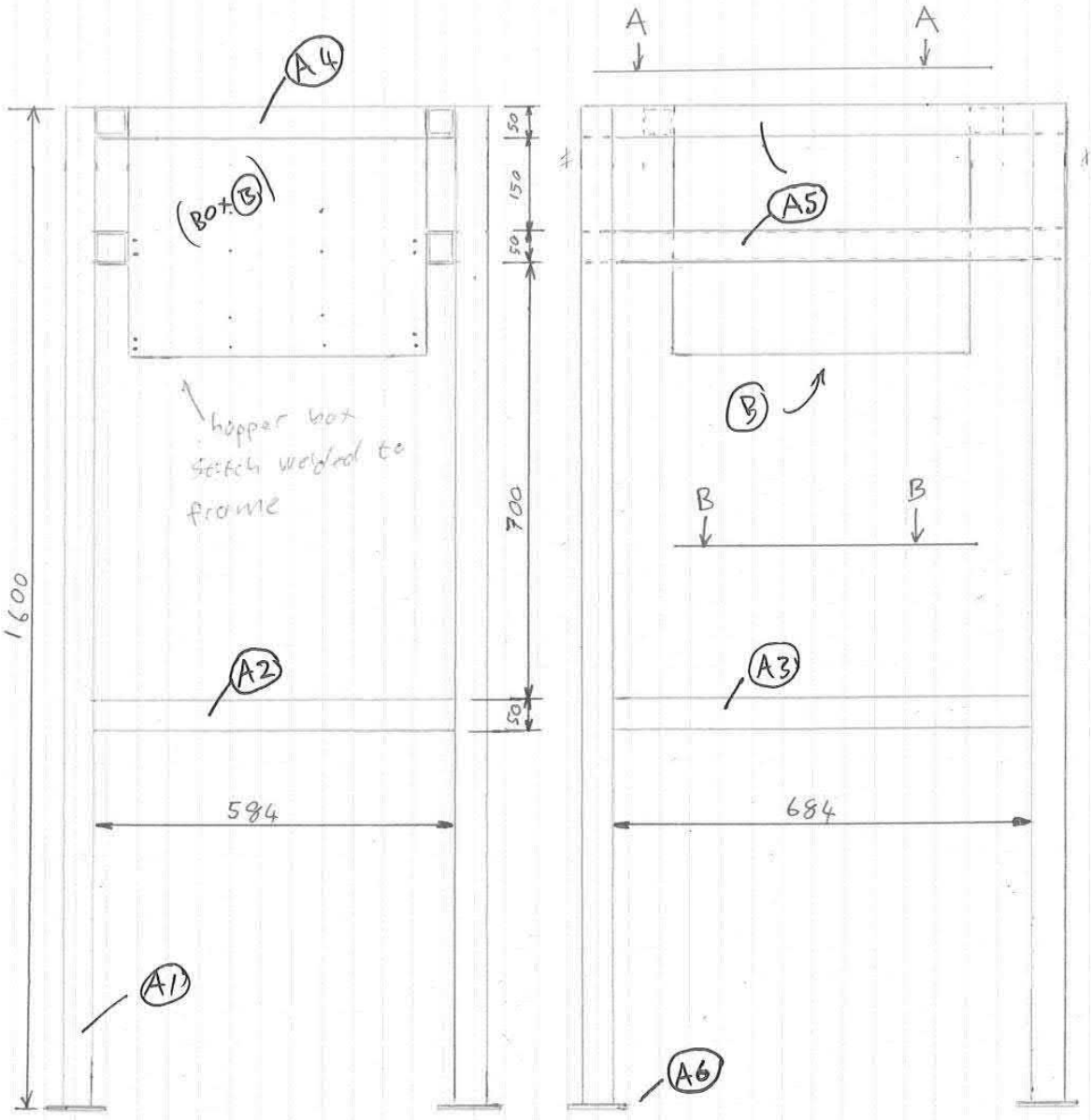
Appendix H Test Rig Design Drawings



TITLE: Main Frame and Hopper Box detail - Elevation Views Assembly A

HATCH GOBA Member of the Hatch Group

PROJECT No	WBS REF No.	CALC. REF No.	DESIGNER	CHECKED	DATE
					2016/04/08

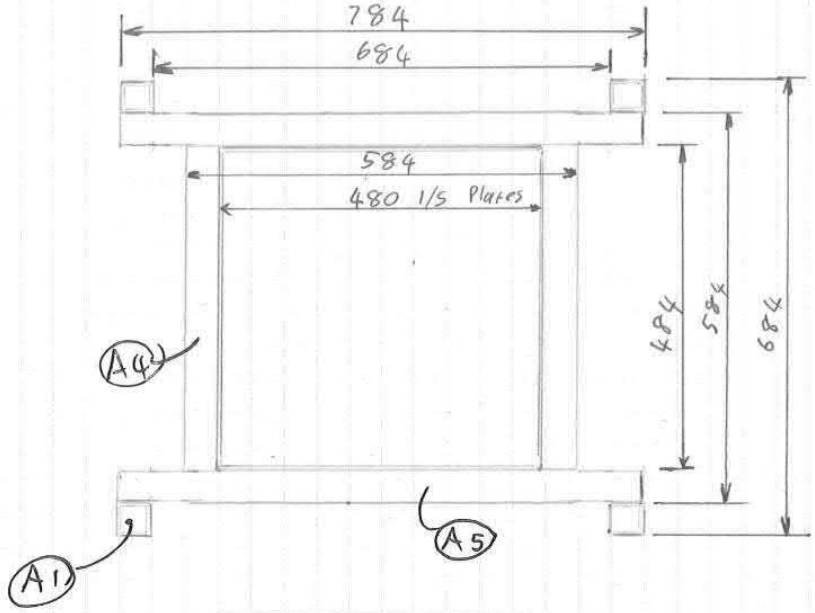


SHEET 2 OF 18

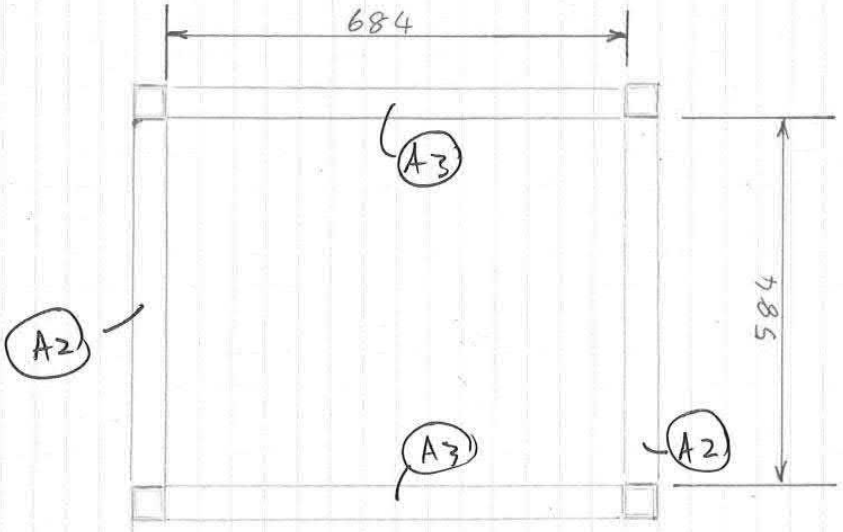
TITLE: Main Frame Plan Details

HATCH GOBA
Member of the Hatch Group

PROJECT No	WBS REF No.	CALC. REF No.	DESIGNER	CHECKED	DATE
					2016/04/08



VIEW A-A



VIEW B-B

SHEET 3 OF 18

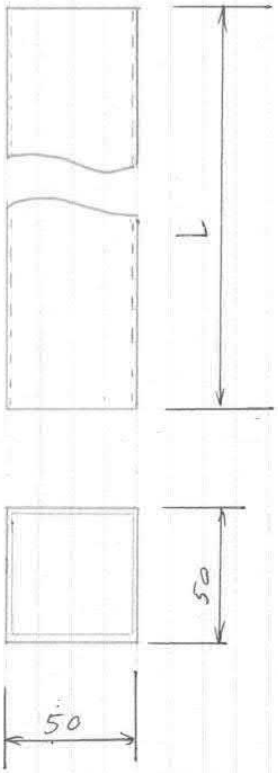
TITLE:

HATCH Member of the Hatch Group GOBA

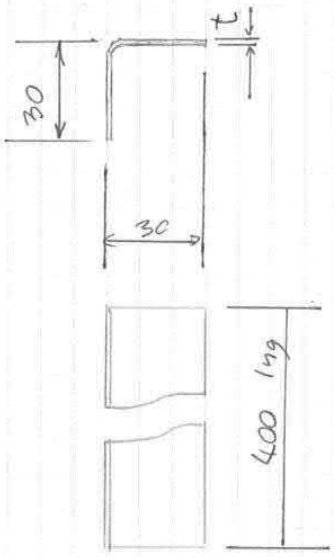
PROJECT No	WBS REF No.	CALC. REF No.	DESIGNER	CHECKED	DATE

50 x 50 Square tube detail

→ for main frame assembly



PART No.	Name	L(mm)	Qty
A1	Verticals	1600	4
A2	Front/rear lower brace	584	2
A3	Side lower brace	684	2
A4	Front/rear upper brace	484	2
A5	Side upper brace	784	4



30 x 30 Manufactured angle [for box assembly]

thickness 't', as available from mild steel sheet,

t = 0.6 to 1.5 mm thk.

Require 4 off

PART (B1)

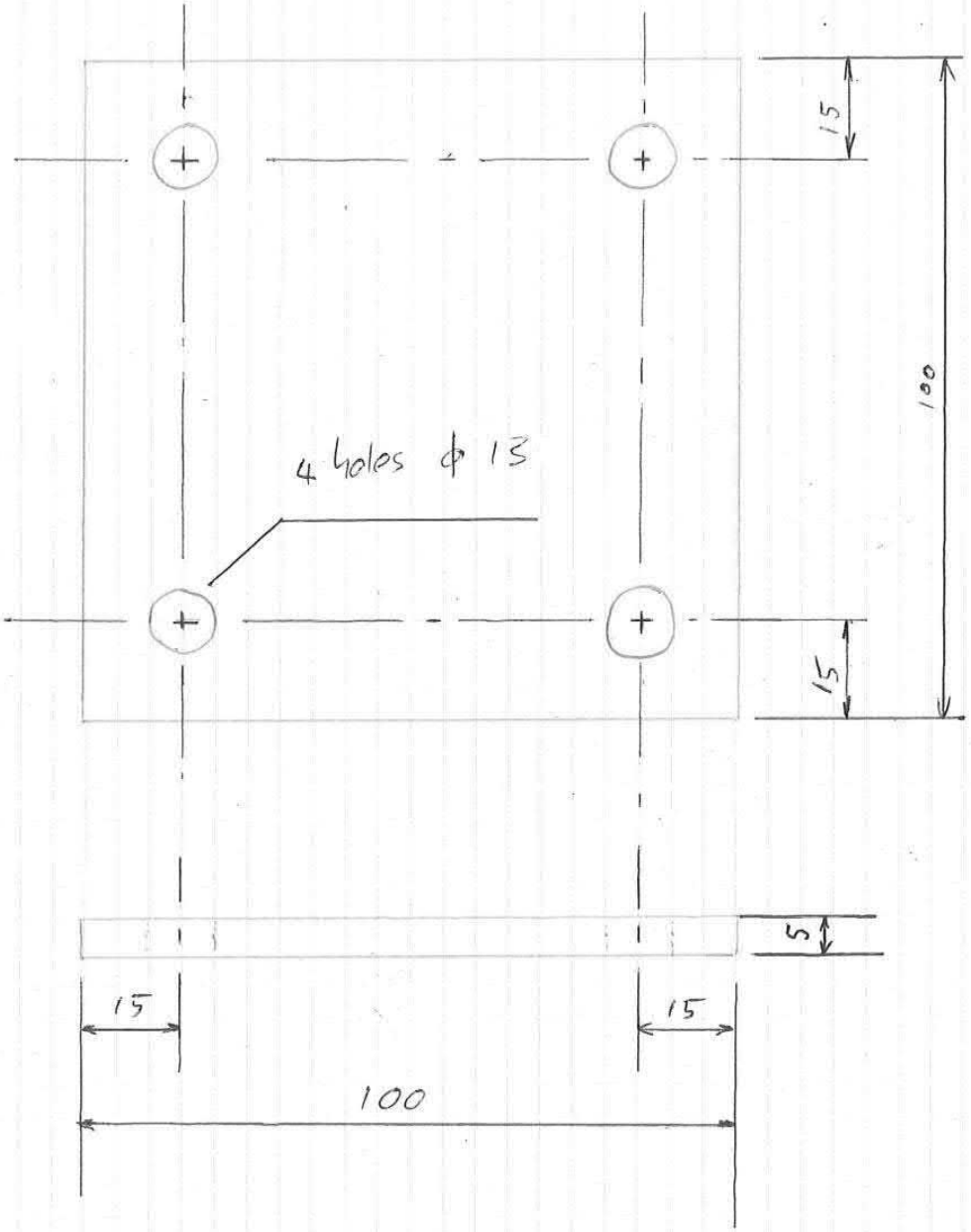
SHEET 4 OF 18

TITLE: Main frame baseplates.
4 - required

HATCH GOBA
Member of the Hatch Group

PROJECT No	WBS REF No.	CALC. REF No.	DESIGNER	CHECKED	DATE
					2016/04/08

PART (A6)



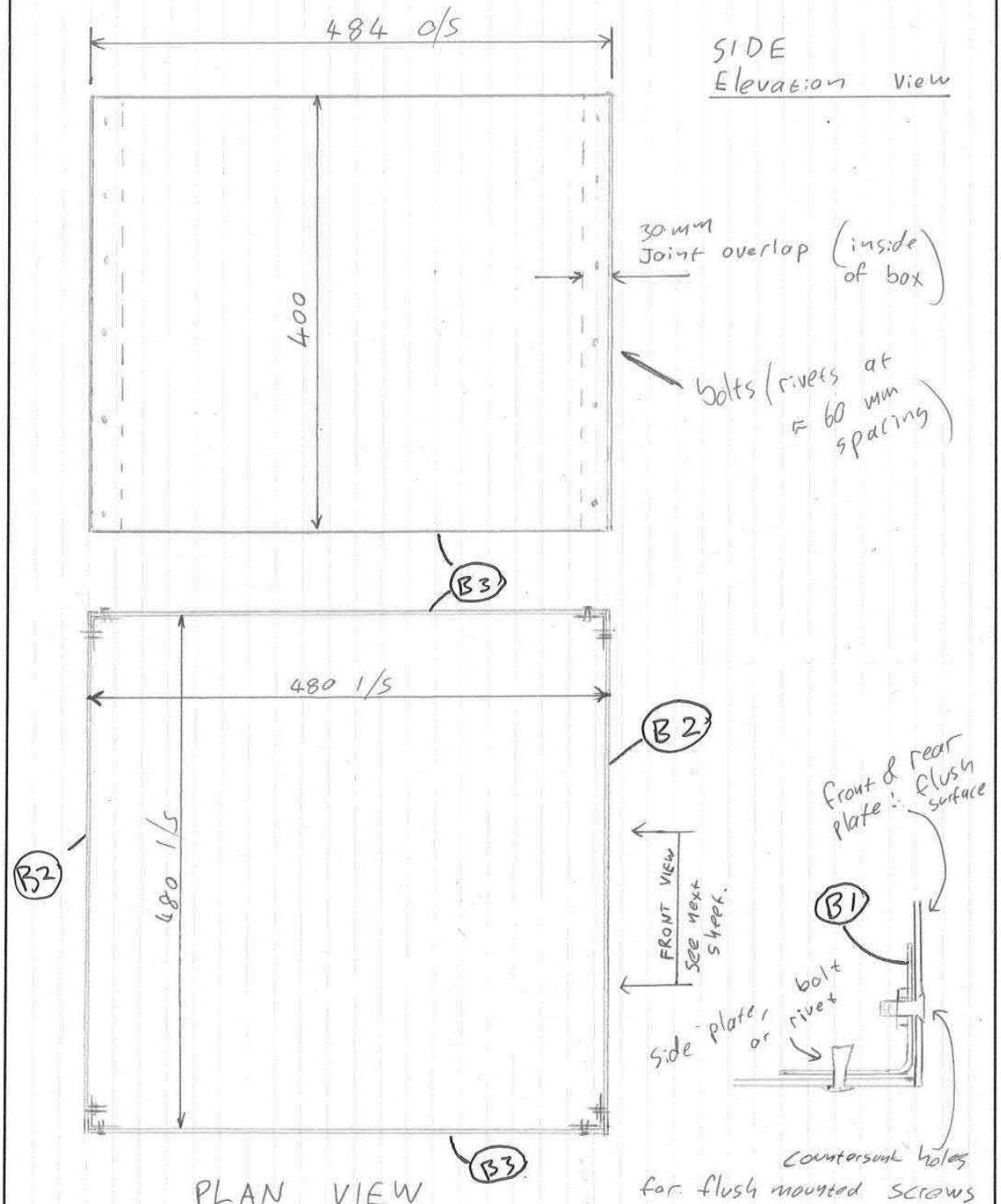
SHEET 5 OF 18

TITLE: Hopper Box detail Assembly (B)

Developed from 2mm thk MS plate, 400 x 1996 mm

HATCH GOBA Member of the Hatch Group

PROJECT No	WBS REF No.	CALC. REF No.	DESIGNER	CHECKED	DATE
					2016/04/08



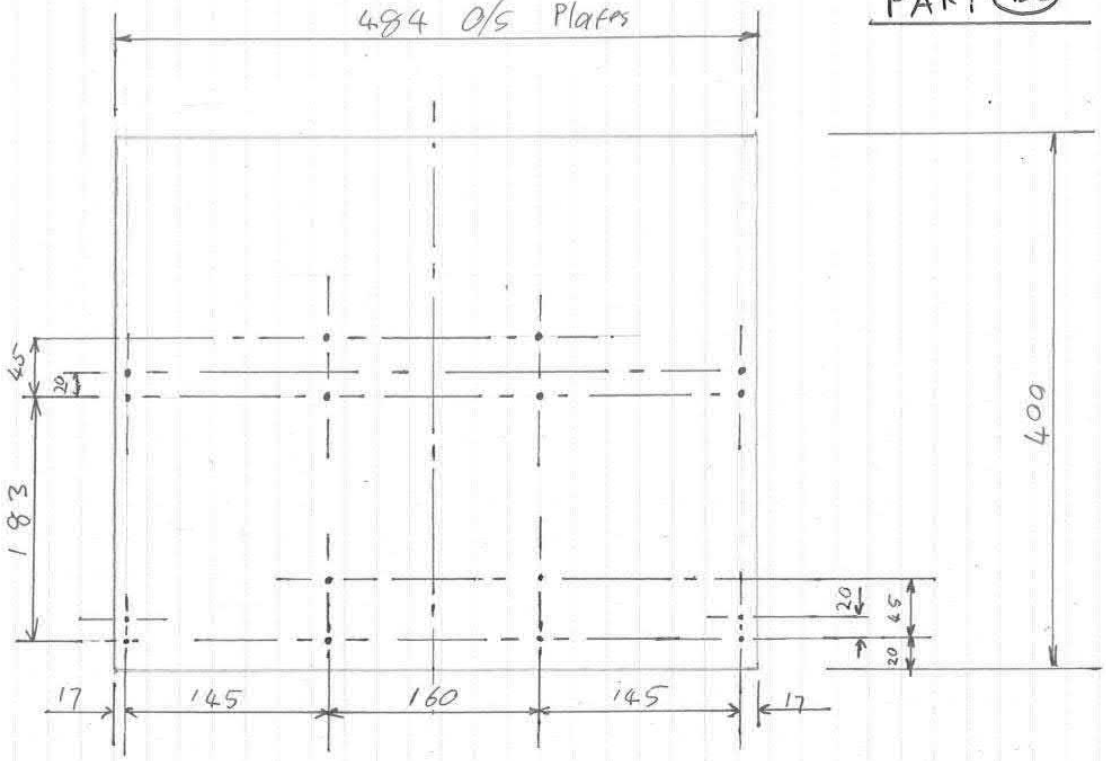
SHEET 6 OF 18

TITLE: Hopper Box detail - Front view & drilling plan - 2 Required

HATCH GOBA Member of the Hatch Group

PROJECT No	WBS REF No.	CALC. REF No.	DESIGNER	CHECKED	DATE
					2016/04/08

PART (B2)



Front view and drilling plan.

Drillings in front and rear to identical Pattern

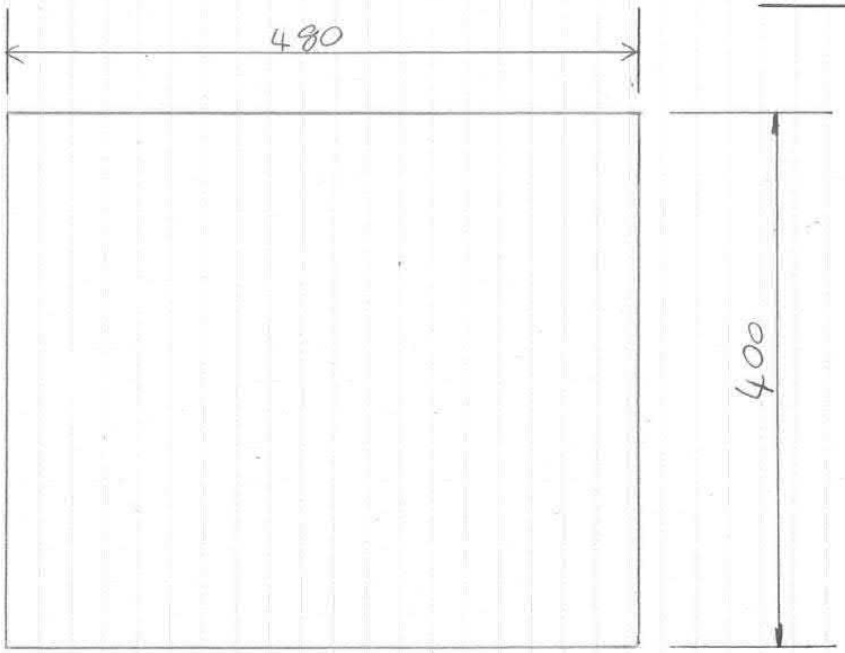
SHEET 7 OF 18

TITLE: Hopper Box side plate detail
2- Required

HATCH
Member of the Hatch Group GOBA

PROJECT No	WBS REF No.	CALC. REF No.	DESIGNER	CHECKED	DATE

PART (B3)



Material : 2mm MS Plate

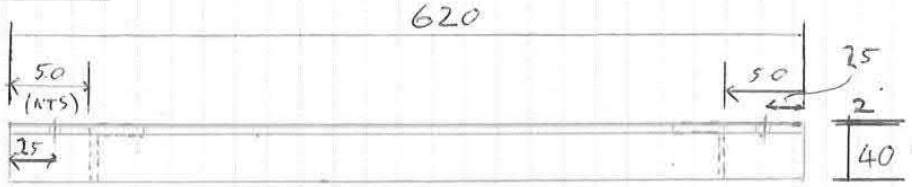
SHEET 8 OF 18

TITLE: Bottom plate Assembly (C)

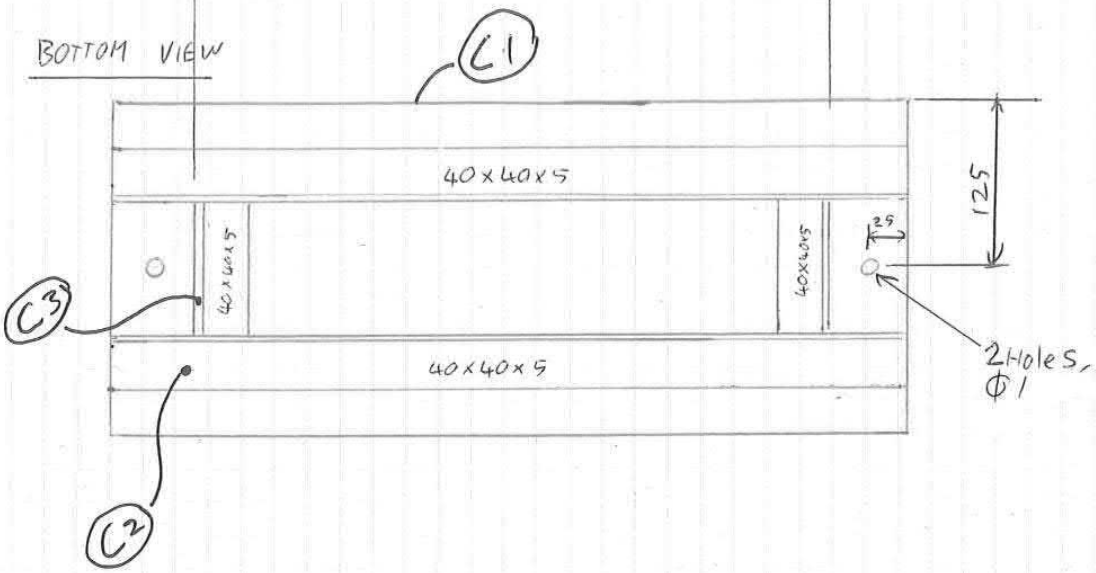
HATCH Member of the Hatch Group GOBA

PROJECT No	WBS REF No.	CALC. REF No.	DESIGNER	CHECKED	DATE
			C. Haupt	082 900 6713	2016/01/26

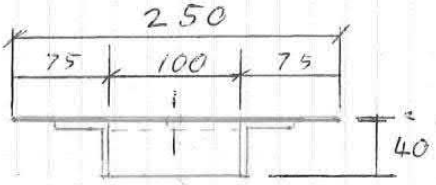
SIDE VIEW



BOTTOM VIEW



FRONT VIEW



40x40x5 : 2x 620 lng & 2x 100 lng ⇒ 1440 mm @ 2.97kg

plate: 600 x 250 x 2mm fok ⇒ 2.42 kg

4.28 kg.

total : 2.42 + 4.28 = 6.7 kg

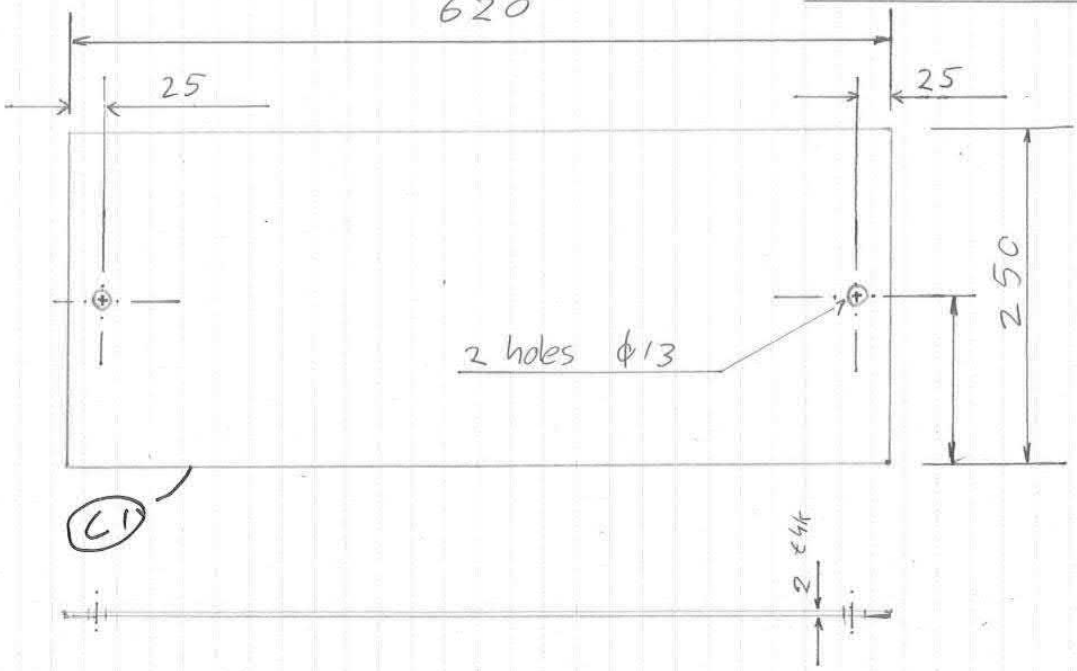
SHEET 9 OF 18

TITLE: Bottom Plate - detail - Require 1
- Require 1

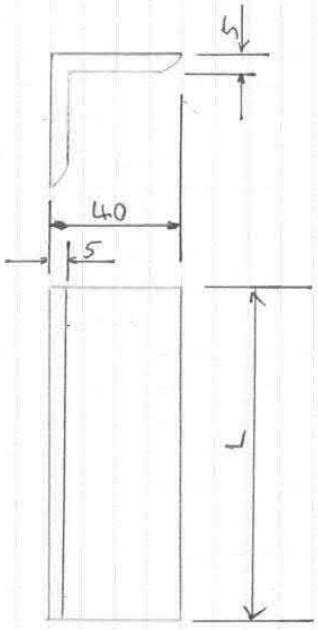
HATCH Member of the Hatch Group GOBA

PROJECT No	WBS REF No.	CALC. REF No.	DESIGNER	CHECKED	DATE

Bottom Plate - Det. - Req. 1



40x40x5 Angle details



NO.	Name	Length(mm)	Qty
C2	Bottom Plate long Stiffener	620	2
C3	Bottom Plate Cross Stiffend	100	2
D1	Loadcell Mount Vertical	140	2

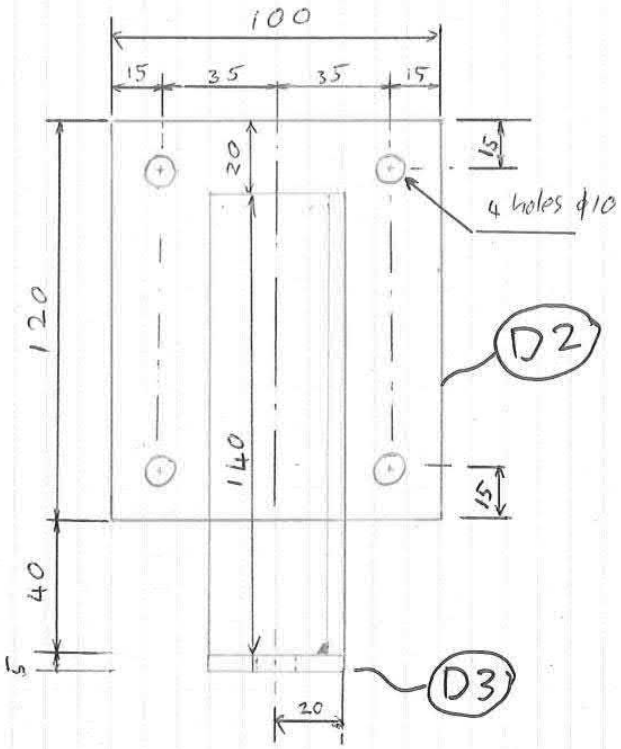
SHEET 10 OF 18

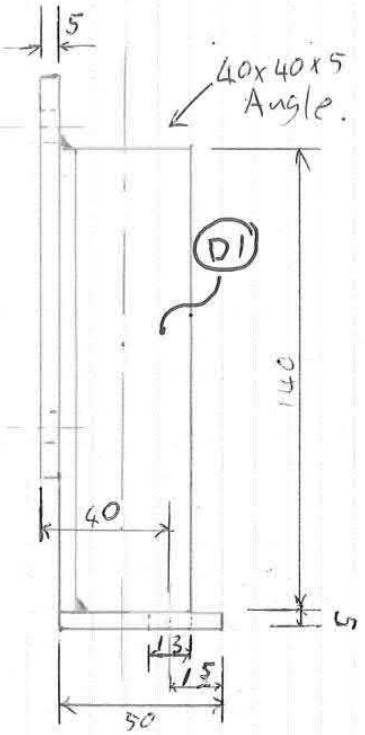
TITLE: Load cell mounting brackets Assembly

2 - required - Assembly (D)

HATCH Member of the Hatch Group GOBA

PROJECT No	WBS REF No.	CALC. REF No.	DESIGNER	CHECKED	DATE
			C. Haupt	082-900-6713	2016/01/26





(12 mm hole through bottom plate.
Centre set back by 16mm

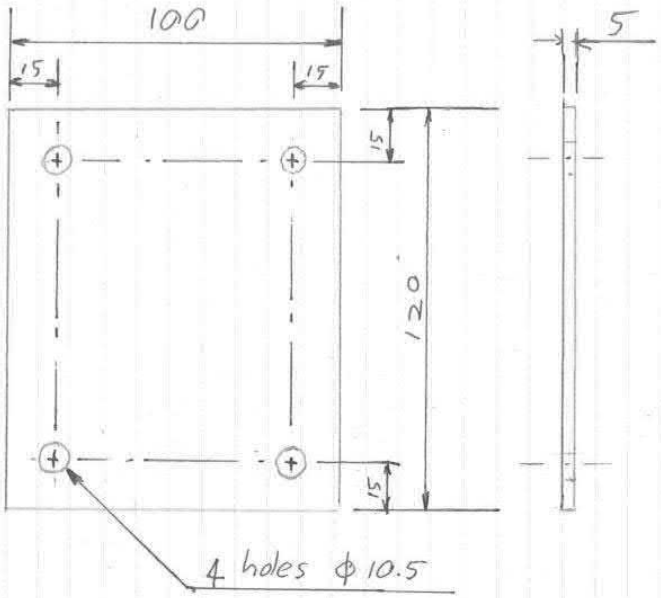
mass, ≈ 0,9 kg ea

SHEET 11 OF 18

TITLE: Loadcell Mounting Bracket, Plate details

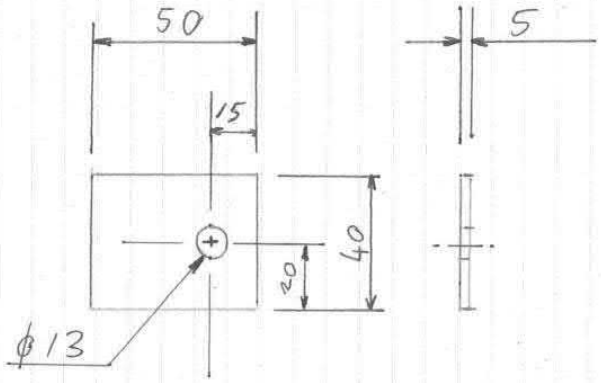
HATCH GOBA
Member of the Hatch Group

PROJECT No	WBS REF No.	CALC. REF No.	DESIGNER	CHECKED	DATE



Mounting Plate to Hopper
- Require 2 off

PART D 2



M Loadcell Mounting plate
- Require 2 off

PART D3

SHEET 12 OF 18

TITLE: Mass Flow Hopper front / rear walls

2 required, one with 2mm steel, one with 8mm Perspex

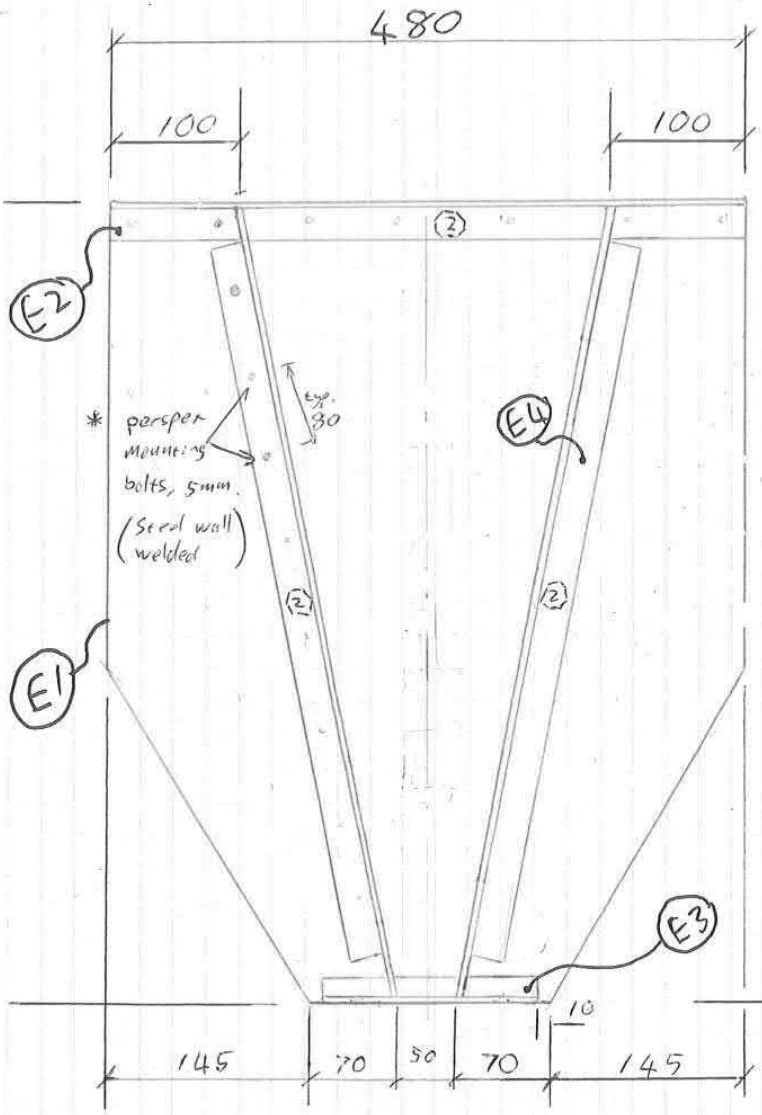
HATCH GOBA Member of the Hatch Group

04/08

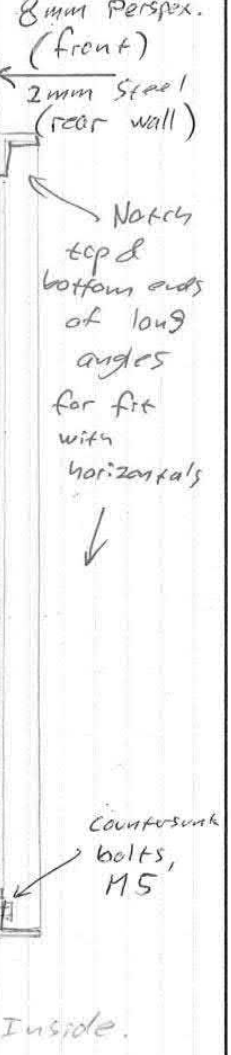
PROJECT No	WBS REF No.	CALC. REF No.	DESIGNER	CHECKED	DATE
			C. Haupt	083-900-6713	2016/01/26

ASSEMBLY E

FRONT VIEW



SIDE VIEW



(2) 30x30x5 angle (2.18 kg/m) 2x710 + 480 + 170 = 2070mm

mass = 2.070 x 2.19 ≈ 4.5 kg.

Backing sheet - Plexiglass, 8mm thk. SG. 1.19 g/cm³ ≈ 2.85 kg.

7.35 kg.

* Countersunk bolts to connect Stiffeners to Plexiglass: M5, every 75-100 mm

SHEET 13 OF 18

TITLE: Hopper bottom Section, front / rear walls, drilling plan

HATCH Member of the Hatch Group GOBA

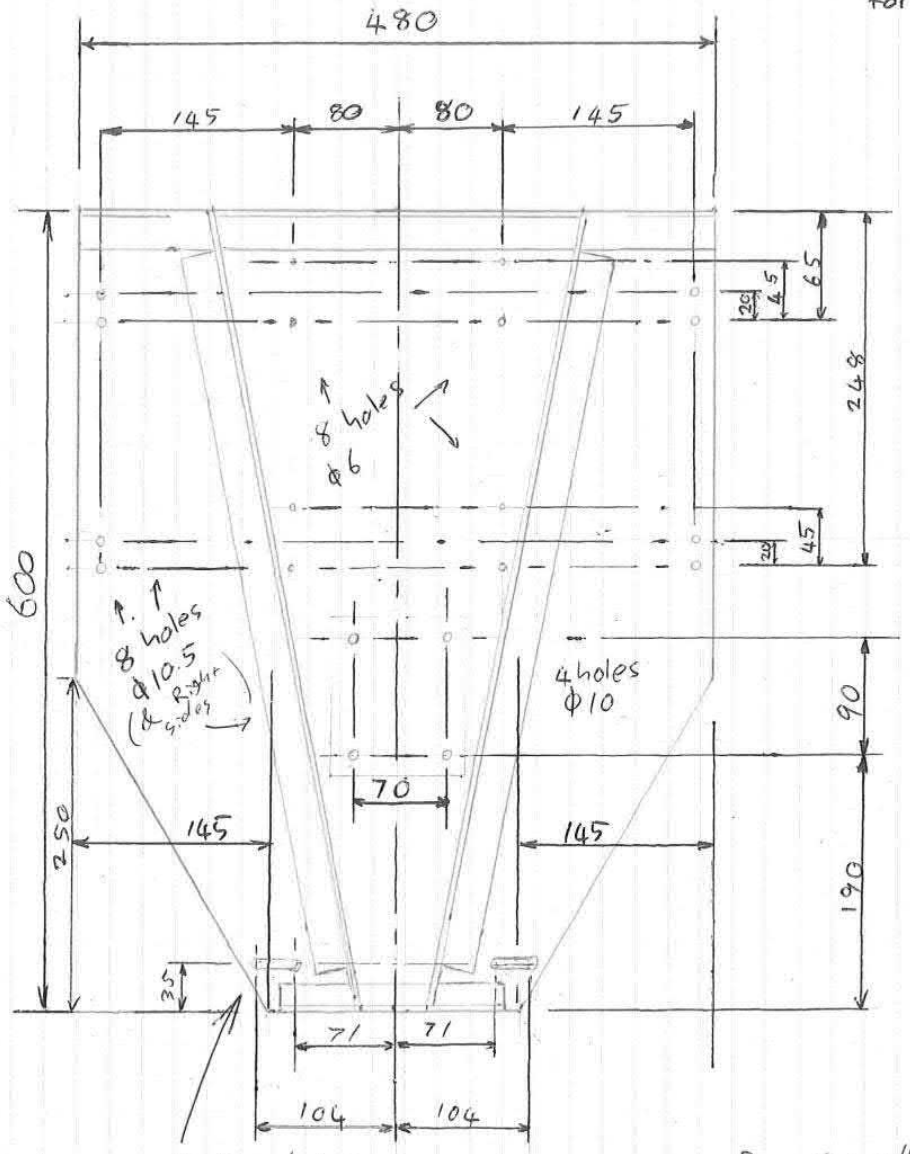
PROJECT No	WBS REF No.	CALC. REF No.	DESIGNER	CHECKED	DATE
					2016/04/08

PART (E1)

E1A - Steel 2mm

E1B - Perspex 8mm

Stiffeners shown for reference only



Rear wall (2 mm mild steel) - Mild steel angle stiffeners welded in place

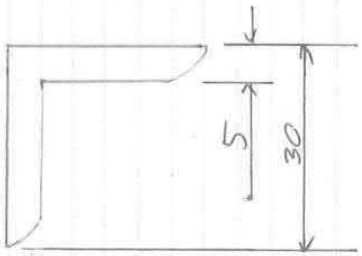
Front wall (8 mm perspex) - Mild steel angle stiffeners joined with 5mm bolts on ≈ 100 mm spacing

SHEET 14 OF 18

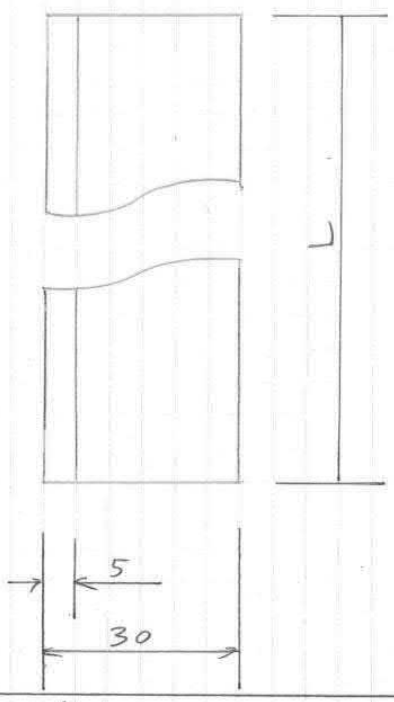
TITLE: 30x5 angle part details

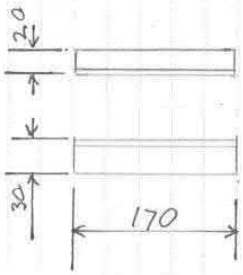
HATCH GOBA
Member of the Hatch Group

PROJECT No	WBS REF No.	CALC. REF No.	DESIGNER	CHECKED	DATE



No	Name	Length	Qty	Detail
E2	front/rear hopper plate top stiffener	480	2	
E3	front/rear hopper plate bottom stiffner	170	2	Detail B
E4	front/rear hopper sloped stiffener	600	4	Notch & Bevel. See Detail A
F2	side hopper plate top/bottom stiffener	484	4	
F3	side hopper plate vertical stiffener	495	6	

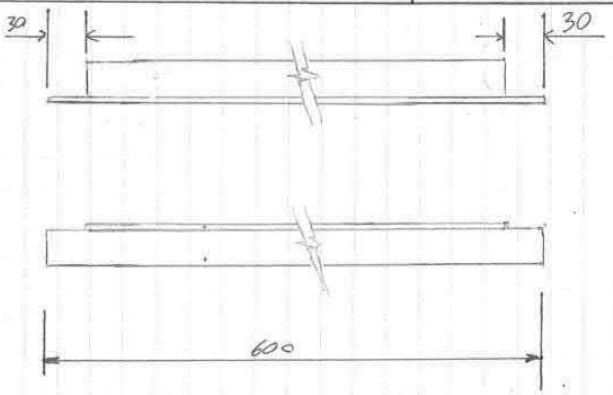




Detail B

trim one flange to 20 mm

PART E3



Detail A

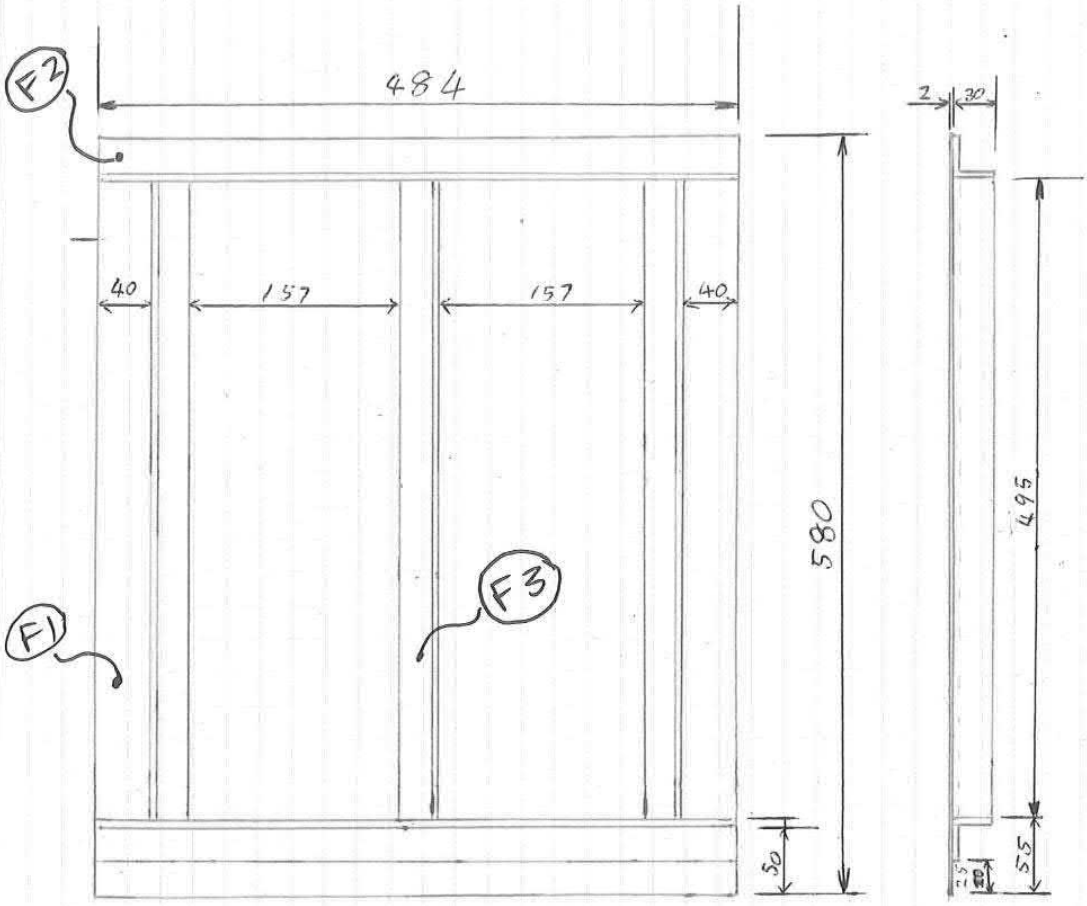
PART E4

SHEET 15 OF 18

TITLE: Mass flow hopper - side walls Require 2
Assembly F

HATCH Member of the Hatch Group GOBA

PROJECT No	WBS REF No.	CALC. REF No.	DESIGNER	CHECKED	DATE
			C. Haupt	082-900-6715	2016/01/26



(2) 30x30x5 angle 2.453 mm @ 2.18 kg/m ⇒ 5.35 kg

plate: 484 x 580 x 2 ⇒ 4.38 kg

total: 9.73 kg each →

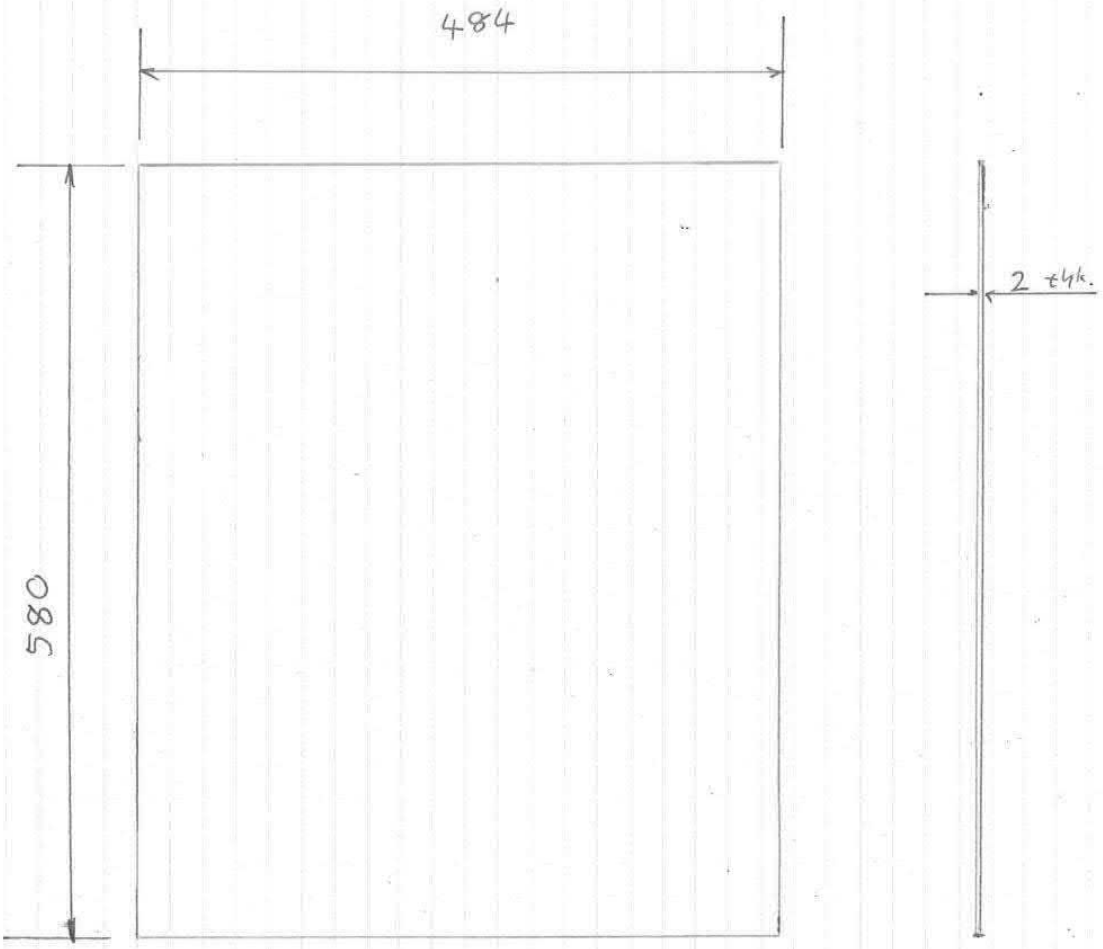
Stiffeners to be stitch welded to plate. 20 mm welds spaced at 100 mm pitch, alternating

SHEET 16 OF 18

TITLE: Mass flow hopper - side walls, plate detail - Require 2

HATCH
Member of the Hatch Group GOBA

PROJECT No	WBS REF No.	CALC. REF No.	DESIGNER	CHECKED	DATE



PART F1

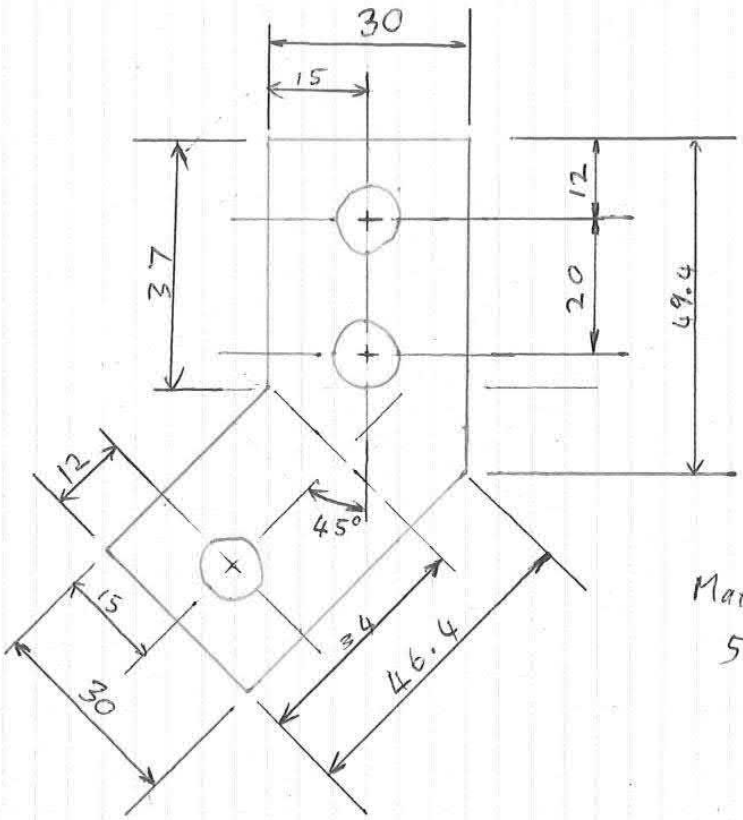
SHEET 17 OF 18

TITLE: Hopper wall mounting brackets, 4 – req.d.

HATCH Member of the Hatch Group GOBA

PROJECT No	WBS REF No.	CALC. REF No.	DESIGNER	CHECKED	DATE
					2016/04/08

PART G



Material, Mild Steel
5-6 mm thk

SHEET 18 OF 18